Methods in Molecular Biology 2910

Springer Protocols

Tolga Soykan
Alexandros Poulopoulos *Editors*

Synapse Development

Methods and Protocols

Second Edition

Humana Press

METHODS IN MOLECULAR BIOLOGY

Series Editor
John M. Walker
School of Life and Medical Sciences
University of Hertfordshire
Hatfield, UK

For further volumes:
http://www.springer.com/series/7651

For over 35 years, biological scientists have come to rely on the research protocols and methodologies in the critically acclaimed *Methods in Molecular Biology* series. The series was the first to introduce the step-by-step protocols approach that has become the standard in all biomedical protocol publishing. Each protocol is provided in readily-reproducible step-by-step fashion, opening with an introductory overview, a list of the materials and reagents needed to complete the experiment, and followed by a detailed procedure that is supported with a helpful notes section offering tips and tricks of the trade as well as troubleshooting advice. These hallmark features were introduced by series editor Dr. John Walker and constitute the key ingredient in each and every volume of the *Methods in Molecular Biology* series. Tested and trusted, comprehensive and reliable, all protocols from the series are indexed in PubMed.

Synapse Development

Methods and Protocols

Second Edition

Edited by

Tolga Soykan

FMP Cellular Imaging Facility, Leibniz-Forschungsinstitut für Molekulare Pharmakologie, Berlin, Germany

Alexandros Poulopoulos

Department of Pharmacology, Physiology, and Drug Discovery, University of Maryland, Baltimore, MD, USA

Humana Press

Editors
Tolga Soykan
FMP Cellular Imaging Facility
Leibniz-Forschungsinstitut für
Molekulare Pharmakologie
Berlin, Germany

Alexandros Poulopoulos
Department of Pharmacology, Physiology, and Drug Discovery
University of Maryland
Baltimore, MD, USA

ISSN 1064-3745 ISSN 1940-6029 (electronic)
Methods in Molecular Biology
ISBN 978-1-0716-4445-4 ISBN 978-1-0716-4446-1 (eBook)
https://doi.org/10.1007/978-1-0716-4446-1

Preface

Synapse development is a phenomenon that spans scales by orders of magnitude. It encompasses the macroscopic projections of neuroanatomy, the mesoscale organization of synaptic target fields, the microscale processes of synaptogenesis, and reaches down to the nanoscale structures of synaptic holocomplexes. The manifestations of synapse development across these scales require a correspondingly diverse toolkit for its study.

In this second edition of *Synapse Development: Methods and Protocols*, we have compiled methods that address phenomena across these scales. Several of the most useful chapters from the first edition have been updated to reflect methodological refinements and are framed within the context of the latest literature. These updates ensure that researchers have access to the most current and effective protocols for studying synapse development.

Importantly, since the first edition in 2017, entirely new methodologies have matured and become integral to cellular and developmental neuroscience. Notable among these advancements is the emergence of genome editing technologies, as well as new advances and refinements of protocols for generating specific neuronal subtypes from human pluripotent stem cells. These models provide powerful platforms for studying human neural development and neurological disorders in model systems.

The volume is organized into three parts:

- *Part I: Forming and Manipulating Synapses in a Dish* focuses on methods for in vitro formation and manipulation of synapses, including cutting-edge approaches for neuron differentiation and genomic modification.
- *Part II: Analyzing Synaptic Structure and Constituents* presents methods for dissecting synaptic components at high resolution, utilizing advanced imaging and purification techniques. These analytical techniques enable researchers to understand the intricate details of synaptic architecture and molecular composition.
- *Part III: Mapping Synaptic Connectivity and Activity* offers approaches for studying synaptic networks and activity patterns in their native contexts. This includes methods for labeling, tracing, and quantifying components of developing neural circuits.

As with the previous edition, we have chosen to exclude electrophysiological methods from this volume. While electrophysiology is indispensable for the study of synapse development, it encompasses a vast array of techniques that merit a dedicated volume of their own.

Our aim with this collection is to minimize barriers for researchers seeking to integrate new approaches with existing expertise. By bringing together methods that span from the macroscopic to the nanoscale, we hope to foster novel perspectives and encourage interdisciplinary integration. The study of synapse development remains a challenging yet profoundly rewarding endeavor, and we trust that the protocols assembled in this volume will serve as valuable resources in advancing our understanding of how synapses form, transform, and transmit.

We extend our sincere gratitude to all the contributors for sharing their expertise. We believe their efforts will inspire and support the next wave of discoveries in synapse development.

Berlin, Germany — *Tolga Soykan*
Baltimore, MD, USA — *Alexandros Poulopoulos*

Contents

Part III Mapping Synaptic Connectivity and Activity

Contributors

Sung Min Ahn • *Brain Science Division, Korea Institute of Science and Technology, Seoul, Republic of Korea; Division of Bio-Medical Science and Technology, Korea University of Science and Technology, Daejeon, Republic of Korea*

Maria Florencia Angelo • *Univ. Bordeaux, CNRS, Interdisciplinary Institute for Neuroscience, IINS, UMR 5297, Bordeaux, France*

Mathias Bähr • *Department of Neurology, University Medical Center Göttingen, Göttingen, Germany*

Bradley J. Baker • *Brain Science Division, Korea Institute of Science and Technology, Seoul, Republic of Korea; Division of Bio-Medical Science and Technology, Korea University of Science and Technology, Daejeon, Republic of Korea*

Stefan Bonn • *Institute for Medical Systems Biology, Center for Biomedical AI, Center for Molecular Neurobiology (ZMNH), University Medical Center Hamburg-Eppendorf, Hamburg, Germany*

Miquel Bosch • *RIKEN-MIT Neuroscience Research Center, Saitama, Japan; The Picower Institute for Learning and Memory, Department of Brain and Cognitive Sciences, Massachusetts Institute of Technology, Cambridge, MA, USA; Universitat Internacional de Catalunya, Barcelona, Spain*

Cheryl Brandenburg • *Department of Pharmacology and Physiology, University of Maryland School of Medicine, Baltimore, MD, USA*

Jorge Castro • *The Picower Institute for Learning and Memory, Department of Brain and Cognitive Sciences, Massachusetts Institute of Technology, Cambridge, MA, USA; MBF Bioscience, Williston, VT, USA*

Gustav Y. Cederquist • *The Center for Stem Cell Biology, Developmental Biology Program, Sloan-Kettering Institute for Cancer Research, New York, NY, USA*

Xuyao Chang • *Center for Stem Cell and Organoid Medicine (CuSTOM), Division of Developmental Biology, Cincinnati Children's Hospital Medical Center, Cincinnati, OH, USA*

Laura Cocas • *Department of Biology, Santa Clara University, Santa Clara, CA, USA; Department of Neurology, University of California San Francisco, San Francisco, CA, USA*

Katalin Czöndör • *University of Bordeaux, CNRS UMR 5297, Interdisciplinary Institute for Neuroscience, IINS, Bordeaux, France*

Luca Della Santina • *College of Optometry, University of Houston, Houston, TX, USA*

Reha S. Erzurumlu • *Department of Neurobiology, University of Maryland School of Medicine, Baltimore, MD, USA*

Gloria Fernandez • *Department of Biology, Santa Clara University, Santa Clara, CA, USA*

Maksims Fiosins • *Institute for Medical Systems Biology, Center for Biomedical AI, Center for Molecular Neurobiology (ZMNH), University Medical Center Hamburg-Eppendorf, Hamburg, Germany*

Corey Flynn • *Atomic Insights, Inc, Poway, CA, USA*

Nazarii Frankiv • *Brain Science Division, Korea Institute of Science and Technology, Seoul, Republic of Korea; Division of Bio-Medical Science and Technology, Korea University of Science and Technology, Daejeon, Republic of Korea*

Pretty Garg • *Department of Neurology, University Medical Center Göttingen, Göttingen, Germany; Cluster of Excellence "Multiscale Bioimaging: from Molecular Machines to Networks of Excitable Cells" (MBExC), University of Göttingen, Göttingen, Germany*

Claudia Gualtieri • *Department of Biological Sciences, University of Maryland Baltimore County (UMBC), Baltimore, MD, USA*

Volker Haucke • *Leibniz-Forschungsinstitut für Molekulare Pharmakologie (FMP), Berlin, Germany; Department of Biology, Chemistry, Pharmacy, Freie Universität, Berlin, Germany; NeuroCure Cluster of Excellence, Charité Universitätsmedizin, Berlin, Germany*

Yasunori Hayashi • *RIKEN-MIT Neuroscience Research Center, Saitama, Japan; The Picower Institute for Learning and Memory, Department of Brain and Cognitive Sciences, Massachusetts Institute of Technology, Cambridge, MA, USA; Brain Science Institute, RIKEN, Wako, Saitama, Japan; Saitama University Brain Science Institute, Saitama University, Saitama, Japan; School of Life Science, South China Normal University, Guangzhou, China; Department of Pharmacology, Kyoto University Graduate School of Medicine, Kyoto, Japan*

Etienne Herzog • *Univ. Bordeaux, CNRS, Interdisciplinary Institute for Neuroscience, IINS, UMR 5297, Bordeaux, France*

Mrinalini Hoon • *Department of Ophthalmology and Visual Sciences, University of Wisconsin-Madison, Madison, WI, USA*

Maesoon Im • *Brain Science Division, Korea Institute of Science and Technology, Seoul, Republic of Korea*

Olaf Jahn • *Neuroproteomics Group, Department of Molecular Neurobiology, Max Planck Institute for Multidisciplinary Sciences, Göttingen, Germany; Translational Neuroproteomics Group, Department of Psychiatry and Psychotherapy, University Medical Center Göttingen, Göttingen, Germany*

Younginha Jung • *Bioimaging Data Curation Center, Ewha Womans University, Seoul, Republic of Korea*

Sebastian Kügler • *Department of Neurology, University Medical Center Göttingen, Göttingen, Germany*

Haeun Lee • *Brain Science Division, Korea Institute of Science and Technology, Seoul, Republic of Korea; Division of Bio-Medical Science and Technology, Korea University of Science and Technology, Daejeon, Republic of Korea*

Noa Lipstein • *Synapse Biology Group, Leibniz-Forschungsinstitut für Molekulare Pharmakologie (FMP), Berlin, Germany*

Mareike Lohse • *Synapse Biology Group, Leibniz-Forschungsinstitut für Molekulare Pharmakologie (FMP), Berlin, Germany; Department of Molecular Neurobiology, Max Planck Institute for Multidisciplinary Sciences, Göttingen, Germany*

Marta Maglione • *Institute for Biology, Freie Universität Berlin, Berlin, Germany; NeuroCure Cluster of Excellence, Charité Universitätsmedizin, Berlin, Germany; Institute for Chemistry and Biochemistry, SupraFAB, Freie Universität Berlin, Berlin, Germany*

Corinne A. Martin • *Department of Pharmacology and Physiology, University of Maryland School of Medicine, Baltimore, MD, USA; Department of Bioengineering, University of California, Berkeley, CA, USA*

Ryuichi Nakajima • *Brain Science Division, Korea Institute of Science and Technology, Seoul, Republic of Korea*

Polina Oberst • *The Center for Stem Cell Biology, Developmental Biology Program, Sloan-Kettering Institute for Cancer Research, New York, NY, USA*

Vincent Paget-Blanc • *Univ. Bordeaux, CNRS, Interdisciplinary Institute for Neuroscience, IINS, UMR 5297, Bordeaux, France*

Marlene E. Pfeffer • *Univ. Bordeaux, CNRS, Interdisciplinary Institute for Neuroscience, IINS, UMR 5297, Bordeaux, France*

Nathalie Piette • *University of Bordeaux, CNRS UMR 5297, Interdisciplinary Institute for Neuroscience, IINS, Bordeaux, France; Alveole S.A., Paris, France*

Celine Plachez • *Department of Neurobiology, University of Maryland School of Medicine, Baltimore, MD, USA*

Alexandros Poulopoulos • *Department of Pharmacology and Physiology, University of Maryland School of Medicine, Baltimore, MD, USA*

Marie Pronot • *Univ. Bordeaux, CNRS, Interdisciplinary Institute for Neuroscience, IINS, UMR 5297, Bordeaux, France*

Ryan R. Richardson • *Department of Pharmacology and Physiology, University of Maryland School of Medicine, Baltimore, MD, USA*

Filiz Sila Rizalar • *Leibniz-Forschungsinstitut für Molekulare Pharmakologie (FMP), Berlin, Germany*

Colin D. Robertson • *Department of Pharmacology and Physiology, University of Maryland School of Medicine, Baltimore, MD, USA*

Andrea J. Romanowski • *Department of Pharmacology and Physiology, University of Maryland School of Medicine, Baltimore, MD, USA*

Stephan J. Sigrist • *Institute for Biology, Freie Universität Berlin, Berlin, Germany; NeuroCure Cluster of Excellence, Charité Universitätsmedizin, Berlin, Germany*

Yoon-Kyu Song • *Graduate School of Convergence Science and Technology, Seoul National University, Seoul, Republic of Korea*

Marilyn Steyert • *Department of Pharmacology and Physiology, University of Maryland School of Medicine, Baltimore, MD, USA; Weill Institute for Neurosciences, University of California San Francisco, San Francisco, CA, USA*

Lorenz Studer • *The Center for Stem Cell Biology, Developmental Biology Program, Sloan-Kettering Institute for Cancer Research, New York, NY, USA*

Vincent Studer • *University of Bordeaux, CNRS UMR 5297, Interdisciplinary Institute for Neuroscience, IINS, Bordeaux, France*

Siqi Sun • *Synapse Biology Group, Leibniz-Forschungsinstitut für Molekulare Pharmakologie (FMP), Berlin, Germany; Department of Biology, Chemistry, and Pharmacy, Freie Universität Berlin, Berlin, Germany*

Mriganka Sur • *The Picower Institute for Learning and Memory, Department of Brain and Cognitive Sciences, Massachusetts Institute of Technology, Cambridge, MA, USA*

Jason Tchieu • *Center for Stem Cell and Organoid Medicine (CuSTOM), Division of Developmental Biology, Cincinnati Children's Hospital Medical Center, Cincinnati, OH, USA*

Béatrice Tessier • *University of Bordeaux, CNRS UMR 5297, Interdisciplinary Institute for Neuroscience, IINS, Bordeaux, France*
Olivier Thoumine • *University of Bordeaux, CNRS UMR 5297, Interdisciplinary Institute for Neuroscience, IINS, Bordeaux, France*
Theodoros Tsetsenis • *Division of Neurology, Department of Pediatrics, The Children's Hospital of Philadelphia, Philadelphia, PA, USA*
Fernando J. Vonhoff • *Department of Biological Sciences, University of Maryland Baltimore County (UMBC), Baltimore, MD, USA*
Pedro Zamorano • *Laboratorio de Microorganismos Extremófilos, Instituto Antofagasta, Departamento Biomédico, Facultad de Ciencias de la Salud, Universidad de Antofagasta, Antofagasta, Chile*

Part I

Making and Manipulating Synapses in a Dish

Chapter 1

Synaptogenic Assays Using Primary Neurons Cultured on Micropatterned Substrates

Katalin Czöndör, Nathalie Piette, Béatrice Tessier, Vincent Studer, and Olivier Thoumine

Abstract

One of the difficulties for studying the mechanisms of synaptogenesis stems from the spatial unpredictability of contact formation between neurons, and the involvement of many parallel adhesive pathways mediating axon-dendrite recognition. To circumvent these limitations, we describe here a method allowing for the investigation of biomimetic synaptic contacts at controlled locations with high precision and statistics. Specifically, primary neurons are cultured on micropatterned substrates comprising arrays of micron-scale dots coated with purified synaptogenic adhesion molecules. Coating the substrates with the homophilic adhesion molecule SynCAM1 triggers the formation of functional presynaptic structures in axons, while neurexin-1β elicits postsynapses in dendrites from neurons expressing the counter receptor neuroligin-1. This assay can be combined with various optical imaging techniques, including immunocytochemistry to screen the accumulation of synaptic components, long-term live cell recordings to probe the kinetics of neurite growth and synapse differentiation, as well as high-resolution single-molecule tracking.

Key words Synapse formation, Micropatterned substrates, Adhesion molecules, Neurexin, Neuroligin, SynCAM

1 Introduction

Assembly of the myriad of synapses between neurons during the development of the central nervous system represents a pivotal process which determines the generation, maintenance, and function of neural circuitries. At the level of individual axon/dendrite contacts, synaptogenesis is a complex multi-step process initiated by specific adhesion proteins [1, 2]. Once the contact is stabilized, scaffolding molecules and functional receptors, which are essential for the transmission of information from one neuron to the other,

Katalin Czöndör and Nathalie Piette are co-first authors.

Vincent Studer and Olivier Thoumine are co-senior authors.

Tolga Soykan and Alexandros Poulopoulos (eds.), *Synapse Development: Methods and Protocols*, Methods in Molecular Biology, vol. 2910, https://doi.org/10.1007/978-1-0716-4446-1_1,

are recruited to contact sites [3]. Importantly, the type of the presynaptic neurotransmitter machinery (glutamate versus GABA), and the corresponding postsynaptic receptors and scaffolding proteins assembled at the synaptic contact determines whether the synapse is excitatory or inhibitory. Once formed, synapses remain very dynamic, as they undergo both structural and functional alterations in response to activity changes in the neuronal network [4]. Given such molecular complexity, heterogeneity, and dynamics, unraveling the mechanisms underlying synaptogenesis and synapse function is highly challenging. Thus, the development of simplified experimental systems which aims at triggering synaptogenesis in a controlled way, and where the role of specific cell adhesion molecules can be isolated, is highly needed.

Indeed, adhesion molecules play an important role in the initial stages of synapse formation, by strengthening the contact between the pre- and the postsynaptic membranes, and by mediating a variety of cell signaling processes, including through the phosphorylation of specific protein binding motifs [5–8]. Some adhesion molecules, such as the heterophilic neurexin/neuroligin complex or the homophilic adhesion proteins SynCAMs, were also found to play key roles in inducing synapse assembly by recruiting essential synaptic molecules to contact sites [9]. In the last two decades, several biomimetic assays were developed to demonstrate the ability of certain adhesion molecules to induce synapse formation, including co-cultures [10–13], synapse microarrays [14], microspheres [11, 15–17], and protein clusters [5, 18, 19]. These existing methods share the principle of using synaptogenic adhesion molecules to induce the assembly of hemi-synapses, thus reducing the complexity of native synaptic contacts to a great extent. However, the spatial and temporal resolutions provided by these assays often do not allow high statistical production at the level of individual synaptic structures.

Here, we describe in technical detail robust methods developed to spatially control synaptic differentiation, by culturing neurons on micropatterned substrates comprising arrays of individual micron-scale dots coated with adhesion proteins and surrounded by a cytophobic agent [20]. The dots are specifically coated with SynCAM1 or neurexin1β (Nrx1β), which triggers the selective differentiation of functional pre- or postsynapses, respectively. Coating of recombinant proteins is made via fluorescently labeled secondary antibodies or streptavidin, allowing both proper orientation of the adhesive ectodomain and fluorescent visualization of the micropatterns. After this coating step, dissociated neurons are plated and cultured on the substrates as regular neuronal cultures. Neurite architecture is highly determined by the specific adhesion to the micron-scale dots, and the development of hemi-synapses is thus defined by the topology of the patterns, leading to the spatial control of synapse formation at a micron-scale resolution.

Importantly, micropatterned substrates can be manipulated just as regular glass coverslips, and therefore be combined with a wide range of microscopy techniques including immunocytochemistry to screen the accumulation of synaptic components, long-term live cell recordings to probe the kinetics of synapse differentiation, local photo-activation to probe functional synaptic properties, and high-resolution single-molecule tracking of membrane receptors. Considering the simple coating protocol, this assay can theoretically be adapted to a wide range of other newly reported synaptogenic adhesion proteins, including leucine-rich repeat transmembrane proteins which also bind neurexins [21–23], opening the way to the targeted and selective study of the mechanisms underlying synapse formation with unprecedented spatial resolution and statistical power.

2 Materials

2.1 Culturing Neurons on Micropatterned Substrates Coated with Adhesion Proteins

1. Coating buffer: 0.2 M boric acid (e.g., Sigma-Aldrich B6768), pH 8.5.
2. Goat Anti-Human IgG, Fcγ fragment-specific, minimal cross-reactivity with other species, unlabeled or conjugated to Alexa647 (Jackson ImmunoResearch, 109-005-098 and 109-605-098 respectively).
3. Recombinant proteins: Home-made Nrx1β-Fc for inducing postsynapses [24], and SynCAM1-Fc for inducing presynapses [25].
4. Plating medium: Minimum Essential Medium (e.g., Gibco MEM 21090–022), 2 mM GlutaMAX supplement 1X (e.g., Gibco 35050038), 4.5 g/l glucose (e.g., Sigma-Aldrich G8769), 10% horse serum (e.g., Gibco 26050088).
5. Neurobasal medium (without red phenol) (e.g., Gibco 12348017) + Neuromix (PAA; 50x; no longer commercialized) + 2 mM L-glutamine (PAA, M11–004, no longer commercialized) or Neurobasal-Plus + B27-Plus (e.g., Gibco A365340) + 1x GlutaMAX.
6. Effectene transfection reagent (Qiagen 301425), if overexpression of the receptor for the coated ligand is necessary.

2.2 Experiments on Fixed Samples

1. Phosphate Buffer Solution (PBS, Euromedex ET-330).
2. Fixation buffer: Paraformaldehyde 4% (PFA), 4% sucrose in PBS.
3. Quenching buffer: 50 mM NH_4Cl in PBS.
4. Permeabilization buffer: 0.1% Triton X-100 (e.g., Sigma-Aldrich X100) in PBS.

5. Bovine Serum Albumin (BSA) (e.g., Sigma-Aldrich A7030).
6. Primary and secondary antibodies of interest: rat anti-HA (Roche 11867423001), mouse anti-PSD-95 (Thermo Scientific MA1–046), mouse anti-synaptotagmin1 luminal domain conjugated to Oyster 550 (Synaptic Systems 105311C5), mouse anti-synapsin (Synaptic Systems 106001), rabbit anti-SynCAM1 (Abcam 216585), donkey anti-rat-FITC (Jackson Immunoresearch 712–095-153), donkey anti-mouse-Rhodamine (Jackson Immunoresearch 715–295-150).
7. Mounting medium: Mowiol (Calbiochem 475904) or equivalent.
8. Fluorescence microscope (Nikon Eclipse TiE or equivalent) equipped with a 20x/0.75 NA or 60x/1.40 NA oil immersion objective, appropriate filter sets from Semrock/Chroma, and a digital CMOS camera (ORCA-Flash 4.0, Hamamatsu).

2.3 Live Cell Imaging

1. Ludin open sample holder (Life Imaging Services), manufactured to fit the 20 × 20 mm square micropatterned coverslips.
2. Penicillin/Streptomycin (e.g., Gibco 15140–122).
3. For long-term imaging experiments: BioStation CT (Nikon).
4. For short-term imaging experiments (up to 5 h): an inverted microscope (Nikon TiE or equivalent) equipped with filter sets appropriate for the fluorophores used, 40× or 60× oil immersion objectives, a thermostatic box providing 37 °C and 5% CO_2 (Life Imaging Systems), and a CCD camera (e.g. CoolSnap, Roper Scientific, Evry, France).

2.4 Universal Point Accumulation in Nanoscopic Topography (uPAINT)

1. Tyrode solution: 108 mM NaCl, 5 mM KCl, 2 mM $MgCl_2$, 2 mM $CaCl_2$, 10 mM HEPES, 15 mM Glucose, pH 7.4.
2. Monoclonal anti-GluA2 antibodies (gift of E. Gouaux, Vollum Institute, Portland, OR, USA) conjugated to ATTO 647 N (Attotec) according to the manufacturer protocol.
3. Microscope equipped with a 100 mW, 633 nm laser line and TIRF illumination arm (Nikon Ti-E Eclipse), 100X /1.49 NA oil immersion objective, dichroic mirror (Di01-R635, SemRock), 676/29 nm emission filter (SemRock) placed on a filter wheel (Suter) and an EM-CCD Camera (e.g. Evolve, Roper Scientific, Evry, France).

3 Methods

The method we initially exploited to obtain micropatterned substrates relied on the use of a photomask containing microfeatures to locally irradiate with deep UV light an antifouling substrate,

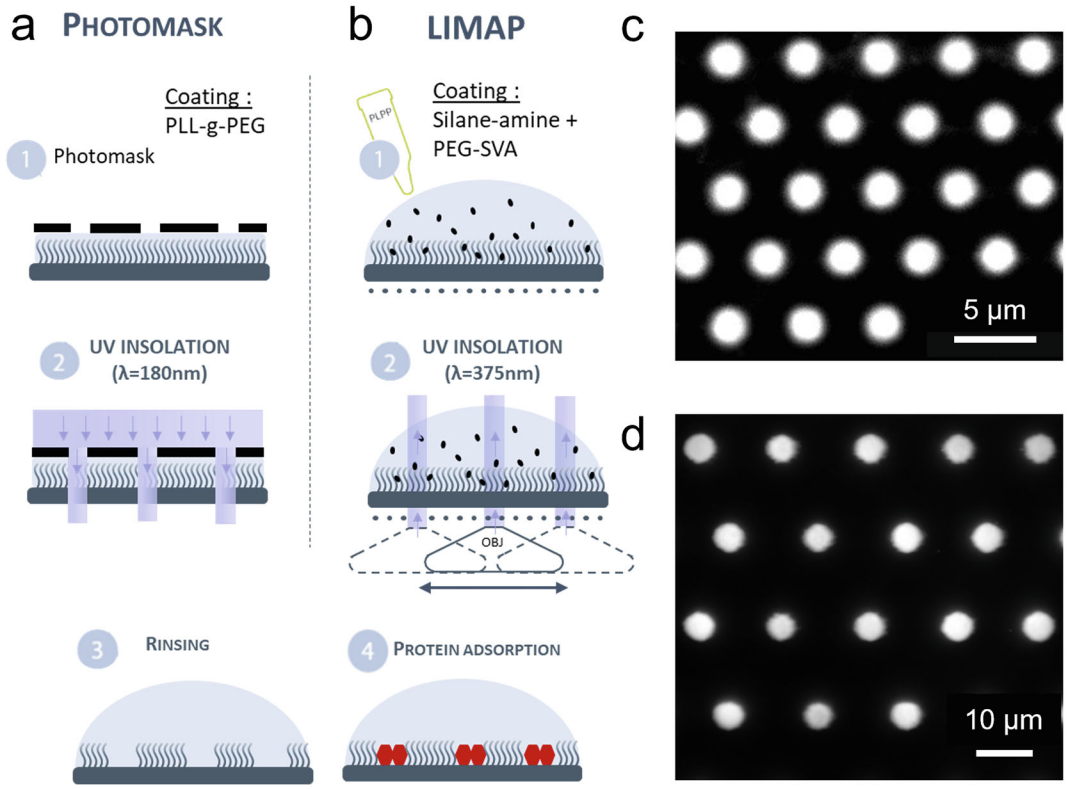

Fig. 1 Comparison of mask- and DMD-based micro-photopatterning technologies. Both methods rely on the use of glass coverslips coated with a cytophobic PEG reagent. (**a**) The first method consists in insolating the coverslip by projecting UV light from a lamp emitting at a wavelength of 180 nm through a quartz photomask containing microfeatures. (**b**) The second method allows for wide-field spatially modulated UV light illumination from a 375 nm laser plugged on a microscope and pattern shape is controlled through a digital micromirror device. (**c, d**) Examples of hexagonal arrays of circular patterns created with the two techniques, respectively. Images show the secondary anti-Fc antibody conjugated to Alexa-647, or streptavidin conjugated to Alexa-647, respectively

making it locally adsorbing for proteins [26]. This solution was directly offered by the company CYTOO (https://cytoo.com) with which we had a collaboration (Fig. 1a). Over the years the collaboration was discontinued, and we adopted another protocol to produce our own micropatterned substrates. This technique called *Light-Induced Molecular Adsorption of Proteins* (LIMAP) [27] is also based on the local ablation of a cytophobic substance by targeted UV light, but is maskless and contactless (Fig. 1b). Here, we will describe the two methods sequentially. Pros and cons of the two strategies, as well as alternative technologies to produce micropatterned substrates in the laboratory, are given in **Notes 1** and **2**, respectively.

3.1 Preparing Micropatterned Glass Substrates with the Photomask Method

In the first method, the UV insolation of the pattern geometry is made by using a photoresist mask (Fig. 1a). The photomask was based on a pre-defined geometry designed by ourselves and its production was custom-ordered to another company, but stayed the property of the purchaser. In this particular configuration, micropatterned substrates were made of 20 × 20 mm square glass coverslips and contained a hexagonal array of chemically activated dots of 1.5 μm diameter, separated by 5 μm and surrounded by a cytophobic polyethylene glycol (PEG) layer (Fig. 1c). A slight dilation of the actual patterned area is possible (e.g., up to 2.5 μm), especially after several uses of the same mask. The dots on the substrates were further coated with 50 μg/mL poly-L-lysine by the manufacturer, dried, and shipped at room temperature. They could be stored for up to 2 months at 4 °C after production. Micropatterned substrates used for this assay are specifically designed with the aim of locally inducing synaptogenesis at the micron-scale, comparable with the size of native synapses. The specific coating of the substrates is done one day before plating the neurons, as described in the following steps (*see* **Note 3**).

3.2 Preparing Micropatterned Glass Substrates with the Maskless Method

The LIMAP system is now commercialized under the name PRIMO by the company Alveole (https://www.alveolelab.com). In this technology, the shape of the micropatterns can be changed on demand by loading binary or grayscale Tiff images in the dedicated Leonardo software. Then, light from an expanded 375 nm laser beam is projected on a digital micromirror device (DMD) whose individual positions are controlled by the computer to create the imposed micropattern (Fig. 1b). UV light is then reflected on a dichroic mirror placed in the filter turret of a microscope and passes through a 20X/0.75 N.A. S-Fluor objective before reaching the sample, allowing us to make patterns with a precision on the order of 1 μm (Fig. 1d).

For this protocol, we used 18-mm round clean coverslips that were first activated for 5 min in a plasma cleaner (Harrick Plasma), then placed for 1 h in a closed dish containing (3-aminopropyl)-triethoxysilane (Sigma-Aldrich). Then 150 μL of 5 kDa mPEG-SVA (Laysan Bio, Inc) dissolved at 100 mg/mL in carbonate buffer (10 mM, pH 8) was incubated for one hour on the coverslip. Coverslips were then rinsed with distilled water and dried with a nitrogen flow. A mix of 33 μL absolute ethanol and 3 μL PLPP gel (photo-initiator) was deposited in each coverslip, and let dry for 30 min at RT, resulting in the formation of a transparent photo-initiator gel in the wells. The micropatterns were created on these coverslips using the PRIMO device docked on an inverted microscope (Nikon TiE Eclipse). The micropatterns were projected by PRIMO at a UV dose between 10 and 50 mJ/mm^2. The combined action of UV and PLPP gel locally degraded the PEG anti-fouling coating by photo-scission [27].

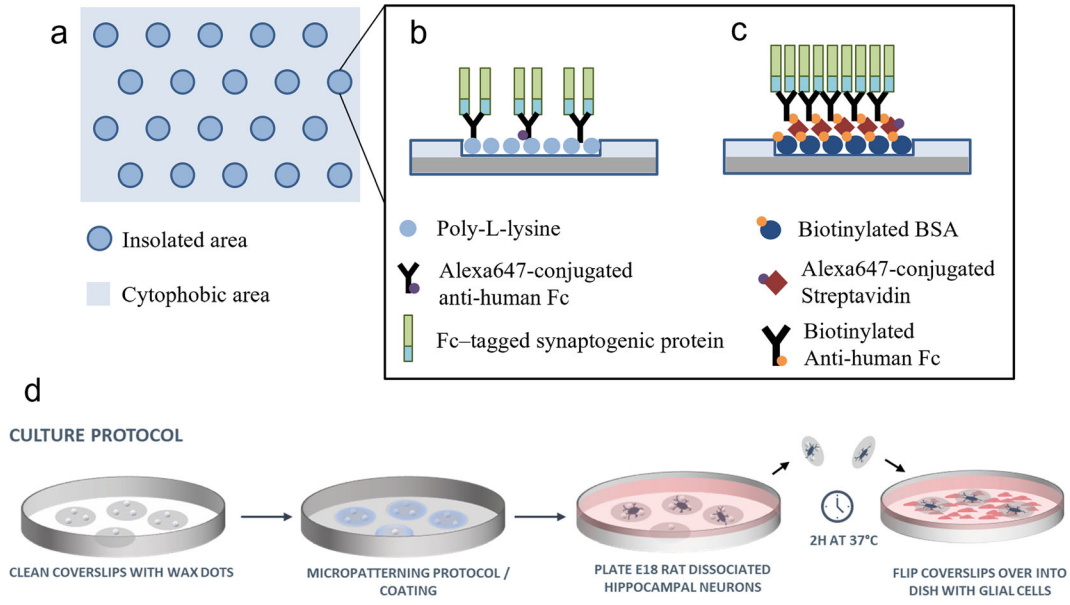

Fig. 2 Protein coating and neuron culture protocols on micropatterned substrates. (**a**) Schematic view of the micropattern geometry. Micropatterned substrates contain a hexagonal array of adhesive dots (1.5 μm) surrounded by a cytophobic PEG reagent (light blue). Two different coating protocols are used depending on the method to produce micropatterned substrates. (**b**) In the mask-based method, poly-L-lysine-coated dots are first coated with anti-human Fc antibodies conjugated to Alexa-647, then with either Fc-tagged Nrx1β or SynCAM1. (**c**) For the LIMAP method, the reactive dots are coated sequentially with biotinylated BSA, streptavidin Alexa-405 or -647, biotinylated anti-Fc antibody, then the Fc-tagged synaptogenic protein. (**d**) Illustration of the culture of dissociated rat hippocampal neurons on micropatterned substrates. In the method using a photomask, neurons were fed with conditioned medium harvested from parallel glial cell cultures, whereas in the LIMAP method, paraffin dots acting as spacers were stuck to the glass substrate, and coverslips were flipped onto a glial cell feeder layer, allowing for longer-term culture

3.3 Coating the Micropatterned Glass Substrates Prepared with the Photomask Method

1. Poly-L-lysine-coated micropatterned substrates made with the mask-based method are first incubated with goat anti-human Fc antibody at 0.023 mg/mL final concentration diluted in coating buffer (Fig. 2a, b). This secondary antibody layer ensures the proper orientation of the adhesive ectodomain of the protein (*see* **Note 4**). Importantly, a combination of unlabeled and Alexa-647 conjugated antibodies in a 9:1 ratio is used to allow for the fluorescent visualization of the micropatterns. Before incubation, the diluted antibodies are centrifuged for 10 min at 20,000× *g* and 4 °C to remove potential aggregates. To minimize antibody consumption, substrates are flipped onto a 160 μl drop of the antibody mixture on Parafilm (previously sterilized with UV for 1 h). The substrates are then incubated with the antibody mix at RT for 2–5 h.
2. The substrates are flipped into 6-well plates and carefully washed with coating buffer (*see* **Note 5**).

3. After washing, the substrates are incubated overnight at 4 °C with 160 µL purified Nrx1β-Fc to induce postsynaptic differentiation or with SynCAM1-Fc to promote presynaptic differentiation (both at 0.04 mg/mL in coating buffer; centrifuged for 10 min at 20,000× *g*, 4 °C) again on Parafilm covering 6-well plates (*see* **Notes 6** and **7**).
4. The second day, the substrates are placed into a new 6-well plate, washed three times with coating buffer and once with plating medium, and left for 1–2 h in the incubator (37 °C, 5% CO_2) in 2 mL plating medium containing 10% horse serum. Indeed, we found that the adsorption of serum proteins was important for neuronal development and could not be omitted.

3.4 Coating the Micropatterned Glass Substrates Prepared with the Maskless Method

For the LIMAP technique, we refined our initial strategy combining anti-Fc antibody and Fc-tagged proteins, and designed a robust and amplified chain of molecular interactions based on the biotin-streptavidin interaction to immobilize larger quantities of synaptogenic proteins on the micropatterns allowing for long term cultures (Fig. 2a, c).

1. After UV insolation, the gel of PLPP is rinsed with demineralized water and the coverslip is dried with airflow.
2. A film of poly-dimethyl-siloxane (PDMS, BISCO HT-6240, Rogers Corporation Carol Stream, IL, USA) with a 15 × 15 mm round hole in the middle was adjusted on each coverslip, thereby defining a central area for using a limited volume (100 µL) of proteins during incubation steps (*see* **Note 8**).
3. All proteins are solubilized in PBS, and three washes with PBS are made between each step. BSA-biotin (ThermoFisher Scientific, Pierce 29,130) 100 µg/mL for 3 min; Streptavidin-AlexaFluor 405 or AlexaFluor 647 (ThermoFisher Scientific S32351 and S21374, respectively) 50 µg/mL for 3 min; biotinylated goat anti-human Fc (Jackson Immunoresearch 109–065) 50 µg/mL for 10 min.
4. After washing, the substrates are incubated overnight at 4 °C with purified SynCAM1-Fc at 50 µg/mL.
5. The second day, the substrates are placed into a 60 mm dish, washed three times with PBS and once with conditioned medium, and left for 1–2 h in the incubator (37 °C, 5% CO_2).

3.5 Plating and Culturing Neurons on Micropatterned Substrates

Primary hippocampal neurons are prepared from embryonic day 18 (E18) Sprague-Dawley rats, as described previously [28].

1. Dissociated neurons are plated at a density of 100,000 cells/substrate (250 cells/mm^2 of coverslip) and are allowed to attach to the substrate for 2–4 h in plating medium.

2. 2–4 h after plating, the substrates are carefully washed with conditioned Neurobasal medium (culture medium), which was previously incubated for 4 days in dishes containing glial cell layer (*see* **Note 9**). The cells can be kept in this medium up to 10 days, however, a part of the medium needs to be replaced by new conditioned culture medium every 3–4 days.
3. On micropatterned substrates made with the LIMAP method, neurons could be kept for up to 21 days in vitro (DIV), yet with an alternative culture protocol. Three or four paraffin dots are deposited on the coverslips before contactless micropatterning; neurons are seeded on the substrates as described before. After neurons have adhered (around 2 h), the coverslips are flipped onto the glial cell layer (Fig. 2d). Here glial cells are sufficient to replenish the medium continuously. This alternative culture method also limits the shear stress on the neurons during medium replacement.
4. In order to induce postsynapse formation with Nrx1-β-Fc-coated micropatterns, neuroligin-1 (Nlg1), the heterophilic binding partner of Nrx1β needs to be overexpressed in neurons (*see* **Note 10**). To this aim, neurons are transfected 3 days after plating using Effectene, according to the manufacturer's instructions. 1 μg DNA per substrate is used for a single transfection, and 2 μg total DNA is used for co-transfections (e.g., HA-Nlg1 and PSD-95-GFP). Conditioned culture medium is used for the transfection procedure (*see* **Note 11**).
5. In the case of SynCAM1-Fc-coated substrates, the cells do not need to be transfected since endogenous SynCAM levels in neurons seem to be sufficient to induce presynaptic development [20]. This might be possible through the establishment of both homophilic and heterophilic interactions between various SynCAM isoforms [29].

3.6 Live Cell and Fixed Cell Image Acquisition

Micropatterned substrates are suitable for several types of optical microscopy observations, just as regular 170 μm-thick glass coverslips. In the following section, we will focus on some of the possible applications aiming at studying the dynamics and the structure of synapse formation and function.

3.6.1 Phase Contrast Imaging of Neurite Development on Micropatterned Substrates

In order to monitor the growth of neurons on micropatterned substrates or to investigate the effect of the adhesion molecule specifically bound to the patterns on neurite development, the substrates are kept in a compact 37 °C/CO_2 cell incubator and monitoring system (Nikon BioStation) after plating. This system provides consistent environmental control of temperature, humidity, and gas concentration in combination with live cell imaging (Fig. 3).

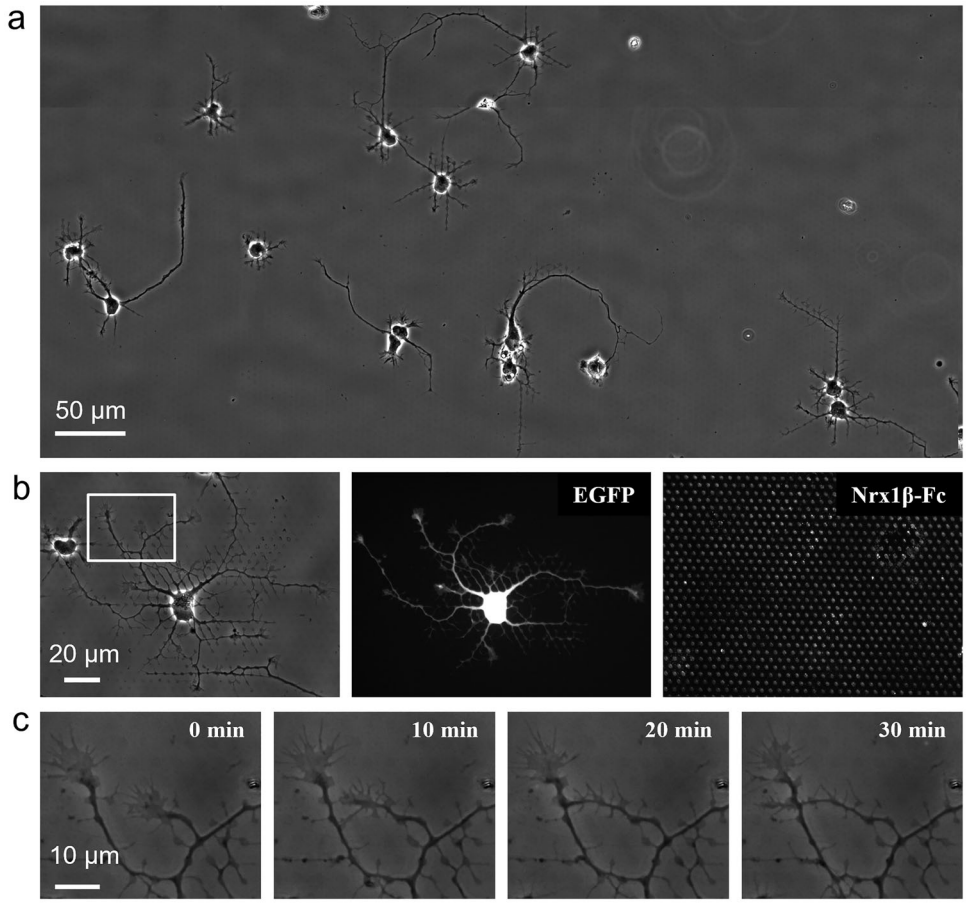

Fig. 3 Neurite growth of neurons cultured on Nrx1β-coated micropatterned substrates**.** (**a**) Phase contrast mosaic image of a neuronal culture growing on Nrx1β-Fc-coated micropatterned substrates for 3 days in vitro. (**b**) Phase contrast (left) and fluorescence image middle) of a neuron expressing GFP and HA-Nlg1, and the corresponding image showing the Nrx1β-Fc-coated micropattern (right). (**c**) Time-lapse images of neurite growth, taking the rectangular area highlighted in (**b**). Note the motion of leading dendritic growth cones along the dots

1. After neurons have fully attached to the substrate (i.e., 4–6 h after plating), the substrates are mounted in a chamber suitable for imaging.
2. The cultures are kept in the plating medium containing antibiotics (Penicillin-Streptomycin), since the sterility of the culture in an open chamber cannot be ensured.
3. Images are taken every 10 min to monitor the short-scale growth of neurites, while images taken every hour allow the observation of overall neurite elaboration over several days (Fig. 3b, c).

Studying the isolated role of specific interactions, like for example Nrx/Nlg adhesion, is also possible by electroporating the neurons with HA-Nlg1 before plating them on substrates coated with

Nrx1β-Fc. By co-expressing a fluorescent protein, such as eGFP, the growth of neurons overexpressing HA-Nlg1 can be selectively monitored by fluorescent imaging and the effect on neuronal development can be directly compared to non-expressing neurons from the same cultures (Fig. 3b).

3.6.2 Studying Postsynapse Assembly Using Nrx1β-Coated Micropatterns

In the following part, we describe an example protocol for investigating the development of excitatory postsynapses in neurons cultured on Nrx1β-Fc-coated micropatterned substrates prepared with the photomask method (Fig. 4a). Three days after plating neurons are transfected with HA-Nlg1, then fixed and immunostained 4 days later (Fig. 4b, c).

1. Cells are fixed in Fixation buffer at RT for 10 min, and carefully washed three times with PBS (*see* **Note 5**). To saturate the remaining active sites of the PFA, the culture is incubated for 15 min in Quenching buffer, followed by careful washing with PBS.
2. To label intracellular proteins, cultures are treated with permeabilization buffer for 5 min, followed by careful washing with PBS.
3. Non-specific binding is blocked by incubation with PBS containing 1% BSA, for 1 h.
4. Neurons are first incubated for 1 h with primary antibodies, including rat anti-HA to stain HA-Nlg1 and mouse anti-PSD-95 to stain the major scaffolding protein of excitatory synapses. Primary antibodies are diluted 1:400 in PBS containing 1% BSA (*see* **Note 12**).
5. After washing carefully with PBS containing 1% BSA, neurons are incubated for 1 h with secondary antibodies: anti-rat-FITC and anti-mouse-Rhodamine at a 1:800 dilution (*see* **Note 13**).
6. Neurons are washed carefully once with PBS containing 1% BSA, then at least three times with PBS.
7. Substrates are mounted on glass slides in approximately 20 μL Mowiol.
8. 16-bit images of the three fluorescence channels are acquired on an inverted epifluorescence microscope, equipped with the appropriate filter sets. A confocal laser scanning microscope can also be used here.

3.6.3 Single-Molecule Tracking of AMPA Receptors

Dynamic aspects of synapse organization, such as receptor diffusion, can also be studied by carrying out single-molecule tracking experiments in neurons cultured on micropatterned substrates prepared with the photomask method. As an example, we describe the protocol for tracking the lateral movement of endogenous AMPA receptors (AMPARs) in relation to Nrx/Nlg adhesions

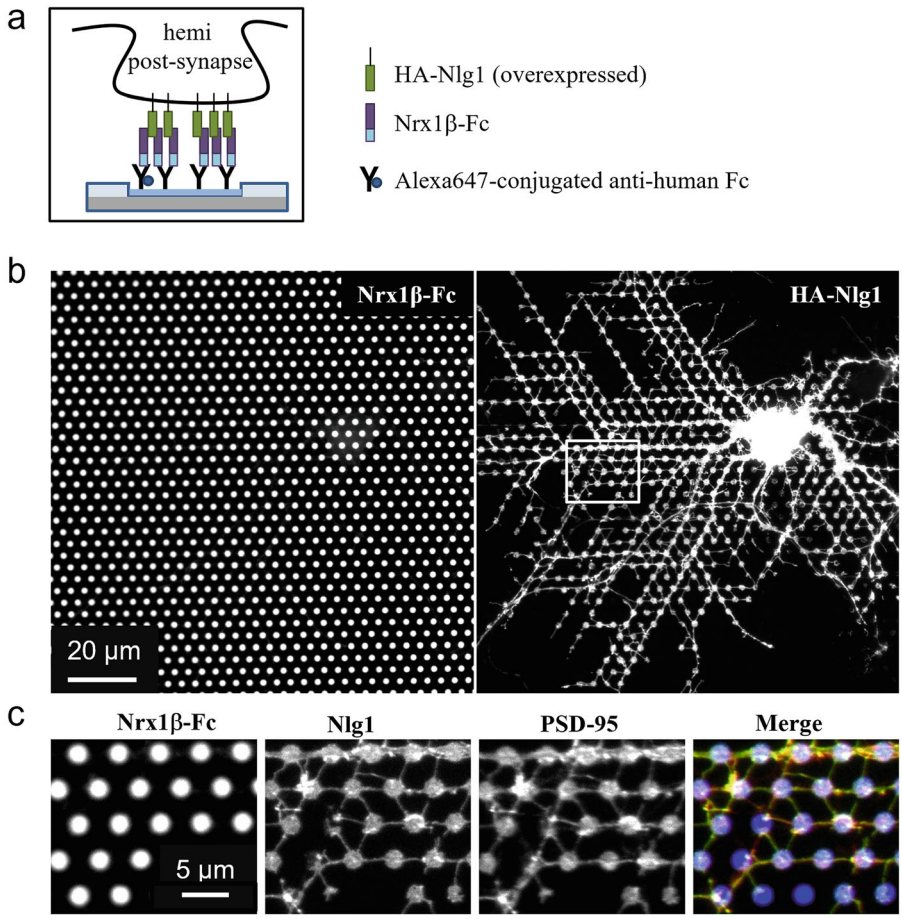

Fig. 4 Dendritic arborization and postsynaptic differentiation in neurons cultured on Nrx1β-Fc-coated micropatterned substrates. (**a**) Schematic view of the molecular interactions between Nlg1 in the dendritic membrane and a Nrx1β-Fc-coated dot, resulting in postsynapse development. (**b**) Neurons were plated on micropatterned substrates coated with Nrx1β-Fc, transfected with HA-Nlg1, and immunostained for anti-HA and endogenous PSD-95 at DIV 10. Note the development of a highly patterned dendritic arborization. (**c**) Insets from the rectangular area highlighted in (b) show the selective accumulation of Nlg1 (green) and PSD-95 (red) at Nrx1β-Fc-coated dots (blue)

(Fig. 5). In general, we incubate neurons with antibodies against the GluA2 subunit of AMPA receptors, which are conjugated to photostable fluorophores. We keep the antibodies in solution to allow for constant labeling, while imaging neurons in oblique illumination to focus on antibodies bound to the cell surface, as described previously [30, 31]. In this experiment, primary hippocampal neurons growing on Nrx1β -Fc-coated micropatterned substrates are transfected with HA-Nlg1 and Homer1c-GFP at days in vitro (DIV) 3–4, and used for single-molecule tracking experiments at DIV 7–8.

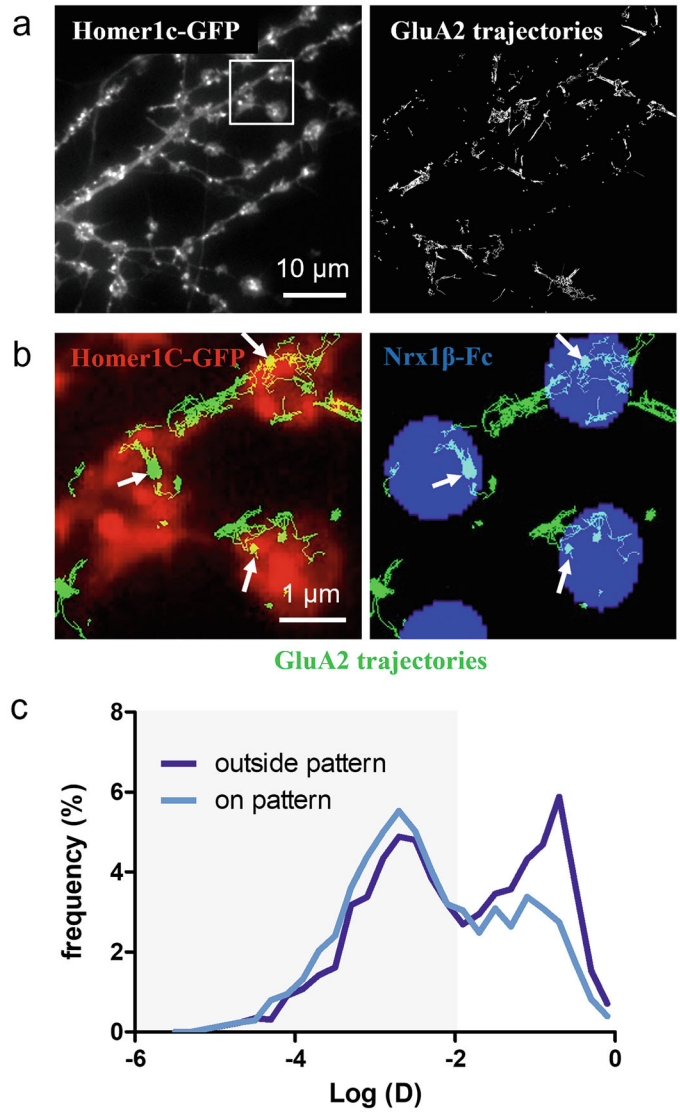

Fig. 5 Trapping of surface-diffusing AMPA receptors at Nrx1β-coated micropatterns. (**a**) Dendritic segment of a neuron co-transfected with HA-Nlg1 and Homer1C-GFP, cultured for 7 DIV on micropatterned substrates coated with Nrx1β-Fc (left). The diffusion of surface AMPARs was followed by stochastic labeling of GluA2 subunits, and trajectories of individual AMPARs were reconstructed based on recordings of 4000 consecutive images (right). (**b**) Enlarged region taken from (**a**) (white box) showing reconstructed trajectories of GluA2 diffusion (green). Note the immobilization of AMPARs when entering the region of dendrites (left) overlapping with the Nrx1β-Fc-coated dots (right), suggesting the trapping of AMPARs at postsynapses labeled by Homer-1c-GFP (arrows). (**c**) Graph showing the distribution of the diffusion coefficient (D) of single GluA2 trajectories in logarithmic scale, when computed inside or outside the micropatterns. The gray area represents slowly mobile AMPARs ($D < 10^{-2}$ µm^2/s), most likely trapped at hemi-synapses induced by Nrx1β-Fc-coated micropatterns, or at regular synapses outside micropatterns

1. The substrate is mounted in Tyrode solution in an open observation chamber and placed on an inverted microscope equipped with an EMCCD camera, a thermostatic box providing air at 37 °C, and an APO TIRF 100X/1.49 NA oil objective.
2. Antibodies against GluA2 subunit conjugated to ATTO 647 N are added directly in the chamber to the Tyrode solution at a 1:6000 dilution.
3. Samples are imaged using oblique illumination performed with the 633-nm line of a HeNe laser in order to allow the selective imaging of surface diffusing receptors.
4. Five stacks of 4000 consecutive frames are obtained per cell, with an integration time of 50 ms.
5. The diffusion coefficient of single AMPAR trajectories is computed as described in Subheading 3.7.2. Note the reduction in the mobile AMPAR pool ($D > 10^{-2}$ $\mu m^2/s$) and corresponding increase in the immobile pool ($D < 10^{-2}$ $\mu m^2/s$) on Nrx1β-Fc-coated micropatterns, reflecting the diffusional trapping of AMPARs at hemi postsynapses (Fig. 5c).

3.6.4 Studying Neurite Growth and Presynapse Differentiation Using SynCAM1-Coated Micropatterns

The protocol described above for Nrx1β-Nlg1 adhesion can be easily adapted to study different synapse types, e.g., based on N-cadherin adhesion [32], or to investigate presynaptic differentiation, for example by staining SynCAM1 and synapsin (presynaptic marker) in neurons cultured on SynCAM1-Fc-coated substrates prepared with the photomask method (Fig. 6a-c). Immunostaining reveals the accumulation of endogenous SynCAM1 on SynCAM1-Fc-coated dots, and presence of molecules such as synapsin in the assembled hemi-synapse, but does not give information about the functionality. One way to address whether the presynapses developed on SynCAM1-Fc-coated micropatterns are functional is to label the active synapses by antibody-feeding assay (Fig. 6d).

1. Cells are incubated for 10 min at 37 °C with anti-synaptotagmin lumenal domain conjugated to Oyster 550 fluorophore, diluted 1:200 in culture medium.
2. Cells are carefully washed with warm conditioned medium to remove the excess antibodies which were not taken up by active presynapses.
3. Labeling of active synapses can be either visualized directly under the microscope, by mounting the substrate in Tyrode solution into the open chamber, or it can be fixed and observed later, with the possibility to immunostain another protein in parallel.

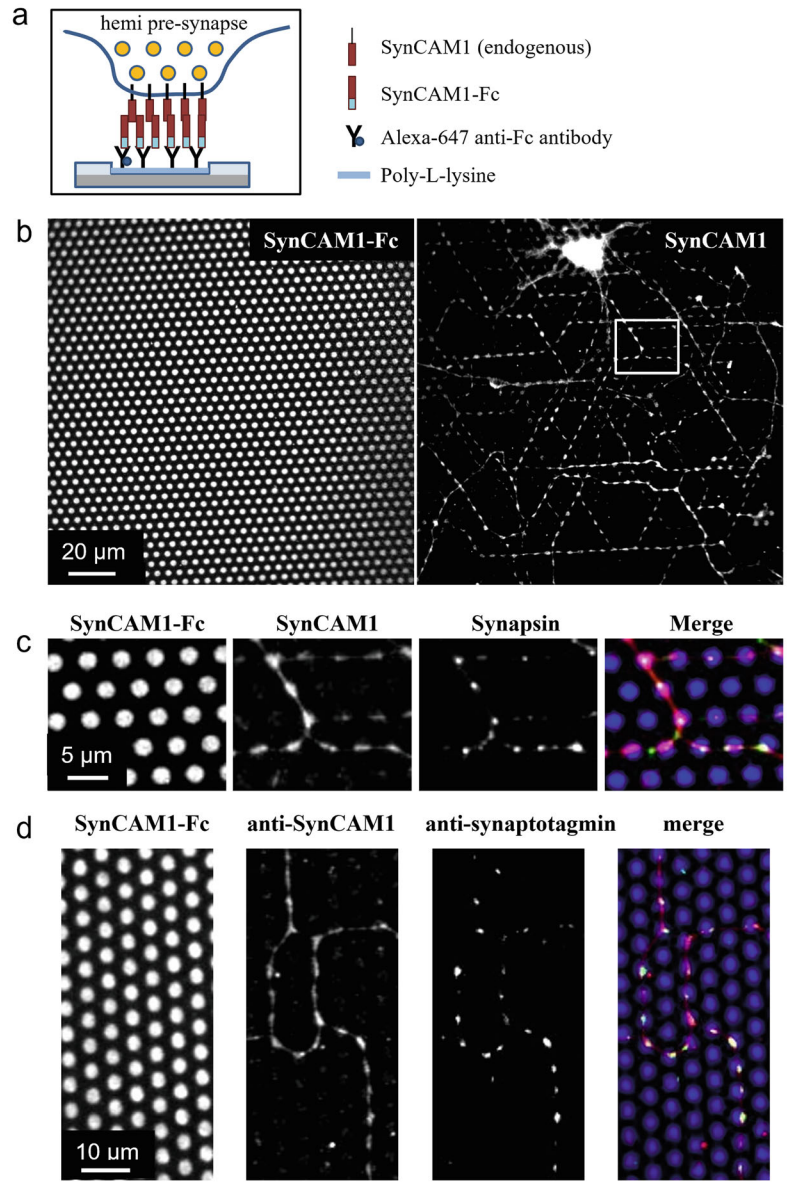

Fig. 6 Axonal arborization and presynaptic differentiation in neurons cultured on SynCAM1-Fc-coated micropatterns. (**a**) Schematic view of the molecular interactions between endogenous SynCAM1 in the axonal membrane axons and a SynCAM1-Fc-coated dot, resulting in presynapse formation. (**b**) Neurons were plated on micropatterned substrates coated with SynCAM1-Fc (left), and immunostained for endogenous SynCAM1 (right) and synapsin at DIV 10. Note the development of a highly patterned axonal network. (**c**) Insets show the selective accumulation of SynCAM1 (red) and synapsin (green) at SynCAM1-Fc-coated dots (blue). (**d**) Live labeling with antibodies to the synaptotagmin lumenal domain indicates the location of active synapses. Cells were immunostained for endogenous SynCAM1 after fixation. Note the strong accumulation of endogenous SynCAM1 (red) and synaptotagmin (green) at the dots (blue)

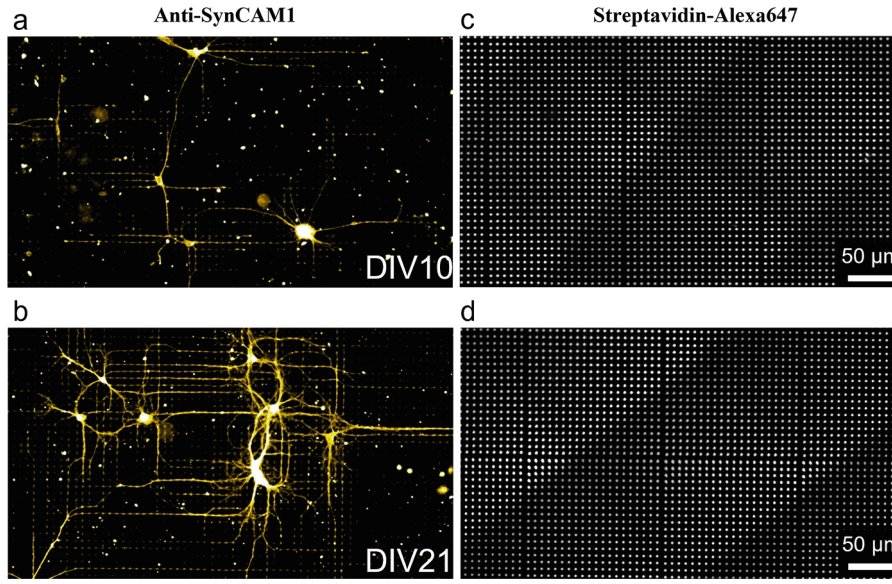

Fig. 7 Long-term cultures of neurons of SynCAM1-Fc-coated substrates. (**a, b**) Neuronal development on micropatterned substrates produced with the LIMAP method and coated with SynCAM1-Fc, at two different ages (DIV 10 and 21, respectively). Neurons were immunostained for endogenous SynCAM1. Note that neurites follow the imposed micropatterns. (**c, d**) Corresponding images showing the micropatterned dots (5 µm separated by 10 µm), based on the streptavidin-Alexa647 fluorescence

The combination of the LIMAP protocol with high protein coating density, and the use of paraffin spacers to allow a close contact between neurons and astrocytes, allows for the long-term culture of neurons on micropatterned substrates. As with the substrates made with the photomask method, neurons also exhibit patterned neurite arborization guided by SynCAM1-Fc-coated micropatterns on substrates prepared with the maskless method (Fig. 7). However, we have not tested yet if there is presynaptic differentiation on SynCAM1-Fc-coated dots in these specific coating and culture conditions.

3.7 Image Analysis

3.7.1 Quantification of Synaptic Protein Accumulation at Micropatterns in Fixed Samples

We developed two independent criteria to measure the recruitment of synaptic proteins at micropatterns. The first procedure relies on quantifying an enrichment index measuring the ratio between fluorescence intensities of a given protein at micropatterns, compared to nearby regions on the same neurite segment. It was written as a program in Metamorph (Molecular Devices), but could be written in any other image analysis software. The second procedure quantifies the degree of colocalization of synaptic clusters with micropatterns, and uses a custom program developed as a plugin for Image J (NIH) [19]. Both programs are available upon request.

Enrichment of Synaptic Proteins at Micropatterns

The first technique is described for neurons growing on Nrx1-β-Fc-coated micropatterns and immunostained for Nlg1 and PSD-95, but this protocol can be equally applied to any other synaptic protein. Here are the basic steps:

1. The potential background in the Nlg1, PSD-95, and micropattern images is subtracted.
2. A dendritic region is selected on the fluorescent image of Nlg1 staining and the corresponding area is also selected on the images highlighting the PSD-95 staining and the micropatterns.
3. The neurite outline is determined using the threshold function on the Nlg1 image.
4. A threshold is also applied to the image of the micropatterns, yielding the outlines as individual regions, which are then transferred to the Nlg1 and PSD-95 images.
5. Only micropatterns which overlap with the neurite area above threshold are used for further quantification, while patterns outside the neuron are eliminated.
6. The fluorescence intensity within each pattern for the area above threshold is determined on both Nlg1 and PSD-95 stained images, as well as the average fluorescence of the neuronal regions located outside the patterns.
7. An enrichment index is calculated by dividing the fluorescent intensities measured in neurite parts on the patterns by the average intensity measured from dendritic parts located outside patterns.
8. This procedure is repeated for three randomly chosen dendritic areas of each neuron, and values are averaged for each neuron. 10–20 neurons are quantified per condition. Enrichment factors above 1.2 are usually considered significant, and can go up to 1.8 or 2 in the case of very strong recruitments.

Apposition of Synaptic Clusters with Micropatterns

The second procedure is explained for the localization of synapsin or PSD-95 clusters at SynCAM-Fc-coated micropatterns.

1. Synapsin or PSD-95 signals of axonal or dendritic segments, respectively, and Alexa-647 signals corresponding to micropatterns are separately segmented using a wavelet-analysis program [33].
2. The segmented images of synapsin or PSD-95 staining are overlaid with the segmented image of the micropattern.
3. The overlapping area of synaptic and micropattern signals is then calculated on the overlaid image, and the percentage of synapsin or PSD-95 signal overlapping more than 50% with a micropattern is determined and averaged on a per cell basis.

4. The value for a random distribution of puncta is calculated as the fractional area of micropatterns occupying the field of view, i.e., around 35%. Values well above this threshold are considered as significant.

3.7.2 Computation of AMPA Receptor Diffusion Coefficients from Single-Molecule Trajectories

Detection of single AMPARs in the 4000-image stacks is performed using an algorithm based on image wavelet segmentation and single particle centroid determination, written as a program running in the Metamorph® software (Molecular Devices), called PALM-Tracer and described earlier [34, 35]. This program allows the identification of each molecule as an individual object, and connects successive positions within a certain diffusion distance (typically 2 pixels of 160 nm). The instantaneous diffusion coefficient, D, is calculated for each trajectory, from linear fits of the first four points of the mean square displacement (MSD) function versus time. The diffusion coefficient is then plotted on a logarithmic scale and allows the comparison of various biological conditions or compartments, such as here the dendritic regions inside or outside Nrx1β-Fc-coated micropatterns. Values of D smaller than 10^{-2} $\mu m^2/s$ typically reflect the trapping of AMPARs at postsynapses [31, 36].

3.8 Future Perspectives Offered by the LIMAP Method

The LIMAP protocol offers two significant improvements compared to the method relying on the use of a photomask. First, it allows for a local control of the density of proteins that are coated on the micropatterns. Indeed, the 255 gray levels of the TIFF images loaded in the Leonardo software are computed into relative UV doses (Fig. 8a), thereby allowing for a local control of the patterning intensity and protein quantity (Fig. 8b, c). This property can be used for instance to investigate the relationship between the density of ligands grafted on the adhesive dots and the corresponding accumulation of counter-receptors expressed in the membrane of the cells that grow on micropatterned substrates, as well as the recruitment of pre- and postsynaptic scaffolding proteins associated with the functional assembly of synapses.

The second improvement of the LIMAP method is the possibility of multi-protein patterning. In fact, by repeating the patterning protocol sequentially, this system allows for several proteins to be micropatterned at different locations on the same substrates [27]. This property can be exploited for instance to spatially segregate neurite adhesion from synapse development. We show here an example of micropatterned substrates containing lines coated with laminin intended to promote neurite outgrowth, and dots coated with streptavidin (followed by biotinylated anti-Fc antibodies and SynCAM1-Fc) intended to induce hemi-synapses (Fig. 8d, e). A neuron cultured on this type of substrate and labeled for MAP-2 is shown (Fig. 8f).

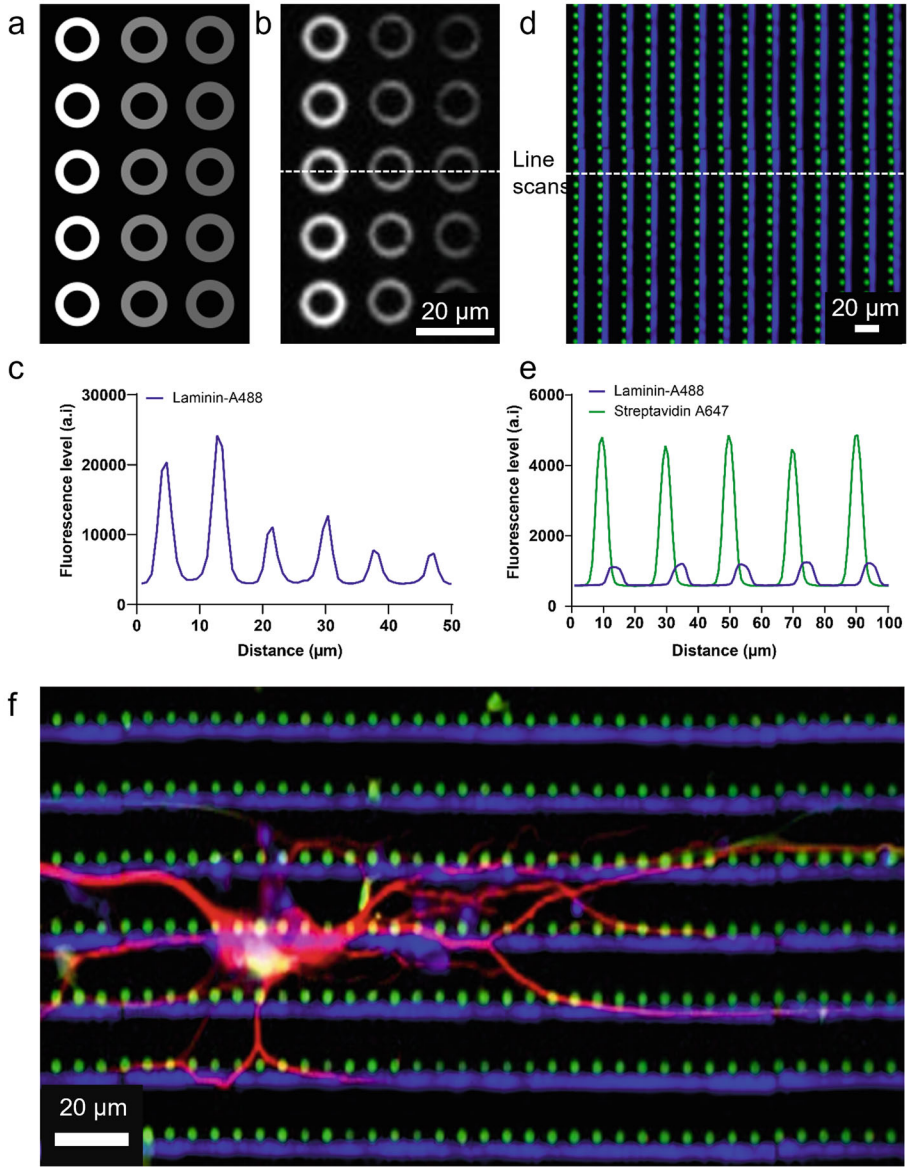

Fig. 8 Control of protein density and dual-protein photopatterning using LIMAP. (**a**) Examples of doughnut geometries (Tiff image) entered in the software. (**b**) Resulting micropatterns filled with Alexa488-conjugated laminin. (**c**) Graph showing the fluorescence intensity line scan through the doughnuts of different intensities. (**d**) Dual micropatterns made sequentially with Alexa647 conjugated streptavidin (green dots) and Alexa488-conjugated laminin (blue lines), later coated with biotinylated anti-Fc antibody and SynCAM1-Fc. (**e**) Graph showing the fluorescence intensity levels for laminin-Alexa488 (blue) and streptavidin-Alexa647 (green) across a horizontal line scan made through the micropatterns. (**f**) Example of a DIV 14 neuron growing on this dual-micropatterned substrate and immunostained for MAP2 (red)

4 Notes

1. The photomask-based production of micropatterns used in this assay can be implemented in the laboratory, according to the protocol described previously [26], but it remains challenging, especially when micropatterns reach length scales of the order of a micron. In particular, the establishment of a tight contact between the photomask and the glass substrates can be difficult and may result in non-reproducible patterns. The other difficulty is that holes in the photomask can gradually get clogged, resulting in non-patterned areas on the substrates. Extensive washing of the photomask is then required, or even its replacement by a new (and thus expensive) mask. On the other hand, as compared to photomask-based technologies where UV light is sent at once throughout the whole sample (i.e., a large coverslip of 10 × 10 cm, later cut into smaller pieces of 20 × 20 mm), one limitation of the LIMAP method is the efficiency. Indeed, the substrate insolation is done by projecting UV light in a mosaic of adjacent fields through a microscope objective, and can be quite time-consuming. For example, it takes approximately 5 min to micropattern a typical area of 5 × 5 mm.
2. Other "soft lithographic" methods can be used to produce micropatterned substrates compatible with high-resolution live cell imaging, and with similar geometries as ours. These include printing of adhesion proteins on silanized glass coverslips using a microfabricated un-alterable master pattern such as an elastomeric stamp [37], or UV cross-linking [38]. Simpler and inexpensive techniques can be found, such as ink-jet printing methods, which consists in depositing microscopic adhesive droplets on a non-adhesive substrate such as one coated with polyethylene glycol, but the size resolution is usually poor (100–200 μm), although other studies report a few microns precision [39]. An alternative approach called micro-photopatterning used computer-controlled two-photon laser photo-ablation of an anti-adhesive poly-vinyl-alcohol film, giving access to many different types of geometries [40].
3. In the case when fabrication of the substrates is not conducted in sterile conditions, the substrates need to be sterilized before coating, for example by exposing them to a UV lamp (365 nm) for 40 min under a laminar flow hood.
4. Attempts to directly conjugate a Cy5 fluorophore by NHS chemistry to accessible lysine groups on the Nrx1β-Fc protein resulted in a loss of function of Nrx1β, losing the ability to bind neuroligin-1 on the cell surface. Using the same strategy,

SynCAM1-Fc conjugated to Cy5 showed reduced homophilic binding affinity compared to unconjugated SynCAM1-Fc. Hence the use of the antibody layer that binds the non-adhesive Fc part of the chimeric proteins.

5. It is very important to keep the substrates always wet, i.e., the liquid should never be completely removed from the substrates while washing. Because of the hydrophobic background, the dewetting of the surface generates strong forces which can lead to the disruption of the antibody layer on the substrate.
6. The recombinant proteins used for coating are classically produced and purified in the laboratory. However, one has to keep in mind that this procedure can take several months, because the production has to be made in heterologous HEK 293 T cells to provide the post-translational changes needed to preserve the adhesive function of the proteins. A detailed protocol explaining the procedure was described previously [24]. Alternatively, those chimeric proteins can be purchased commercially (R&D systems, refs. 5268-NX for human Nrx1β-Fc and 1459-S4 for SynCAM1-10His, respectively, Fc tagged SynCAM1 being discontinued).
7. Alternatively, the substrates can be incubated with the antibody overnight at 4 °C, and the next day with the adhesion protein for 2–4 h at RT.
8. Although both micropatterning methodologies are based on PEG degradation, the nature of the PEG coating and the photochemical reactions at work are different. In turn, the protein binding and the antifouling properties of the native PEG layer can be different. The major difference lies in the fact that neurons are able to adhere non-specifically outside the micropatterns with the photomask protocol, but less likely with the maskless LIMAP protocol where no poly-L-lysine was added. Indeed, some non-specific adhesion of axons to free poly-L-lysine on the micropatterns may itself participate in presynaptic differentiation [17].
9. Since the density of the culture is relatively low, it is very important to keep the neurons in conditioned medium obtained from glial cell cultures. Although the medium contains the Neuromix supplement, additional factors secreted by glial cells are essential for cell survival.
10. In our E18 rat hippocampal Banker cultures observed at DIV 7–15, the expression levels of endogenous Nlg1 seem fairly weak, as judged by the low level of surface staining obtained with Nrx1β-Fc, used in place of a good antibody against Nlg1 suitable for live cell labeling [24, 41]. These expression levels seem insufficient to mediate a strong recognition of Nrx1β-Fc

immobilized on micropatterns, and thereby postsynaptic differentiation. Another possibility is that the amount of Nrx1-β-Fc that is adsorbed to the secondary antibody layer is not high enough to bind enough endogenous Nlg1 and mediate synaptic differentiation. Thus, there seems to be a limiting amount of either exogenous Nrx1β-Fc or endogenous Nlg1 that prevents postsynaptic differentiation, whereas endogenous SynCAMs seem to be in sufficient amounts to mediate presynaptic differentiation.

11. Alternatively, neurons can be electroporated prior to plating, which will typically result in a lower expression level and a higher ratio of cells overexpressing the given protein.
12. In order to minimize the volume of antibodies used, substrates can be placed on Parafilm, so that a drop of 200 μL is sufficient to cover their surface.
13. When choosing secondary antibodies, it is important to avoid using the same fluorescent label which was used for visualizing the micropattern. In the given example, one also has to be careful to use secondary antibodies for rat and mouse primary antibodies which are specifically developed for minimal cross-reactivity between host species. Such antibodies are available at Jackson Immunoresearch Labs.

Acknowledgments

We thank P. Scheiffele, T. Biederer, and S. Okabe for the generous gift of plasmids; E. Gouaux for the gift of the anti-GluA2 antibody and M. Sainlos for its fluorescent conjugation; C. Breillat for initial work on SynCAM1-Fc; Y. Rufin at the biochemical facility of the Bordeaux Neurocampus (Bioprot) for the purification of Fc-tagged proteins, F. Neca, Z. Karatas, S. Benquet, and M. Munier for molecular biology; E. Verdier and N. Retailleau at the Cell culture facility of the Institute; R. Sterling and J. Gilardin for logistics; A. Azioune for help on coating protocols, J.B. Sibarita, A. Kechkar, and C. Butler for the gift of the PALM-Tracer single-molecule image analysis software; S. Lafosse and H. Delobel for the temporary loan of the Nikon BioStation.
This work received funding from the Fondation pour la Recherche Médicale ("Equipe FRM" DEQ20160334916), French Ministry of Research, Agence Nationale de la Recherche (grants "Synthe-Syn" ANR-17-CE16-0028-01), ERA-NET Neuron "Synpathy" (ANR-15-NEUR-0007-04), Investissements d'Avenir Labex BRAIN (ANR-10-LABX-43), and grants from the Conseil Régional de Nouvelle-Aquitaine.

References

1. Kurshan PT, Shen K (2019) Synaptogenic pathways. Curr Opin Neurobiol 57:156–162
2. Südhof TC (2017) Synaptic Neurexin complexes: a molecular code for the logic of neural circuits. Cell 171:745–769
3. Friedman HV, Bresler T, Garner CC et al (2000) Assembly of new individual excitatory synapses: time course and temporal order of synaptic molecule recruitment. Neuron 27: 57–69
4. Blanpied TA, Kerr JM, Ehlers MD (2008) Structural plasticity with preserved topology in the postsynaptic protein network. Proc Natl Acad Sci USA 105:12587–12592
5. Poulopoulos A, Aramuni G, Meyer G et al (2009) Neuroligin 2 drives postsynaptic assembly at perisomatic inhibitory synapses through gephyrin and collybistin. Neuron 63:628–642
6. Giannone G, Mondin M, Grillo-Bosch D et al (2013) Neurexin-1β binding to Neuroligin-1 triggers the preferential recruitment of PSD-95 versus Gephyrin through tyrosine phosphorylation of Neuroligin-1. Cell Rep 3:1996–2007
7. Letellier M, Szíber Z, Chamma I et al (2018) A unique intracellular tyrosine in neuroligin-1 regulates AMPA receptor recruitment during synapse differentiation and potentiation. Nat Commun 9:3979
8. Bemben MA, Shipman SL, Hirai T et al (2013) CaMKII phosphorylation of neuroligin-1 regulates excitatory synapses. Nat Neurosci 17: 56–64
9. Missler M, Südhof TC, Biederer T (2012) Synaptic cell adhesion. Cold Spring Harb Perspect Biol 4:a005694
10. Scheiffele P, Fan J, Choih J et al (2000) Neuroligin expressed in nonneuronal cells triggers presynaptic development in contacting axons. Cell 101:657–669
11. Graf ER, Zhang X, Jin SX et al (2004) Neurexins induce differentiation of GABA and glutamate postsynaptic specializations via neuroligins. Cell 119:1013–1026
12. Biederer T, Sara Y, Mozhayeva M et al (2002) SynCAM, a synaptic adhesion molecule that drives synapse assembly. Science 297:1525–1531
13. Ko J, Zhang C, Arac D et al (2009) Neuroligin-1 performs neurexin-dependent and neurexin-independent functions in synapse validation. EMBO J 28:3244–3255
14. Shi P, Scott MA, Ghosh B et al (2011) Synapse microarray identification of small molecules that enhance synaptogenesis. Nat Commun 2: 510
15. Dean C, Scholl FG, Choih J et al (2003) Neurexin mediates the assembly of presynaptic terminals. Nat Neurosci 6:708–716
16. Heine M, Thoumine O, Mondin M et al (2008) Activity-independent and subunit-specific recruitment of functional AMPA receptors at neurexin/neuroligin contacts. Proc Natl Acad Sci USA 105:20947–20952
17. Lucido AL, Sanchez FS, Thostrup P et al (2009) Rapid assembly of functional presynaptic boutons triggered by adhesive contacts. J Neurosci 29:12449–12466
18. Barrow SL, Constable JR, Clark E et al (2009) Neuroligin1: a cell adhesion molecule that recruits PSD-95 and NMDA receptors by distinct mechanisms during synaptogenesis. Neural Dev 4:17
19. Mondin M, Labrousse V, Hosy E et al (2011) Neurexin-neuroligin adhesions capture surface-diffusing AMPA receptors through PSD-95 scaffolds. J Neurosci 31:13500–13515
20. Czöndör K, Garcia M, Argento A et al (2013) Micropatterned substrates coated with neuronal adhesion molecules for high-content study of synapse formation. Nat Commun 4:2252
21. Linhoff MW, Laurén J, Cassidy RM et al (2009) An unbiased expression screen for synaptogenic proteins identifies the LRRTM protein family as synaptic organizers. Neuron 61:734–749
22. DeWit J, Sylwestrak E, O'Sullivan ML et al (2009) LRRTM2 interacts with Neurexin1 and regulates excitatory synapse formation. Neuron 64:799–806
23. Liouta K, Chabbert J, Benquet S et al (2021) Role of regulatory C-terminal motifs in synaptic confinement of LRRTM2. Biol Cell 113: 492–506
24. Mondin M, Tessier B, Thoumine O (2013) Assembly of synapses: biomimetic assays to control Neurexin/Neuroligin interactions at the neuronal surface. In: Current protocols in neuroscience. Wiley, Hoboken
25. Breillat C, Thoumine O, Choquet D (2007) Characterization of SynCAM surface trafficking using a SynCAM derived ligand with high homophilic binding affinity. Biochem Biophys Res Commun 359:655
26. Azioune A, Carpi N, Tseng Q et al (2010) Protein micropatterns. A direct printing protocol using deep UVs. Methods Cell Biol 97: 133–146
27. Strale P-O, Azioune A, Bugnicourt G et al (2016) Multiprotein printing by light-induced

molecular adsorption. Adv Mater 28:2024–2029

28. Kaech S, Banker G (2006) Culturing hippocampal neurons. Nat Protoc 1:2406–2415
29. Fogel AI, Akins MR, Krupp AJ et al (2007) SynCAMs organize synapses through heterophilic adhesion. J Neurosci 27:12516–12530
30. Giannone G, Hosy E, Levet F et al (2010) Dynamic superresolution imaging of endogenous proteins on living cells at ultra-high density. Biophys J 99:1303–1310
31. Nair D, Hosy E, Petersen JD et al (2013) Super-resolution imaging reveals that AMPA receptors inside synapses are dynamically organized in Nanodomains regulated by PSD95. J Neurosci 33:13204–13224
32. Chazeau A, Garcia M, Czöndör K et al (2015) Mechanical coupling between transsynaptic N-cadherin adhesions and actin flow stabilizes dendritic spines. Mol Biol Cell 26:859–873
33. Racine V, Hertzog A, Jouanneau J et al (2006) Multiple-target tracking of 3D fluorescent objects based on simulated annealing. In: 3rd IEEE international symposium on biomedical imaging, pp 1020–1023
34. Izeddin I, Boulanger J, Racine V et al (2012) Wavelet analysis for single molecule localization microscopy. Opt Express 20:2081–2095
35. Kechkar A, Nair D, Heilemann M et al (2013) Real-time analysis and visualization for single-molecule based super-resolution microscopy. PLoS One 8:e62918
36. Czöndör K, Mondin M, Garcia M et al (2012) Unified quantitative model of AMPA receptor trafficking at synapses. Proc Natl Acad Sci USA 109:3522–3527
37. Rozkiewicz DI, Kraan Y, Werten MWT et al (2006) Covalent microcontact printing of proteins for cell patterning. Chem – A Eur J 12: 6290–6297
38. Fink J, Théry M, Azioune A et al (2007) Comparative study and improvement of current cell micro-patterning techniques. Lab Chip 7:672–680
39. Sanjana NE, Fuller SB (2004) A fast flexible ink-jet printing method for patterning dissociated neurons in culture. J Neurosci Methods 136:151–163
40. Doyle AD, Wang FW, Matsumoto K et al (2009) One-dimensional topography underlies three-dimensional fi brillar cell migration. J Cell Biol 184:481–490
41. Chamma I, Letellier M, Butler C et al (2016) Mapping the dynamics and nanoscale organization of synaptic adhesion proteins using monomeric streptavidin. Nat Commun 7: 10773

Chapter 2

Generation of Glutamatergic Human Neurons from Induced Pluripotent Stem Cells

Filiz Sila Rizalar and Volker Haucke

Abstract

Generation of human induced pluripotent stem cells (iPSCs) provided a unique platform for human brain development studies, in vitro disease modeling, and therapeutic strategy development. Human stem cells can be rapidly and efficiently differentiated into several distinct subpopulations of brain cells. These stem cell-derived systems are gaining acceptance as a viable alternative in the neuroscience field as they can mimic interactions between various brain cells, and help recapitulate brain regions with specific functions. Here, we describe a method to generate functional, postmitotic, excitatory cortical-like neurons from iPSCs by expressing the NGN2 transgene from a stably integrated doxycycline-inducible promoter. These induced neurons (iNs) can be utilized to study the development and function of human cortical neurons. They also allow studying disease mechanisms by comparing normal and pathophysiological conditions and enable reliable screens for testing of therapeutic approaches.

Key words Stem cells, iPSCs, Human neurons, Differentiation, NGN2, Synapse

1 Introduction

Human induced pluripotent stem cells (iPSCs) are becoming an increasingly accepted alternative for modeling neuronal development and neurogenetic diseases since they recapitulate the formation of the developing nervous system, are amenable to genetic manipulation, and provide temporally unrestricted sampling.

Several methods have been developed to generate central nervous system neurons in vitro. These distinct methods can be employed depending on the research question as each method confers unique advantages and limitations. These approaches can be broadly categorized into two. The first group is based on the formation of isolated neural cassettes or neural progenitors, which spontaneously differentiate toward neurons under non-self-renewing conditions. These protocols eliminate growth factors such as FGF2 or EGF while additionally enhancing the speed of

Tolga Soykan and Alexandros Poulopoulos (eds.), *Synapse Development: Methods and Protocols*, Methods in Molecular Biology, vol. 2910, https://doi.org/10.1007/978-1-0716-4446-1_2,

differentiation or directing the neuronal differentiation toward specific neuronal subtypes by the use of small molecules [1, 2]. Two major limitations in this approach are the relatively long culturing of developing neurons (i.e., 60–90 days in vitro) to achieve the desired neuronal subtypes and the generation of mixed population of neurons and glia. The latter requires additional selection steps such as FACS sorting if pure mature neurons need to be obtained [3]. Alternatively, iPSCs can be directly stimulated into the neuronal lineage via neuronal lineage-specific transcription factors. This way, intermediate steps such as the formation of neural rosettes and neural progenitor cells can be skipped and the resulting differentiation protocol can be significantly shortened, i.e., to 16–30 days in vitro. Initially, three transcription factors (BRN2, ASCL1, and MYT1L) were transiently expressed to generate human induced neurons (iNs) [4]. Later it was shown that expression of a single neuronal transcription factor Neurogenin 2 (NGN2) alone was sufficient to generate excitatory cortical neurons [5]. Similarly, expression of ASCL2 and DLX2 transcription factors have been demonstrated to generate pure GABAergic iNs [6].

To avoid lentiviral overexpression of transcription factors to generate excitatory cortical iNs, the NGN2 transgene was later stably integrated under a doxycycline-inducible promoter into a safe-harbor locus in iPSCs [7]. The maturity and physiological activity of NGN2-containing iNs have been reported in several studies [7–11]. Here we provide a detailed step-by-step protocol for the generation of developing or mature glutamatergic iNs via expression of NGN2 (Fig. 1).

2 Materials

2.1 Buffers, Solutions, and Media

1. Coating solution: 400 µl Matrigel™ dissolved in 20 mL OPTI-MEM™.
2. PBS (phosphate-buffered saline): pH 7.4, without calcium, magnesium or Phenol Red.
3. Dissociation solution: 1X PBS with 0.5 M EDTA.
4. Astrocyte medium: Dulbecco's Modified Eagle's Medium (DMEM) with 4.5 g/l glucose (e.g., Gibco), 10% (v/v) Fetal bovine serum (heat-inactivated) 100 U/ml Penicillin, 0.1 mg/mL Streptomycin.
5. StemFlex medium: StemFlex™ Basal Medium (e.g., Thermo Fisher) containing 1X StemFlex™ supplement.
6. F12/N2 iN differentiation medium: 1X DMEM/F12 (Dulbecco's Modified Eagle Medium/Nutrient Mixture F-12, e.g., Thermo Fisher), 1X N2 supplement, 1X NEAA, 10 ng/mL

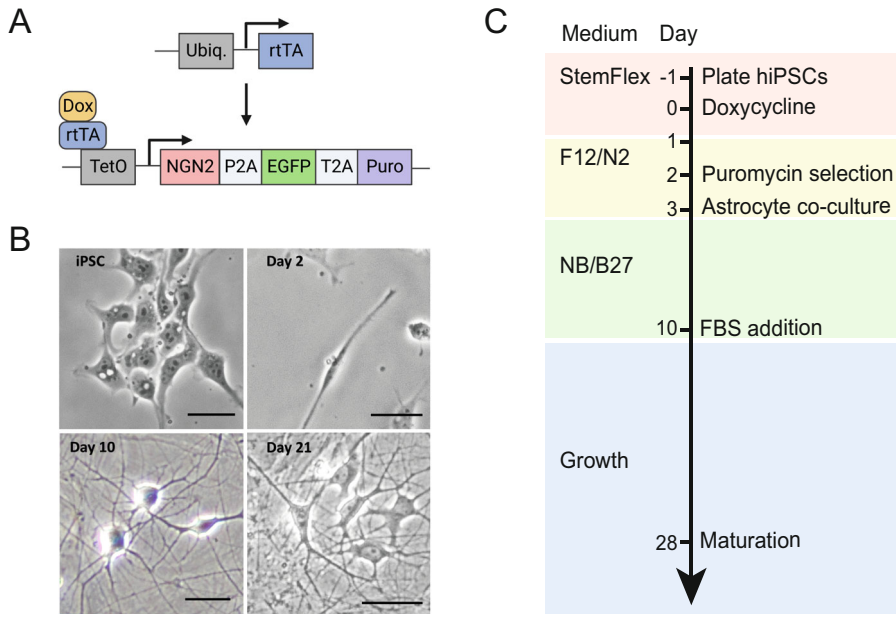

Fig. 1 Generation of excitatory cortical neurons from human iPSCs. (**a**) Expression constructs used for neuronal differentiation (adapted from [5]). Both cassettes are located at the safe-harbor locus of the human iPSC line. Doxycycline binds to rtTA and enables NGN2 transcription by activating the tetracycline response element (TetO). Upon initiation of neuronal differentiation, nuclear EGFP expression is used as a reporter of the activated NGN2 cassette. (**b**) Timeline for neuronal differentiation. Expression of the NGN2 cassette is activated at day 0 by doxycycline treatment. Astrocyte cultures are prepared from mouse cortices and added to the differentiating iNs at day 3 to support neuronal growth. (**c**) Brightfield images of human iPSCs and iPSC-derived iNs at day 2, 10, and 21 during neuronal differentiation. Scale bars, 50 μm

Human BDNF, 10 ng/mL Human NT-3, 0.2 μg/mL Mouse laminin, 2.5 μg/mL Doxycycline, 100 U/mL Penicillin, 0.1 mg/mL Streptomycin.

7. NB/B27 iN differentiation medium: 1X NBA (Neurobasal-A Medium, e.g., Gibco), 1X B27 supplement, 1X GlutaMAX™, 10 ng/mL Human BDNF, 10 ng/mL Human NT-3, 0.2 μg/mL Mouse laminin, 2.5 μg/mL Doxycycline, 100 U/mL Penicillin, 0.1 mg/mL Streptomycin.
8. Basic medium: 1X MEM (Minimum Essential Media), 5 g/l Glucose, 200 mL/l $NaHCO_3$, 100 mg/l Transferrin.
9. Growth medium for iNs: 1X Basic medium, 5% (v/v) FCS, 0.5 mM L-glutamine, 2% (v/v) B27-supplement, 50 U/ml Penicillin, 50 μg/mL Streptomycin.
10. Stem cell freezing media (serum-free) (e.g., Bambanker).
11. Accutase Cell Detachment Solution (e.g., Thermo Fisher).
12. Trypsin (0,25%) (e.g., Thermo Fisher).
13. HBSS (Hank's balanced salt solution): Without calcium, magnesium or Phenol Red.

2.2 Additional Reagents

1. ROCK inhibitor (Y-27632).
2. Dimethyl sulfoxide (DMSO) (≥99,5%, BioScience Grade, nuclease free).
3. Poly-L-Lysine (PLL) (e.g., Sigma P4832) (stock solution prepared by dissolving 5 mL PLL in 28 mL ddH_2O).
4. Cytosine arabinoside (AraC) stock (4 mM), 2000X.

2.3 Equipment

1. Falcon tubes (15 and 50 mL).
2. 1.5 mL centrifuge tubes.
3. Tubes for cryopreservation of cells.
4. 6-well, 10-cm and 3.5-cm tissue culture dishes.
5. Cell counter.
6. Surgical scissors, smooth fine forceps, flat tip forceps.
7. Freezing box, liquid nitrogen tank.
8. Centrifuge, incubator, laminar flow hood.
9. Stereomicroscope, brightfield and fluorescence microscope.

3 Methods

3.1 Human iPSC Culture

Feeder-free human iPSC lines, characterized as positive for the pluripotency markers OCT4, SOX2, NANOG, and SSEA4, are SNP karyotyped and tested for the absence of human pathogenic viruses (HIV, HBV, HCV) and can be used for this protocol. The differentiation protocol focuses on the use of an iPSC line containing a doxycycline-inducible NGN2-EGFP-Puromycin expression cassette in their genome at a safe harbor locus (Fig. 1).

Human iPSC cultures are maintained on plates coated with Matrigel in StemFlex medium at 37 °C in humidified atmosphere containing 5% CO_2. The iPSC medium StemFlex is changed every second or third day. All steps of the following procedure should be performed in a laminar flow hood using the standard sterile techniques.

1. Coat 6-well plates by adding 1.5 mL of Matrigel-containing coating solution per one well and incubating at 37 °C for 1 h. Amount of coating solution used can be adapted according to different sizes of culture plates (*see* **Note 1**).
2. Thawing of frozen iPSCs: Turn on the water bath at 37 °C and prepare 10 mL of StemFlex medium in a falcon tube at RT. Transfer the frozen cells rapidly to the water bath and incubate until there is a small amount of ice remaining. Then spray with ethanol and transfer the cryotube under the cell culture hood. Using a 5 mL serological pipette, slowly transfer the iPSCs into the falcon tube containing StemFlex medium

while slowly swirling the falcon tube. Centrifuge the cells at 200× *g* for 5 min at RT. Resuspend cell pellet in StemFlex supplemented with 5 μM Y-27632 to reduce apoptosis of single iPSCs after dissociation and plate cells on dishes coated with Matrigel.

3. For passaging, iPSCs should reach 80% confluency. There are two methods for passaging of iPSCs.
   (a) For regular passaging (twice a week), wash cells once with 1X PBS, aspirate the PBS and detach cells from the wells by adding 0.5 mL of dissociation solution (1X PBS containing 0.5 M EDTA) per one well of a 6-well plate and incubating the plate for 5 min at 37 °C. During the incubation time, the edges of iPSC colonies start to detach from the plates. After confirming the initiation of the detachment under a brightfield microscope, remove the dissociation solution, carefully resuspend cell clumps in StemFlex medium and transfer onto Matrigel-coated plates at a ratio of 1:4–1:10.
   (b) For single-cell seeding and counting, similarly wash cells with 1X PBS and dissociate iPSCs by incubating in 1 ml of Accutase Cell Detachment Solution for 5 min at 37 °C. Dilute single-cell suspension with 5 mL StemFlex medium and centrifuge at 200× *g* for 5 min at RT. Resuspend the cell pellet in StemFlex supplemented with 5 μM Y-27632. Count and seed the cells on Matrigel-coated plates.
4. Cryopreservation of iPSCs: Dissociate 80–90% confluent iPSCs using Accutase cell detachment solution as described in 4b. Resuspend cell pellet in 1 mL Bambanker freezing medium, and transfer to cryovials. Freeze cells at −80 °C in cryofreezing containers before transferring them to liquid nitrogen for long-term storage.

3.2 Initiation of Reprogramming of iPSCs

1. Day −1: Dissociate NGN2 cassette-containing iPSCs into single cells and plate on Matrigel-coated 6 wells (2×10^5 iPSCs/well) containing 2 ml StemFlex medium with 5 μM Y-27632. Alternatively, the NGN2 cassette can be delivered by overexpression (*see* **Note 2**).
2. Day 0: Initiate neuronal differentiation by changing the StemFlex medium to F12-N2 medium containing 2.5 μg/ml doxycycline to induce NGN2 expression.
3. Day 1: Exchange the medium once more to F12-N2 medium containing fresh doxycycline. On this day, the nuclear GFP signal in the differentiating cells containing the NGN2 cassette is visible under the fluorescence microscope.

4. Day 2: Change F12-N2 medium to fresh F12-N2 medium containing fresh doxycycline and supplemented with 10 μg/mL Puromycin to apply a negative selection and enrich for cells in which the NGN2 expression cassette has been successfully activated (*see* **Note 3**). Apply Puromycin selection for a minimum of 24 h although the selection can be extended up to 48 h, until no undifferentiated cells are observed in wells.

3.3 Isolation and Plating of Cortical Astrocytes

Astrocytes are prepared from mouse pups on post-natal day 1–3. On average 4 mouse pup cortices per 2 × 10 cm dish are used, therefore the volumes in the protocol are calculated for 4 pups.

1. Prewarm 30 mL astrocyte medium before starting the procedure.
2. Prepare surgical scissors, smooth fine forceps, flat tip forceps, paper towels, 2 × 3.5 cm dishes containing 2 mL of ice-cold HBSS and 70% ethanol.
3. Mouse is sacrificed by decapitation using the scissors. By using a midline incision along the scalp, reveal the skull.
4. Disconnect the cranium from the skull base by cutting the cranium carefully from neck to nose and introducing additional cuts at the anterior of the olfactory bulbs and at the inferior of the cerebellum.
5. Take out and place the brain into the dissecting dish containing HBSS by using forceps. Dish must be kept on ice until all brains are harvested.
6. After the brains are collected remove the olfactory bulbs and cerebellum using the fine dissecting forceps under a stereomicroscope.
7. Perform a midline incision between the hemispheres from the posterior side to anterior end. Then, keeping the posterior end attached by the forceps, insert a second set of forceps to the created grove. Finally, peel away the thin plate of the cortex structure from the brain.
8. Collect the cortices in the second dish in HBSS, cut into small pieces with scalpel and collect into a falcon tube.
9. Following removal of supernatant, wash the cortices three times with 5 mL cold HBSS. After the last wash, add 5 mL Trypsin (37 °C) and 10 μl DNase and incubate tissues at 37 °C for 15 min.
10. After trypsinization, wash the cortices again three times with 5 mL HBSS each. Resuspend the tissue in 2 mL astrocyte media containing 10 μl DNase.

11. Triturate the tissue first by using 1 ml pipette tips and then using glass Pasteur pipettes with narrowed pore size until no particles were observed.
12. Divide the material into two falcon tubes, each containing 10 mL of astrocyte medium, and centrifuge for 8 min at 200× *g* at 4 °C.
13. Resuspend cell pellets in 1 mL astrocyte medium and plate onto 10 cm dishes.
14. The day after plating, wash astrocytes with 1X PBS to remove debris and change medium to fresh DMEM containing 10% FBS and P/S.
15. Culture is confluent approximately 7 days after preparation.
16. Astrocytes can be passaged by washing with 1X PBS and incubating with 1 mL trypsin for 5 min (37 °C). After they are centrifuged for 5 min at 200× *g* at 4 °C, cells are resuspended and seeded on 10 cm plates containing 10 mL of astrocyte medium.
17. When astrocytes are passaged after the preparation, they can be stored in cryovials in liquid nitrogen for future use. Astrocytes are frozen in 10% DMSO in FBS and to reach maximum cell recovery, they should be thawed in Matrigel™ or PLL-coated plates.

3.4 Co-seeding of Human iNs and Mouse Astrocytes

On day 3, differentiating iNs were co-cultured with mouse astrocytes to support neuronal growth. Glia cultures prepared from P0/P1 mouse cortices and passaged at least one time after their preparation (*see* Subheading 3.2; *see* **Notes 3** and **4**) were used for co-culture.

1. Wash astrocytes with PBS and detach from the dish by 5-min incubation with 1.5 mL trypsin at 37 °C.
2. Centrifuge astrocytes at 200 g for 5 min, resuspend the pellet in 1 ml NB-B27 iN differentiation medium and count cells.
3. Wash iNs once with 1X PBS to remove dead cells and puromycin. Detach the cells by 3-min incubation with Accutase Cell Detachment Solution at 37 °C.
4. Following centrifugation at 200× *g* for 5 min, resuspend cell pellet in NB-B27 iN differentiation medium (max. 500 μl per 6 wells to achieve higher cell density) and count cells.
5. Seed iNs and mouse astrocytes in a 5:1 ratio, respectively. Of note, this ratio might be changed depending on the particular experiment and astrocytes could be completely omitted for experiments requiring iNs to develop no longer than 13 days (*see* **Note 5**).

6. Seed iN-astrocyte mix on Matrigel™-coated plates or coverslips. To achieve dense iN cultures, only the center of wells/coverslips should be coated with Matrigel™ and a total number of 80–150 x 10^3 cells should be seeded per coverslip in a 30–50 μl drop. When using this technique, plates are first incubated with cell drops at 37 °C for 1 h until iNs and astrocytes attach to coverslips, and then NB-B27 medium containing fresh doxycycline is added (2 mL per one well of a 6-well plate) (*see* **Note 6**).

3.5 Culturing of iNs until Maturity

After day 3, iN medium is only partially exchanged (see below).

1. Day 6: Remove half of the NB-B27 iN differentiation medium and add fresh NB-B27 medium containing fresh doxycycline.
2. Day 8: Repeat the same procedure as on day 6.
3. Day 10: Remove half of the NB-B27 medium and add Growth Medium containing FBS. After this point doxycycline is no longer added to the medium, and instead AraC is included to inhibit overgrowth of mitotic glial cells.
4. After day 10: Feed iN cultures only weekly, by removing 100 μl of the old media and adding 150 μl of fresh growth media for 6-well coverslips. Mature neurons are harvested after day 28.

4 Notes

1. Matrigel™ is stored at −20 °C and is liquidized at 0 °C. If it remains longer at room temperature (RT) it acquires a gel form and its solubility in OPTI-MEM™ decreases. Thus, it should be carefully thawed and immediately mixed with OPTI-MEM™. After coating, Matrigel™ solution can be re-collected and kept at 4 °C for later use. Similarly, previously coated plates can also be sealed with Parafilm and stored at 4 °C for weeks.
2. In case that the iPSC line to be differentiated into neurons does not contain the NGN2 differentiation cassette in its genome, the cassette must be administered to iPSCs by lentiviral delivery of the NGN2 and rtTA cassettes 6 h post-seeding. iPS cells should then be incubated with the lentivirus overnight. An additional EGFP-expression cassette may be delivered as a fluorescent reporter. Several studies in which iPSCs were generated from patient cells have opted for this approach as genetic reprogramming of iPSCs for more than one round might pose challenges with respect to pluripotency and/or viability.
3. Puromycin selection is essential for obtaining a clean iN-astrocyte co-culture. If omitted, stem cells which have not activated their differentiation cassette will remain as contaminants, divide, and eventually dominate the culture. The ideal

puromycin concentration may vary depending on cell line and should be determined in an initial experiment, in which different concentrations of Puromycin are applied to day iNs on day 2 post-differentiation for 48 h.

4. To be co-cultured with human iNs, mouse astrocytes have to be passaged at least once to make sure there are no residual mouse neurons contaminating the human neuron preparation. Astrocytes from postnatal days 1 (P1) until 3 can be used for co-seeding. It is not recommended to use astrocytes older than P3 as after this stage cell division becomes progressively slower. Importantly, the number of astrocytes required for a co-seeding experiment is limited and is significantly less than the number of iNs (approximately only 1/5 ratio). However, when astrocytes are isolated from mouse cortex the starting material should be sufficient to achieve proper astrocyte density. In order to make use of all astrocytes that are isolated and plated, cultured cells can be split at a comparably lower density (i.e., 1:10) such that several plates containing P1 astrocytes can be stored frozen for future experiments.
5. Although human iNs develop and mature (e.g., formation of functional synapses) most efficiently when mouse astrocytes are added, it is possible to culture iNs in the absence of astrocytes. The limiting factor here is the duration of culturing. In our hands, iNs can be cultured without astrocytes for up to 15 days in vitro without observing detachment from coverslips or cell death. Depending on the scope and duration of the experiments astrocyte-iN co-culturing may thus be omitted from the protocol.
6. As an alternative to using mouse primary astrocytes, iNs can also be co-seeded with commercially available human iPSC-derived astrocytes [12–14]. In this case, astrocyte isolation and plating is discarded and only the co-seeding procedure is followed.

References

1. Koch P, Opitz T, Steinbeck JA et al (2009) A rosette-type, self-renewing human ES cell-derived neural stem cell with potential for in vitro instruction and synaptic integration. Proc Natl Acad Sci USA 106(9):3225–3230
2. Borghese L, Dolezalova D, Opitz T et al (2010) Inhibition of notch signaling in human embryonic stem cell-derived neural stem cells delays G1/S phase transition and accelerates neuronal differentiation in vitro and in vivo. Stem cells (Dayton, Ohio) 28(5): 955–964
3. Yuan SH, Martin J, Elia J et al (2011) Cell-surface marker signatures for the isolation of neural stem cells, glia and neurons derived from human pluripotent stem cells. PLoS One 6(3):e17540
4. Pang ZP, Yang N, Vierbuchen T et al (2011) Induction of human neuronal cells by defined transcription factors. Nature 476(7359): 220–223
5. Zhang Y, Pak C, Han Y et al (2013) Rapid single-step induction of functional neurons from human pluripotent stem cells. Neuron 78(5):785–798

6. Yang N, Chanda S, Marro S et al (2017) Generation of pure GABAergic neurons by transcription factor programming. Nat Methods 14(6):621–628
7. Wang C, Ward ME, Chen R et al (2017) Scalable production of iPSC-derived human neurons to identify tau-lowering compounds by high-content screening. Stem Cell Rep 9(4): 1221–1233
8. Yi F, Danko T, Botelho SC et al (2016) Autism-associated SHANK3 haploinsufficiency causes Ih channelopathy in human neurons. Science 352(6286):aaf2669
9. Nehme R, Zuccaro E, Ghosh SD et al (2018) Combining NGN2 programming with developmental patterning generates human excitatory neurons with NMDAR-mediated synaptic transmission. Cell Rep 23(8): 2509–2523
10. Rizalar FS, Lucht MT, Petzoldt A, Kong S, Sun J, Vines JH, Telugu NS, Diecke S, Kaas T, Bullmann T, Schmied C, Loewe D, King JS, Cho W, Hallermann S, Puchkov D, Sigrist SJ, Haucke V (2023) Phosphatidylinositol 3,5-bisphosphate facilitates axonal vesicle transport and presynapse assembly. Science 382:223–230
11. Steinke S, Kirmann T, Nerlich J et al (2022) NMDA-receptor-Fc-fusion constructs neutralize anti-NMDA receptor antibodies. bioRxiv:2022.04.29.490085
12. Canals I, Ginisty A, Quist E et al (2018) Rapid and efficient induction of functional astrocytes from human pluripotent stem cells. Nat Methods 15(9):693–696
13. Li X, Tao Y, Bradley R et al (2018) Fast generation of functional subtype astrocytes from human pluripotent stem cells. Stem Cell Rep 11(4):998–1008
14. Tchieu J, Calder EL, Guttikonda SR et al (2019) NFIA is a gliogenic switch enabling rapid derivation of functional human astrocytes from pluripotent stem cells. Nat Biotechnol 37(3):267–275

Chapter 3

Generation of Prefrontal Cortex Neurons from Human Pluripotent Stem Cells Under Chemically Defined Conditions

Gustav Y. Cederquist, Polina Oberst, Xuyao Chang, Jason Tchieu, and Lorenz Studer

Abstract

Human pluripotent stem cells (hPSCs) have the potential to differentiate into all human somatic cell types allowing for an experimental platform to access otherwise inaccessible tissues through directed differentiation protocols. Access to tissue is especially critical for neurobiology where functional human tissue is rare. The prefrontal cortex is an evolutionarily expanded addition to the cerebral cortex, associated with higher order cognitive function. Here, we present a method to generate neural progenitors and post-mitotic neurons with a prefrontal cortical identity through the directed differentiation of hPSCs under defined conditions. Neural induction is achieved by inhibiting TGF beta and BMP signaling (termed dual-SMAD inhibition) and neural progenitors are subsequently patterned toward the prefrontal cortex lineage using recombinant FGF8. Cells generated using this protocol open possibilities to study the unique developmental and synaptic properties of the prefrontal cortex, as well as to understand its selective vulnerability in a number of human brain disorders.

Key words Human pluripotent stem cells, Prefrontal cortex, Directed differentiation, Human disease modeling, Neurodevelopment

1 Introduction

Human pluripotent stem cells (hPSCs) are derived from the inner cell mass of the blastocyst and have the developmental potential to differentiate into all human somatic cell types [1]. Work over the past few decades has elucidated the key signaling events during early development that can be co-opted to direct hPSC differentiation along specific developmental lineages. Regarding neural development, early studies in Xenopus showed that inhibition of BMP signaling is critical for dorsal specification and neural induction [2, 3]. Capitalizing on these early observations, Chambers et al. devised a highly efficient method for neural induction of hPSC cultures via chemical inhibition of two SMAD pathways

Tolga Soykan and Alexandros Poulopoulos (eds.), *Synapse Development: Methods and Protocols*, Methods in Molecular Biology, vol. 2910, https://doi.org/10.1007/978-1-0716-4446-1_3,

(dual-SMAD inhibition), downstream of BMP and TGFb signaling [4]. The original method uses a small molecule, SB431542, as a TGFb inhibitor and recombinant noggin as a BMP inhibitor, but it was later shown that the LDN193189 compound could substitute for noggin, resulting in highly efficient and consistent neural induction [5]. Dual-SMAD inhibition is now the backbone of many neural-directed differentiation protocols such as cortical neurons [6], subcortical interneurons [7], spinal motor neurons [8], and sensory neurons [5].

However, within each of the aforementioned broad cell types lies even more fine-grained specializations. Glutamatergic cortical neurons, which arise from the dorsal pallial progenitors [9, 10], are parcellated into functional areas that underlie specific behaviors such as movement, vision, and hearing. These behaviors map to spatially distinct and reproducible areas known as the motor cortex, the visual cortex, and the auditory cortex. Cortical arealization is specified by the concerted activity of key morphogenetic gradients including FGFs, BMPs, and WNTs [11]. Morphogenetic gradients impose a cartesian coordinate system onto dorsal pallial progenitors, whereby a progenitor interprets its position in the coordinate system, and hence future function, by reading the local concentration of morphogens. This principle is elegantly demonstrated by the diffusible factor FGF8, which is released from the anterior neural ridge and is required for frontal cortex patterning. Ectopic expression FGF8 from outside the anterior neural ridge duplicates the area map [12]. Thus, FGF8 acts as a classic organizer and specifies frontal cortex identity.

The human frontal cortex and prefrontal cortex exhibit unique developmental and functional features and are selectively vulnerable to disease. As an example of the unique neurophysiology in the prefrontal cortex, synaptic spines in this area maintain their dynamic exuberance and pruning behavior well into adulthood, suggesting a protracted phase of synaptic plasticity in this region [13]. In addition, the anterior cingulate and fronto-insular cortex exclusively house a specific cell type known as Von Economo neurons, which are large bipolar spindle-shaped cells found in layer Vb of humans and other primates [14]. Abnormalities in prefrontal cortex development and function have been associated with autism [15], as well as a number of neuropsychiatric disorders [16]. In addition, the frontal cortex selectively degenerates in a form of dementia known as fronto-temporal dementia. Thus, a hPSC-directed differentiation protocol to generate this area serves as an important experimental reagent. Here we present a facile method for generating prefrontal cortex neural progenitors and neurons from hPSCs using chemically defined media conditions (Fig. 1). In brief, neural induction of an hPSC monolayer is achieved using dual-SMAD inhibition in minimal media. Subsequently, neural progenitors are plated at high density to induce rosette formation and patterned toward prefrontal cortical identity using

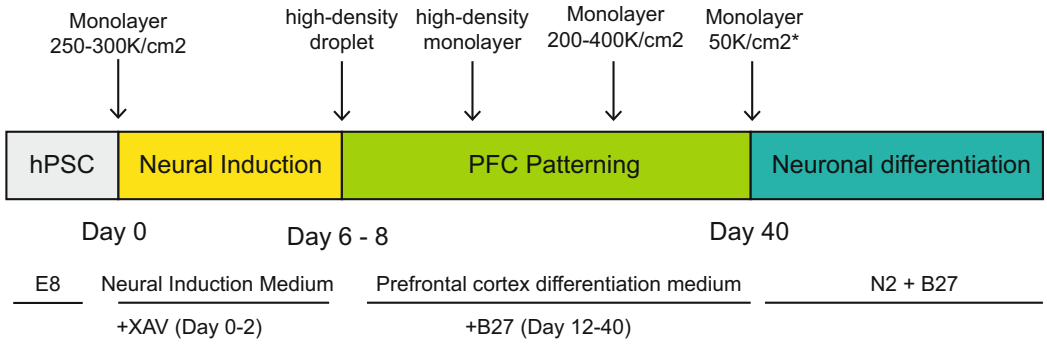

Fig. 1 Schematic of differentiation. Colored boxes indicate major phases of differentiation protocol, with timing indicated. Down arrows represent passages. Media is listed on the bottom row

recombinant FGF8. Finally, neural progenitors are passaged to low density to induce neuronal post-mitotic differentiation. Prefrontal cortex neurons generated using this protocol have a variety of downstream applications including the study of lineage development, neurodevelopmental disorders, and drug screening. Future iterations of prefrontal cortex differentiation protocols may aim to generate even more specific functional subdivisions [17, 18] or later maturation stages.

2 Materials

All tissue culture work should be done in a dedicated and sterile tissue culture fume hood, using sterile technique. Always aliquot stock reagents and store at appropriate temperatures. Once aliquots are removed from the freezer, they can be stored at 4 °C for up to 2 weeks. BSA/PBS diluent is filter sterilized**.** Add small molecules and growth factors from stock to solution on the day of use. Do not store small molecules and growth factors at working concentration.

2.1 General Tissue Culture Reagents

1. Dulbecco's Phosphate buffered saline: PBS without calcium and magnesium.
2. Bovine serum albumin (BSA).
3. 6-well tissue culture treated plates.
4. 10-cm tissue culture treated plates.
5. hPSC dissociation reagent: 0.5 M EDTA in DPBS, pH 8.0 (Thermo Fisher Scientific 15575020).
6. Vitronectin: 5 mg/mL in DPBS, diluted from 100x stock solution (Thermo Fisher Scientific A14700).

7. Dissociation reagent: Accutase® (Innovative Cell Technologies AT104–500).
8. Matrigel: (BD Biosciences 356234) (*see* **Note 1**).
9. Poly-L-Ornithine solution: stock solution is 15 mg/mL (Sigma Aldrich P3655) in 0.1% BSA/PBS. Dilute 1:1000 in DPBS to make working solution.
10. Laminin/Fibronectin solution: Stock solution of laminin is purchased (R&D 3400–010-1) and Stock solution of Fibronectin 1 mg/mL (Corning 356008) in 0.1% BSA/PBS. Dilute laminin 1:500 and Fibronectin 1:500 in DPBS to make working solution.
11. B27 without vitamin A 50x (Thermo Fisher Scientific 17504044).
12. Stem-Cellbanker (Amsbio 11890).

2.2 Media Recipes

1. E8 media (stem cell maintenance media): Thaw E8 supplement (10 mL) overnight at 4 °C or at room temperature (~30 min) and add to base media (500 mL) (Thermo Fisher Scientific A1517001).
2. Neural induction media: E6 base media purchased from the manufacturer (Thermo Fisher Scientific A1516401) with 100 nM LDN193189 and 10 μM SB431542 added.
3. Prefrontal cortex differentiation media: N2 media (1 L DMEM/F12, 1 mL 2-mercaptoethanol 1000x (Life Technologies # 21985–023), 2.0 g Sodium Bicarbonate (Sigma # S5761-1KG), 1.56 g D-(+)-Glucose (Sigma # G7021-1KG), 20ul 1 mM progesterone), 10 mL N2 supplement B (Stem Cell Technologies 07156), 10 mL of penicillin/streptomycin (100x). Add FGF8 fresh each day, at 1:1000 dilution to a final concentration of 50 ng/mL.

2.3 Small Molecules and Proteins

1. Y-27632 (ROCKi) 1000x stock solution: 10 mM in ultrapure ddH2O (R&D 1254).
2. SB431542 (SB) 1000x stock solution: 10 mM in 200 proof ethanol (R&D 1614).
3. LDN193189 (LDN) 5000x stock solution: 500 mM in DMSO (Stem Cell Technologies 72147).
4. XAV-939 (XAV) 5000x stock solution: 10 mM in DMSO (R&D 3748) (*see* **Note 2**).
5. Recombinant human FGF8 1000x stock solution: 50 mg/mL in 0.1% BSA/PBS (R&D 423-F8).
6. Recombinant human SHH stock solution: 10 mg/mL diluted in 0.1% BSA/PBS (R&D 1845-SH).

2.4 Antibodies for Validation

1. Rabbit Anti-PAX6 Biolegend 901301, RRID: AB_2565003.
2. Rabbit Anti-FOXG1 Clontech M227, RRID: AB_2827749.
3. Rabbit Anti-NKX2.1 Abcam ab76013, RRID: AB_1310784.
4. Rabbit Anti-SOX2 Biolegend 630802, RRID: AB_2195784.
5. Mouse Anti-COUPTF-1 [H8132] Abcam ab41858, RRID: AB_742210.
6. Goat Anti-SP8 Santa-Cruz sc-104661, RRID: AB_2194626.

2.5 Sequencing Primers for Validation

Dorsal Forebrain Validation

1. PAX6_F CAACACACCTAGTCATATTCCTATC.
2. PAX6_R CTGGGGACTGGGGGTTG.
3. DLX1_F ACTCACACAGACTCAGGTCAAGAT.
4. DLX1_R CGGATGAAGAGTTAGGGTTCCAGC.
5. TBR1_F GACTCAGTTCATCGCCGTCA.
6. TBR1_R CAGCCGGTGTAGATCGTGTC.
7. FOXG1_F CAACGGCATCTACGAGTTCA.
8. FOXG1_R TGTTGAGGGACAGATTGTGG.

Enriched in Prefrontal Cortex

9. CYP26A1_F TTTGAATTAAATGGATACCAGATTC.
10. CYP26A1_R TTCTTTGCCTACACAGCTCCT.
11. COL2A1_F ATTTCAGCTATGGAGATGACAATC.
12. COL2A1_R TGAACCTGCTATTGCCCTCT.
13. SPHK1_F TCCTTGAACCATTATGCTGGCTATG.
14. SPHK1_R TCTCCCCCAGACGCCGATAC.
15. ZIC1_F AGGACGCACACAGGGGAGAAG.
16. ZIC1_R AGGATTCGTGGACCTTCATG.
17. WNT3_F CACGACTATCCTGGACCA.
18. WNT3_R TGGGTGGCTTGAAGAGCG.
19. DPP7_F CGGGATTCGGAGGAACCTGAGTG.
20. DPP7_R GCTGGCTGCTGCTCACGC.
21. SOCS2_F AGACAGGATGGTACTGGGGAAGTATG.
22. SOCS2_R ATAGAGTCCAATCTGAATTTT.

Enriched in Occipital Cortex

23. COUPTF1_F AAGCGGTTCAGCGAGGAAGAATG.
24. COUPTF1_R GATGCCCATAATGTTGTTGG.
25. FGFR3_F CGCAAGGCTGTCCTCAGG.

26. FGFR3_R TCAGTGGCATCGTCTTTCA.
27. UNC5A_F CTATCCATCCACGATGTGCCCAG.
28. UNC5A_R CAAACCTTGTGTCCTTGGTGATGTT.
29. EPHA3_F AAGGAGTTGTTACCAAAAGTAAG.
30. EPHA3_R TTACACACCAAGTTACTGTTGA.
31. TLE2_F ACTGCCTGAACCGAGACAACT.
32. TLE2_R GTCCCAGACCACAATGTTGC.
33. NEGR1_F TTGTCAACTTTGCTCCTACTATTC.
34. NEGR1_R CAGCCACACAGGTATAATT.

3 Methods

3.1 Maintenance of hPSC Culture

1. Coat a 10 cm tissue culture plate with vitronectin. To do so, thaw a vial of vitronectin stock at room temperature. Then dilute 1:100 in DPBS to a final concentration of 5 mg/mL. Ensure the entire surface of plate is covered in liquid. We typically use 7 mL for a 10 cm dish. Leave at room temperature for 1 h (*see* **Note 3**).
2. Aspirate vitronectin solution and add 10 mL of E8 media to dish.
3. Remove frozen vial of hPSC from liquid nitrogen and thaw in 37 °C water bath until most of the vial is thawed, but there is a small amount of frozen cells left (*see* **Note 4**).
4. Using a P1000 pipette transfer thawed cells into 5 mL of DMEM/F12 in a 15 mL conical tube. Rinse vial with 1 mL of DMEM/F12 and add this to conical tube. DMEM/F12 should be pre-warmed to 37 °C.
5. Pellet cells using centrifugation 200× *g* for 4 min.
6. Aspirate the medium without disturbing the cell pellet. Tilting the conical tube to about a 45-degree angle can help.
7. Gently resuspend cells in 6 mL of E8 using a 5 mL pipette (*see* **Note 5**).
8. Plate the resuspending hPSC colonies to roughly 20–40% confluency on the 10 cm vitronectin-coated plate, from **step 2** (*see* **Note 6**).
9. Feed cells daily, by replacing media with 10 mL of fresh E8 (*see* **Note 7**).
10. Check daily that cells are healthy. When cells reach 80% confluency it is time to passage (*see* **Note 8**).

11. To passage cells, first wash once with DPBS, then add 6 mL of hPSC dissociation reagent to plate. Incubate at room temperature for 4 min. After 4 min, aspirate hPSC dissociation reagent and allow cells to sit for another 2 min without any media. After 2 min tap the side of the dish to dislodge the colonies from the plate. Add 10 mL of DMEM/F12 to the 10 cm plate and swirl. At this point there should be free floating hPSC colonies. Gently pipette up and down one time using a 10 mL pipette. Then passage colonies. Generally, a 1:7 to 1:10 ratio works well. Cells should be passaged as colonies, and not as single cells.

3.2 Neural Induction (Day −2 to Day 7)

1. Coat a 6-well dish with Matrigel at least a day prior to beginning the differentiation. To do this, thaw an aliquot of Matrigel overnight on ice in a 4 °C cold room (Day −2). The next day dilute Matrigel 1:50 in 4 °C DMEM/F12. Add 1 to 1.5 mL of diluted Matrigel solution to each well of a 6 well dish. Wrap the dish with parafilm and place overnight in a 4 °C cold room. The Matrigel dish is ready to use the next day (*see* **Note 9**).
2. Aspirate Matrigel solution and add 3 mL of E8 medium with 10 mM ROCKi to each well of a 6 well dish.
3. When hPSCs reach 80% confluency of a 10 cm dish, they are ready to begin differentiation. Dissociate hPSCs to single cell by washing in DPBS once, then incubating in 10 mL hPSC dissociation reagent at 37 °C for 6 min (*see* **Note 10**).
4. Triturate cells using a 10 mL pipette, ensuring that all cells are lifted off the plate. Move cells in hPSC dissociation reagent to a 50 mL conical tube. Add 15 mL of DMEM/F12 to this tube as well. Pellet cells via centrifugation at 200× *g* for 4 min.
5. Resuspend cells in 1 mL of E6 medium in the 50 mL conical tube. Gently triturate with a P1000 pipette, about 5 times to dissociate to single cells.
6. Count total number of cells in suspension.
7. Plate cells in E8 media + ROCKi from **step 2**, at a density of 250,000–300,000 cells/cm^2.
8. The next day (day 0), aspirate E8 media and rinse once with DPBS. Aspirate DPBS and add 3 mL of Neural induction medium plus 2 μM XAV to each 6-well plate (*see* **Note 11**). Feed with neural induction medium plus 2 μM XAV on day 1 and day 2, by replacing old media with 3 mL of fresh media per well.
9. From day 3 to day 7, feed cells daily neural induction medium without XAV (*see* **Note 12**).

3.3 Neural Rosette Formation (Day 7 to Day 12)

1. On day 6 of differentiation, begin coating a 10 cm dish with poly-ornithine/laminin/fibronectin. To do this, add poly-ornithine solution to 10 cm dish overnight. Then rinse three times with DPBS. On day 7 add laminin/fibronectin solution and incubate at 37 °C for at least 3 h (*see* **Note 13**).
2. Aspirate laminin/fibronectin solution and allow plate to dry completely. It is critical that the plate be completely dry (*see* **Note 14**).
3. Dissociate monolayer cultures by washing with DPBS once, then incubating with Accutase for 30 min at 37 °C. Generally, we use 2 mL of Accutase per well of a 6-well dish.
4. After the incubation gently triturate cells with a P1000 pipette 5 times to dissociate to single cells.
5. Add cells from two to three wells of a 6-well dish into a 50 mL conical tube, prefilled with 20 mL of DMEM/F12.
6. Pass the DMEM/F12 cell mixture through a 45 μm cell strainer into a clean 50 mL conical tube.
7. Pellet the cells by centrifugation at 200× *g* for 4 min.
8. Resuspend cells in 25 mL of DMEM/F12 and pellet again.
9. Resuspend cells in 1 mL of prefrontal cortex differentiation media with 1x ROCKi.
10. Plate 20 μL droplets of the high-density cell resuspension on the dried laminin/fibronectin plates. Typically, a 20 μL droplet will contain about 400,000 cells. To do this, aspirate cells using a 20uL pipette. Gently eject cells from the pipette tip so a small droplet is hanging off the tip. Touch this droplet to the dried laminin/fibronectin plate. The droplet should adhere to the plate, with the surface tension of the liquid helping to maintain the droplet's form (*see* **Note 15**).
11. Once 25 to 30 droplets are plated on the 10 cm dish, move the dish to the 37 °C incubator for 2 h. Take care not to disturb the droplets.
12. After 2 h, carefully remove the plate from the incubator back into the tissue culture hood. Gently add 15 mL of prefrontal cortex differentiation media by dripping the media down the side of the 10 cm dish, taking care not to disturb the high-density cell droplets. Return to cells to the incubator and do not disturb them until day 10 (*see* **Note 16**).
13. On day 10, replace media with 15 mL of fresh prefrontal cortex differentiation media (*see* **Note 17**).

3.4 Prefrontal Cortex Patterning (Day 12 to Day 40)

1. On day 12, dissociate high-density droplets with 0.05% trypsin. First, rinse cells with DPBS once. Then dissociate by incubating with 7 mL of prewarmed 0.05% trypsin for 8 min at 37 °C (*see* **Note 18**).

2. After incubation, gently triturate cells with a 10 mL pipette to break up all large clumps. Add trypsin cell mixture to a 50 mL conical tube prefilled with 20 mL of DMEM/F12 + 10% FBS.
3. Pellet cells by centrifugation at 200× *g* for 4 min and resuspend cells in 25 mL of DMEM/F12 without FBS. Do this two times to ensure serum is washed out.
4. Finally passage cells using a 1:2 ratio onto new 10 cm poly-ornithine/laminin/fibronectin-coated plates. These plates do not need to be dried.
5. From day 12 to day 20, feed every other day, by replacing media with 10 mL of fresh prefrontal cortex differentiation media plus B27. Cells should reform rosettes at this stage (*see* **Note 19**).
6. On day 20, passage cells to lower density with Accutase. First, rinse cells with DPBS once. Then incubate cells with 7 mL Accutase for 30 min.
7. After incubation gently triturate cells to break up large clumps. Add Accutase cell mixture to a 50 mL conical tube prefilled with 20 mL of DMEM/F12 + 10% FBS.
8. Pellet cells by centrifugation at 200× *g* for 4 min and resuspend cells in 25 mL of DMEM/F12 without FBS. Do this two times to ensure serum is washed out.
9. Finally, resuspend cells in 10 mL of prefrontal cortex differentiation medium and count total cell number. Cells can be frozen and banked at this stage for later use (*see* **Note 20**).
10. Replate cells at a density of 200,000 to 400,000 cells/cm^2 in prefrontal cortex differentiation medium on poly-ornithine/laminin/fibronectin-coated plates. Either 10 cm, 6-well, or 24-well plates can be used, depending on what suits downstream analysis. We suggest plating an extra well of a 6-well plate for quality control at day 30 (*see* **Note 21**).
11. Feed cells with prefrontal cortex differentiation medium through day 40, by replacing with fresh medium every other day.

3.5 Prefrontal Cortex Neuronal Differentiation (Day 40 +)

1. On day 40, passage prefrontal cortex culture to low density to promote neuronal differentiation. First, rinse cells with DPBS once. Then incubate with Accutase for 30 min at 37 °C.
2. After incubation gently triturate cells to break up large clumps. Add Accutase cell mixture to a 50 mL conical tube prefilled with 20 mL of DMEM/F12 + 10% FBS.
3. Pellet cells by centrifugation at 200× *g* for 4 min and resuspend cells in 25 mL of DMEM/F12 without FBS. Do this two times to ensure serum is washed out.

4. Resuspend cells in 10 mL of N2 Medium + B27 and count total cell number.
5. Plate cells at a density of 50,000 cells/cm^2 on poly-ornithine/laminin/fibronectin coated plates (*see* **Note 22**).
6. Maintain cells in N2 Medium + B27, feeding every other day (*see* **Note 23**).

4 Notes

1. There is minor lot-to-lot variability of Matrigel, which can influence hPSC and differentiation quality. Growth factor reduced Matrigel is a more defined version of the product, with less lot variability. Growth factor reduced Matrigel can be attempted if one experiences variability between differentiation replicates.
2. Check XAV aliquot for a white precipitate before each use. If there is a white precipitate, warm in a 37 °C water bath to try to dissolve. Discard aliquot if white precipitate cannot be dissolved.
3. We generally use 7 mL of vitronectin solution for a 10 cm plate and 1 mL per well of a 6-well dish. Vitronectin dishes can be stored at 4 °C for up to 1 week, wrapped in parafilm. Ensure plates are stored flat.
4. It is important to minimize the time thawed hPSCs sit in DMSO cryopreservation solution (10% DMSO/E8). To expedite thawing, gently move the frozen vial back and forth through the water bath, and check for thawing every 15 seconds. Move to the next step once the vial is 50% thawed.
5. hPSCs should remain in colonies rather than single cells upon re-suspension. Using a 5 mL pipette rather than a P1000 pipette is gentler on cells and does not dissociate them to single cell. It is also therefore important to freeze hPSC stocks as colonies rather than single cells.
6. To achieve a 20–40% confluency when plating thawed hPSCs, we typically split a thawed vial across three 10 cm plates. That is, resuspend a thawed vial in 6 mL of E8, and add 2 mL to each of three 10 cm dishes. When freezing cells for storage, cells are grown to 80% confluency in a 10 cm dish, then split into 3 cryopreservation vials.
7. Consider using E8 Flex to avoid feeding cells on weekends (Thermo Fisher Scientific A28558501). This is a special E8 formulation designed so that cells can be left without feeding for 48 h or more. Passage cells on Thursday, then double feed cells on Friday with 20 mL of E8 Flex as per the manufacturer's

suggestion. Passage cells on Monday, then feed with 10 mL of E8 Flex on Tuesday. Passage cells on Thursday and repeat. It may take some trial and error to achieve the appropriate passage density, so colonies are 80% confluent on Monday and Thursday. In our hands, passaging colonies between 1:10 and 1:15 dilutions were typically sufficient.

8. If cells are not healthy the day after thawing and plating, this could be due to a number of factors including poor cryopreservation, thawing cells and plating them too slowly, or improper vitronectin coating. Make new vitronectin-coated plates, and re-thaw cells plating them at a higher density. One can also plate cells in the presence of ROCKi to promote survival after thawing.
9. Matrigel is typically purchased in 10 mL glass vials. Thaw the Matrigel stock overnight on ice in a 4 °C cold room and aliquot into 1 mL cryotubes the next day. Pre-chill the cryotubes on ice. Store Matrigel aliquots at −20 °C. Do not re-freeze Matrigel more than once. After coating, Matrigel dishes can be stored at 4 °C for up to two weeks. We have used Matrigel diluted from various concentration ranging from 1:20 to 1:100 in DMEM/F12 without noticing clear difference in differentiation efficiency. More dilute concentrations, for example, 1:50 to 1:100 may result in better neuron health in long-term cultures. Additionally, the protein content can vary from lot to lot. One can calculate Matrigel dilutions based on the total protein content to standardize the final Matrigel concentration across differentiations. The total protein content is found on the Matrigel datasheet.
10. It is essential to start out the differentiation with high-quality and healthy hPSCs. hPSCs should have uniform morphology. Colonies should not be overgrown nor have spontaneous differentiation. The edges of hPSC colonies should just be starting to touch each other, but not for more than one day.
11. One of the major areas of inconsistency with dual SMAD inhibition is forebrain induction, indicated by FOXG1 expression. It is advisable to assay FOXG1 expression either by quantitative real-time PCR (qRT-PCR) or immunocytochemistry to ensure consistent forebrain induction. We typically add 2 μM XAV from day 0–2 of the differentiation to suppress early WNT signaling as WNT signaling can promote midbrain identities [19].
12. High-density droplets can be made between day 6 and day 8 of the protocol. Waiting until after day 8 reduces the efficiency of rosette formation.

13. Ensure adequate DPBS rinses after poly-ornithine incubation as this can be toxic for cells. Laminin/fibronectin plates can be stored at 4C for up to one week.
14. Ensuring that the poly-ornithine/laminin/fibronectin plates are completely dry is crucial before plating high-density droplets. We aspirate the laminin/fibronectin solution then prop up the 10 cm dish at a 45 to 60-degree angle by leaning against a pipette tip box, in the tissue culture hood with the lid of the dish off. After a few minutes of drying, aspirate the liquid that has settled at the bottom edge of the dish. Leave dishes for at least 30 min to dry. A thin translucent uniform film should develop on the bottom of the plate, indicating the dish is completely dry.
15. If the plate has any moisture on it, the droplet will dissipate and spread out over the dish.
16. If needed, an occipital cortex control can be generated in parallel. To generate occipital cortex, use the same protocol except add 25 ng/mL of recombinant SHH to N2 media, instead of FGF8.
17. One should monitor for neural rosette formation around day 10 using a light microscope (Fig. 2). At the same time, monitor for the appearance of delaminating flat cells. These flat cells migrate away from the high-density droplets and into the spaces between. They have a flat morphology. The appearance of these cells often signals a failed differentiation, as these cells will continue to proliferate and take over the culture, especially after passaging. One potential strategy to deplete flat cells is based on their quick detachment from the plate with trypsin. On day 12, when passaging cells with trypsin, monitor for the

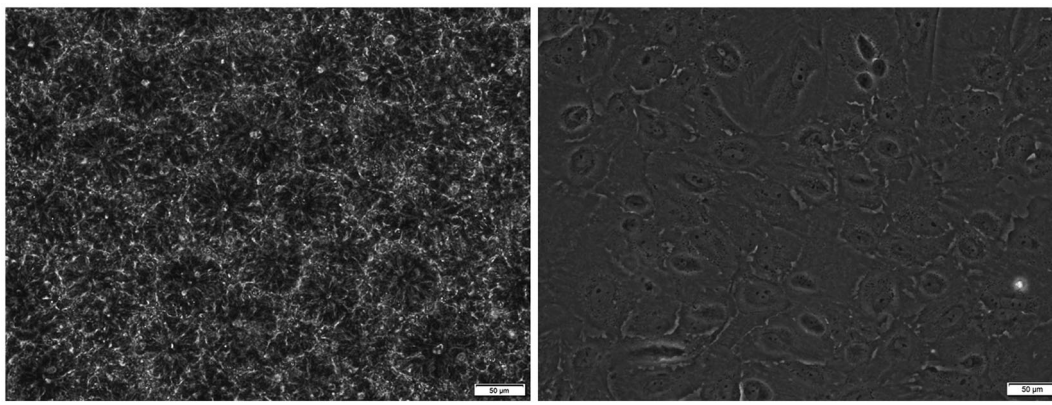

Fig. 2 Neural rosette morphology. Phase contrast images of neural rosettes (left). Also shown are characteristic morphology of flat cells demarginating from the high-density droplet, which indicate a poor-quality neural differentiation (right). Scale bars are 50 μm

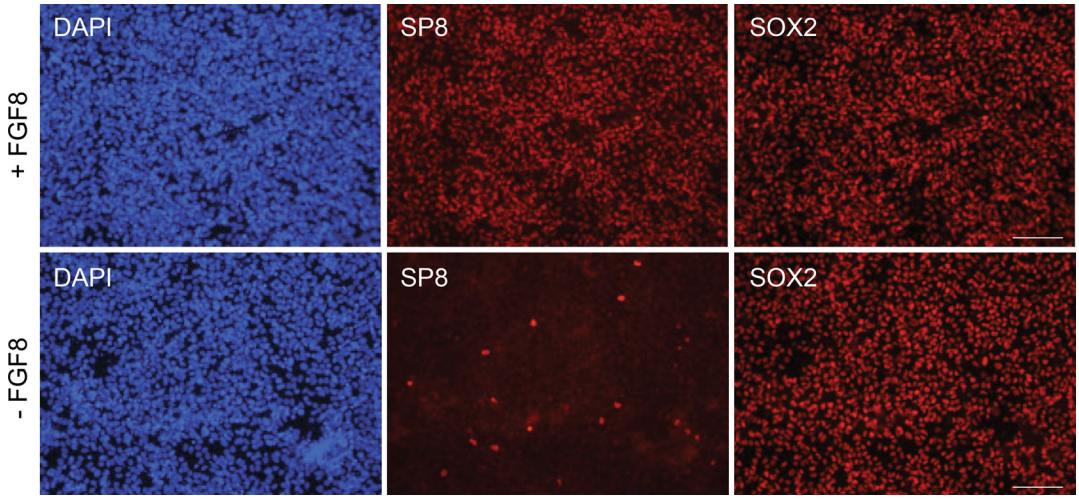

Fig. 3 Immunocytochemistry showing induction of SP8 expression with prefrontal cortex differentiation medium (+FGF8) by day 18. Prefrontal cortex neural progenitors should have near-uniform expression of SP8 and SOX2. Occipital cortex neural progenitors, grown in the absence of FGF8 (-FGF8), should not express SP8. Prefrontal cortex neural progenitors should express FOXG1 and PAX6, and should not express COUP-TF1 or NKX2.1 (not shown). We typically assay cells between day 18 and 20, however expression of these proteins turns on earlier. Scale bars are 50 μm

timepoint at which the flat cells begin to detach from the plate. This should occur after about 4 min of trypsin incubation at 37 °C. Gently tap the side of the dish and aspirate trypsin, then rinse once with DPBS. The intended effect is to wash out flat cells. The high-density droplets which are more adherent to the dish should remain. Add additional trypsin and incubate at 37 °C for 3 more min and proceed to the next step of the protocol.

18. If the high-density droplets are not dissociating and instead remain as large clumps of cells, then incubate the cells with trypsin for an additional 3 min.
19. Quality control should be performed at day 20 using immunocytochemistry to assess for forebrain induction (Fig. 3). Cells should express PAX6, FOXG1, SOX2, and SP8 (prefrontal cortex) or COUPTF1 (occipital cortex). See materials section for antibodies.
20. It is possible to cryofreeze the differentiation when passaging at day 20. At this point, cells are still predominantly neural progenitors and be cryopreserved in prefrontal cortex differentiation medium with 10% DMSO. An alternative is to freeze using Stem-Cell banker.
21. Quality control should be performed at day 30 qRT-PCR to assess for dorsal forebrain induction and prefrontal cortex patterning. Dorsal forebrain cells will consist of both progenitors

and neurons, and should express *PAX6*, *FOXG1*, and *TBR1*, but have relatively lower expression of *DLX1*. Additional primers to compare prefrontal versus occipital identity are provided in the materials section. It is helpful to have an occipital cortex control differentiation for this comparison.

22. The plating density at this step may vary depending on the final downstream application and the time neurons will spend in culture. If planning for immunocytochemistry-based analysis, we plate cells on poly-ornithine/laminin/fibronectin-coated glass coverslips at day 40.
23. Since cultures will contain both progenitors and post-mitotic neurons, cells may start to clump together as progenitors continue to proliferate. One can consider using the Notch inhibitor, DAPT, to induce neuronal differentiation at this stage, however we have not tested whether this impacts maintenance of prefrontal cortex identity.

References

1. Thomson JA, Itskovitz-Eldor J, Shapiro SS, Waknitz MA, Swiergiel JJ, Marshall VS et al (1998) Embryonic stem cell lines derived from human blastocysts. Science 282:1145–1147
2. Smith WC, Harland RM (1992) Expression cloning of noggin, a new dorsalizing factor localized to the Spemann organizer in Xenopus embryos. Cell 70:829–840
3. Hemmati-Brivanlou A, Kelly OG, Melton DA (1994) Follistatin, an antagonist of activin, is expressed in the Spemann organizer and displays direct neuralizing activity. Cell 77:283–295
4. Chambers SM, Fasano CA, Papapetrou EP, Tomishima M, Sadelain M, Studer L (2009) Highly efficient neural conversion of human ES and iPS cells by dual inhibition of SMAD signaling. Nat Biotechnol 27:275–280
5. Chambers SM, Qi Y, Mica Y, Lee G, Zhang XJ, Niu L et al (2012) Combined small-molecule inhibition accelerates developmental timing and converts human pluripotent stem cells into nociceptors. Nat Biotechnol 30:715–720
6. Qi Y, Zhang XJ, Renier N, Wu Z, Atkin T, Sun Z et al (2017) Combined small-molecule inhibition accelerates the derivation of functional cortical neurons from human pluripotent stem cells. Nat Biotechnol 35:154–163
7. Maroof AM, Keros S, Tyson JA, Ying SW, Ganat YM, Merkle FT et al (2013) Directed differentiation and functional maturation of cortical interneurons from human embryonic stem cells. Cell Stem Cell 12:559–572
8. Steinbeck JA, Jaiswal MK, Calder EL, Kishinevsky S, Weishaupt A, Toyka KV et al (2016) Functional connectivity under Optogenetic control allows modeling of human neuromuscular disease. Cell Stem Cell 18:134–143
9. Noctor SC, Flint AC, Weissman TA, Dammerman RS, Kriegstein AR (2001) Neurons derived from radial glial cells establish radial units in neocortex. Nature 409:714–720
10. Rakic P (1988) Specification of cerebral cortical areas. Science 241:170–176
11. O'Leary DD, Chou SJ, Sahara S (2007) Area patterning of the mammalian cortex. Neuron 56:252–269
12. Fukuchi-Shimogori T, Grove EA (2001) Neocortex patterning by the secreted signaling molecule FGF8. Science 294:1071–1074
13. Petanjek Z, Judas M, Simic G, Rasin MR, Uylings HB, Rakic P et al (2011) Extraordinary neoteny of synaptic spines in the human prefrontal cortex. Proc Natl Acad Sci USA 108:13281–13286
14. Nimchinsky EA, Gilissen E, Allman JM, Perl DP, Erwin JM, Hof PR (1999) A neuronal morphologic type unique to humans and great apes. Proc Natl Acad Sci USA 96:5268–5273
15. Courchesne E, Mouton PR, Calhoun ME, Semendeferi K, Ahrens-Barbeau C, Hallet MJ et al (2011) Neuron number and size in prefrontal cortex of children with autism. JAMA 306:2001–2010

16. Hare BD, Duman RS (2020) Prefrontal cortex circuits in depression and anxiety: contribution of discrete neuronal populations and target regions. Mol Psychiatry 25:2742–2758
17. Shibata M, Pattabiraman K, Lorente-Galdos B, Andrijevic D, Kim SK, Kaur N et al (2021) Regulation of prefrontal patterning and connectivity by retinoic acid. Nature 598:483–488
18. Cholfin JA, Rubenstein JL (2008) Frontal cortex subdivision patterning is coordinately regulated by Fgf8, Fgf17, and Emx2. J Comp Neurol 509:144–155
19. Kim TW, Piao J, Koo SY, Kriks S, Chung SY, Betel D et al (2021) Biphasic activation of WNT signaling facilitates the derivation of midbrain dopamine neurons from hESCs for translational use. Cell Stem Cell 28:343–355. e5

Chapter 4

Differentiation of Mature Dopaminergic Neurons from Human Induced Pluripotent Stem Cells

Pretty Garg, Mathias Bähr, and Sebastian Kügler

Abstract

Reprogramming of somatic cells like blood cells and fibroblasts to obtain human induced pluripotent stem cells (hiPSCs) has become a state-of-the-art tool to study human diseases. The self-renewable hiPSCs offer ease of genetic modifications and can be differentiated into any cell type of the human body ranging from hepatocytes, cardiac myocytes, and subtypes of neurons. Dopaminergic (DA) neurons are one such neuronal subtype that is largely present in the midbrain region of the human brain and controls several functions like voluntary movement, reward, addiction, and stress. Loss of DA neurons is associated with one of the most common neurological disorders, Parkinson's disease (PD). Here, we describe a small molecule-directed approach for the generation of functionally mature dopaminergic neurons through the differentiation of hiPSCs. Differentiated DA neurons can be used to study their role in (patho)physiology.

Key words Induced pluripotent stem cells, Dopaminergic neurons, Astrocytes, Network activity, Differentiation, Patterning

1 Introduction

The generation of induced pluripotent stem cells (iPSC) from rodents and humans [1, 2] has proved to be a "game-changer for medicine" [3]. With their self-proliferating capability, differentiation potential toward cell types of all three germ layers, and ease of genetic modification, iPSCs provide a great platform to understand the role of different cell types in human diseases. For neurodegenerative disorders, iPSCs-derived cells are of utmost importance to studying disease-associated mechanisms that can be further confirmed using in vivo models. Furthermore, differentiated cells can be utilized for large-scale drug screening [4]. Additionally, iPSCs possess a great advantage for cell transplantation as they use autologous cells thereby reducing the risks of rejection. Besides this, 3D cultures of iPSCs to generate cerebral organoids, bone, optic vesicle-like structures, functional liver buds, cardiac muscle tissue,

Tolga Soykan and Alexandros Poulopoulos (eds.), *Synapse Development: Methods and Protocols*, Methods in Molecular Biology, vol. 2910, https://doi.org/10.1007/978-1-0716-4446-1_4,

primitive and pancreas islet cells have started a new generation of tissue bioengineering [5]. Together with the range of their applications, iPSCs serve as a promising tool for the advancement of personalized medicine.

1.1 Differentiation of Human Induced Pluripotent Stem Cells Toward Dopaminergic Neurons to Study Parkinson's Disease

Almost 90% of the dopaminergic (DA) neurons reside in the ventral part of the mesencephalon constituting substantia nigra pars compacta (SNpc) and ventral tegmental area (VTA). Although constituting 1% of the total number of neurons in the brain, DA neurons regulate important functions like movements, reward system, motivation, and working memory [6]. Loss of DA neurons in SNpc causes Parkinson's disease (PD) which is the second most common neurodegenerative disorder. A substantial decrease in DA neurons and thus secreted dopamine in PD is marked by motor symptoms like bradykinesia, tremor, rigidity, and loss of postural control. Considering the role of DA neurons in physiology and disease, their development in the brain has been widely studied to replenish the pool of lost neurons by either triggering DA neurons differentiation or by engrafting their differentiated progenitors [7, 8].

Over the last 15 years of iPSC discovery, hundreds of protocols have been described to differentiate subtypes of neurons. All of these differentiation approaches rely on the knowledge of developmental pathways that can be activated or blocked using small molecules and growth factors [9, 10] or viral-vector-mediated gene regulation [11, 12]. Here, we describe a protocol to generate functional DA neurons from hiPSCs using stepwise treatment with small molecules and growth factors (Fig. 1). The first step of the

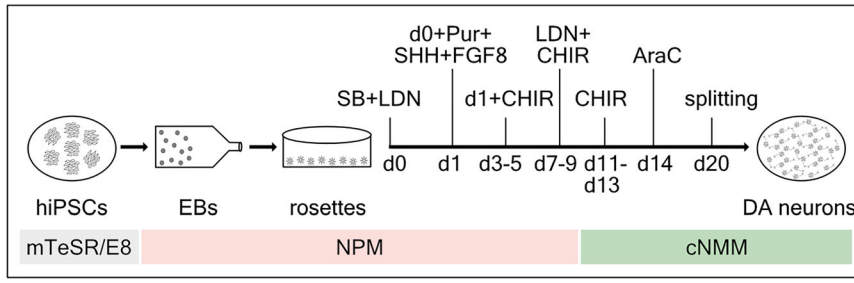

Fig. 1 Schematic of dopaminergic (DA) neurons differentiation protocol. Human induced pluripotent stem cells (hiPSC) are cultured until enough cells are ready to generate embryoid bodies (EB). After plating EBs into a 10 cm dish to generate rosettes, they are neuralized and patterned to differentiate into DA neurons using a small molecule-based approach. The medium formulation for each stage of differentiation is indicated at the bottom. The timeline of patterning is indicated from d0-d14 along with the combination of small molecules to be used. After 14 days of patterning, cells are treated with Ara-C for 4–5 days and dissociated at d20. DA neurons are plated as single cells on Poly-l-ornithine (PLO) coated surfaces with or without rat primary astrocytes. NPM: neuronal patterning media, cNMM: complete neuronal maturation media, SB: SB431542, LDN: LDN193189, SHH: sonic hedgehog, Pur: purmorphamine, CHIR: CHIR99021, Ara-C: arabinofuranosyl cytidine

protocol employs small molecules, SB431542 and LDN193189, to inhibit tumor growth factor β (TGF-β) and bone morphogenetic proteins (BMP), thus causing dual SMAD inhibition and inducing neuralization of iPSCs [13]. In the second step, the resulting neuroepithelial cells are patterned toward midbrain floor-plate precursors by activating sonic hedgehog and canonical Wnt signaling. Midbrain precursors are further proliferated with fibroblast growth factor 8 (FGF8). Subsequently, differentiated midbrain neurons undergo maturation in the presence of growth factors like brain-derived neurotrophic factor (BDNF) and glia-derived neurotrophic factor (GDNF). Postmitotic neurons are selected by application of a mitotic inhibitor, arabinofuranosyl cytidine (Ara-C). This protocol results in a heterogeneous neuronal population with >80% NeuN and >50% of tyrosine hydroxylase (TH) expressing neurons which is the maximum number of TH-positive cells reported with small molecule-directed differentiation. The method can be applied to different iPSC lines with similar differentiation efficiency as long as there are no spontaneously differentiating cells. Several modified versions of this protocol with an elaborate functional characterization of the differentiated DA neurons have been previously reported [10, 14, 15].

Furthermore, several studies have shown that astrocytes regulate neuronal synapse maturation [9] by providing guidance cues in the form of membrane-bound, cytoplasmic, or secreted proteins [16, 17]. Therefore, the co-culture of differentiated DA neurons with rodent astrocytes helps to accelerate their functional maturation that can be evaluated by spontaneous network bursts and the release of dopamine without external stimuli.

2 Materials

All solutions should be prepared in a Laminar Flow hood following standard sterile technique. All microfuge tubes to be used for aliquoting should be pre-autoclaved. Make sure that all solutions to be used for cell culture are sterile (pass through a 0.2 μm filter if required).

2.1 General Cell Culture Reagents and Plasticware

1. Matrigel (growth factor reduced, Corning 354230): 1:100 diluted in sterile 1X PBS or DMEM/F12 (*see* **Note 1**).
2. Poly-L-ornithine (PLO): 0.1 mg/mL PLO (Sigma P3655) in H_2O (*see* **Note 2**).
3. Laminin: Freshly dilute 1 mg/mL Laminin stock (Sigma L2020) to 20 μg/mL working concentration in sterile PBS (*see* **Note 3**).
4. Dissociation agents: 0.5 mM EDTA (*see* **Note 4**) prepared in PBS or Accutase (Merck A6964) (*see* **Note 5**).

5. Knock-out serum replacement (KOSR, ThermoFisher Scientific 10828010) (*see* **Note 6**).
6. Dimethyl sulfoxide (DMSO, Sigma D4540) (*see* **Note 7**).
7. 7.5% Bovine serum albumin (BSA): Dilute 7.5% BSA (ThermoFisher Scientific 15660037) to 0.2% in sterile PBS, pH 7.4 (*see* **Note 8**).
8. T25 tissue culture-treated flask (Sarstedt 83.3910.002).
9. 6-well tissue culture-treated plate (Sarstedt 83.3920).
10. 10 cm tissue culture-treated petri dish (Sarstedt 83.3902).
11. Frosty Boy (ThermoFisher Scientific 5100–0001).
12. Cryovials (ThermoFisher Scientific 377267).
13. 0.2 μm filter (VWR 28145–477).
14. 70 μm cell strainer (Miltenyi Biotec 130-098-462).

2.2 Media Composition

All media unless otherwise stated should be stored at 4 °C and used up within 2 weeks.

1. mTeSR/E8: mTeSR/E8 (Stemcell Technologies 5990) (*see* **Note 9**).
2. Neuronal patterning medium (NPM): 1% Glutamax, 1% B27 without retinoic acid, 1% N2 supplement, 1% NEAA, 50 μM β-mercaptoethanol in DMEM/F12 (ThermoFisher Scientific 11330032) (*see* **Note 10**).
3. Neuronal Maturation Medium (NMM): 1% Glutamax, 1% B27 with retinoic acid in Neurobasal medium (ThermoFisher Scientific 21103049).
4. Complete Neuronal Maturation Medium (cNMM): 20 ng/mL BDNF, 20 ng/mL GDNF, 10 ng/mL NT3, 0.25 mM dcAMP, 1 ng/mL TGFβ3, 0.2 mM AA, and 10 μM DAPT in NMM.
5. Serum-free rat cortical astrocyte medium (sfRCAM): 1% Penstrep, 1% Glutamax, 1% B27 without retinoic acid, 1% N2 supplement, 1% NEAA, 10 μg/mL CNTF in DMEM/F12 (ThermoFisher Scientific 11330032).
6. Cryomedium for iPSCs: mTeSR/E8 with 10% DMSO and 20% KOSR (*see* **Note 11**).

2.3 Reconstitution of Small Molecules and Growth Factors

Dissolve and aliquot the small molecules and growth factors following the sterile tissue culture approach (*see* **Notes 12–15**).

1. ROCK inhibitor (RI) 1000X stock solution: Reconstitute 2 mg of RI (Tocris 1254) in 1.25 mL of DMSO to make a stock of 5 mM. Make 10 and 50 μL aliquots.

2. SB431542 1000X stock solution: Reconstitute 5 mg of SB431542 (Tocris 1614) in 1.3 mL of DMSO to make a stock of 10 mM. Make 10 and 50 μL aliquots.
3. LDN193189 100,000X stock solution: Reconstitute 2 mg of LDN193189 (Tocris 6053) in 417.2 μL of DMSO to make a stock of 10 mM. Make 2.5 and 5 μL aliquots. Protect from light.
4. SHH C25II 2000X stock solution: Reconstitute 200 μg of SHH C25II (R & D systems 464-SH-200/CF) in 1 mL of sterile PBS to make a stock of 200 μg/mL. Make 10 and 20 μL aliquots.
5. Purmorphamine 5000X stock solution: Reconstitute 5 mg of Purmorphamine (Stemgent 04–0009) in 960.4 μL of DMSO to make a stock of 10 mM. Make 5 and 10 μL aliquots.
6. Fibroblast growth factor 8 (FGF8) 250X stock solution: Reconstitute 25 μg of FGF8 (Peprotech AF-100-25) in 1 mL of sterile 0.2% BSA (prepared in PBS) to make a stock of 25 μg/mL. Make 40 and 200 μL aliquots.
7. CHIR99021 5000X stock solution: Reconstitute 10 mg of CHIR99021 (Tocris 4423) in 1.43 mL of DMSO to make a stock of 15 mM. Make 5 and 10 μL aliquots.
8. Brain-derived neurotrophic factor (BDNF) 1000X stock solution: Reconstitute 20 μg of BDNF (Peprotech 450–02) in 1 mL of sterile 0.2% BSA (prepared in PBS) to make a stock of 20 μg/mL. Make 25 and 50 μL aliquots.
9. Glia-derived neurotrophic factor (GDNF) 500X stock solution: Reconstitute 10 μg of GDNF (Peprotech 450–10) in 1 mL of sterile 0.2% BSA (prepared in PBS) to make a stock of 10 μg/mL. Make 50 and 100 μL aliquots.
10. Ascorbic Acid (AA) 250X stock solution: Reconstitute 100 mg of AA (Sigma A4403-100MG) in 11.35 mL of sterile H_2O to make a stock of 50 mM. Make 40 and 200 μL aliquots.
11. Dibutyryl cAMP (dcAMP) 200X stock solution: Reconstitute 25 mg of dcAMP (Sigma D0260-25MG) in 1.02 mL of sterile H_2O to make a stock of 50 mM. Make 50 and 100 μL aliquots.
12. Tumor growth factor β3 (TGFβ3) 2000X stock solution: Reconstitute 2 μg of TGFβ3 (Peprotech 100-36E) in 1 mL of 4 mM HCl containing 0.2% BSA (prepared in PBS) to make a stock of 2 μg/mL. Make 25 and 100 μL aliquots.
13. DAPT 2000X stock solution: Reconstitute 10 mg of DAPT (Cayman 13,197) in 1.16 mL of DMSO to make a stock of 20 mM. Make 5 and 25 μL aliquots.

14. Neurotrophin 3 (NT3) 1000X stock solution: Reconstitute 10 μg of NT3 (Peprotech AF-450-03) in 1 mL of sterile 0.2% BSA (prepared in PBS) to make a stock of 10 μg/mL. Make 10 and 50 μL aliquots.
15. Ciliary neurotrophic factor (CNTF) 1000X stock solution: Reconstitute 20 μg of CNTF (Peprotech 450–13) in 2 mL of sterile 0.2% BSA (prepared in PBS) to make a stock of 10 μg/mL. Make 10 and 50 μL aliquots.
16. Arabinofuranosyl cytidine (Ara-C) 1000X stock solution: Reconstitute 1 mg of Ara-C (Sigma C-6645) in 1.65 mL of sterile cell-culture grade water to make a stock of 2.5 mM. Make 10 and 50 μL aliquots.

3 Methods

All procedures should be performed under the standard sterile technique. Medium-containing growth factors or small molecules should be brought to room temperature for 30 min followed by warming at 37 °C for 5 min. Prolonged warming results in the degradation of growth factors. All reagents and equipment should be sterilized thoroughly with 70% Ethanol before bringing them in the laminar-flow hood.

3.1 Maintenance and Cryopreservation of Human iPSCs

This protocol describes the hiPSC culture starting from a commercial source in the form of a cryopreserved stock.

1. Coat 2 wells in a 6-well plate with matrigel. Incubate for 30 min at 37 °C or 1 h at room temperature (*see* **Note 16**).
2. Calculate the required amount of mTeSR/E8 medium required with and without RI from **steps 3, 4**, and 7. Warm the medium and then add 5 μM RI to the required amount of mTeSR/E8.
3. After sufficient incubation, aspirate Matrigel, and wash the plate once with PBS followed by adding 2 mL of mTeSR/E8 with RI to each well.
4. Pre-fill one 15 mL conical tube with 8 mL of mTeSR/E8 medium without RI.
5. Take out the iPSC cryovial from dry ice or liquid nitrogen and thaw the cells in a 37 °C water bath until almost completely thawed. Using a P1000 pipette, transfer the cells from the cryovial to a 15 mL conical tube filled with media in **step 4**. Centrifuge the conical tube at 200 g for 5 min to pellet the cells (*see* **Note 17**).

6. Aspirate the medium without disturbing the pellet, and gently resuspend the cells in 1 mL of mTeSR/E8 with RI (*see* **Note 18**).
7. Divide the cell suspension equally in two wells of the matrigel-coated 6-well plate (*see* **Note 19**).
8. Observe the cells on the following day to confirm their attachment and survival (*see* **Note 20).**
9. Feed the cells with fresh medium without RI on the second day after plating the cells. After that medium should be replaced every day (*see* **Note 21**).
10. Once the cells reach 75–80% confluency, they should be transferred into a new plate by splitting. To split the cells, coat the required number of wells, and warm the required amount of 0.5 mM EDTA (1 mL per well) and medium at 37 °C. Post warming, add RI to the required amount of medium. Aspirate medium from the well, and add 1 mL of prewarmed EDTA. Incubate the cells with EDTA for 5–10 min at 37 °C. Wash the detached cells with fresh mTeSR/E8 medium and collect in a 15 mL conical tube. Centrifuge the tube at 200 g for 5 min to pellet the cells (*see* **Note 22**).
11. Aspirate the medium without disturbing the pellet, and gently resuspend the cells in 1 mL of mTeSR/E8 with RI. Plate the cell suspension in the predetermined number of matrigel-coated wells. Observe the cells the next day and proceed following **steps 8–10**.
12. iPSC stock can be cryopreserved in liquid nitrogen following these steps. Pre-cool Frosty box at 4 °C for 2–3 h. Estimate the number of vials to be made and label cryovials with the details of the cells. Determine and prepare the amount of cryomedium required (1 mL/cryovial). Perform splitting as described in **step 10** using accutase instead of EDTA. Aspirate the medium without disturbing the pellet, and gently resuspend the cells in 1 mL of cryomedium. Make up the volume of the cell suspension to the calculated amount by adding more cryomedium. Mix the cells uniformly and pipette 1 mL cell suspension per cryovial. Carefully close the vials without touching the lids and place them in the Frosty box. Let Frosty box cool down further at −80 °C overnight. The following day, transfer the cells to liquid nitrogen (*see* **Note 23**).

3.2 Formation of Embryoid Bodies

When the cells reach 75–80% confluency, they can be used to generate three-dimensional, multicellular aggregates called embryoid bodies (EB). This step improves intercellular communication and enhances differentiation efficiency.

1. Aspirate mTeSR/E8 from confluent iPSCs, wash the cells once with warm PBS and add 4 mL of NPM to each well. Incubate the cells in NPM for 2 days (*see* **Note 24**).
2. Aspirate NPM from the cells and wash them once with warm PBS (pH 7.4). Aspirate PBS and dissociate the cells with warm EDTA (1 mL/well). Incubate at 37 °C for 5 min. Add 2 mL of warm NPM to the cells and triturate them using P1000. Collect the cells in a 15 mL conical tube. Wash the well twice with 2 mL of warm NPM and collect the content in the same 15 mL tube. Centrifuge the conical tube at 200 g for 5 min to pellet the cells.
3. Aspirate the medium without disturbing the pellet and gently resuspend the cells in 1 mL of NPM (*see* **Note 25**).
4. Transfer the cell suspension to a non-coated T25 flask containing 5 mL of warm NPM. Incubate at 37 °C and observe the cells the next day for the formation of small spheres called EBs (*see* **Note 26**).
5. To change the medium of EBs, tilt the flask at a 45° angle and let it sit for 5 min to allow EBs to settle at the bottom and then carefully aspirate the medium making sure not to aspirate EBs. Feed the cells with 5 mL of warm NPM. Perform medium change every day for the next two days (*see* **Note 27**).
6. For dopaminergic differentiation, transfer the contents of the T25 flask containing EBs to a matrigel-coated 10 cm dish containing 5 mL warm NPM. Incubate at 37 °C for one day (*see* **Note 28**).

3.3 Patterning Toward Dopaminergic Lineage

After generating EBs from undifferentiated iPSCs, they are neuralized using dual SMAD inhibition followed by patterning toward the midbrain lineage. Differentiating neurons start to appear at D9–10 at the edge of plated rosettes. Stages of differentiation starting from iPSCs, differentiating rosettes, and differentiated neurons plated with astrocytes are displayed in Fig. 2.

1. Day 0: Make sure that EBs are well attached to the dish before starting patterning. To begin patterning toward the dopaminergic lineage, aspirate the medium from the dish containing EBs and replace it with 10 mL NPM containing 10 μM SB and 100 nM LDN (*see* **Note 29**).
2. Day 1: Aspirate the medium and replace it with 10 mL NPM containing 10 μM SB, 100 nM LDN, 100 ng/mL SHH, 2 μM Purmorphamine, and 100 ng/mL FGF8.
3. Day 3–5: On days 3 and 5, aspirate the medium and replace it with 10 mL NPM containing 10 μM SB, 100 nM LDN, 100 ng/mL SHH, 2 μM Purmorphamine, 100 ng/mL FGF8, and 3 μM CHIR.

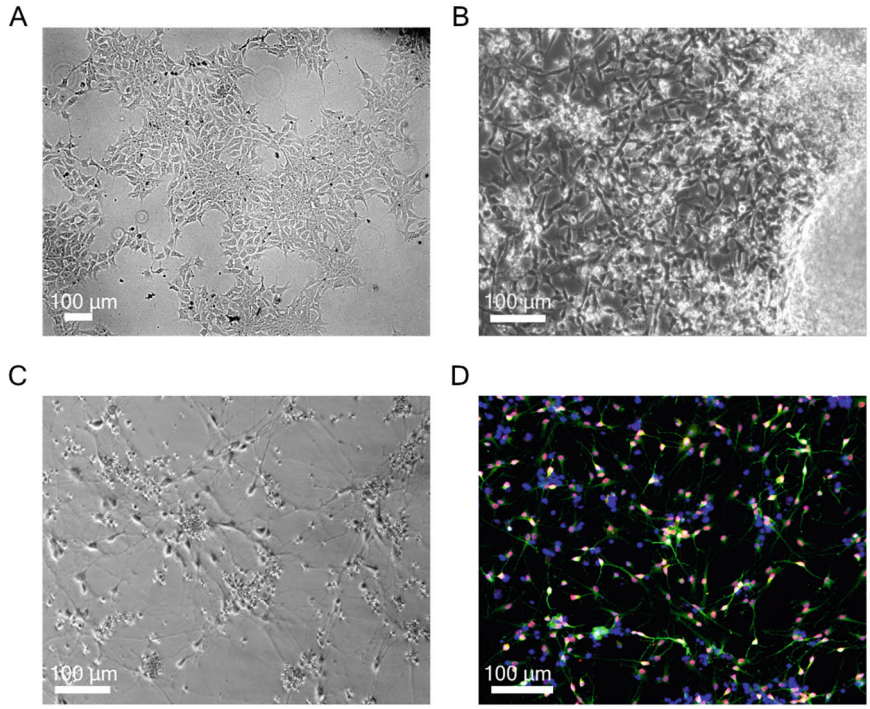

Fig. 2 Representative images of cells during the differentiation protocol. (**a**) Human iPSC stem cell culture showing a uniform undifferentiated morphology to start with DA neuron differentiation. (**b**) Neural rosettes undergoing patterning with differentiating neurons at the edges, while the thick clumps on the right represent rosettes. (**c**) Representative image of day 5 DA neurons plated with astrocytes on a PLO-coated dish. Note that neurons would develop a dense network over time in culture. (**d**) Immunostaining for NeuN (red), tyrosine hydroxylase (TH) (green), and DAPI (blue) on day 4 after plating hiPSC-derived DA neurons with astrocytes. Note that >50% of NeuN-expressing cells are positive for TH

4. Day 7–9: On days 7 and 9, aspirate the medium and replace it with 10 mL NPM containing 100 nM LDN and 3 μM CHIR (*see* **Note 30**).
5. Day 11–13: On days 11 and 13, aspirate the medium and replace it with 10 mL cNMM containing 3 μM CHIR.
6. Day 14: Aspirate the medium and replace it with 10 mL cNMM containing 2.5 μM Ara-C. Incubate the cells for 3 days. After 3 days of Ara-C treatment, replace the medium with cNMM without Ara-C and incubate for one more day (*see* **Note 31**).

3.4 Preparation of Plates for Plating hiPSC-Derived Dopaminergic Neurons

Differentiated dopaminergic neurons can be plated on several coated surfaces like poly-l-ornithine or poly-d-lysine followed by laminin, matrigel, or glial cells (*see* **Note 32**). The coating can either be done by following the below-mentioned protocol or commercially available pre-coated plated might be used.

3.4.1 Preparation of PLO-Laminin Plates

This protocol describes the volume of solutions required for each well in a 24-well plate.

1. Coat the plates or coverslips with PLO at least 48 h before plating the differentiated neurons and incubate at 4 °C for 48 h (*see* **Note 33**).
2. On the day of plating neurons, aspirate PLO from the wells and wash them 3 times with sterile water with 10 min incubation each.
3. After the last wash, incubate the plate with laminin at 37 °C for at least 2 h before plating the cells.
4. To plate the cells, remove laminin and add 500 μL of cNMM followed by plating of neurons. Plate 150,000 neurons/well after dissociation.

3.4.2 Preparation of Plates with a Monolayer of Astrocytes

This protocol describes the volume of solutions required for each well in a 24-well plate.

1. Serum-free, primary rat cortical astrocyte-enriched culture can be generated as described previously [18].
2. To obtain a uniform astrocyte monolayer, plate the glia 4 days before plating of neurons. Add 500 μL of warm sfRCAM/well to PLO-coated plates.
3. Dissociate astrocytes using accutase and plate 50,000 glia/well in a 24-well plate.
4. On the day of plating dopaminergic neurons, replace sfRCAM with cNMM 2–3 h before plating neurons. Plate 150,000 neurons/well after dissociation.

3.5 Dissociation and Plating of Differentiated Dopaminergic Neurons

1. After Ara-C treatment post patterning, aspirate the medium from the wells and carefully wash the cells with warm PBS (*see* **Note 34**).
2. Aspirate the PBS and add 5 mL/10 cm dish warm accutase. Incubate at 37 °C for 20 min (*see* **Note 35**).
3. Collect accutase-treated cells with 10 mL of warm NB media in a conical tube and pellet the cells at 200 g for 5 min.
4. Aspirate the medium and resuspend the pellet in 1 mL of warm cNBM. Triturate the cells 15–20 times with P1000 to break the pellet and to obtain a homogenous suspension of cells. Add another 1 mL of warm cNBM to the cells and filter the cell suspension through a 70 μm nylon cell strainer to remove any cell clumps (*see* **Note 36**).
5. Count the cells using a hemocytometer or an automated cell counter. Adjust the volume of the cell suspension to have 150,000 neurons/100 μL of the medium.

6. Gently plate 100 μL of the cell suspension per well in a 24-well plate and very carefully incubate the plate at 37 °C (*see* **Note 37**).
7. Maintain the neurons on cNBM with 40% medium change every 3 days until used for experiments (*see* **Note 38**).

4 Notes

1. Thaw matrigel for 4–5 h at 4 °C for aliquoting. Since thawed, liquid matrigel can form a gel at room temperature, it is important to pre-cool labeled tubes and tips to be used for aliquoting. Snap freeze the aliquots using dry ice and store at −80 °C for prolonged stability of up to 6 months. We recommend making working size aliquots of 30, 60, 90, and 120 μL in 2 mL tubes that can be easily thawed by adding 1 mL of PBS/DMEM-F12 and then making up the final volume.
2. Reconstitute 50 mg PLO in 1 mL of 0.15 M sterile Borate buffer to make a stock of 50 mg/mL. Make 50 μL aliquots, and store at −20 °C. Working dilution should be freshly prepared and sterilized using a 0.2 μm filter before use.
3. Laminin stock should be thawed for 2–3 h at 4 °C, aliquoted (e.g., 25 μL) in pre-cooled labeled tubes, and stored at −80 °C. Plates can be coated with just enough laminin to cover the well surface.
4. EDTA powder dissolves only when the pH of the solution reaches around 8.0. Therefore, to get EDTA easily dissolved, slowly add 5 M NaOH until the EDTA solution reaches a pH of 8.0.
5. Thaw accutase overnight at 4 °C, make 5 and 10 mL aliquots and store at −20 °C to avoid repeated freeze-thaw cycles.
6. Thaw KOSR overnight at 4 °C, make 10 mL aliquots and store at −20 °C to avoid repeated freeze-thaw cycles.
7. Keep DMSO protected from light by covering the tube with aluminum foil.
8. BSA should be kept on ice all the time during use. It is recommended to make 1 mL aliquots of 7.5% BSA and store at −20 °C for extended stability.
9. Prepare the medium following the manufacturer's instructions. Make 45 mL aliquots, and freeze at −20 °C for later use. Thaw the medium at 4 °C one day before use. Since this medium contains a lot of growth factors, bring it to room temperature for 30 min and then warm shortly at 37 °C for 5 min before use.

10. β-mercaptoethanol is very unstable in solution and therefore it is recommended not to store this medium for more than 3–4 days.
11. Protect this medium from light. The medium does not need to be warmed at 37 °C, room temperature is enough. White precipitate might form upon mixing DMSO and KOSR in the media. They will go off by mixing for 1–2 min. This medium should always be prepared fresh on the day of use.
12. Small molecules and growth factors are mostly sold as lyophilized powder that tends to stick to the walls and lid of the vial. Collect down the contents of the vial by centrifuging at 900 rpm for 2 min before opening the vial.
13. Reconstitution should be done in steps. e.g., when the final volume is 1 mL, first add 500 μL of reconstitution agent like water/DMSO/BSA to the vial and incubate it on ice for 10 min (except for reagents dissolved in DMSO as it will freeze at 4 °C). Take a sterile 1.5 mL tube and transfer the dissolved 500 μL of the substance to it. Now 'wash' the original vial with another 250 μL of the reconstitution agent and add it to the first 500 μL collected in a 1.5 mL tube. Repeat this step to achieve a final volume of 1 mL. Such stepwise reconstitution allows collecting any undissolved powder sticking to the walls of the original vial.
14. Perform all reconstitutions under sterile culture conditions. To avoid weighing small molecules and growth factors, predetermine their required amount to be ordered based on usage. Weighing, if necessary, should be done under sterile conditions or the small molecule or growth factor weighed under non-sterile conditions should be filter-sterilized before aliquoting. Since most of the small molecules and growth factors are reconstituted in small amounts (1–2 mL), filter-sterilization usually results in a massive loss of volume and potential binding of the concentrated factors to the filter's membrane resulting in a variable stock concentration. We, therefore, recommend maintaining sterile conditions during the reconstitution and aliquoting steps. If sterility of any component is doubtful, it is recommended to filter-sterilize the culture media using a 0.20 μm filter after the addition of small molecules and growth factors.
15. All small molecules and growth factors should be aliquoted at predetermined volumes to avoid repeated freeze-thaw cycles. We recommend two aliquot sizes that should be sufficient for small (e.g., 10 mL) and higher volumes (e.g., 50 mL) of culture media. For prolonged stability of up to 6 months, small molecules should be stored at −20 °C, and growth

factors should be stored at −80 °C. Thaw growth factors on ice before use. Thawed growth factors can be stored at 4 °C for up to 1 week.

16. Use up to 1.5 mL matrigel per well in a 6-well plate or 3 mL for a T25 flask. Plates can be pre-coated with matrigel and stored at 4 °C for up to 1 week.
17. Keep swirling the cryovial in the water bath until only a small sphere of ice remains. At this point, take the cryovial to the hood and transfer the cells to a prefilled conical tube with the medium. This helps to minimize exposure of cells to the high DMSO concentrations present in the cryoprotectant suspension. Cell suspension should be added to the medium in a gentle, drop-wise manner using a P1000 pipette.
18. Resuspension of the cells should be done gently. This is best done by setting P1000 at 800 μL and resuspending gently as it avoids the formation of froth.
19. Usually one million cells are plated per well. If the number of cells in the cryovial is unknown, and the pellet (milky white) looks very small, it is advised to plate the cells in just one well to allow better survival.
20. If the cells are more than 60% confluent, change the medium without adding RI. If there are a lot of dead cells, replace the medium with fresh RI to allow better survival of the remaining cells.
21. iPSC must maintain an undifferentiated morphology at all times. Irregular medium change is usually a major reason for spontaneous differentiation that results in a heterogeneous population of cells and inefficient differentiation.
22. Whenever the cells are split, they should be plated in the medium containing RI as it allows better attachment and survival of iPSCs. When splitting a 75–80% confluent well, the splitting ratio can be kept between 1:4–1:6 to allow a good cell survival and density. EDTA-based splitting usually results in clumps of cells that cannot be counted. If the cells do not come off easily with EDTA, or if a definite number of cells has to be plated, replace EDTA with accutase.
23. Each 75–80% confluent well of a 6-well plate can be used to make 2 cryovials to have a good density of cells for thawing. Cryomedium contains a high amount of DMSO that is toxic to cells. Therefore, prolonged incubation of cells in cryomedium in a non-frozen state should be strictly avoided. To achieve a uniform cell suspension, invert the tube 2–3 times.
24. This step helps to accustom the cells to new media. If there is a lot of cell death after one day of culture in NPM, feed the cells by replacing the old medium with fresh NPM.

25. Too rigorous mixing while resuspension will result in increased cell death. Pipetting up and down 2–3 times with a P1000 pipette is sufficient to resuspend the cells. It is recommended to pool the cells from two wells to generate a good number of EBs.
26. If good spheres are already seen on day 1, then proceed with the medium change. Else wait for one day.
27. This step needs to be done carefully as at the initial stages EBs are small and it will take 4–5 min for EBs to settle well at the bottom. The medium might appear a bit turbid due to dead cells. In the following days, EBs grow bigger and are easy to settle, and the medium gets much clearer as the dead cells are removed.
28. After placing the dish in the incubator, swirl it 2 times clockwise and once in a counter-clockwise motion to ensure a uniform spread of EBs.
29. If the EBs do not attach or come off during medium changes, increase the matrigel concentration to 1:80. Once the cells start to differentiate, EBs usually do not detach afterward. 40–50 EBs per plate is a good density to start differentiation.
30. Cells would still proliferate during patterning. The amount of media to be added might need to be increased if the density gets too high. An easy way to access it is by observing the medium color. If medium turns yellow within a day, either add more medium on the day of medium change or perform medium changes more often.
31. Ara-C treatment to restrict the proliferation of mitotic cells is important since there are a lot of undifferentiated cells that would interfere with the downstream assays.
32. The surface is usually chosen depending on the duration of culture duration and downstream applications. If the experiments will be performed within a week of plating, glial cells are not required. To avoid neuronal clumping in a long-term culture or for downstream assays measuring neuronal activity, plating on glial cells is strongly recommended.
33. 500 μL of PLO and 300 μL of laminin are sufficient to cover a well in a 24-well plate. For other formats, the amount of PLO or laminin sufficient to cover the surface should be chosen.
34. Cells might appear as an easily detachable film and therefore washing should be done very carefully. If the cells are already detached as a thin layer, collect them in a conical tube centrifuge at 50 g for 2 min. Aspirate the medium and then wash the cells once with PBS.
35. Do not stop accutase treatment as soon as the layer of cells detaches from the plate as this is not sufficient to form single

cells. If the cells were collected in a conical tube in the previous step, then accutase treatment can be done in the same tube by incubating at a 37 °C water bath.

36. Breaking the clumps requires rigorous trituration to form single cells. Passing through a cell strainer is required only if trituration does not result in single cells.
37. Care should be taken to pipette the cells in the center of the well. Cells suspension tends to move toward the edge of the wells and therefore extreme care should be taken when placing the plate with freshly plated cells in the incubator. Close the door very carefully.
38. Do not aspirate the medium using a suction pump as neurons are very delicate. The best way is to use P1000 to remove and add the media gently.

References

1. Takahashi K, Yamanaka S (2006) Induction of pluripotent stem cells from mouse embryonic and adult fibroblast cultures by defined factors. Cell 126:663–676. https://doi.org/10.1016/j.cell.2006.07.024
2. Takahashi K, Tanabe K, Ohnuki M et al (2007) Induction of pluripotent stem cells from adult human fibroblasts by defined factors. Cell 131: 861–872. https://doi.org/10.1016/j.cell.2007.11.019
3. Inoue H, Nagata N, Kurokawa H, Yamanaka S (2014) iPS cells: a game changer for future medicine. EMBO J 33:409–417. https://doi.org/10.1002/embj.201387098
4. Rowe RG, Daley GQ (2019) Induced pluripotent stem cells in disease modelling and drug discovery. Nat Rev Genet 20:377–388. https://doi.org/10.1038/s41576-019-0100-z
5. Liu C, Oikonomopoulos A, Sayed N, Wu JC (2018) Modeling human diseases with induced pluripotent stem cells: from 2D to 3D and beyond. Dev 145:1–6. https://doi.org/10.1242/dev.156166
6. Schultz W (1997) Dopamine neurons and their role in reward mechanisms. Curr Opin Neurobiol 7:191–197. https://doi.org/10.1016/S0959-4388(97)80007-4
7. Hegarty SV, Sullivan AM, O'Keeffe GW (2013) Midbrain dopaminergic neurons: a review of the molecular circuitry that regulates their development. Dev Biol 379:123–138. https://doi.org/10.1016/j.ydbio.2013.04.014
8. Wang S, Zou C, Fu L et al (2015) Autologous iPSC-derived dopamine neuron transplantation in a nonhuman primate Parkinson's disease model. Cell Discov 1:1–11. https://doi.org/10.1038/celldisc.2015.12
9. Klapper SD, Garg P, Dagar S et al (2019) Astrocyte lineage cells are essential for functional neuronal differentiation and synapse maturation in human iPSC-derived neural networks. Glia 67:1893–1909. https://doi.org/10.1002/glia.23666
10. Kriks S, Shim J-W, Piao J et al (2012) Floor plate-derived dopamine neurons from hESCs efficiently engraft in animal models of PD. Nature 480:547–551. https://doi.org/10.1038/nature10648.Floor
11. Ng YH, Chanda S, Janas JA et al (2021) Efficient generation of dopaminergic induced neuronal cells with midbrain characteristics. Stem Cell Rep 16:1763–1776. https://doi.org/10.1016/j.stemcr.2021.05.017
12. Wang C, Ward ME, Chen R et al (2017) Scalable Production of iPSC-Derived human neurons to identify Tau-lowering compounds by high-content screening. Stem Cell Reports 9: 1221–1233. https://doi.org/10.1016/j.stemcr.2017.08.019
13. Chambers SM, Fasano CA, Papapetrou EP et al (2009) Highly efficient neural conversion of human ES and iPS cells by dual inhibition of SMAD signaling. Nat Biotechnol 27:275–280. https://doi.org/10.1038/nbt.1529
14. Kirkeby A, Grealish S, Wolf DA et al (2012) Generation of regionally specified neural

progenitors and functional neurons from human embryonic stem cells under defined conditions. Cell Rep 1:703–714. https://doi.org/10.1016/j.celrep.2012.04.009

15. Mahajani S, Raina A, Fokken C et al (2019) Homogenous generation of dopaminergic neurons from multiple hiPSC lines by transient expression of transcription factors. Cell Death Dis 10:898. https://doi.org/10.1038/s41419-019-2133-9
16. Pfrieger FW (2010) Role of glial cells in the formation and maintenance of synapses. Brain Res Rev 63:39–46. https://doi.org/10.1016/j.brainresrev.2009.11.002
17. Kucukdereli H, Allen NJ, Lee AT et al (2011) Control of excitatory CNS synaptogenesis by astrocyte-secreted proteins Hevin and SPARC. Proc Natl Acad Sci USA 108:E440–E449. https://doi.org/10.1073/pnas.1104977108
18. Schroeter CB, Herrmann AM, Bock S et al (2021) One brain—all cells: a comprehensive protocol to isolate all principal cns-resident cell types from brain and spinal cord of adult healthy and eae mice. Cells 10:1–25. https://doi.org/10.3390/cells10030651

Chapter 5

Prime Editing of Mouse Primary Neurons

Colin D. Robertson, Ryan R. Richardson, Marilyn Steyert, Corinne A. Martin, Corey Flynn, and Alexandros Poulopoulos

Abstract

Prime editing is a hybrid genome editing technology that introduces small edits on the genome with high precision. It combines nickase Cas9 with reverse transcriptase to prime and synthesizes edited DNA from RNA, reducing unintended insertions and deletions on the genome. This protocol describes the design of prime editing guide RNAs (pegRNAs), cloning of plasmids, nucleofection of mouse primary neurons, and preparation for next-generation sequencing. Directions are given for pegRNA and PE3b gRNA design and construction using PegAssist, a publicly available webtool and plasmid set. Prime editing in neurons allows genome manipulation while maintaining endogenous gene expression, making it ideal for studying protein structure/function relationships and pathogenic variants in a native neuronal context.

Key words Prime editing, CRISPR, Neurons, Genome editing, pegRNA, Nucleofection, PegAssist

1 Introduction

The advent of genome editing technologies has been a boon for biomedical research. CRISPR/Cas9-based editing in particular has provided unmatched control over genomic sequences both in vitro and in vivo. Cas9-based techniques broadly operate through the association of the Cas9 nuclease with a guide RNA which directs the complex to a specific genomic locus [1, 2]. Once bound to the target sequence on genomic DNA (**gDNA**), Cas9 induces a double-strand break (**DSB**) at a defined position. The DSB activates the non-homologous end joining (**NHEJ**) machinery for repair, but with repeated cleavage and ligation the error rate in this process causes insertions and deletions (**indels**) on nucleotides resulting in frameshift mutations and a functional knock-out (**KO**) of the gene of interest [1, 3–6]. This strategy is highly effective for frameshift and loss-of-function mutations. However, when wanting

Tolga Soykan and Alexandros Poulopoulos (eds.), *Synapse Development: Methods and Protocols*, Methods in Molecular Biology, vol. 2910, https://doi.org/10.1007/978-1-0716-4446-1_5,

to study specific mutations for structure-function analyses, or to study the effects of specific variants associated with disease, more refined editing techniques are required [7].

Earlier advances in specific genome editing approaches included homology-directed repair (**HDR**)-mediated genomic knock-in (**KI**) and base editing. While each improves on the specificity of genomic outcomes, they are still limited in application. HDR methods rely on DSB, which increases the propensity of indels [8]. Base editors do not cause indels, but do have specificity issues when it comes to nearby bases, and are currently limited to four transition mutations (A > G, G > A, T > C, and C > T). Additionally, both strategies are prone to widespread off-target effects.

An alternative genome editing strategy, termed Prime Editing (**PE**), uses Cas9 targeting of specific sequences on the genome without causing DSBs, limiting indels and off-target editing [9]. To prevent DSBs, PE uses the H840A nickase variant of Cas9 (**nCas9**) [1], which cuts only the non-complementary strand of DNA. nCas9 is fused to an engineered reverse transcriptase (**RT**) which synthesizes DNA with the desired edit based on an RNA template (Fig. 1). Both the guide RNA (**gRNA**) that targets the nCas9 and the template RNA for the RT are encoded in a single prime editing guide RNA (**pegRNA**) containing four sequence modules: spacer (a standard guide sequence designed for all CRISPR/Cas9 applications), scaffold (required for Cas9 binding),

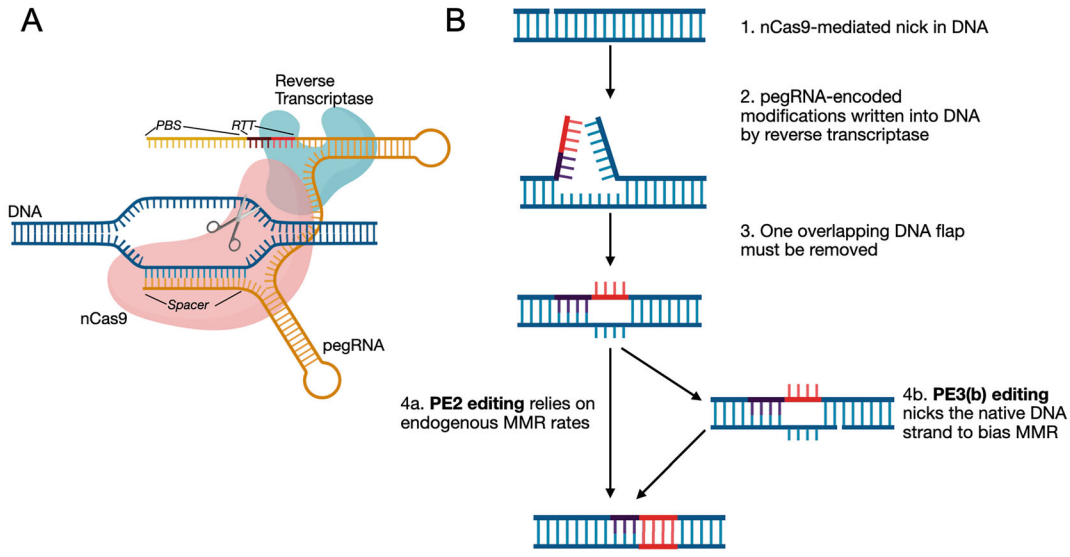

Fig. 1 Mechanism of prime editing. A. Schema representing prime editor (pink nCas9 and blue reverse transcriptase) bound to target DNA (dark blue) with relevant regions labeled. B. The target DNA progresses through four stages for successful incorporation of the written strand (red and purple). PE3 strategy is depicted on the left, and PE3b strategy is shown on the right. (Created with BioRender.com)

primer-binding sequence (PBS; will hybridize to the cleaved 3′ strand of DNA to prime the RT), and reverse transcriptase template (RTT; encodes the desired edit). Successful incorporation of the desired edit is dependent on two molecular coin flips: first the incorporation of transcribed product, and second the correction of the newly formed mismatch. The mismatch repair can be biased by the inclusion of a second nicking gRNA in an approach termed PE3 (there is also PE3b which binds and nicks after RT activity due to proximity to the spacer PAM sequence) [9]. The PE3 approach increases efficiency at the cost of also increasing indel rates (these still tend to be minority products unlike DSB approaches), so specific experimental considerations should be weighed when selecting an approach [9].

All told, PE approaches allow for highly specific genome editing while maintaining design flexibility, reducing indels, and nearly eliminating off-target effects. The major sacrifice of this approach is its low efficiency for larger edits, though adaptor technologies are being developed to mitigate that.

Prime editing excels at precisely introducing point variants or small and specific insertions and deletions. Although limited in applications, this aligns well with the needs of neuroscience research. In addition to aiding in studies of protein structure and function, almost 70% of the 6000 known monogenic diseases affect the nervous system [10]. The high precision of this editing approach enables genome editing without stringent requirements for selection and expansion of correct edits. This could expand the utility of powerful in vitro models like primary neuronal cultures for structure/function studies, analysis of single-nucleotide variants [11–13], and even correction of pathogenic variants. This protocol will focus on nucleofecting prime editing plasmids in developing neurons in culture: pegRNA design, cloning, nucleofection, primary neuron culture, and preparation for next-generation sequencing of the gene target.

2 Materials

2.1 Cloning and Preparation of Plasmid Containing pegRNA and PE3b gRNA Plasmids

1. Synthesized pegRNA fragment (sequence given by PegAssist.app).
2. Forward and reverse oligonucleotides for PE3b (sequence given by PegAssist.app).
3. Plasmids:

   P457 (pJ2.2.U6 < pegRNA scaffold), Addgene plasmid #226288.

   P396 (pJ2.U6 < gRNA scaffold), Addgene plasmid #226289.

   P387 (pJ2.17v2), Addgene plasmid #226290.

4. Primers:
   prRR940 (pegRNA_1.0_F): GGTCTCAggagTTTCCCC-GAAAAGTGCCAC.
   prRR918 (pegRNA_2.0_R): GGTCTCAagtaGCCGATTCA TTAATGCAGCG.
   prRR941 (PE3b_2.0_F): GGTCTCAtactTTTCCCCGAAAA GTGCCAC.
   prRR921 (PE3b_7.0_R): GGTCTCAagcgGCCGATTCA TTAATGCAGCG.
5. BbsI and BsaI restriction enzymes.
6. T4 DNA ligase and 10x ligase buffer.
7. Chemically competent *E. coli*.
8. SOCS medium.
9. LB agar plates supplemented with ampicillin.
10. LB supplemented with ampicillin.
11. Plasmid miniprep kit.
12. Polymerase master mix and PCR buffer (*see* **Note 1**).
13. DNase-free water.
14. Gel DNA recovery/extraction kit.
15. PCR tubes.
16. Agarose.
17. Glycerol.
18. Cryogenic Tubes.
19. Sterile cotton swab.
20. Plasmid miniprep kit.

2.2 Neuron Culture and Nucleofection

1. P0 mouse pups (*see* **Note 2**) (Approximately 2 pups per 9.5 cm^2 culture plate).
2. poly-L-lysine.
3. Glass coverslips (*see* **Note 3**).
4. Borosilicate Pasteur pipettes.
5. Sterile, autoclaved MilliQ water.
6. Culture Medium—Neurobasal Plus with 1x B-27 Plus and Penicillin-Streptomycin (*see* **Note 4**).
7. Dissection medium—1x HBSS (Mg- and Cl-), 10 mM HEPES, 30 mM glucose, and 12 mM magnesium sulfate in MilliQ water; filter sterilize through 0.22-micron filter.
8. Papain.

9. 10x Papain activation buffer—68 mM Cysteine-HCL, 0.01% β-mercaptoethanol, and 12 mM EDTA pH 8.0 in MilliQ water; filter sterilize through 0.22-micron filter.
10. Activated papain solution—1:1 papain with 2x papain activation buffer (*see* **Note 5**).
11. Electroporation medium—Combine 120 mM KCl, 10 mM KH_2PO_4, 2 mM EGTA, 25 mM HEPES, 5 mM $MgCl_2$, and 0.5 mM $CaCl_2$ adjusted pH 7.5–7.6. Add 5 mM reduced glutathione GSSG and 2 mM ATP immediately before use or freezing. This can be stored at −80 °C (*see* **Note 6**).
12. Plasmid expressing pegRNA/PE3(b) (constructed and prepared in **part 2**).
13. Plasmid TU516 pJ2.CAG < EGFP-2A-PE2.
14. 15 mL screwcap tube.
15. Latex pipette bulb.
16. 15 mL pipettes.
17. 50 mL conical tubes.
18. Trypan blue.
19. Hemocytometer.
20. Microcentrifuge tubes.
21. 0.4 cm electroporation cuvettes.

2.3 Instrumentation

1. Thermocycler.
2. Shaking heat block.
3. Nanodrop or spectrophotometer.
4. Autoclave.
5. Laminar flow hood.
6. Amaxa Nucleofector II.
7. CO_2 incubator.

2.4 Software

1. Genome browser genome.ucsc.edu or benchling.com.
2. Pegassist.app or other pegRNA design tool.

3 Methods

3.1 Design of pegRNA and PE3(b) Guides

1. Import the desired gene of interest using the Benchling.com gene importer. If not using benchling, the following steps can also be completed using UCSD Genome Browser, NCBI gene viewer and Ensembl to identify specific gene regions.
2. Identify and annotate specific locus intended for editing (*see* **Note 7**).

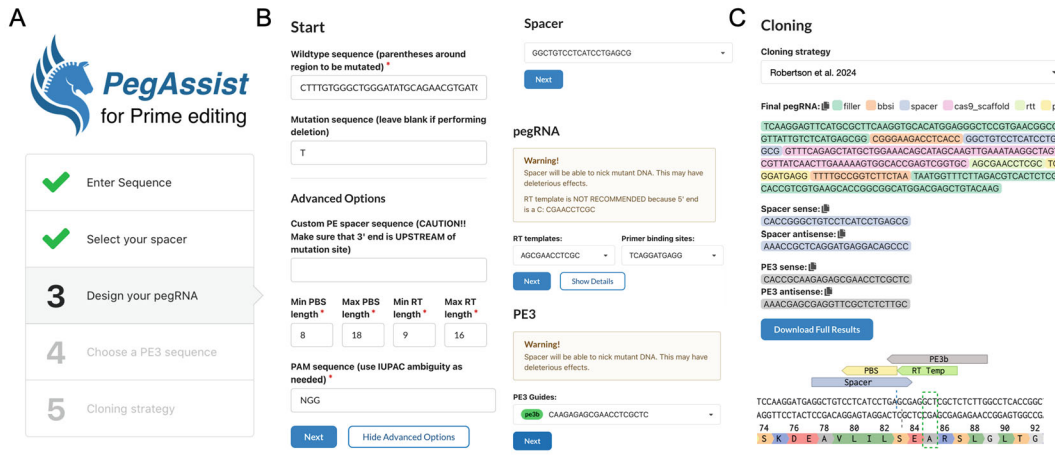

Fig. 2 Using PegAssist.app to design prime editing guides. (**a**) The PegAssist.app workflow. (**b**) An example wildtype sequence and mutation sequence allows PegAssist.app to generate options for Spacer, RT Template, Primer binding site (PBS), and optional PE3(b) guides. PegAssist will display relevant warning messages dependent on the sequence and provide final options to facilitate cloning. (**c**). Alignment of the chosen pegRNA and PE3b guide regions on the target DNA. The direction and orientation of spacer, PBS, and RT template in relation to one another is crucial for successful prime editing. Nicking sites for the pegRNA (blue dashed line) and PE3b guide (gray dashed line), and the region to be modified (green dashed box) are shown on the DNA sequence. (Partially created with Benchling.com)

3. Copy the nucleotide sequence with 150 bases upstream and downstream of the intended edit.
4. Paste the sequence in a separate document labeled "Wild-type sequence."
5. Copy and paste ~300 nucleotide sequence in the "Wildtype sequence" box on pegassist.app. PegAssist provides a user-friendly interface to design and select optimal pegRNAs (Fig. 2), though other pegRNA design tools can be used equivalently (*see* **Note 8**).
6. In the "Mutation sequence" box, input the sequence desired within the parentheses. Example inputs:

   Substitution G > T

   Wildtype: GATC(G)TGTCC;

   Mutation sequence: T

   Deletion

   Wildtype: GATC(G)TGTCC;

   Mutation sequence: *leave blank*

   Insertion

   Wildtype: GATC()GTGTCC;

   Mutation sequence: A

7. Prime editing parameters can be left at the default settings for initial designs.

   PBS length: 8–18 nucleotides

   RTT length: 9–16 nucleotides

   PAM sequence: NGG

8. PegAssist will display available spacer sequences. Once a spacer sequence is selected (*see* **Note 9**), the options for compatible PBS and RTT are listed (*see* **Note 10**). Select the desired spacer, PBS, RTT, and optional PE3(b) (*see* **Note 11**) sequences.
9. Double check the compatibility of these parts by annotating the known genomic sequence. Copy these individual selections and paste into a separate file. Annotate the Wild-type sequence to confirm the sequences will bind in the desired locations and orientation (*see* **Note 12**).
10. Order the oligonucleotides and double-stranded DNA fragment required for cloning (*see* **Note 13**). PegAssist will display the parts with necessary cloning elements in the "Cloning" section.

3.2 Cloning of pegRNA

The following steps will produce a single vector with the pegRNA and PE3(b) guides present in duplex and under the control of independent U6 promoters. This is beneficial for downstream applications as it limits the total number of plasmids required for prime editing.

3.2.1 Preparing the pegRNA

1. Bring the synthetic pegRNA to a concentration of 100 ng/μL using DNAse/RNAse-free water (*see* **Note 14**).
2. Perform a Golden Gate Assembly (GGA) to subclone the pegRNA into the first vector backbone. In a PCR tube, mix 100 ng of the pegRNA, 100 ng P457, 1 μL BbsI, 1 μL T4 DNA ligase, and 2 μL 10x T4 ligase buffer. Bring the final volume of 20 μL using DNAse/RNAse-free water.
3. Place the PCR tube in a thermocycler and run a standard GGA protocol for 15–50 cycles (*see* **Note 15**).
4. Transform the GGA mixture using the following method: Add 4 μL of the resulting mixture to TOP 10 chemically competent *E. coli* or an equivalent strain. Rest on ice 30 min. Heat-shock the mixture at 42 °C for 30 s in a heating block (*see* **Note 16**). Return to ice for 2 min. Add SOCS medium using sterile technique and incubate at 37 °C with shaking for 30 min. Plate this mixture on LB agar plates supplemented with ampicillin and incubate overnight at 37 °C.
5. Using a sterile pipette tip, pick individual colonies and inoculate small volumes (~4 mL) of LB supplemented with ampicillin. Grow these liquid cultures overnight at 37 °C with shaking.

6. Pellet the cultures by centrifugation. Extract plasmid DNA using a plasmid miniprep kit according to the manufacturer's protocol and sequence the plasmid using a U6 universal primer (*see* **Note 17**) to confirm proper insert of the pegRNA. Select one clone with the correct sequence and proceed to the next step.
7. Perform a PCR on the pegRNA plasmid using primers prRR940 and prRR918. Combine 100 ng of the pegRNA plasmid, 10 ng each primer, 12.5 μL KAPA HiFi HotStart ReadyMix, and DNAse-free water in a final volume of 25 μL. A standard hot start PCR protocol can be used with a 60 °C annealing temperature and 1 min extension time.
8. Run the PCR product on a 1% agarose gel and purify the 740 bp band using a Gel DNA Recovery/Extraction Kit according to the manufacturer's instructions. Save this purified PCR band at 4 °C as "Part I" for a future GGA.

3.2.2 Preparing the PE3 (b) Guide

1. Resuspend the forward and reverse oligonucleotides for the PE3(b) guide in DNase/RNase-free water to a final concentration of 100 μM. Add 1 μL of each oligo to a PCR tube with 1 μL 10x T4 ligase buffer and 7 μL DNase/RNase-free water. Place the sample in a thermocycler and denature at 95 °C for 5 min followed by a descending temperature ramp of 0.1 °C per second to 25 °C to anneal the oligos.
2. Perform a GGA using 1 μL annealed oligo mixture, 100 ng P396, 1 μL BbsI, 1 μL T4 DNA ligase, 2 μL 10x T4 ligase buffer, and DNase/RNase-free water to a final volume of 20 μL.
3. Repeat the steps from the pegRNA cloning section to perform a GGA, transform in *E. coli*, culture, miniprep plasmids, and sequence with a U6 universal primer.
4. After confirming proper plasmid sequence perform a PCR as above using primers prRR941 and prRR921. Run the product on a 1% agarose gel and purify the 1000 bp band using a Gel DNA Recovery/Extraction Kit according to the manufacturer's instructions. Save this purified PCR band at 4 °C as "Part II" for a future GGA.

3.2.3 Constructing the pegRNA/PE3(b) Plasmid

1. Perform a GGA using 100 ng Part I, 100 ng Part II, 100 ng P387, 1 μL BsaI, 1 μL T4 DNA ligase, 2 uL 10x T4 ligase buffer, and DNase/RNase-free water to a final volume of 20 μL. Place this reaction tube in a thermocycler and run a GGA protocol with 50 cycles.
2. Refer to the steps above to transform the GGA and culture the bacteria to isolate plasmid clones. Confirm the sequence by Sanger sequencing using primer prRR945.

3. Make a glycerol stock of the bacteria containing the proper sequence by combining 800 μL of bacteria in suspension in LB broth with 500 μL sterile 80% glycerol in a cryogenic tube. Store the glycerol stock at −80 °C. This stock can be used to prepare plasmid DNA for experimental applications.
4. Using the wooden end of a sterile cotton swab, scrape the top layer of the glycerol stock and use this to inoculate 220 mL LB broth supplemented with ampicillin in a 1 L flask (*see* **Note 18**). Incubate the flask at 37 °C with shaking overnight up to 18 h. Use a Plasmid Midiprep Kit to purify the plasmid DNA. Quantify the total DNA concentration using a NanoDrop Spectrophotometer by applying 1.5 μL plasmid to the NanoDrop (*see* **Note 19**).
5. For short-term storage and repeated use, keep plasmid DNA at 4 °C. For long-term storage, keep the DNA at −20 °C. Aliquot as needed to avoid repeated cycles of freeze/thaw.

3.3 Primary Culture of Neonatal Mouse Cortical Neurons and Nucleofection of Prime Editing Plasmids

1. Two days prior to culturing neurons, prepare culture dishes and pipettes. Coat dishes with poly-L-lysine (P4832) by adding a 1/12 solution of poly-L-lysine in 1x PBS equal to the culturing volume of the dish/plate. Incubate this dish in a cell culture incubator until the day of culture. Borosilicate Pasteur pipettes should be flame-polished by rotating the tip over the flame of a Bunsen burner to decrease the size of the opening and round the glass edges (*see* **Note 20**). Autoclave the flame-polished pipettes and place in a sterile laminar flow hood in preparation for culturing.
2. At least one hour prior to culturing cells, while working in a sterile laminar flow hood, aspirate the poly-L-lysine from the culture dish and wash 3x with equal volume sterile water. Add culture medium to the dish and return to cell culture hood.
3. On the day of cell culture prepare dissection medium and activated papain buffer (*see* **Note 21**). Warm electroporation medium to room temperature. Measure and mix DNA in microcentrifuge tubes (*see* **Note 22**).
4. Fill a 50 mm petri dish with ice-cold dissection media. Under a dissecting microscope, dissect the brain of a p0 mouse neonate by first euthanizing via rapid decapitation using sterilized surgical scissors. Grasp the head using a Kimwipes tissue and make an incision in the scalp along the midline of the skull. Pull pack the skin layer to expose the underlying skull and cut the skull along the midline. Peel the skull away from the incision site using sterile tweezers to expose the brain. Remove the brain to the dish with cold dissection media.
5. Under a dissecting microscope, remove the cerebellum. Remove the pia from the cortical surface using sharp-tipped tweezers and separate the hemispheres (*see* **Note 23**). Cut and

discard the subcortical structures from the overlying cortex for both hemispheres. Transfer the cortical tissue to a 15 mL screwcap tube containing 1 mL dissection media on ice.

6. While working in a sterile laminar flow hood, aspirate the dissection media until around 0.5 mL remains with the cortical tissue. Add 30 μL activated papain solution and incubate in a 37 °C water bath for 30 min.
7. Return the tube containing cortical tissue to the laminar flow hood. Inactivate papain by washing tissue 3x with 10 mL dissection media (*see* **Note 24**). Add 5 mL growth media to tissue pieces. Using a flame-polished Pasteur pipette with a latex pipette bulb, gently triturate the tissue 4–8 times. Use a 15 mL pipette to transfer the cell suspension. Pass the suspension through a 70 μm cell strainer into a 50 mL conical tube. Bring the total volume of the suspension to 10 mL. Take a 10 μL sample of the suspension and transfer to a tube containing 10 μL trypan blue. Pipette this mixture into a hemocytometer and count viable cells in each quadrant to estimate the density of viable cells.
8. For a 6-well plate aliquot the suspension to microcentrifuge tubes so that at least 720,000 cells are present in each aliquot (*see* **Note 25**). For other plate sizes a density of 75,000 cells/cm^2 should be retained.
9. Spin down the cells at 1000 RCF for 2 min.
10. In the laminar flow hood, aspirate and discard the media. Resuspend the pelleted cells in 300 μL of electroporation buffer. Add 1–3 μg of DNA mixture. Gently transfer this suspension to a 0.4 cm electroporation cuvette. Place the cuvette in an Amaxa Nucleofector II and select program O-005. Immediately after electroporation transfer the cell suspension to the coated culture dish containing pre-warmed culture media (*see* **Note 26**). Incubate the cells in a cell culture incubator. After four hours, replace the medium with fresh, prewarmed growth medium to remove non-adherent cell debris.
11. Change medium again 24 h after plating.
12. Results of the nucleofection should be detectable by fluorescence within 24–48 h of nucleofection (*see* **Note 27**). The efficiency of co-electroporation can be appreciated by the fluorescence imaging of neurons and glia at DIV 2 (Fig. 3).
13. Media should be changed every other day by removing 50% of the total culture media and replacing with fresh, prewarmed culture media. Transfected cells can be identified by green fluorescence encoded on the TU516 plasmid.

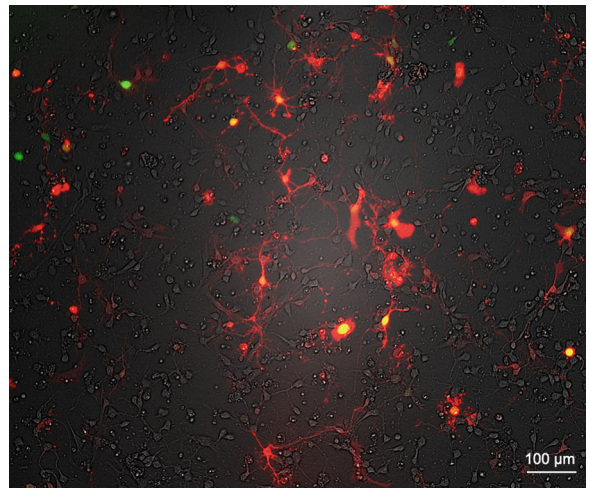

Fig. 3 Primary cortical culture following AMAXA nucleofection. A. Cells include neurons and glia shown at DIV 2 following plasmid nucleofection. RFP (red) and nuclear-GFP (green) on separate plasmids are co-electroporated to appreciate efficiency of co-expression. Observed overall efficiency is typically between 10–30%. Scale bar 100 µm

3.4 Preparation for Next-Generation Sequencing

While these cells can be used for a multitude of downstream assays, it is critical to first validate the editing approach. While deconvolution of Sanger sequencing is possible, it is unlikely to provide proper fidelity to detect and assay editing precision. Instead, next-generation sequencing (NGS) should be employed. The following steps will provide the necessary guidance to begin a NGS preparation. After these steps are followed, further library preparation can be done either by the user or passed on to a third-party company or core facility.

1. Design PCR oligos to amplify the region surrounding the desired edit. The resulting amplicon should be 250–500 base pairs in length, with at least 40% of the total length downstream of the PAM sequences recognized by the pegRNA and PE3 (b) guides. To make these oligos compatible with NGS applications, attach the following Illumina universal adapter sequences: Forward ACACTCTTTCCCTACACGA CGCTCTTCCGATCT—[Oligo Sequence] and Reverse GA CTGGAGTTCAGACGTGTGCTCTTCCGATCT—[Oligo Sequence] (*see* **Note 28**).
2. Genomic DNA can be isolated using the salting-out method [14] (*see* **Note 29**). Cells can be collected by the addition of minimal 0.25% trypsin/EDTA. Incubate cells at 37 °C for 5 min, then gently pipette to remove remaining adherent cells.

3. Transfer the suspended cells into a microcentrifuge tube containing 3-4x volume lysis buffer containing 0.2 mg/mL proteinase K, 150 mM NaCl, 10 mM Tris, 10 mM EDTA, and 0.1% sodium dodecyl sulfate. Incubate this tube at 55 °C overnight.
4. Add 0.5 total volume saturated NaCl to precipitate proteins. Mix by inversion and spin at max speed in a benchtop centrifuge for 2 min.
5. Retain the supernatant and ethanol precipitate by adding 0.1 total volume 3 M sodium acetate and 3 total volumes ice cold 100% isopropanol.
6. Chill at −80 °C for 20 min. Spin down at max speed at 4 °C for 10 min.
7. Remove the supernatant. Add ice-cold 100% ethanol to the pelleted DNA and mix by flicking the tube. Centrifuge at maximum speed at 4 °C for 10 min.
8. Remove the supernatant and dry the tube at room temperature. Resuspend the pellet in DNA resuspension buffer with 10 mM Tris pH 8.5 and 0.1 mM EDTA.
9. Quantify DNA concentration using a NanoDrop.
10. Use 10–50 ng of genomic DNA for a PCR using the oligos designed for NGS. Combine genomic DNA with 10 ng each primer, 12.5 μL KAPA HiFi HotStart ReadyMix, and DNase-free water in a final volume of 25 μL (*see* **Note 30**).
11. The resulting PCR product can be purified and used to generate an NGS library.

4 Notes

1. A high-fidelity polymerase should be used to decrease error rate when cloning. Commonly used polymerases are available with error rates lower than 0.5 in 10^5 nucleotides.
2. Approximately two mouse neonates will provide enough cells for a single 9.5 cm^2 culture plate.
3. Consider the size of the culture wells when selecting coverslips. If the coverslips are too large, removing them for fixation and mounting will be difficult. If mounted coverslips for imaging is not required, glass bottom plates can be used instead.
4. Culture medium should be aliquoted and kept frozen for long-term storage. An aliquot in active use can be stored at 4 °C for seven days.
5. Both the papain and the activation buffer will be suspensions requiring thorough mixing before pipetting.

6. Prolonged storage will oxidize glutathione and lower electroporation efficiency. Always note electroporation efficiency, and if substantial decreases are observed prepare fresh buffer.
7. Mismatches between the targeting guide RNA and the genomic locus will reduce editing efficiency. Multiple reference genome assemblies may be listed for any given species. Best practice would include checking the desired target locus across each assembly. Additionally, Sanger sequencing of the target locus using genomic DNA prepared from sample animals can eliminate uncertainty in the nucleotide sequence at the target locus.
8. PegAssist.app will aid in the design of and construction of prime editing guide RNAs, but other webtools exist. It may be beneficial to use multiple webtools to identify strong candidates for high editing efficiency. Other options include (*in alphabetical order*) Easy-Prime [15], PE-Designer [16], peg-Finder [17], PINE-CONE [18], PnB Designer [19], Prime-Design [20], and multicrispr [21].
9. The PBS and RTT sequences are determined by the site of the DNA nick and are therefore determined by the spacer sequence. For highest efficiency editing choose a spacer that has a compatible PE3b guide. If no spacers are displayed, a PAM sequence is not located within the search window. Increase the maximum allowable RTT length in the search parameters to expand the search window.
10. The resulting PBS and RTT sequences differ only in total length. A high-throughput analysis of pegRNAs found that the highest editing efficiency is achieved with a PBS 11- or 12-nt in length, and an RTT 12+/−2- nt in length [22]. There may still be variability in overall efficiency dictated by the genomic locus, so multiple pegRNAs can be designed and compared empirically.
11. Preference should be given for a PE3b guide over a PE3 guide. The PE3b guide will bind closer to the pegRNA cut site resulting in sequential binding and nicking of genomic DNA and decreasing rates of unintended gene knock-out [23].
12. The spacer should cut upstream (5′) of the desired edit. The PBS should bind on the strand opposite of the spacer. The RTT should directly abut the PBS and contain the desired mutation.
13. The “final pegRNA” displays the full pegRNA sequence with the selected spacer, PBS, and RTT as well as BbsI cloning sites and stretches of “filler” sequence. This sequence should be ordered as synthesized double-stranded DNA. The filler is only necessary if the company used to synthesize the pegRNA requires a minimum number of base pairs and will be removed in subsequent cloning steps. The “Spacer sense” and “Spacer

antisense" sections can be ignored if ordering the "final pegRNA" in full. The optional "PE3(b) sense" and "PE3 (b) antisense" sequences contain additional nucleotides for cloning compatibility and should be ordered as displayed from an oligonucleotide synthesis company (like IDT).

14. This pegRNA part can be used directly in a GGA, or it can be subcloned using a TOPO TA Cloning Kit (Thermo Scientific, K4575J10).
15. An example GGA protocol follows: (1) Initial digest at 37 °C for 15 min. (2) Digest at 37 °C for 2 min. (3) Ligation at 16 °C for 5 min. (4) Return to "**step 2**" 15–50 times. (5) Final digest at 37 °C for 15 min. (6) Heat inactivation at 65 °C for 20 min. (7) Hold at 4 °C. The final digest is meant to cleave any remaining backbone vector without the desired insert and should improve cloning success. Heat inactivation will destroy the enzymes and prevent ligation during the "Hold" step. When selecting the cycle number for a GGA, the major consideration is the number of parts being inserted into a backbone. With 1–2 inserts a 15-cycle GGA is typically sufficient. If cloning efficiency is low, the cycle number can be increased to 50.
16. For any steps involving a heating block, water can be added to the well prior to inserting a tube to distribute heat more evenly.
17. If the service provider does not offer commonly used universal primers, the following sequence can be ordered as an oligonucleotide to submit for Sanger sequencing: GACTATCATATGCTTACCGT.
18. The volume of this culture should not exceed ~1/5 total capacity of the culture flask. Larger volumes will not be properly aerated and plasmid quality and yield could be impacted. In this case, an extra 20 mL is initially added to account for evaporation during the long growth period.
19. The expected concentration of plasmid is 2–4 μg/μL. Check that the A260/A280 ratio is around 1.8. Values of 2.0 or above could suggest RNA contamination. Check that the A260/230 ratio is between 2.0 and 2.2. Lower values suggest impurities are present in the sample.
20. Flame polishing the pipettes is essential for cell viability and quality. The process rounds the edges at the opening of the pipette to reduce mechanical stress on the dissociated cells.
21. Dissection medium should be kept cold on ice. Activated papain should be incubated at 37 °C for at least 30 min before adding to tissue.
22. The plasmids should be mixed at an even molar ratio to promote co-electroporation.

23. The pia can be difficult to remove. Gently scrape the surface of the brain with sharp tweezers until the pia is slightly furrowed. Grab the furrowed region with the tweezers and pull parallel to the surface of the brain to peel the pia. If not properly removed dissociation of the tissue may be more difficult.
24. The tissue is very delicate and can easily be aspirated during pipetting. Allow the tissue to fully settle to the bottom of the tube before pipetting.
25. Viability of cells after nucleofection decreases dramatically if fewer cells are used in the suspension during the cuvette electroporation. For high viability, aim to have over 10^6 cells per electroporation.
26. After adding the cell suspension to the culture plate, rock the plate in a figure eight motion to promote even distribution of the cells.
27. Other plasmid transfection methods, including lipofection, polyethylenimine, or calcium phosphate co-precipitation also work with neurons. However, in our hands, the efficiency of plasmid transfection and co-transfection are order-of-magnitudes lower compared to nucleofection.
28. These NGS-compatible primers have a universal adapter sequence that is recognized in a second PCR during library preparation. Primers with unique barcode sequences will prime each sample independently and then samples can be pooled. The barcodes enable sorting of individual samples after sequencing.
29. As an alternative, there are also commercially available kits that make genomic DNA isolation from these samples easy and quick.
30. The annealing temperature for this PCR will be variable based on the design of the primers. Care should also be taken to avoid saturation during PCR. To test for saturation, a sample can be collected at the second to last cycle and compared to a sample from the final sample on an agarose gel. The amplicon should nearly double between these samples.

References

1. Jinek M, Chylinski K, Fonfara I et al (2012) A programmable dual-RNA-guided DNA endonuclease in adaptive bacterial immunity. Science 337(6096):816–821
2. Knott GJ, Doudna JA (2018) CRISPR-Cas guides the future of genetic engineering. Science 361(6405):866–869
3. Lykke-Andersen S, Jensen TH (2015) Nonsense-mediated mRNA decay: an intricate machinery that shapes transcriptomes. Nat Rev Mol Cell Biol 16(11):665–677
4. Haapaniemi E, Botla S, Persson J et al (2018) CRISPR-Cas9 genome editing induces a p53-mediated DNA damage response. Nat Med 24(7):927–930
5. Nambiar TS, Baudrier L, Billon P, Ciccia A (2022) CRISPR-based genome editing

through the lens of DNA repair. Mol Cell 82(2):348–388

6. Altas B, Romanowski AJ, Bunce GW, Poulopoulos A (2022) Neuronal mTOR outposts: implications for translation, signaling, and plasticity. Front Cell Neurosci 16. https://doi.org/10.3389/fncel.2022.853634
7. Anzalone AV, Koblan LW, Liu DR (2020) Genome editing with CRISPR-Cas nucleases, base editors, transposases and prime editors. Nat Biotechnol 38(7):824–844
8. Santiago Y, Chan E, Liu P-Q et al (2008) Targeted gene knockout in mammalian cells by using engineered zinc-finger nucleases. Proc Natl Acad Sci USA 105(15):5809–5814
9. Anzalone AV, Randolph PB, Davis JR et al (2019) Search-and-replace genome editing without double-strand breaks or donor DNA. Nature 576(7785):149–157
10. Condò I (2022) Rare monogenic diseases: molecular pathophysiology and novel therapies. Int J Mol Sci 23(12):6525
11. Lin J, Liu X, Lu Z et al (2021) Modeling a cataract disorder in mice with prime editing. Mol Ther Nucleic Acids 25:494–501
12. Newby GA, Liu DR (2021) In vivo somatic cell base editing and prime editing. Mol Ther 29(11):3107–3124
13. Robertson CD, Davis P, Richardson RR et al (2023) Rapid modeling of an ultra-rare epilepsy variant in wild-type mice by in utero prime editing. bioRxiv. https://doi.org/10.1101/2023.12.06.570164
14. Minematsu T, Sugiyama M, Tohma Y et al (2004) Simplified DNA extraction methods for sexing chick embryos. J Poult Sci 41(2):147–154
15. Li Y, Chen J, Tsai SQ, Cheng Y (2021) Easyprime: a machine learning-based prime editor design tool. Genome Biol 22(1):235
16. Hwang G-H, Jeong YK, Habib O et al (2021) PE-designer and PE-analyzer: web-based design and analysis tools for CRISPR prime editing. Nucleic Acids Res 49(W1):W499–W504
17. Chow RD, Chen JS, Shen J, Chen S (2021) A web tool for the design of prime-editing guide RNAs. Nat Biomed Eng 5(2):190–194
18. Standage-Beier K, Tekel SJ, Brafman DA, Wang X (2021) Prime editing guide RNA design automation using PINE-CONE. ACS Synth Biol 10(2):422–427
19. Siegner SM, Karasu ME, Schröder MS et al (2021) PnB designer: a web application to design prime and base editor guide RNAs for animals and plants. BMC Bioinformatics 22(1):101
20. Hsu JY, Grünewald J, Szalay R et al (2021) PrimeDesign software for rapid and simplified design of prime editing guide RNAs. Nat Commun 12(1):1034
21. Bhagwat AM, Graumann J, Wiegandt R et al (2020) multicrispr: gRNA design for prime editing and parallel targeting of thousands of targets. Life Sci Alliance 3(11):e202000757
22. Yu G, Kim HK, Park J et al (2023) Prediction of efficiencies for diverse prime editing systems in multiple cell types. Cell 186(10):2256–2272.e23
23. Aida T, Wilde JJ, Yang L, Hou Y, Li M, Xu D et al (2020) Prime editing primarily induces undesired outcomes in mice. bioRxiv. https://doi.org/10.1101/2020.08.06.239723

Part II

Analyzing Synaptic Structure and Constituents

Chapter 6

Purification of Afference-Specific Synaptosome Populations Using Fluorescence-Activated Synaptosome Sorting

Vincent Paget-Blanc, Marie Pronot, Marlene E. Pfeffer, Maria Florencia Angelo, and Etienne Herzog

Abstract

The central nervous system contains a complex intermingled network of neuronal, glial, and vascular cells, and for several decades, neurobiologists have used subcellular fractionation methods to analyze the molecular structure and functional features of the different cell populations. Biochemists have optimized fractionation protocols that enrich specific compartments such as synapses (called "synaptosomes") and synaptic vesicles to reduce this complexity. However, these approaches suffered from a lack of specificity and purity, which is why we previously extended the conventional synaptosome preparation to purify fluorescent synaptosomes from VGLUT1^{venus} knock-in mice on a cell sorter. We adapted our previous protocol to sort from single neuronal projections and small target regions of the brain as we did in the present example by labeling dopaminergic projections to the striatum. We proved that our newest method allows a steep enrichment in fluorescent dopaminergic synaptosomes containing presynaptic varicosities and associated postsynaptic elements and a substantial depletion in glial contaminants. Here we propose a detailed procedure for implementing projection-specific fluorescence-activated synaptosome sorting.

Key words Synaptosome, Fluorescence-activated synaptosome sorting, Synapse, Subcellular fractionation, Flow cytometry, Micro-particle sorting, Dopamine

1 Introduction

The brain contains a complex meshwork of neurons, glial cells, and blood vessels, and the daunting complexity of this tissue represents a challenge for research on synapses and micro-structures (0.5–2 μm on average) formed between neurons. Numerous subcellular fractionation approaches were developed to enrich isolated synaptic particles (called synaptosomes) and synaptosome-derived sub-synaptic compartments [1–6]. Synaptosomes are functional synaptic particles consisting of a resealed presynaptic compartment and part of the postsynaptic element [7, 8]. A wealth of knowledge

Tolga Soykan and Alexandros Poulopoulos (eds.), *Synapse Development: Methods and Protocols*, Methods in Molecular Biology, vol. 2910, https://doi.org/10.1007/978-1-0716-4446-1_6,

about synapse structure, composition, and function [1, 5, 9], together with generic proteomes of synaptic structures, were derived from synaptosome preparations. These previous studies enabled researchers to define the average composition of synapses and corresponding substructures in the brain [5, 6, 10–12].

A major limitation of the conventional synaptosome-based preparations used so far is the presence of synapse types mixture (49.1% of all particles) with neuronal and non-neuronal contaminations (50.9% of all particles) [3, 13, 14]. This lack of specificity and the significant contamination by non-synaptic compartments confound the interpretation of synaptosome-derived data and limit the identification of new synapse-specific proteins in synaptic subpopulations. To circumvent these issues, an effort to dissect molecular scaffolds isolated through co-immunoprecipitation assays has been made, and contaminations are partly removed in this manner. However, the output material is limited to medium-sized (1000–5000 kD) macromolecular scaffolds [15], while the resolution of isolated complexes is limited by regional tissue dissections combining several synaptic origins within the explants [16]. Proximity labeling strategies also provide the ability to perform subcellular-selective analysis of neuronal compartments but are either restricted to nanoscale environments [17–20] or whole neuronal cells [21]. In both paradigms, proximity labeling cannot encompass the proteome of the whole synapse between 2 or more cell types. Another strategy to study synaptic subpopulation is to combine synaptosome immunolabeling with flow cytometry. Nevertheless, uncertainties regarding the efficiency of these methods remain, and they still have to be successfully implemented on unfixed samples [22–24].

To reach specificity and higher purity of unfixed synaptosome samples, we established the first protocol for fluorescence-activated synaptosome sorting (FASS) of subpopulations of synapses. We applied it to VGLUT1 synapses from the VGLUT1^{venus} knock-in mouse model [25] and identified novel proteins at excitatory synapses [26]. We successfully applied FASS to the comparison of VGLUT1 synapse proteomes in a model of synucleinopathy and identified new synaptic markers of the pathology at early stages [27]. More recently, we adapted FASS for local transcriptome screening [28] and projection-specific synaptosomes targeting [29, 30]. We updated the protocol to target new types of synapses, starting with the dopaminergic synaptosomes in the striatum. To that end, we used a mouse line expressing the recombinase CRE under the control of the dopamine transporter (DAT) promoter together with stereotaxic injections of an adeno-associated viral vector (AAV) driving the CRE-dependent expression of a green fluorescent protein [31, 32]. To enhance the yield and quality of synaptosome sorting, we switched from an EGFP probe to mNeongreen [30, 33]. This enhanced FASS method allows

high-resolution separation of synaptic and extra-synaptic components of neurons from projection-specific synapse populations. FASS-purified synaptosomes can then be studied using immunofluorescence, electron microscopy, immunoblotting, transcriptomic and proteomic techniques [26–30]. This updated method enabled us to characterize multipartite dopamine synapses that we named Dopamine Hub Synapses [30].

We propose here to detail all steps necessary to sort and collect a given synapse population with the recent optimizations added to the original protocol [34]. Beyond the efficient sorting of dopaminergic synapses in our example, extensions of FASS to other populations of synapses and different types of labeling approaches can be envisioned. Finally, this FASS methodology may serve as a base for the adaptation to the purification of other biological microparticles/organelles.

2 Materials

2.1 Fluorescence-Traced Animals

The molecular genetic strategy designed to label your projection of interest has to be optimized before the first sorting experiment. Validation of the selectivity, coverage, and strength of labeling should be carefully performed in histology. The detailed description of the stereotaxic injection protocol goes beyond the scope of this article. Mouse brain stereotaxic injections should be performed according to standard protocols [35].

2.2 Synaptosome Preparation

1. Dissection tools, including curved thin tweezers and razor blades.
2. Two glass Petri dishes.
3. Glass Pasteur pipettes.
4. Stainless steel brain matrix (e.g., Kent Scientific 0.5 mm Mouse brain coronal matrix #RBMS-205C) or any other mouse brain coronal matrix.
5. One stereomicroscope (e.g., Leica MZ10F) coupled to a CCD camera (e.g., Leica DFC3000 G) connected to a fluorescent lamp.
6. Drill-type homogenizer (e.g., Heidolph RZR 2102 control).
7. Glass/Teflon potter with a capacity of 2 cm^3.
8. Plate shaker.
9. Benchtop centrifuge with fixed angle rotor (we use an Eppendorf Centrifuge 5424 R).
10. Ultracentrifuge with a swing-bucket rotor (e.g., Beckman-Coulter Optima LE80K ultracentrifuge with SW40Ti rotor or Thermo WX Ultra 90 ultracentrifuge with TH 641 rotor).

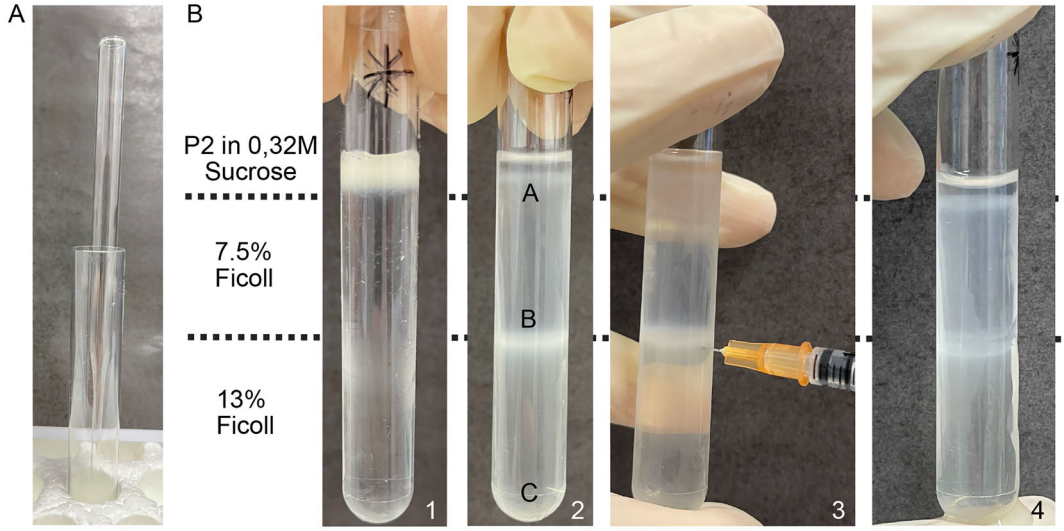

Fig. 1 Bottom-up discontinuous gradient preparation using a glass Pasteur pipette. The gradient is filled through the Pasteur pipette with the 7.5% Ficoll layer poured first and the 13% Ficoll layer poured last (**a**) and handled for final synaptosome fractionation (**b**). 1: Crude synaptosomes (P2) in 0.32 M sucrose are layered on the gradient. 2: After ultracentrifugation, 3 fractions A, B, and C are visible; the A fraction is prominently populated by myelin sheath fragments, the B fraction is the synaptosome-rich fraction, and the C pellet contains denser debris and free mitochondria as described earlier. 3: the B fraction is collected by inserting a 29-gauge 0.5 mL syringe from the side of the tube below the B fraction. During collection, the level is descending, and one should adjust the needle orientation to fully grasp the bulk of the synaptosome interface. 4: at the end of the procedure, the synaptosome interface is nearly cleared, and no contamination has been added from the top myelin-rich layer

11. Ultra-clear ultracentrifuge tubes for your swinging bucket rotor (e.g., Beckman Coulter 344059 that fit in SW40Ti; *see* Fig. 1).
12. Isosmolar Buffer: 0.32 M sucrose 4 mM HEPES pH 7.4 (15 mL per prep).
13. 7.5% Ficoll: 7.5% Ficoll (e.g., Sigma Ficoll® 400 #F2637-100G), 0.32 M sucrose 4mM HEPES pH 7.4 (15 mL per prep).
14. 13% Ficoll: 13% Ficoll (e.g., Sigma Ficoll® 400 #F2637-100G), 0.32 M sucrose, 4 mM HEPES pH 7.4 (15 mL per prep).
15. Phosphate Buffered Saline.
16. PES Vacuum Filter Units (e.g., Nalgene™ Rapid-Flow™ #568-0020 by ThermoFischer).
17. FM4-64 from Interchim (FP-41109C) or any other provider.
18. Protease Inhibitors: Protease inhibitor cocktail 80 μM Aprotinin, 5 mM Bepstatin, 1.5 mM E-64, 2 mM Leupeptin, 1 mM Pepstatin A. For other commercial protease inhibitor cocktails,

ensure it is compatible with downstream applications. Check with your proteomics facility for a cocktail of inhibitors compatible with mass spectrometry (i.e., without AEBSF, such as Halt Protease and Phosphatase Inhibitor Cocktail from Thermo Scientific).

2.3 FACS Analysis and Sorting Steps

1. 5 mL Polystyrene Round-Bottom Tube 12 * 75 mm style (e.g., Falcon #352058 by BD Labware, *see* **Note 1**).
2. 15 mL Centrifuge tubes (e.g., Sarstedt #62.554.502).
3. FACSAria cell sorter from Becton-Dickinson Inc. (*see* **Note 2**) with a 20 mW 488 nm laser, a square flow cell for side population sorting, and a sample collection cooling unit.
4. Sheath fluid (e.g., BD FACSFlow ref: 342003).

2.4 Filtration of Sorted Samples

1. Analytical filter holder 13 mm (e.g., Merck-Millipore ref: XX3001240), EZ-Fit™ manifold (e.g., Merck-Millipore ref: EZFITH0LD3), or glass reusable filtration unit and rotary vane vacuum pump.
2. 0.1 μm hydrophilic PVDF filter (e.g., Durapore® PVDF filter, Merck-Millipore VVLP01300).
3. SDS-PAGE loading buffer: 2.5% SDS, 0.002% Bromophenol Blue, 0.7135 M (5%) β-mercaptoethanol, 10% glycerol, 62.5 mM Tris with HCl to pH 6.8 or Biorad premixed 4× Laemmli Sample Buffer #1610747 supplemented with 1:3 β-mercaptoethanol.

2.5 Synaptosome Fixation on Coverslips

1. Coverslip holder.
2. 12 mm coverslips.
3. 24-well flat-bottom plates.
4. Centrifuge with microplate swing rotor (e.g., Beckman-Coulter J-26 XP centrifuge with JS 5.3 rotor).
5. Chrome Alum Gelatin Slide Coating: 1% Gelatin, 1% Chromium potassium sulfate, in distilled water.
6. PFA Sucrose Buffer: 4% paraformaldehyde, 4% sucrose in PBS.

3 Methods

On the day preceding the experiment, prepare all materials and buffers. Buffers should be stored at 4 °C. Wash the required glass/Teflon potter(s) by rinsing 3 times with distilled water, brushing 3 times with distilled water, brushing 3 times with 70% ethanol, rinsing 3 times with 70% ethanol, and drying overnight. The following morning, brush the potter(s) 3 times with acetone, rinse 3 times with Milli-Q water, and let it dry. Place on ice until

use, and add protease inhibitors to Isosmolar Buffer and PBS (volume needed to do synaptosome dilution, typically 30 mL for 2 striatal samples pooled from 3 animals each).

3.1 Brain Tissue Dissection

1. Organize four areas on the bench to sacrifice the mouse, extract the brain, dissect regions of interest, and homogenize tissue samples.
2. Keep all the tools used for dissection on ice, including the brain matrix and razor blades that are washed 3 times with 70% ethanol and 3 times with Milli-Q water.
3. Sacrifice the first mouse by cervical dislocation (follow the local regulatory guidelines regarding ethics on animal handling). Decapitate the mice, cool down the head in liquid nitrogen for 3 s, and extract the brain that should not be frozen.
4. Clean and maintain the brain at 4 °C by placing it in ice-cold PBS (without protease inhibitors). If needed, cut a piece of mouse tail to secure a genotyping biopsy backup and freeze it at −20 °C. While working in the cold room is advisable but not mandatory, perform all subsequent steps on the ice.
5. Dissect the regions of interest. For the DAT-Cre fluorescent striatum, dissection proceeds as follows. Place the cortices facing the bottom of the brain matrix. While keeping the brain matrix on a dish containing ice, place it under the microscope. Olfactory tubercules should be fluorescent and visible together with the more posterior part of the striatum. Place a sharp razor blade in front at the limit of the olfactory tubercule fluorescence and another at the posterior part of the striatum (a razor blade can be placed between those two endpoints if you wish to do the dissection in two steps). Remove the first razor blade and discard the olfactory bulbs. Remove the second razor blade and place the coronal slice on the glass surface of the Petri dishes filled with ice. Place the Petri dishes under the binoculars. Without using fluorescence, separate the two hemispheres with a scalpel blade. Move the left hemispheres outside of your field of view. From the right hemisphere, dissect out the corpus callosum, cortices, lateral septal nucleus, diagonal band nucleus, and olfactory tubercules. Turn the remaining tissue containing the striatum at 90° to the right using tweezers. Using fluorescence, dissect and discard the left (posterior) non-fluorescent part containing the hypothalamus, thalamus, BST, and globus pallidus. Continue to turn the striatum with a 90° angle to dissect out lesser fluorescent parts. This step is crucial to increase the representation of fluorescent particles in the final gradient preparation (*see* **Note 3**). Once the dissection is completed, proceed with the other hemisphere. At the end of the dissection, take a picture of the two striata and place each in

100 μL of ice-cold Isosmolar Buffer in a 1.5 mL micro-centrifuge tube. Keep the tube in ice until the end of the dissection.

6. Repeat steps in 3.1 for each mouse. We routinely performed our FASS with a minimum of 6 mouse striata (3 pairs). Select the most fluorescent striata by comparing each picture and discarding the rest.

3.2 Tissue Homogenization

1. Weigh each sample if you need to measure the yield of your fractionation. Introduce tissue samples into a 2 cm^3 clean ice-cold glass/Teflon potter using a glass Pasteur pipette. The final volume is 1 mL of ice-cold Isosmolar Buffer into the potter. Connect to the homogenizer rotor. Homogenize tissue with 12 strokes at 900 rpm. Keep the potter ice-cold as much as possible during homogenization and avoid bubble formation by not having the Teflon get out of the homogenate during strokes.
2. Collect the homogenate in a 2 mL micro-centrifuge tube. Add 0.25 mL of ice-cold Isosmolar Buffer to the glass potter. Rinse the potter with 3 manual strokes and add the wash to the homogenate tube. Further, rinse the Teflon potter by running 0.25 mL ice-cold Isosmolar Buffer, letting it collect in the glass tube, and adding it to the homogenate. Mix the homogenate by inverting the tube 3 times. The final homogenate should be at least 5 volumes of the tissue sample (grams of tissue/mL buffer) for proper subsequent fractionation. Aliquot 50 μL of homogenate (H fraction) before proceeding. Repeat this step for each sample.

3.3 Synaptosome Fractionation

1. Equilibrate the weight of the homogenates in pairs to balance the centrifuge by adding Isosmolar buffer if needed, then centrifuge at 1000 g for 5 min at 4 °C (we use Eppendorf Centrifuge 5424 R with fixed rotor).
2. Transfer each supernatant (S1, around 1.5 mL) to new 2 mL micro-centrifuge tubes, mix by inverting each tube 3 times, and aliquot 50 μL of S1.
3. Resuspend the pellet (P1) in 0.250 mL of ice-cold Isosmolar Buffer and keep it as an aliquot.
4. Equilibrate S1 weights in pairs, then centrifuge at 12,500 g for 8 min at 4 °C (we use Eppendorf Centrifuge 5424 R with fixed rotor).
5. During this centrifugation step, lay discontinuous Ficoll gradients in new (*see* **Note 4**) ultracentrifuge tubes (we use 14 × 89 mm Beckman Coulter 344059). Through a glass Pasteur pipette, add the first 5 mL of ice-cold 7.5% Ficoll solution, then slowly add 5 mL of 13% Ficoll (*see* Fig. 1a).

6. Aliquot slowly all of the supernatant (S2); beware that P2 can resuspend in S2 during its collection; if it is the case, leave the rest of S2, it should not be more than 100 µL.
7. Resuspend P2 pellets by adding Isosmolar buffer for a final volume of 350 µL of P2. Resuspend with several up and down strokes with a p200 micropipette. Aliquot 50 µL of P2 and slowly layer the remaining P2 on top of sucrose gradients with a p1000 micropipette (*see* Fig. 1b).
8. Precisely equilibrate the weights of the gradients in the ultracentrifuge tubes using Isosmolar buffer.
9. Centrifuge at 50,000 g for 70 min at 4 °C in the ultracentrifuge swinging rotor (TH 641 or SW40Ti). Set the acceleration to 6 of 10 and the deceleration to 4 of 10 to preserve the gradient layering.
10. After the centrifugation, collect synaptosomes (B fraction) with a 0.5 mL U-100 29G insulin syringe (pierce the tube below the B fraction interface; *see* Fig. 1b and **Note 4**). Collect the fraction in a 2 mL micro-centrifuge tube; mix by inverting the tube 3 times (avoid vortexing). Aliquot 50 µL of the B fraction for protein titration and western-blot analysis and keep the rest for synaptosome sorting.
11. Protect the suspension from light by wrapping the tube with aluminum foil. These samples correspond to the master samples for analysis and sorting in the FACS.

3.4 Synaptosomes Analysis and Sorting

1. The cell sorter (*see* **Note 2**) should be set as follows: 70 µm Nozzle, sample shaking at 300 rpm, sample temperature at 4 °C, FSC neutral density filter 0.5, 488 nm Laser on, Area Scaling 0.91, Window Extension 0.7, FSC Area Scaling 0.81, Sort Precision: 0-16-0. Thresholding on FM4-64 with a threshold value of 500. Optical parameters should be set as appeared in Table 1.
2. All samples should be diluted in 0.22 µm filtered PBS with protease inhibitors until reaching approximately 20,000 events per second at a flow rate between 1 and 3 (*see* **Note 5**). Dilute

Table 1
Optical parameters for mNeongreen FASS analysis

Channel	Filter and gain
FSC	ND 0.5, 340 V
SSC	488/10 nm, 300 V
FITC (mNeongreen)	530/30 nm, 660 V
PerCP (FM4-64)	675/20 nm, 630 V

100 µL of synaptosomes in 2 mL ice-cold 0.22 µm filtered PBS with protease inhibitors. Mix by inverting the tube 3 times. From this first 1/20 dilution, perform a second 1/10 dilution placing 100 µL of diluted sample in 0.9 mL ice-cold 0.22 µm filtered PBS with protease inhibitors (a 1/200 dilution factor was determined empirically for 6 striata; *see* **Note 5**). The intermediate 1/20 step allows for adapting dilutions based on the initial sample concentration. Sample shaking should run at 300 rpm and the temperature set to 4 °C.

3. The detection threshold is read on FM4-64 fluorescence. Stain each sample by adding 2 µg/mL of FM4-64 before loading in the cell sorter (*see* **Note 6**).
4. Noise baseline check with PBS: Load PBS + FM4-64. Run the sample for 1 min at a flow rate of 11. Lower to flow rate 3 and record for 1 min. Noise events should be down to 200/min approximately. Should noise rise above 400–500 events/min (*see* **Note 1**), run ultra-pure water for 10 min at the maximal flow rate, then rerun PBS with a flow rate of 3. Repeat wash steps until the baseline falls below 400 events/min. If problems persist, change the box of tips used to prepare solutions.
5. Auto-fluorescence baseline check with WT sample and gating strategy: Add FM4-64 and mix by inverting the tube 3 times. Flow the sample for 1 min in the sorter at flow rate 11 before recording one hundred thousand events at a flow rate of 3 (*see* **Note 5**). Slide the P1 gate toward the lower forward scatter channel (FSC) and side scatter channel (SSC) scores to include 80–85% of the total detected events in this gate (Fig. 2a). P1 represents the non-aggregated population of particles in the Ficoll synaptosome sample (singlets). Create a second contour plot graph displaying the fluorescence channel peak area (FITC channel for EGFP or mNeongreen) in Y and the FSC peak area in X. Restrict the display to the singlets (P1) population in this new graph (*see* Fig. 2b). Center P2 gate on the WT auto-fluorescent population. Set the FASS gate (P3) above to get 0.1% events in this gate having P3 close to P2 (Fig. 2b). Put a P5 gate around the aggregating diagonal population to follow unwanted aggregation processes over time (Fig. 2a). An additional P6 gate can be placed to track the whole aggregates population containing small and big aggregates (Fig. 2a). Additional graphs in the sheet may help monitor the sample, but they are not critical for the gating strategy.
6. Fluorescence analysis with mNeongreen sample: Let the sample flow at flow rate 11 for 1 min in the sorter before recording one million events at a flow rate of 3.0 (*see* **Note 5**). Adjust the FASS (P3) top gate to include all highly mNeongreen fluorescent particles (Fig. 2c).

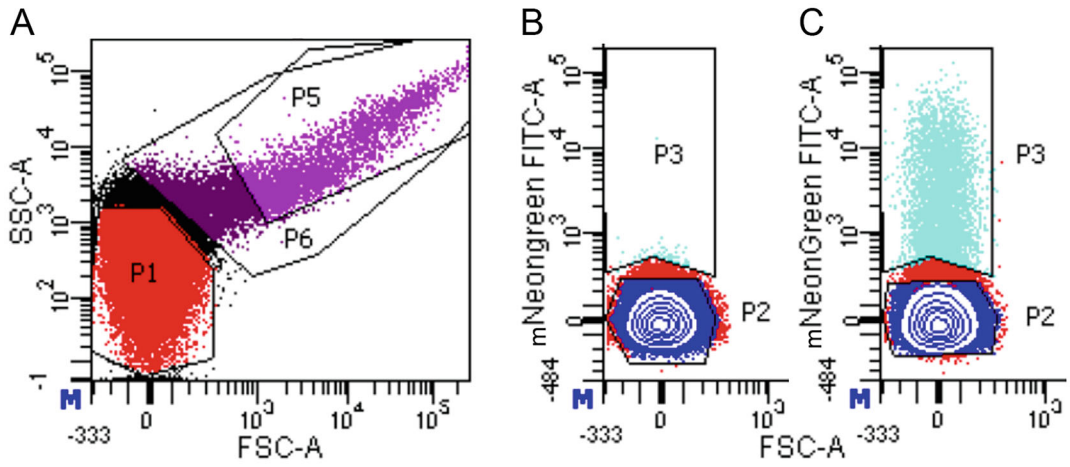

Fig. 2 Analysis and gating of DAT-Cre$^{mNeongreen+}$ synaptosomes. (**a**) light scattering of all particles detected through the FM4-64 threshold. P1 gate represents single particles (singlets) and generally accounts for 85% of the total. P1 is shifted to the lower left side of the main population as we observed small aggregates in the top right part. The P5 gate covers large aggregates and allows monitoring aggregation over time. It should remain below 10%. P6 covers both large and small aggregates. P6 is more susceptible to change over time than P5. Note that FACSAria cannot resolve size differences in the singlets synaptosomes. The singlets (P1) gated population is displayed in a new contour plot (**b** and **c**). (**b**) Wild-type non-fluorescent singlets population (P1) allows to set the baseline autofluorescence in the FITC/mNeonGreen channel. The P2 gate is positioned to cover the whole WT P1 population. P3 (FASS sample) is set to represent 0.1% of the entire singlets (P1) population in the WT. (**c**) DAT-Cre$^{mNeongreen+}$ samples provide a significant fluorescent population above the P2. P3 (FASS sample) is designed to cover this population and exclude the WT baseline

7. Sorting fluorescent synaptosomes: The number of events/s should remain stable between 18,000 and 25,000 events/s with a flow rate of 3.0 or below. Use the 15 mL Falcon tube collection device cooled to 4 °C. The left tube will receive FASS gated events (P3, mNeongreen fluorescent particles), while the right tube will collect non-fluorescent P2 gated events that will eventually be discarded (*see* **Note 7**). Perform a test sort for quality control of the streams and make sure left and right streams fall in their respective tubes. Place new 15 mL tubes. Open the sorting sheet. Set sorting precision to 0-16-0 (*see* **Note 7**), and add the FASS (P3) gate to the left side and the P2 gate to the right side. Start sorting and keep the speed of analysis below 22,000 events/s roughly and the sorting efficiency above 80% by modulating the flow-rate speed during the procedure. The rate of particle aggregation seen in gate P5 should remain below 10% of total events. Otherwise, prepare a fresh mNeongreen tube. On average, a new sample tube has to be prepared every hour. Check the volume of the collected sample directly into the collection tube. On average, 1 million events generate 1 mL of the collected sample. Do not sort more than 14 million events in one 15 mL Falcon tube.

8. Sorting control: Use the gate singlets (P1) to sort the non-aggregated population of synaptosomes. The procedure is the same as for the FASS gate (P3). Singlets (P1) synaptosome counts are usually lower than FASS (P3) and need to be adjusted by sorting more. Re-analysis of the singlets sample (P1) will help determine singlets counts (*see* **Note 8**).
9. Sort re-analysis: The first quality control of the sort is performed through the re-analysis of sorted samples in the sorter. Use at least 500 µL of the sorted sample to perform the re-analysis. Perform a minimum of 1 min sample line backflush between each analysis. Add FM4-64, mix and run this sample first 1 min at a flow rate of 11, then 1 min at a flow rate of 3.0 before recording for 1 min. This procedure thoroughly cleans the sample line from any contamination with the unsorted sample processed before and stabilizes the flow of sorted events. The flow of events in re-analysis usually runs between 100 and 200 events/s (roughly 100-fold slower than during analysis and sorting). A good sort for a minor initial fluorescent population is indicated by more than 50% of events seen in the FASS sample (P3 gated) and below 30% in P2 (*see* Fig. 3). Additionally, sorted synaptosomes should display a more compact population in FSC/SSC scatter plots (*see* Fig. 3c). Eventually, one may monitor the global fluorescent population in the sorted sample (see the inset graph in Fig. 3c). Total fluorescence in a good sort represents more than 60% of the total

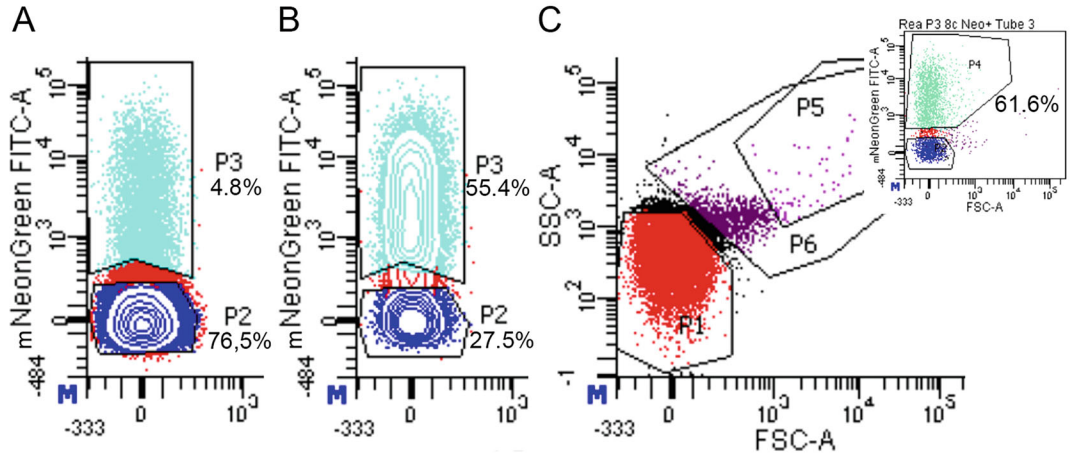

Fig. 3 Re-analysis of sorted samples. (**a**) same graph as Fig. 2c. On a good day, around 5% of the total sample is in P3 (FASS sample) and about 77% in P2. (**b**) Re-analysis of sorted P3 (FASS) population. FASS population rises to 55–65% of the total while P2 negative particles drop to less than 30%. (**c**) On a light scatter plot, the sample seems now more compact in the P1 gate, though aggregation still takes place after sorting. In the inset, we estimate the total fluorescence in the sorted sample as all particles originating from FASS (P3). P4 usually rises to 60–68%

events. If your samples are processed via proteomics approaches, the rest of the reanalyzed sample can be placed back into its 15 mL Falcon tube. If your sample is processed through immunofluorescence, discard the re-analysis tube (*see* **Note 9**). Note that each 15 mL tube of sorted synaptosome should be reanalyzed individually prior to collection for subsequent analysis. Indeed, subtle changes in the sort quality during the day might occur, and it happens that one of the tubes doesn't meet the quality criteria to be included in the analysis.

3.5 FASS Sample Processing

1. FASS sample concentration for proteomics approaches: After the quality control re-analysis has been validated, FASS synaptosomes collected in 15 mL tubes are concentrated by filtration on 13 mm diameter PVDF filters with 0.1 μm pores at 4 °C. This step may be very long if the vacuum is not strong enough. We, therefore, recommend optimizing the filtration setup on Ficoll samples before the first sorting day. Overlay all FASS samples of the same origin onto the filter over the afternoon of sorting. For a typical day of sorting, we collect around 35 million synaptosomes.
2. After completion of the filtration, remove the filter with tweezers. Place the filter straight onto a 0.5 mL micro-centrifuge tube. To keep the bottom of the 0.5 mL tubes clean, put them into a 50 mL Falcon tube. Freeze them in liquid nitrogen and store them at −80 °C until use. Do not wait more than 2–3 weeks to process your frozen filters (*see* **Note 10**).
3. Thaw your 0.5 mL tubes containing filters at 4 °C. Prepare 1.5 mL tubes filled with 1.2 mL ultrapure water and one for 1× SDS-PAGE loading buffer (we use Biorad premixed 4× Laemmli Sample Buffer #1610747 supplemented with 1:3 β-mercaptoethanol). Warm the tubes filled with water and SDS-PAGE loading buffer for 5 min at 70 °C in a thermomixer. Resuspend filtered proteins in 70 μL of SDS-PAGE warm loading buffer. Incubate the 0.5 mL tubes with loading buffer at 70 °C for 3 min in the tubes containing 1.2 mL ultrapure water (for complete denaturation while preserving complex hydrophobic proteins like neurotransmitter transporters) (*see* **Note 11**) while shaking at full speed. Quickly open and close the lid to remove the pressure formed during the heating. Put the sealed 0.5 mL tube top-down with most of the sample on the cover. Pierce the bottom of the 0.5 mL tube 3 times with a clean 25 gauge needle and place it in a clean 1.5- or 2-mL tube. Centrifuge for 1 min at full speed 4 °C in a micro-centrifuge to collect the sample in the larger tube, rotate the 0.5 mL tube so that the cap faces the other direction, and centrifuge again for 1 min at full speed 4 °C.

4. FASS sample protein titration: Ficoll synaptosome proteins should be titrated using standard methods (Bradford, Lowry, or others). Then FASS samples are titrated using silver staining performed on SDS-PAGE gels against a standard curve of sucrose synaptosomes. Following titration, samples are loaded the same day in western blot gels. We use precast gels for reproducibility (e.g., 10 wells of 7.5% Biorad precast gels) using around 0.2–0.5 μg of proteins and processing through mass spectrometry. Samples can also be kept at −80 °C and analyzed by immunoblot; we use the automated capillary-based immunoblot WES system (i.e., Bio-Techne Protein Simple, WES) because of its sensitivity and reliability.

3.6 FASS Sample Recovery on Coverslips

1. Gelatinize coverslips: place 12 mm coverslips in a coverslip holder and immerse in Chrome Alum Gelatin Slide Coating for 4 min; remove and air dry in a 60 °C oven for at least 2 h minimum.
2. Place gelatinized coverslips into a 24-well flat-bottom microplate.
3. Add 1 mL of sorted synaptosomes per well (adapt the singlets P1 gated synaptosomes volume to re-analysis counts; *see* **Note 8**).
4. Centrifuge microplate for 34 min at 6800 g on a microplate swing-rotor centrifuge (we use JS 5.3 rotor using Beckman J-26XP centrifuge). Discard supernatant.
5. Fix with 500 μL of 4% PFA Sucrose Buffer. Incubate at room temperature for 20 min under slow shaking.
6. Eliminate PFA and wash 3 times for 5 min with PBS at room temperature under slow shaking. Store at 4 °C in PBS until use.
7. Upon immunofluorescence staining, coverslips may be mounted on glass slides using standard procedures for downstream imaging applications.

4 Notes

1. FM4-64-based thresholding of particle detection requires one to be extremely careful regarding noise issues. Indeed, FM4-64 will fluoresce in the presence of detergent or hydrophobic molecules. Any unwanted release of particles or molecules prone to providing a hydrophobic milieu to FM4-64 molecules will induce noise in the experiment. We faced this problem with certain plasticware and when the cell sorter was not thoroughly rinsed with water after the cleaning procedure from Becton-Dickinson (BD). Hence, we suggest being extremely cautious

when changing/testing plasticware (including tips used for solution preparation) and constantly checking the noise baseline at the beginning of a sort. This noise will not harm sample sorting at high event rates but damages the re-analysis of sorted samples at low event rates.

2. Our experience of synaptosome sorting is successful with the FACSAria cell sorter from BD Bioscience which doesn't mean that it may not work with any other cell sorter. Indeed, from the FSC/SSC scatter plots, the FACSAria is nearly blind in this size range of biological samples. Much could probably be done to optimize microparticle detection and sorting with this equipment. However, we had the opportunity to work for several years with another cell sorter, the Moflo XDP from Beckmann-Coulter, with very little success. One chief aspect of the success of a sorting day is the stability of the fluidics system of the sorter over time. This criterion was never met with the Moflo XDP, even though some short sorting sequences were promising in the re-analysis. Overall, a correctly set FACSAria can easily be stable for a full day. Notably, the quality of the objective lens and gel coupling to the analysis chamber should be checked by the maintenance team from the provider, as optimal quality is critical with our small and dim particles. Upon lens replacement, we gained a lot of signals on our current system.
3. The amount of input material in the cell sorter is critical for very small brain microdissection based on fluorescence, like for DAT-Cre mNeongreen mice. By pooling the strictly fluorescent explants from 6 striata, we obtained enough samples for a complete sorting day. A critical aspect is to have a high level of fluorescent particles in the model to lower the time spent analyzing unwanted events. Indeed, the larger the population in the FASS gate (P3) is, the faster the sorting will be. Along these lines, we did try to use post-nuclear pellet 2 fractions in the sorter, but the quality and speed of sorts suffered from this. Another critical issue regarding the sample quality is to ensure intense labeling of the target compartment. In the case of dopaminergic synaptosomes, we achieved this using DAT-Cre mice coupled to AAV expression of mNeongreen protein. Switching from EGFP to mNeongreen protein allowed us to obtain more robust staining of the dopaminergic synaptosomes [30]. Further refinement with other fluorescent proteins can be envisioned. We tried to backcross the DAT-Cre mouse line with other reporter lines like Ai9-tomato. Unfortunately, the fluorescence intensity in the litter was not enough to enable FASS. This limiting factor needs to be taken into account when implementing the method with another labeling approach.

4. The aggregation of particles is a critical parameter for the success of FASS. With DAT-Cre mNeongreen labeling, only a small proportion of the population of synapses is fluorescent; hence unlike VGLUT1^{Venus}, fewer aggregates contain fluorescent particles. However, small aggregates that escape FSC resolution tend to be sorted with the single particles when particles aggregate. Also, an increasing aggregated population (seen in P5) is removing events of interest in the FASS sample (P3 gated), and sort rates will drop. Even though we do not fully understand which parameter is responsible for the aggregation process on conventional gradient samples, we suspect that myelin and bacteria/fungi derived trace contaminants from catalyzing it. We identified several critical parameters to block the process almost entirely through methodic comparisons. These include: a thorough cleaning procedure for the potters (see methods section), the use of fresh filter-sterilized buffers, the replacement of sucrose by Ficoll during the last fractionation step, the exclusive use of new tubes for the 3 centrifugation steps (in our case the first 2 centrifugations are using 2 mL micro-centrifuge tubes), syringe based collection of the gradient synaptosome B fraction (*see* Fig. 1), the vortex-free gentle mixing of suspensions using tube inversions, and finally the constant handling of samples at 4 °C (also mandatory for protein handling in general).
5. The optimal focusing of the sample flow in the sorter will positively influence fluorescence detection. Indeed, the flow rate of the sample entering the acceleration chamber can be set from 0 to 11 on the FACSAria. This tuning sets the pressure difference between the sample line and the flow analysis chamber. We observed that changes in the flow rate used on the instrument changed the measurements on our sample. Indeed, at small flow rates, the sample is efficiently sheathed by the sheath fluid and optimally focused on the laser beams. While loose focusing may be harmless for the measurements on a 10–15 μm cell, it becomes critical when dealing with 1 μm particles. Hence, we insist on using a flow rate of 3.0 or less for all analyses and sorts. During re-analysis, we suggest always keeping the same flow rate of 3 to compare the number of sorted particles for each sample. Playing with dilutions during sample preparation will allow for reaching the proper flow rate when higher values are needed. On a similar note, we observed that sample measurements/statistics are mostly not stable before the sample has run for 1 min in the sorter. Hence, we always run the sample for 1 min at the maximum flow rate before refreshing the graphs and recording a sample.
6. We initially used 1 μg/mL of FM4-64; at this concentration, we could see a decrease of events/s after 1 h of sorting on the same dilution due to a washout of the FM. This phenomenon

was exacerbated by long sorting times due to the low representation of dopaminergic particles (5% of the total). Increasing the FM4-64 concentration to 2 μg/mL stabilized events detected over time and did not significantly increase the noise seen during the analysis of PBS.

7. Sorting quality depends on the sorting precision/mask used and on the actual quality of the stream. In our experience, the best results were obtained upon using the 0-16-0 mask that selects events only when they are estimated to fall in the center of the drop of interest (and no contaminant is close by in the flow). In our hands, the simultaneous sorting of P2 non-fluorescent events on the opposite side allowed us to increase the sort quality of the FASS (P3) fluorescent events. We believe this occurs through the better focusing/lower spraying of the central trash flow and the active removal of negative events from the mid-trash flow. We then tried to analyze these P2 gated samples but soon figured out that the silver gel profiles were too different from our sucrose synaptosome standard so that protein titration could be considered accurate. Also, in principle, this P2 gated population is a non-relevant ensemble of particles of many different origins that only share the common feature of being negative to mNeongreen fluorescence.
8. We empirically realized that twice more particles were present in the FASS sample (P3 gated) compared to the singlets (P1 gated), while the sorter claimed identical counts. We confirmed this finding by measuring the protein content of FASS and singlets (P1) gated samples with 1.5- to 2-fold more proteins in the FASS sample. This might be partly explained by the low signal-to-noise ratio of the FM4-64 used for thresholding particle detection. We favored a threshold that ensures the full detection of biological particles rather than a more stringent one that would leave some undetected real particles to navigate randomly in the droplets below the detection threshold and negatively affect sample purity. The price to pay seems to be the inclusion of false positive detections that fall mostly in the global singlet population rather than the green fluorescent synaptosomes of interest. Also, it is likely that the average size of sorted synaptosomes is higher than the average size of singlet microparticles in the gradient sample. Raising FM4-64 concentration to 2 μg/mL improved sorted counts between both samples. When plating synaptosomes on coverslips, sample re-analysis counts can be used for the normalization of particle numbers between the two samples. Silver staining analysis is necessary to normalize protein content for proteomics or immunoblot analysis.

9. When performing a sort that will be processed with immunofluorescence, discard the reanalyzed sample. We noticed that at 2 μg/mL, FM 4-64 tends to be more challenging to wash out from synaptosomes and can still be visible after immunofluorescence post-processing containing multiple wash steps.
10. We noticed an important decay in protein content over time when filtrates were left for more than 2 weeks on the filters at −80 °C. When processing the same quantity of sorted particles 2 weeks and a half after collection, the protein content was 280 ng, while samples processed after 3 weeks contained 220 ng of proteins, and those processed after 3 weeks and a half contained 140 ng of proteins. Therefore, it is critical to rapidly process samples for proteomics and avoid leaving them for too long on filters.
11. After testing 30, 50, or 70 μL recovery volume, we determined that 70 μL of SDS-PAGE loading buffer gave our 13 mm PVDF filters the best yield. Indeed, we recovered, on average, 45% of the proteins filtrated with 30 μL of, 55% with 50 μL, and 92% with 70 μL.

References

1. Whittaker VP (1993) Thirty years of synaptosome research. J Neurocytol 22:735–742. https://doi.org/10.1007/BF01181319
2. Huttner WB, Schiebler W, Greengard P, De Camilli P (1983) Synapsin I (protein I), a nerve terminal-specific phosphoprotein. III. Its association with synaptic vesicles studied in a highly purified synaptic vesicle preparation. J Cell Biol 96:1374–1388. https://doi.org/10.1083/jcb.96.5.1374
3. Cotman CW, Matthews DA (1971) Synaptic plasma membranes from rat brain synaptosomes: isolation and partial characterization. Biochim Biophys Acta 249:380–394. https://doi.org/10.1016/0005-2736(71)90117-9
4. Jones DH, Matus AI (1974) Isolation of synaptic plasma membrane from brain by combined flotation-sedimentation density gradient centrifugation. Biochim Biophys Acta BBA—Biomembr 356:276–287. https://doi.org/10.1016/0005-2736(74)90268-5
5. Boyken J, Grønborg M, Riedel D et al (2013) Molecular profiling of synaptic vesicle docking sites reveals novel proteins but few differences between glutamatergic and GABAergic synapses. Neuron 78:285–297. https://doi.org/10.1016/j.neuron.2013.02.027
6. Weingarten J, Lassek M, Mueller BF et al (2014) The proteome of the presynaptic active zone from mouse brain. Mol Cell Neurosci 59:106–118. https://doi.org/10.1016/j.mcn.2014.02.003
7. Gray EG, Whittaker VP (1962) The isolation of nerve endings from brain: an electron-microscopic study of cell fragments derived by homogenization and centrifugation. J Anat 96:79–88
8. Whittaker VP (1959) The isolation and characterization of acetylcholine-containing particles from brain. Biochem J 72:694–706
9. Bai F, Witzmann FA (2007) Synaptosome proteomics. Subcell Biochem 43:77–98. https://doi.org/10.1007/978-1-4020-5943-8_6
10. Takamori S, Holt M, Stenius K et al (2006) Molecular anatomy of a trafficking organelle. Cell 127:831–846. https://doi.org/10.1016/j.cell.2006.10.030
11. Burré J, Zimmermann H, Volknandt W (2007) Immunoisolation and subfractionation of synaptic vesicle proteins. Anal Biochem 362:172–181. https://doi.org/10.1016/j.ab.2006.12.045
12. Wilhelm BG, Mandad S, Truckenbrodt S et al (2014) Composition of isolated synaptic boutons reveals the amounts of vesicle trafficking proteins. Science 344:1023–1028. https://doi.org/10.1126/science.1252884
13. Henn FA, Anderson DJ, Rustad DG (1976) Glial contamination of synaptosomal fractions.

Brain Res 101:341–344. https://doi.org/10.1016/0006-8993(76)90274-2

14. Dodd P, Hardy JA, Oakley AE, Strong AJ (1981) Synaptosomes prepared from fresh human cerebral cortex; morphology, respiration and release of transmitter amino acids. Brain Res 224:419–425. https://doi.org/10.1016/0006-8993(81)90871-4
15. Schwenk J, Harmel N, Brechet A et al (2012) High-resolution proteomics unravel architecture and molecular diversity of native AMPA receptor complexes. Neuron 74:621–633. https://doi.org/10.1016/j.neuron.2012.03.034
16. Schwenk J, Baehrens D, Haupt A et al (2014) Regional diversity and developmental dynamics of the AMPA-receptor proteome in the mammalian brain. Neuron 84:41–54. https://doi.org/10.1016/j.neuron.2014.08.044
17. Lobingier BT, Hüttenhain R, Eichel K et al (2017) An approach to spatiotemporally resolve protein interaction networks in living cells. Cell 169:350–360.e12. https://doi.org/10.1016/j.cell.2017.03.022
18. Loh KH, Stawski PS, Draycott AS et al (2016) Proteomic analysis of unbounded cellular compartments: synaptic clefts. Cell 166:1295–1307.e21. https://doi.org/10.1016/j.cell.2016.07.041
19. Uezu A, Kanak DJ, Bradshaw TWA et al (2016) Identification of an elaborate complex mediating postsynaptic inhibition. Science 353:1123–1129. https://doi.org/10.1126/science.aag0821
20. Takano T, Wallace JT, Baldwin KT et al (2020) Chemico-genetic discovery of astrocytic control of inhibition in vivo. Nature 588:296–302. https://doi.org/10.1038/s41586-020-2926-0
21. Hobson BD, Choi SJ, Mosharov EV et al (2022) Subcellular proteomics of dopamine neurons in the mouse brain. elife 11:e70921. https://doi.org/10.7554/eLife.70921
22. Wolf ME, Kapatos G (1989) Flow cytometric analysis and isolation of permeabilized dopamine nerve terminals from rat striatum. J Neurosci 9:106–114
23. Wolf ME, Kapatos G (1989) Flow cytometric analysis of rat striatal nerve terminals. J Neurosci 9:94–105
24. Gylys KH, Fein JA, Yang F, Cole GM (2004) Enrichment of presynaptic and postsynaptic markers by size-based gating analysis of synaptosome preparations from rat and human cortex. Cytom Part J Int Soc Anal Cytol 60:90–96. https://doi.org/10.1002/cyto.a.20031
25. Herzog E, Nadrigny F, Silm K et al (2011) In vivo imaging of intersynaptic vesicle exchange using VGLUT1 Venus knock-in mice. J Neurosci 31:15544–15559. https://doi.org/10.1523/JNEUROSCI.2073-11.2011
26. Biesemann C, Grønborg M, Luquet E et al (2014) Proteomic screening of glutamatergic mouse brain synaptosomes isolated by fluorescence activated sorting. EMBO J 33:157–170. https://doi.org/10.1002/embj.201386120
27. Blumenstock S, Angelo MF, Peters F et al (2019) Early defects in translation elongation factor 1α levels at excitatory synapses in α-synucleinopathy. Acta Neuropathol (Berl) 138:971–986. https://doi.org/10.1007/s00401-019-02063-3
28. Hafner A-S, Donlin-Asp PG, Leitch B et al (2019) Local protein synthesis is a ubiquitous feature of neuronal pre- and postsynaptic compartments. Science 364:eaau3644. https://doi.org/10.1126/science.aau3644
29. Hobson BD, Kong L, Angelo MF et al (2022) Subcellular and regional localization of mRNA translation in midbrain dopamine neurons. Cell Rep 38:110208. https://doi.org/10.1016/j.celrep.2021.110208
30. Paget-Blanc V, Pfeffer ME, Pronot M et al (2022) A synaptomic analysis reveals dopamine hub synapses in the mouse striatum. Nat Commun 13:3102. https://doi.org/10.1038/s41467-022-30776-9
31. Turiault M, Parnaudeau S, Milet A et al (2007) Analysis of dopamine transporter gene expression pattern—generation of DAT-iCre transgenic mice. FEBS J 274:3568–3577. https://doi.org/10.1111/j.1742-4658.2007.05886.x
32. Oh SW, Harris JA, Ng L et al (2014) A mesoscale connectome of the mouse brain. Nature 508:207–214. https://doi.org/10.1038/nature13186
33. Shaner NC, Lambert GG, Chammas A et al (2013) A bright monomeric green fluorescent protein derived from Branchiostoma lanceolatum. Nat Methods 10:407–409. https://doi.org/10.1038/nmeth.2413
34. Luquet E, Biesemann C, Munier A, Herzog E (2017) Purification of synaptosome populations using fluorescence-activated synaptosome sorting. In: Poulopoulos A (ed) Synapse development: methods and protocols. Springer, New York, pp 121–134
35. Cetin A, Komai S, Eliava M et al (2006) Stereotaxic gene delivery in the rodent brain. Nat Protoc 1:3166–3173. https://doi.org/10.1038/nprot.2006.450

Chapter 7

Investigating the Molecular Composition of Neuronal Subcompartments Using Proximity Labeling

Mareike Lohse, Siqi Sun, Maksims Fiosins, Stefan Bonn, Pedro Zamorano, Olaf Jahn, and Noa Lipstein

Abstract

The expression pattern of proteins defines the range of biological processes in cellular subcompartments. A core aim in cell biology is therefore to determine the localization and composition of protein complexes within cells. Proximity labeling methodologies offer an unbiased and efficient way to unravel the cellular micro-environment of proteins, providing insights into the molecular networks they participate in. In this chapter, we present a protocol for conducting proximity labeling experiments in primary murine neuronal cultures in vitro based on the proximity-dependent biotinylation identification (BioID) approach. Data acquired through this protocol can be utilized to identify the composition of protein complexes in neurons and to create molecular maps of neuronal subcompartments. This will aid in determining the spatial distribution of biological processes within neurons, and in unraveling fundamental principles of neuronal function and plasticity.

Key words Proximity labeling, Biotinylation identification (BioID), TurboID, Primary neurons, Synapses, Mass spectrometry, Affinity purification

1 Introduction

Neurons are highly compartmentalized cells. A dendritic subcompartment extending from the cell body typically functions to receive and integrate information from upstream neurons, while an axonal subcompartment functions to deliver information to downstream neurons. The different functions mediated by these anatomically distinct subcompartments rely on unique protein complexes. For example, the release of neurotransmitters from axon terminals of presynaptic, information-transmitting neurons, is regulated by a core molecular machinery that mediates the synaptic vesicle cycle and neurotransmitter release. In dendritic and somatic subcompartments, receptor complexes that bind neurotransmitters and

Tolga Soykan and Alexandros Poulopoulos (eds.), *Synapse Development: Methods and Protocols*, Methods in Molecular Biology, vol. 2910, https://doi.org/10.1007/978-1-0716-4446-1_7,

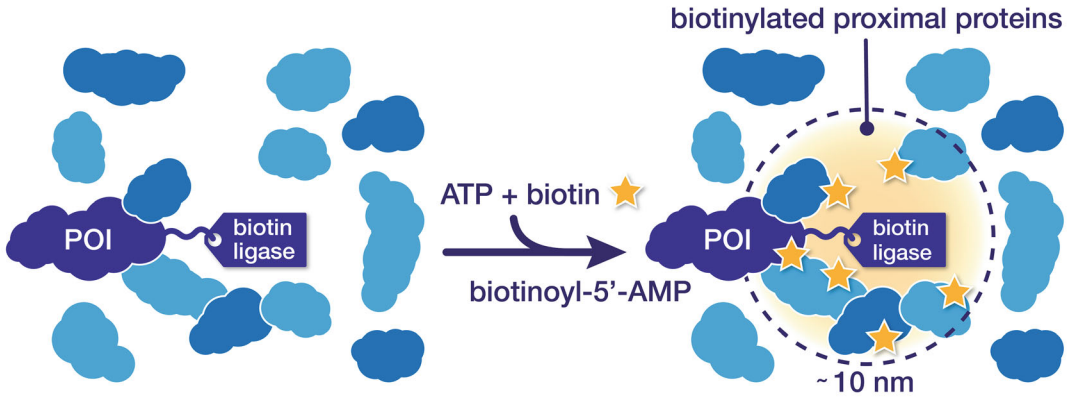

Fig. 1 An enzyme that produces biotin radicals is genetically targeted to protein of interest (POI). Biotin-conjugated reactive intermediates are enzymatically generated upon the addition of biotin derivatives and subsequently diffuse away and react with nearby free primary amines, covalently tagging neighboring endogenous proteins. Only proteins within the radius of the reactive intermediates are biotinylated. After cell lysis, biotinylated proteins are affinity purified and characterized by Western blot or liquid chromatography-mass spectrometry

convey the signal at the postsynaptic, information-receiving neuron, can be found.

The activity of protein complexes that mediate unique neuronal functions is highly regulated. A large group of proteins, including for example G-protein coupled receptors, kinases, phosphates, auxiliary subunits, proteins that mediate metabolic functions and proteostatic proteins are expected to form tight regulatory networks around the core components essential for neuronal and synaptic functions, thereby shaping synapse-specific and neuron-specific properties. However, the localization of many such proteins within specific neuronal subcompartments remains unknown, usually due to the lack of appropriate antibody-based tools for their visualization. Deciphering the spatio-temporal distribution of regulatory proteins in neurons holds the potential to unravel cell biological processes that shape the functional properties of neurons and their synapses.

Proximity labeling is a powerful discovery tool to unravel the composition of protein microenvironments in living cells [1, 2]. Proximity labeling methodologies rely on a still-growing toolkit of enzymes, many of which are engineered, that can catalyze the formation of free biotin radicals. The radicals are released from the catalytic pocket of the enzyme and diffuse freely until they decay or attach covalently onto proteins in their proximity. When a protein of interest (POI) is tagged with a biotinylating enzyme, biotin radicals will label the immediate environment of that POI (Fig. 1), including direct and indirect interactors. The biotinylated proteins are then enriched via a one-step affinity purification on streptavidin beads, and can be characterized in a targeted way by Western blot

approaches or, preferably, in an unbiased way by liquid chromatography-mass spectrometry (LC-MS), providing a snapshot of the molecular environment in question.

Proximity labeling approaches have many advantages over classical biochemical approaches for analyzing protein complexes. First, the labeling occurs in the living cell, which enables the capture of protein complexes under physiological conditions. Second, weak and transient interactions, as well as membrane proteins in proximity can be identified, without changing the reaction conditions and excluding the need for the costly generation of high-quality antibodies. Third, the ultra-high affinity of the streptavidin-biotin interaction [3] enables to conduct affinity purifications under harsh binding and washing conditions (e.g., in the presence of strong detergents) to efficiently suppress unspecific binding of non-biotinylated proteins. Finally, proximity labeling is easy to integrate in molecular biology laboratories, since it only requires simple cloning procedures and standard cellular expression techniques.

Here, we describe a protocol for proximity biotinylation and affinity purification of proteins from neuronal cultures in vitro. We adapted the proximity-dependent biotinylation identification (BioID) approach, which uses mutated versions of the biotin ligase BirA [4, 5]. Specifically, we use an engineered version of BirA called TurboID, which retains the relatively large size (35 kD) of the original BirA, but provides a high biotinylation efficiency [6]. Although proximity labeling has been used in multiple cell types and organisms, there are several particularities in applying it in primary neuron-astrocyte co-cultures, which we highlight here. Our current proximity labeling protocol is well-suited for the investigation of protein organization at neuronal subcompartments, resulting in extremely specific readouts. This protocol can be combined with biochemical fractionation protocols (e.g., to enrich for synaptosomes or synaptic vesicles), to further increase specificity and spatial resolution.

2 Materials

2.1 Reagents for Primary Astrocyte and Neuronal Cultures

1. Papain buffer solution (100 mL): 20 mg L-cysteine (e.g., Sigma-Aldrich C7362), 1 mM $CaCl_2$, 0.5 mM ethylenediaminetetraacetic acid (EDTA) pH 8, add Dulbecco's modified eagle medium (e.g., DMEM; Gibco™ 41966-029) to 100 mL. Aliquot and store at −20 °C.
2. Enzymatic stop solution (100 mL): 250 mg Bovine Serum Albumin (BSA; e.g., Sigma-Aldrich A9418), 250 mg trypsin inhibitor (Sigma-Aldrich T9253), 90 mL DMEM, 10 mL Fetal Bovine Serum, heat inactivated (FBS; e.g., Gibco™ A15-104).

Filter sterile using a 0.22 μm vacuum filter bottle (e.g., Corning® 430771), aliquot, and store at −20 °C.

3. Dulbecco's Phosphate Buffered Saline (DPBS; sterile, e.g., Gibco™ 14190).
4. Poly-L-Lysine (PLL; e.g., Sigma-Aldrich P4707): diluted 1:10 in sterile DPBS.
5. Hanks' Balanced Salt Solution, without calcium and magnesium (HBSS, e.g., Gibco™ 14170-088).
6. Neuronal culture medium: Freshly mix 500 mL Neurobasal™-A medium (NBA; e.g., Gibco™ 10888-022), 10 mL Gibco™ B-27™ Plus Supplement (50×; e.g., Thermo Fisher Scientific 17504044), 5 mL GlutaMAX™ supplement (e.g., Thermo Fisher Scientific 35050-061), and 1 mL Penicillin-Streptomycin (10,000 U/mL), filter sterile, and store at 4 °C for up to 8 weeks.
7. Papain (e.g., Worthington Biochemicals LS003126).
8. 0.05% Trypsin-EDTA.
9. Astrocyte culture medium: Freshly mix 448.5 mL DMEM with GlutaMAX (Gibco™ 31966-021), 50 mL Fetal Bovine Serum, heat inactivated, 0.5 mL Corning® MITO+ Serum Extender (355006) and 1 mL Penicillin-Streptomycin (10,000 U/mL), filter sterile, and store at 5% CO_2, 37 °C for up to 1 month.
10. Floxuridine (FUDR) 1000× stock: 16.5 mg/mL uridine (Sigma-Aldrich U3750), 6.7 mg/mL 5-fluorodeoxyuridine (Sigma-Aldrich F0503) in $_{dd}H_2O$. Filter sterile, aliquot, and store at −20 °C.
11. PDL-collagen-coating solution: 0.1 mg/mL Poly-D-Lysine (PDL; e.g., Sigma-Aldrich P6407), 0.2 mg/mL collagen (Corning® 354236) and 10.2 mM acetic acid in $_{dd}H_2O$.
12. Laminar flow hood equipped with UV-light and standard equipment for cell culture.
13. Stereomicroscope.
14. Dissection tools.
15. CO_2- and temperature-controlled incubator: 5% CO_2, 37 °C.
16. Cell culture dishes.

2.2 Preparation of cDNA Constructs

Before starting, carefully read **Notes 1–7**.

Standard cloning methods are used to generate vectors with the cDNA encoding the selected POI under the human synapsin promoter, to promote selective expression in neurons. Use expression systems for stable expression, for example, lentiviral-based transduction, which results in the integration of the delivered DNA into the genomic DNA. You will need to clone at least two constructs:

1. POI tagged by TurboID: depending on the POI, either an N-terminal or a C-terminal fusion construct should be designed. Make sure the TurboID carries a tag (e.g., ALFA- or FLAG-tag) that will enable a Western blot assessment of the expression levels of your constructs if necessary. We separate the POI and TurboID by a 15 amino acid flexible linker.
2. A positive control construct, where the TurboID enzyme is, for example, constrained to a general subcompartment (i.e., the cytosol). For cytosolic POIs, we use a cytosolic TurboID (V5-TurboID-NES-pCDNA3 cassette in the Addgene plasmid #107169 from the group of Alice Ting [6]), cloned in a lentiviral/adenoviral expression vector under the human synapsin promoter.

2.3 Immunocytochemistry

1. 10× Phosphate-based saline (PBS): 1.37 M NaCl, 27 mM KCl, 100 mM Na_2HPO_4, 18 mM KH_2PO_4.
2. 1× PBS.
3. 4% Paraformaldehyde (PFA) in 1×PBS, pH 7.4.
4. 50 mM glycine in 1× PBS (50 mL).
5. Permeabilization buffer: 0.1% Triton X-100 (e.g., Sigma-Aldrich T8787) and 2.5% normal goat serum (NGS, e.g., Thermo Fisher Scientific 10000C) in 1× PBS.
6. Blocking buffer: 2.5% NGS in 1× PBS.
7. Antibodies against markers of the relevant subcompartments, that can be used for immunostaining. See Table 2 for an example of a combination of antibodies to verify synaptic localization.

2.4 Affinity Purification of Biotinylated Proteins

1. RIPA lysis buffer (500 mL): 150 mM NaCl, 1% IGEPAL CA 630 (NP-40), 1% sodium deoxycholate, 0.1% SDS, 25 mM Tris-HCl pH 7.4. Store at 4 °C. As a working solution, RIPA lysis buffer is always freshly supplemented with 1× protease inhibitors. *Note: the composition of detergents can be modified depending on your protein of interest.*
2. Protease inhibitors mix.
3. Biotin solution. Because biotin is difficult to dissolve at a high concentration, we use a 10× BXT strep-tactin XT elution buffer (500 mM, Iba Lifesciences 2-1042-025).
4. Magnetic streptavidin beads. We use MagStrep® Strep-Tactin®XT Beads (Iba Lifesciences 2-5090-002), because they have a reduced affinity to biotin, which enables competitive elution of biotinylated proteins.
5. CHAPS/Urea elution buffer: 7 M urea, 2 M thiourea, 2% CHAPS, 0.1 M Tris, pH 8.5. Use high-quality reagents (e.g.,

from Serva) as this eluate will directly proceed to in-solution digestion with trypsin (see below).

6. Protein quantification kit (e.g., Bradford or BCA).
7. 3× Laemmli sample buffer: 150 mM Tris–HCl pH 6.8, 30% (v/v) glycerol, 6 mM EDTA, 10% SDS, 150 mM Dithiothreitol (DTT), 0.2% (w/v) Bromophenol Blue, mix well. Aliquot and freeze at −20 °C.
8. Protein molecular weight marker (e.g., PageRuler Plus Prestained Protein Ladder, 10–250 kDa, Thermo Scientific 26619).
9. 4–12% Bis-Tris polyacrylamide gel (e.g., Invitrogen NuPAGE™ NP0322BOX) and SDS-PAGE running system (e.g., Invitrogen A25977).
10. 10× MOPS running buffer: dissolve 0.5 M MOPS, 0.5 M Tris, 35 mM SDS, 10 mM EDTA in $_{dd}H_2O$. Store at 4 °C.
11. Transfer buffer: 25 mM Tris, 0.2 M glycine, 20% methanol in $_{dd}H_2O$. Store at 4 °C.
12. Protein stain kit (e.g., MemCode™ Reversible Protein Stain Kit, Thermo Scientific 24580).
13. 10× Tris-buffered saline (TBS): 1 M NaCl, 100 mM Tris, adjusted to pH 7.4 with HCl.
14. 1×TBST: 1×TBS with 0.1% Tween20.
15. Blocking buffer: 1× TBST with 5% (w/v) low fat milk powder.
16. Streptavidin-HRP conjugate (e.g., Thermo Fisher Scientific S911, diluted 1:2000).
17. Sonicator and probe for small volumes.
18. Cooled bench-top centrifuge (min. 15,000× *g*).
19. Magnetic rack (e.g., DynaMag™-2, Invitrogen 12321D).
20. Temperature-controlled shakers.

3 Methods

Before starting, carefully read **Notes 1–7** and see Fig. 2.

3.1 Overview

- Prepare plates coated with an astrocyte monolayer, or, for immunostaining, with PLL-coated coverslips.
- Day 0: prepare primary neuronal cultures, plate on an astrocyte monolayer/PLL-coated coverslips.
- Day 1: wash the plates to remove dead neurons.
- Day 2–3: infect your cultures with viruses.
- Day 16–18: add biotin solution.

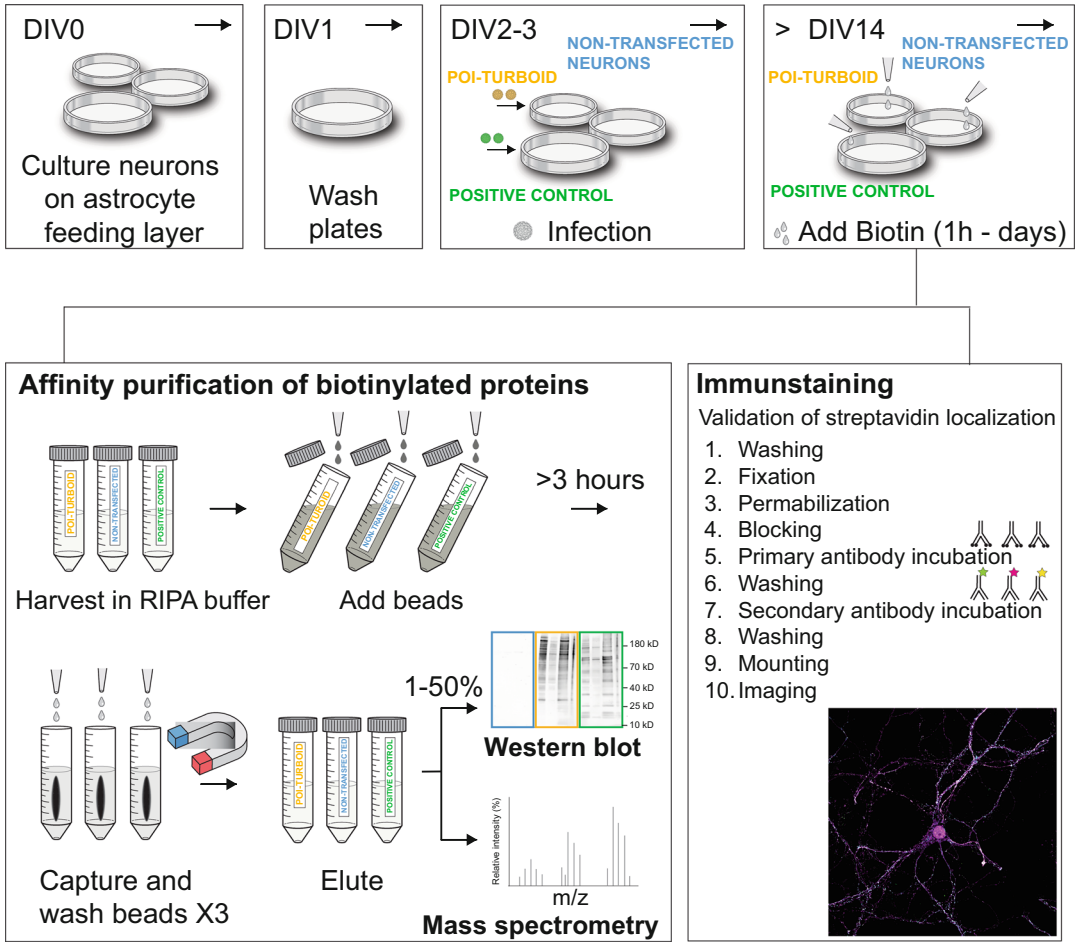

Fig. 2 Primary cortical neurons from P0 wild-type mice are cultured, washed the next day and infected on day in vitro (DIV) 2–3 with lentiviral or adenoviral constructs that mediate the expression of the protein-of-interest (POI) genetically tagged by TurboID, and a cytosolic TurboID (positive control). The same number of plates are left uninfected as negative control. The neurons are incubated with biotin before they are harvested for affinity purification of biotinylated proteins (left) or fixed for the validation of expression and correct localization of the biotinylated proteins (right)

- Harvest the samples (option: store at −80 °C for further processing).
- Sample processing: conduct an affinity purification to prepare samples for downstream analysis by Western blot or mass spectrometry.

3.2 Monolayer Astrocyte Cultures

To ensure the proper development and function of neurons in culture, it is strongly recommended to co-culture them with astrocytes. We prepare the astrocyte cultures separately and use monolayer cultures on which we plate neurons. This is sufficient to support neuronal viability and firing, but maintains the number of

astrocytes low, which aids in reducing the levels of astrocyte proteins in the sample. The protocols for preparing primary astrocytes are adapted from Burgalossi et al. (2012) [7], originally for astrocytic islands for autaptic neuronal cultures. We do not describe this protocol here, but rather start at the point of splitting the astrocyte culture onto plates for the proximity labeling experiments. As an alternative, it is possible to use standard protocols for neuron-glia co-cultures. For immunostaining, it is best to use neuronal cultures without an astrocyte monolayer to reduce the background immunofluorescence during imaging.

1. Prepare in advance PDL-collagen-coated 10 cm cell culture dishes by smearing the PDL-collagen coating solution with a clean cotton swab onto the dishes. Let the coating dry completely. The coated dishes can be stored at room temperature in the dark until use (up to several months). Sterilize the coated dishes with UV light in the cell culture hood for at least 20 min before use.
2. Close a T75 cell culture flask containing primary astrocytes tightly. Vortex at maximum strength for 2–6 min. This step aids in detaching the non-astrocytic cells. Check the astrocyte culture under a microscope every few minutes. When a clear carpet-like astrocyte culture is observed, stop vortexing.
3. Remove the astrocyte medium and foam generated by vortexing and wash the astrocyte culture twice with 10 mL DPBS.
4. Remove the DPBS and add 2–3 mL Trypsin/EDTA at 37 °C for 5 min.
5. Add 10–12 mL astrocyte medium to block the Trypsin activity and resuspend the astrocytes homogeneously for cell counting.
6. Plate at least 500 K astrocytes in each coated 10 cm dish. Distribute the cells evenly. Fill the coated dish with 15 mL astrocyte medium.
7. Check the growth of the astrocytes under a microscope daily. A confluent astrocytic feeding monolayer is usually formed approximately 5–7 days after plating. If you aim for an earlier usage, plate more astrocytes. Once a confluent astrocytic feeding monolayer is formed, add 1×FUDR to the culture to avoid overgrowth of the astrocytes. The addition of FUDR should optimally be done at least one day before seeding the neurons.

3.3 Primary Cortical Neuronal Cultures

1. Thaw an aliquot of the papain buffer solution, freshly add 25 units of papain per 1 mL of prewarmed papain buffer solution to make the digestion solution, and equilibrate with carbogen until the solution becomes clear. Use a 0.22 μm filter unit (e.g., Millipore SLGP033RS) to sterilize the solution. Aliquot 1 mL digestion solution per sample (e.g., tissue from

Table 1
Volumes of buffers and number of neurons seeded per cell culture dish

Application	Biochemistry		Immunostainings	
Dish size	10 cm	6 cm	12-well	24-well
# astrocytes	∽500 k	∽300 k	–	–
# neurons	3–5 × 10^6	0.8–1 × 10^6	100–150 k	50–100 k
Medium (mL)	15–20	4–5	2	1

one mouse brain) in an 1.5 mL Eppendorf tube. Pre-warm the aliquots at 37 °C.

2. Dissect cortices from postnatal day 0 (P0) mouse brains in HBSS without Ca^{2+} or Mg^{2+}. Removing the thin meninges layer surrounding the cortex will result in a healthier culture.
3. Transfer each pair of mouse cortices into 1 mL prewarmed digestion solution and incubate at 37 °C, gently shaking for 1 h.
4. Remove the majority of digestion solution without disrupting or drying the cortices and immediately add 1 mL prewarmed stop solution. Incubate at 37 °C, gently shaking for another 15–20 min.
5. Remove the majority of stop solution and add 200 μL prewarmed neuronal culture medium. Gently dissociate the brain tissue by pipetting it up slowly with a 200 μL pipette tip, and down carefully against the Eppendorf tube wall, letting it flow down to the bottom. Repeat this procedure for 8–9 times.
6. Immediately after dissociation, add 800 μL prewarmed neuronal culture medium to the cell suspension and wait until large tissue pieces sediment to the bottom. Transfer the supernatant containing single neurons into 9 mL of neuronal culture medium. Count the cells.
7. Replace the medium in the target plates to neuronal medium and seed the neurons (see recommendations in Table 1). Keep the cultures in an incubator at 37 °C, 5% CO_2. *Note: we typically obtain 5–10 million cortical neurons from one mouse.*
8. Optional: For neuronal cultures on an astrocytic layer, change the medium carefully at day-in-vitro (DIV) 1. For neuronal cultures on PLL-coated coverslips (*see* **Note 9**), remove almost all medium without drying the neurons and wash the coverslips twice by slowly dropping single drops of prewarmed medium on the neurons. Check the culture under the microscope; debris and dead cells should be largely removed, if not, repeat the washing step one more time.

9. Infect the neurons at DIV1-3 with AAV/lentiviruses containing (a) POI-TurboID and (b) positive control constructs. Keep the same amount of (c) non-transfected plates.
10. Add 10× BXT buffer (500 mM biotin) directly to the neuronal medium of the cultures in a ratio of 1:100–1:1000 to yield a final concentration of 0.5–5 mM biotin 2–3 days before harvesting/fixation.

3.4 Validation of Construct Expression and Localization by Immunostaining

All steps are conducted at room temperature, unless otherwise indicated. Here, use neurons grown on PLL-coated coverslips without astrocytes (*see* **Notes 8–9** and Fig. 3).

1. Wash the coverslips three times with PBS.
2. Fixation: remove the PBS and add 4% PFA in PBS in each well to fix your cells for 18 min.
3. Wash the coverslips three times with PBS for 2–5 min each.
4. Quenching: remove the PBS, add 50 mM glycine in PBS and incubate for 10 min under gentle agitation.
5. Wash the coverslips three times with PBS for 2–5 min each time, incubate the plate under gentle agitation.

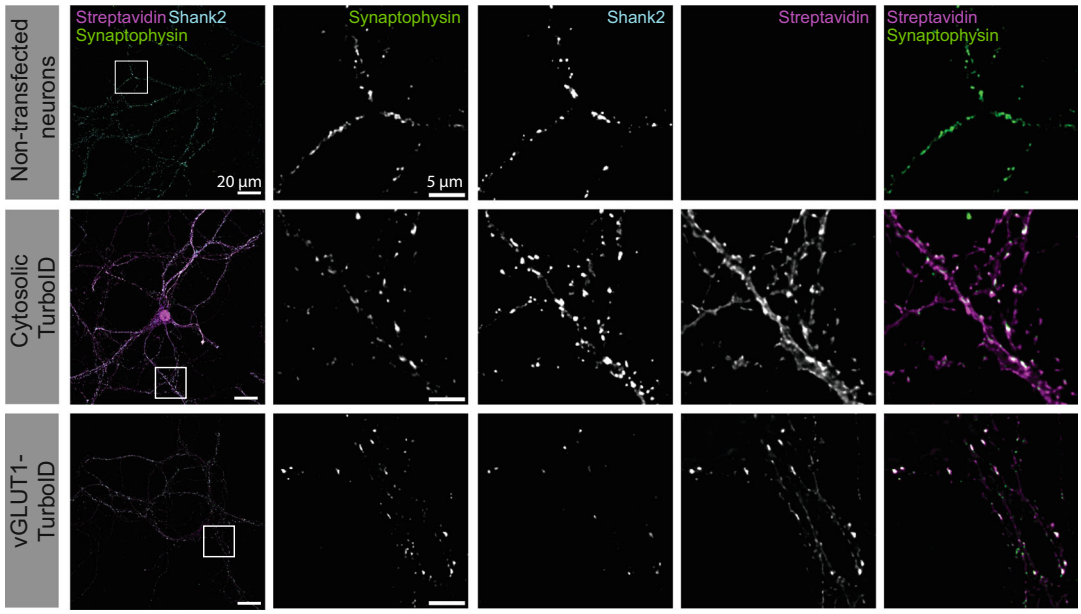

Fig. 3 Immunofluorescence images of non-transfected neurons, neurons expressing cytosolic TurboID, and neurons expressing VGLUT1-TurboID, stained for Map2 (dendritic marker), Synaptophysin 1 (presynaptic marker), Shank2 (postsynaptic marker) and for biotinylated proteins using the antibodies specified in Table 2. Non-transfected neurons do not show a signal for biotinylation (negative control), whereas neurons expressing cytosolic TurboID show a diffused biotinylation signal throughout the cell body and neuronal projections. The signal for biotinylation in neurons expressing VGLUT1-TurboID co-localizes well with that of the presynaptic marker synaptophysin

Table 2
Example for antibody combination to validate biotinylation at synapses

Marker	Primary Ab	Dilution	Secondary Ab/Chemicals	Dilution
Presynaptic compartment	Synaptophysin 1 (rabbit) (e.g., Synaptic Systems #101002)	1:500	Goat anti-rabbit Alexa633 (e.g., Thermo Fisher Scientific A21071)	1:2000
Postsynaptic compartment	Shank2 (Guinea Pig) (e.g., Synaptic Systems #162204)	1:250	Goat anti-guinea pig Alexa488 (e.g., Thermo Fisher Scientific A11073)	1:2000
Dendritic compartment	Map2 (chicken) (e.g., Novus Biologicals #NB300-213)	1:1000	Goat anti-chicken Alexa405 (e.g., Abcam 175674)	1:1000
Biotinylation	–	–	Streptavidin-Alexa555 (e.g., Thermo Fisher Scientific S32355)	1:800

6. Permeabilization: remove the PBS, add permeabilization buffer and incubate for 30 min under gentle agitation.
7. Wash the coverslips twice with blocking buffer for 2–5 min.
8. Incubate the coverslips with the relevant primary antibodies diluted in blocking buffer for 2.5 h at room temperature, to label the compartment under investigation. Note: antibody incubation times may change depending on the antibody. See example in Table 2 for an antibody combination to label the synaptic subcompartment.
9. Wash the coverslips three times for 2–5 min each with permeabilization buffer.
10. Incubate the coverslips with secondary antibodies diluted in blocking buffer for 45 min at room temperature and in the dark. In addition to the secondary antibodies, add streptavidin coupled to a fluorophore to stain the biotinylated proteins.
11. Wash the coverslips three times with blocking buffer for 2–5 min under gentle agitation.
12. Briefly dip each coverslip in $_{dd}H_2O$ before mounting the coverslip on a microscope slide (e.g., with Aqua-Poly/Mount).
13. Use a standard confocal imaging setup to image the samples.
14. Quantify the degree of co-localization between the immunoreactivity of your subcompartment markers (i.e., the signal from a synaptic label) and the signal stemming from the streptavidin-fluorophore channel, using software such as ImageJ or Imaris.

3.5 Sample Preparation for Affinity Purification of Biotinylated Proteins

After harvesting, all experiments are conducted on ice, unless otherwise indicated. Handle all samples, buffers, tubes, and glassware with gloves to avoid contamination with human keratin.

1. Remove the medium and wash the neuronal culture thoroughly with DPBS.
2. Harvest the neurons in 1 mL RIPA lysis buffer freshly supplemented with 1× protease inhibitors. Incubate the culture dish for 1–2 min in the lysis buffer before collecting the cell lysate in Eppendorf tubes.
3. If the sample is very viscous, sonicate it briefly (4–8 pulses at 60% power) to shear the DNA.
4. Centrifuge the cell lysates for 10 min at ~20,000× *g*, 4 °C to pellet DNA and transfer the supernatant to a new tube.
5. Measure the protein concentration of each sample using a standard protein quantification assay (e.g., Bradford or BCA method).
6. Optional: since biotinylation is a covalent modification, cell lysates can be flash-frozen in liquid nitrogen and stored at −80 °C for further processing.

3.6 Affinity Purification of Biotinylated Proteins for Mass Spectrometry

After harvesting, all the experiments are conducted on ice, unless otherwise indicated. Handle all samples, buffers, tubes, and glassware with gloves to avoid contamination with human keratin. Before starting, carefully read **Notes 10–15**.

1. Measure the protein concentration in the input samples. Starting the affinity purification with similar protein concentrations in all samples is important for proper estimation of background levels as well as for downstream analysis of the mass spectrometric data.
2. Use 10–50 μg of the supernatant samples to prepare "input" samples for Western blot analysis. Mix each sample with concentrated Laemmli sample buffer and boil at 99 °C for 10 min.
3. Equilibrate the necessary volume of beads per sample by washing them 3 times with 1–2 mL RIPA buffer. Use a magnetic rack to capture the beads during the removal of solution. Make sure the beads are homogeneously resuspended when adding solution by inverting the tube several times. Avoid vortexing, never let the beads dry. Aliquot in separate Eppendorf tubes according to the number of samples.
4. Capture the beads using a magnetic rack. Remove the RIPA buffer from the beads and add the harvested samples to the beads.
5. Incubate with gentle rolling for minimally 3 h at 4 °C. Overnight incubation is also possible, but not necessary.

6. Capture the beads using a magnetic rack. Collect the supernatant ("flow through") in an Eppendorf tube, and immediately add 1–2 mL of RIPA buffer to the beads. Never let the beads dry.
7. Use 10–50 μg of the collected "flowthrough" sample to prepare a Western blot sample. Mix with concentrated Laemmli sample buffer and boil for 10 min. The efficiency of biotinylated protein capture by the beads can be assessed using this sample (Fig. 4).
8. Wash the beads 3–5 times with 1–2 mL RIPA buffer. Use the magnetic rack to capture the beads, add RIPA buffer, gently invert the tube 4–5 times at each washing step to make sure the beads are fully resuspended, and repeat. Note that washes in additional buffers are also possible in this stage.
9. Use a magnetic rack to capture the beads and remove the RIPA buffer. Add 150 μL CHAPS/Urea elution buffer supplemented with 1xBXT buffer (50 mM biotin) to the beads to elute the proteins. In contrast to disruptive elution with Laemmli sample buffer, this non-disruptive competitive elution leads to cleaner samples with only low avidin contamination and reduced background.
10. Incubate the beads at room temperature for 15 min rolling, or in a thermoshaker at 800 rpm. Do not heat the tubes when preparing samples for LC-MS since heating will lead to the release of avidin into your sample and to the decomposition of urea, the latter resulting in the modification (carbamylation) of proteins.
11. Use a magnetic rack to capture the beads. Collect the supernatant ("eluate"). Use a part of the eluate volume (1–50%) to prepare a Western blot sample, mix with concentrated Laemmli sample buffer and boil for 10 min (Fig. 4).
12. Add 150 μL of 1× Laemmli sample buffer to the remaining beads and boil for 10 min. Using this sample, you will evaluate the efficiency of the competitive elution (Fig. 4).

3.7 Detection of Biotinylation and Identification of Proximal Proteins by Western Blot Analysis

See **Notes 16–17**.

1. Load each Western blot sample into an individual lane of a 4–12% Bis-Tris polyacrylamide gel. See Fig. 4 for an outline of the samples to be loaded. We typically assess 1% of the input and flow-through samples, and 5% of the eluate and bead samples.
2. Run SDS-PAGE in MOPS-SDS Running buffer at a current of 100–200 V until the dye front reaches the bottom of the gel.

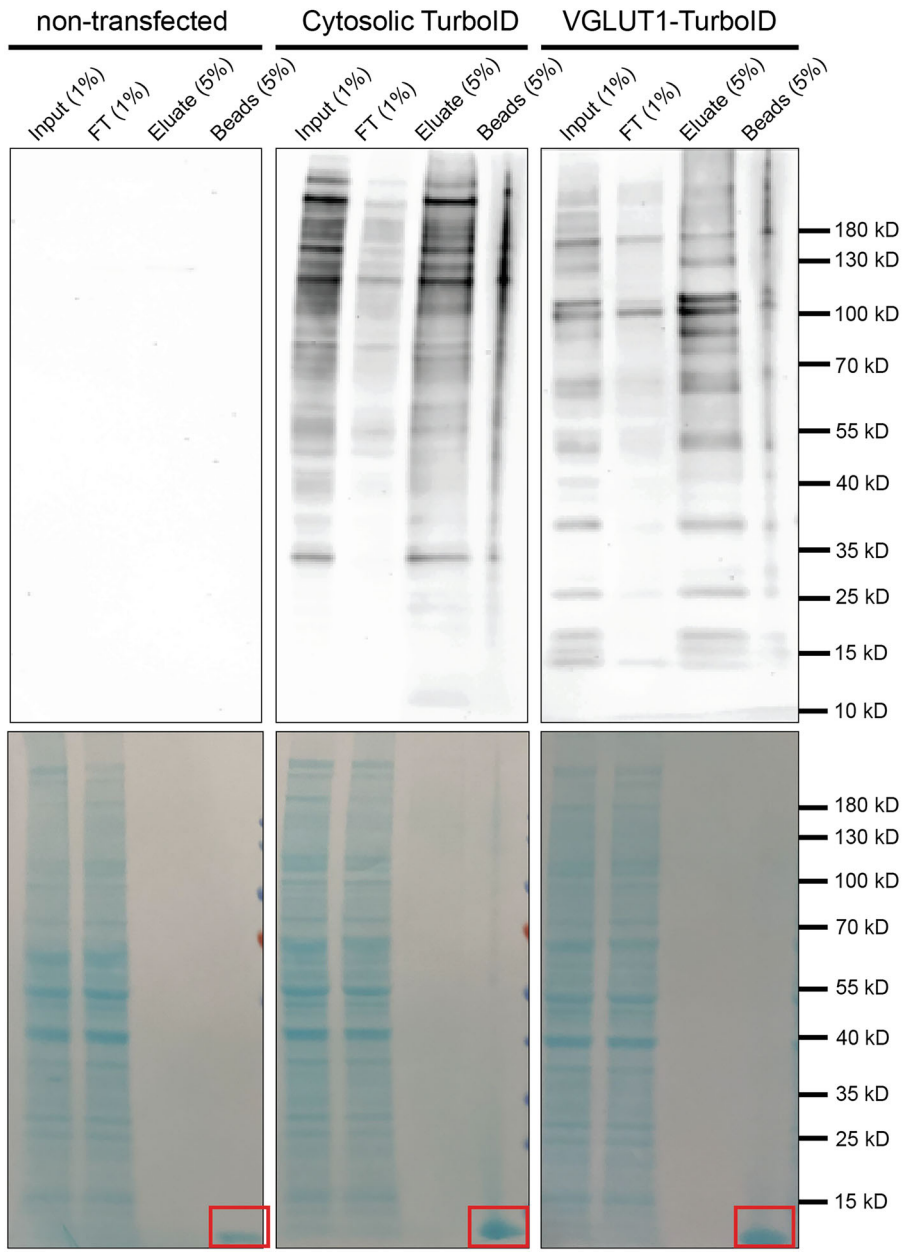

Fig. 4 Western blot analysis of samples obtained by affinity purification of biotinylated proteins from neuronal lysates. Samples include the neuronal lysate (percentages refer to %volume); a sample collected after enrichment and eluted in biotin-CHAPS/Urea buffer ("Eluate"; containing the biotinylated protein fraction for downstream analysis); the flowthrough ("FT"; the fraction of the sample that did not bind to the streptavidin beads); and a sample containing material that was eluted from the beads by boiling in 1x Laemmli in a second elution step after competitive elution with biotin-CHAPS/Urea buffer took place ("Beads"). Staining of the membranes for total protein (lower images; here: MemCode™) shows the amount of proteins that was loaded. Note the negligible avidin contamination in the eluate sample in comparison to the bead sample (see protein band migrating at ~13 kDa, marked by red squares)

3. Transfer the gel to a nitrocellulose membrane in methanol-based transfer buffer with a total current of 1000 mA (e.g., 4 h at 250 mA).
4. Wash the membrane 3 times in $_{dd}H_2O$. Use a protein stain kit according to the manufacturer's instructions, and document the protein stain (Fig. 4). Remove the stain. The protein stain is needed for evaluation of the affinity purification efficiency.
5. Block the membrane with blocking buffer for 30 min–1 h at room temperature.
6. Replace the blocking buffer with a solution containing streptavidin-HRP in blocking buffer, incubate for 1 h at room temperature.
7. Wash the membrane 3 times for 10 min each in TBST.
8. Wash the membrane once with TBS.
9. Develop the chemiluminescence signal using standard HRP signal amplification system and a dedicated image analyzer.

3.8 Data Generation and Initial Inspection

See **Notes 18–20**.

Our quantitative proteomics workflow is based on automated sample preparation, label-free protein quantification by ion mobility-enhanced data-independent acquisition (DIA) mass spectrometry, and a customized data analysis pipeline. It was originally developed for protein detection in synaptic protein fractions and is described in detail elsewhere [8]. As to the experimental design, we typically process samples from three biological replicates and analyze them as technical replicates at injection level to address variability in protein quantification. The description below is relevant for quantitative mass spectrometric data after processing.

1. It is advisable to merge technical replicates, for instance by averaging. Discuss how to deal with missing values at this level with your partner proteomics facility.
2. *Normalization*: Normalize the data by dividing each value by the sum of all values within one sample. This is not necessary for samples from the non-transfected, negative control. Normalization aids in cases where ligase expression levels are dramatically different between conditions. It is essential to do this normalization before imputation of missing values and before removing non-specific entries.
3. *Imputation*: In this step, group-wide missing values (e.g., when a protein has no data in the negative control) are replaced by low, random values according to the statistical distribution of the values in the sample. For this purpose, the measured, non-normalized values per sample are log2-transformed to generate data with approximately normal distribution. The mean and standard deviation (SD) of the data are calculated

to obtain the center and width of their distribution, and these parameters are used to simulate random low values to replace missing values. There are multiple methods for imputation and the settings should be determined according to the nature of your data. While imputation is critical for proper usage of quantitative data, wrong usage of imputation can dramatically alter the experimental results. Discuss alternative imputation approaches with your partner proteomics facility.

4. *Remove non-specific entries*: These may arise due to nonspecific binding to beads, or from endogenously biotinylated proteins in neurons and astrocytes. To remove such background, we use non-transfected neurons as a control. We determine a *specificity ratio* for each entry, calculated as the ratio between the *non-normalized* signal intensity of the POI-TID and that of the non-transfected control. Typically, we consider hits as specific if this ratio is larger than 4, and the difference between the groups is statistically significant after adjusting for multiple comparisons ($p < 0.05$). Note that if you do not impute missing values, you need to include all cases where an abundance value is available for the POI-TurboID but not for the negative control condition.
5. *Evaluate proximity*: In proximity labeling experiments, proteins that are very close to the POI are expected to be intensively biotinylated, and thus their relative fraction in the sample is expected to be high. In contrast, distal proteins would be marginally biotinylated, and their relative fraction in the sample is expected to be low. The *proximity ratio* is calculated for each entry as the ratio between the *normalized* abundance value of the POI-TurboID and the normalized abundance value of the cytosolic TID control. Note that if you do not impute missing values, you need to include all cases where an abundance value is available for the POI-TurboID but not for the positive control condition.
6. *Biological evaluation*: Evaluate your results by comparing the list of significant proteins against available data in the literature. For synaptic POIs, we advise comparing the results with proteins in the SynGO database [9] and with the synaptosomal and SV proteins detected by Taoufiq et al. [10]. Functional enrichment analysis, especially for GO cellular components, may confirm that the proximal proteins are located in the same cellular subcompartment as the POI.

4 Notes

1. If during the experiment you are conducting, you plan to produce samples for downstream LC-MS analysis, first discuss the settings of the experiment with your partner proteomics

facility. Potential adaptations will have to be made with regard to the amount, volume, and buffer composition of the resulting sample.

2. Biotin ligases depend on free biotin for their activity. TurboID is reported to induce biotinylation in an amount sufficient for downstream proteomic analysis within 10 min of the addition of biotin [6]. However, the supplements for neuronal media, critical for the growth of neurons in vitro, contain large amounts of free biotin which cause a moderate and detectable level of biotinylation even before the addition of biotin. This "steady-state biotinylation" does not affect neuronal viability, but hinders the acute induction of biotinylation when using biotin ligase-based approaches in neuronal cultures. Acute activation of biotinylation is possible in other proximity labeling systems (e.g., APEX-based systems) [11].
3. Although we work with cortical neurons (due to the large number of neurons per animal that can be isolated), this protocol is suitable for culturing neurons from other brain structures (e.g., hippocampal neurons). Similarly, mouse lines with different genetic backgrounds can be used. Make sure all licenses for working with animals are in place.
4. Carefully select a negative control as it is particularly important for testing non-specific binding to the beads. Additionally, it can be used to control for potential chromatographic carry-over in LC-MS, which could lead to detection of TurboID in samples from non-transfected neurons. In primary neurons in culture, it is not advisable to use the expression of the POI-TurboID in the absence of biotin as a negative control, due to the steady-state biotinylation in the presence of supplements for neuronal media (*see* **Note 2**). Use non-transfected neurons instead.
5. Carefully select positive controls, depending on your POI. Valid positive controls include proteins with a broad expression pattern in the same cellular subcompartment, and mutants of the POI that affect their cellular localization or complex composition. Suboptimal positive controls include mutants of the POI that reduce its expression levels, and proteins that are expressed in distinct cellular compartments than the POI.
6. CRISPR-based approaches to tag the POI endogenously are highly recommended, as long as they target a large fraction of the neurons in culture to produce sufficient amount of sample for downstream analysis.
7. It is advisable to avoid transient over-expression approaches. When using viral transduction methods, keep in mind the final size of your construct. The size of the cDNA coding for TurboID-V5 is ~1 kb. Lentiviral particles have a limited

packing capacity, such that the insert size can be maximally 8–9 kb. The degree of expression declines as the insert size increases, due to inefficient packing of the DNA. The packing capacity of adenoviruses is lower, and limited to insert sizes of 5–6 kb. At the protein level, make sure that you choose a POI that remains functional, stable, and localizes correctly into its designated cellular subcompartment when tagged. If your POI was not tagged before, it is advisable to generate both N- and C-terminal fusion constructs and validate the localization of the resulting proteins. Lastly, keep in mind the degree of over-expression and assess the expression efficiency of the different constructs you use. Optimally all constructs you test should be expressed at similar levels. If knock-out mice deficient for the POI are available, it is recommended to prove the functionality of the TurboID-fused POI by rescue experiments in cultured neurons using appropriate readouts.

8. Before collecting large samples for LC-MS or Western blot analysis, confirm the localization of your over-expressed POI--TurboID and positive control(s) at the expected subcompartment of the cell by immunostaining.
9. We use poly-L-Lysine (PLL)-coated coverslips to grow neurons for immunostainings, as astrocytes often contribute to a high background signal. Sterilized coverslips are incubated at 37 °C for 1 h in 1:10 diluted PLL solution in DPBS. Longer incubation times are not advisable. After washing for three times with DPBS, the coated coverslips can be maintained under sterile conditions in HBSS or in DPBS in a temperature-controlled incubator until use.
10. The interaction between streptavidin and biotin is one of the strongest non-covalent interactions in nature. This creates a difficulty in eluting the biotinylated proteins from the beads. Boiling the beads will result in successful elution, but will also release a massive amount of Avidin from the beads into the sample, which masks other signals during downstream LC-MS analysis. To avoid this, biotinylated proteins can be eluted by on-bead trypsinization protocols, preferably by using beads with trypsin-resistant streptavidin [12], which are commercially available (ReSyn Biosciences). Alternatively, we recommend a competitive elution strategy with excess free biotin, relying on the MagStrep® Strep-Tactin®XT Beads (Iba Lifesciences 2-5090-002), that carry a mutated form of streptavidin with lower affinity for biotin.
11. We elute the biotinylated proteins in a CHAPS/Urea buffer supplemented with biotin to yield a sample that can be directly subjected to in-solution digestion according to the filter-aided sample preparation (FASP) procedure [13] in preparation for LC-MS analysis.

12. The volume of beads used to capture the biotinylated proteins depends on the provider, stock, and on the amount of biotinylated proteins in your sample. We use 150–200 μL bed volume per 10 cm plate for conditions of low- to mild overexpression. The amount of biotinylated proteins is difficult to estimate, but at least 1 μL magnetic beads per 0.85 nmol biotinylated protein should be used. To experimentally determine the amounts of beads needed, compare the input sample with the recollected flow-through sample during Western blot analysis.
13. Use only wide bore pipette tips while transferring the beads. Alternatively, cut the tip of a 1 mL pipet tip with clean scissors.
14. Despite the specified long shelf life, we recommend to use the beads as fresh as possible, particularly when dealing with samples for downstream LC-MS analysis.
15. Western blot samples can be stored at −20 °C.
16. Control for successful biotinylation: because primary neuronal cultures are limited in scale, the yield of biotinylated proteins is expected to be low and difficult to quantify using standard protein quantification assays, by Coomassie staining, and even by silver staining protocols. Due to the ultra-high binding affinity of streptavidin and biotin, a Western blot analysis using streptavidin-HRP conjugate to identify the biotinylated proteins in the samples will serve as the best tool to assess the success of the experiment, and will provide an estimate for the protein amounts in the sample. Our experience shows that if you identify a signal for biotinylation using streptavidin-HRP conjugate-based detection when loading <30% of your sample, that sample is suitable for LC-MS analysis. Sample analysis by Western blot using standard antibodies (e.g., against a tag) will require loading of large sample amounts, as the affinity of standard antibodies is lower than that of the streptavidin-HRP conjugate.
17. Upscaling your sample size: If the degree of biotinylation is low, consider increasing the number of neuron culture plates, the amount of virus added to each plate (to increase the number of infected neurons), or to extend the time in which excess biotin is present in the medium. In our experience, for well-expressed proteins, 1–2 10 cm dishes per construct and 1–2 days of excess biotin exposure are sufficient.
18. Similar expression levels of the biotin ligase in both experiment and control conditions are optimal for downstream analysis. Sometimes, however, this is hard to achieve, especially in the case of large proteins with reduced expression levels, and a well-expressed positive control such as cytosolic TurboID. In that case, comparison of the quantitative LC-MS data is

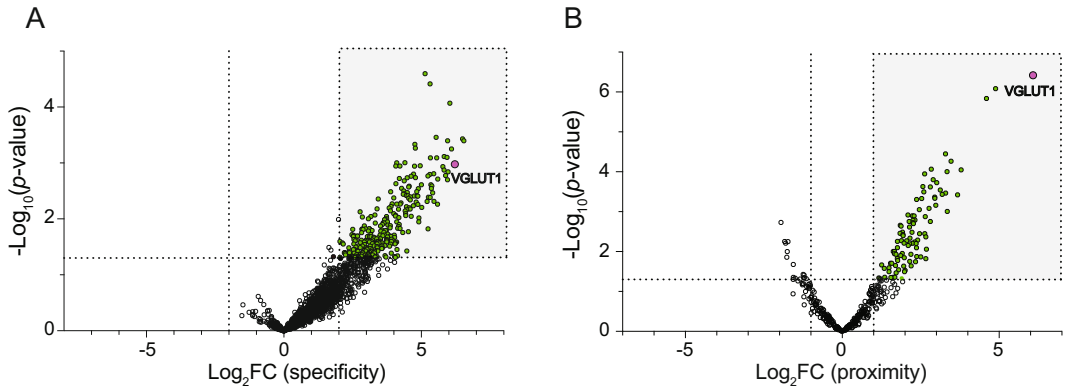

Fig. 5 Volcano plots illustrating two steps of data filtering for an experiment analyzing the proximal environment of the synaptic vesicle protein VGLUT1 (Uniprot Accession: Q3TXX4). VGLUT1 was C-terminally tagged with TurboID and expressed via lentiviral-mediated overexpression in murine cortical neurons in vitro. (**a**) Volcano plot to select proteins that are enriched in comparison to a non-transfected control. We consider specific proteins as those that are enriched >4-fold in comparison to the non-transfected control (x-axis) in a statistically significant manner ($n = 3$, $p < 0.05$; y-axis). 384 hits passed this threshold (green circles). (**b**) Evaluation of proximity: of the 384 hits in A, we defined proximity as the ratio between the normalized abundance of the POI-TurboID and the normalized abundance value of the positive control (here, cytosolic TurboID). We consider 98 proteins (enriched >2-fold, $p < 0.05$) as proximal to VGLUT1. Note that VGLUT1 is highly enriched in both plots

difficult. We use normalization of the values in each sample, which then allows to compare the relative fraction of hits in each sample.

19. Proximity labeling data is best illustrated in volcano plots (Fig. 5). See dedicated protocols and consult your partner proteomics facility on the appropriate statistical analysis that is necessary to produce such plots.
20. A good indication for the success of your experiment is when the tagged POI displays a high proximity ratio with a high statistical confidence.

Acknowledgments

We thank Barth van Rossum for graphic design, Kerstin Steinhagen, Dörte Hesse, Marina Uecker, and Lars Piepkorn for technical assistance, and the LeibnizFMP animal facility for mouse husbandry. This work was supported by the German Research Foundation Excellence Strategy EXC-2049-390688087 (N.L.); CRC 1286 "Quantitative Synaptology" projects A11 (N.L.) and Z2 (M.F. & S.B.), and by the Einstein Center for Neurosciences funded by the Einstein Foundation Berlin, project number EZ-2014-226 (S.S.). P.Z. was supported by MINEDUC-UA project, code ANT 1856.

References

1. Branon T, Han S, Ting A (2017) Beyond immunoprecipitation: exploring new interaction spaces with proximity biotinylation. Biochemistry 56(26):3297–3298. https://doi.org/10.1021/acs.biochem.7b00466
2. Trinkle-Mulcahy L (2019) marcial. F1000Res 8. https://doi.org/10.12688/f1000research.16903.1
3. Sano T, Vajda S, Cantor CR (1998) Genetic engineering of streptavidin, a versatile affinity tag. J Chromatogr B Biomed Sci Appl 715(1):85–91. https://doi.org/10.1016/s0378-4347(98)00316-8
4. Roux KJ, Kim DI, Burke B (2013) BioID: a screen for protein-protein interactions. Curr Protoc Protein Sci 74:Unit 19 23. https://doi.org/10.1002/0471140864.ps1923s74
5. Roux KJ, Kim DI, Raida M, Burke B (2012) A promiscuous biotin ligase fusion protein identifies proximal and interacting proteins in mammalian cells. J Cell Biol 196(6):801–810. https://doi.org/10.1083/jcb.201112098
6. Branon TC et al (2018) Efficient proximity labeling in living cells and organisms with TurboID. Nat Biotechnol 36(9):880–887. https://doi.org/10.1038/nbt.4201
7. Burgalossi A et al (2012) Analysis of neurotransmitter release mechanisms by photolysis of caged Ca(2)(+) in an autaptic neuron culture system. Nat Protoc 7(7):1351–1365. https://doi.org/10.1038/nprot.2012.074
8. Ambrozkiewicz MC et al (2018) Polarity acquisition in cortical neurons is driven by synergistic action of Sox9-regulated Wwp1 and Wwp2 E3 ubiquitin ligases and intronic miR-140. Neuron 100(5):1097–1115 e1015. https://doi.org/10.1016/j.neuron.2018.10.008
9. Koopmans F et al (2019) SynGO: an evidence-based, expert-curated knowledge base for the synapse. Neuron 103(2):217–234 e214. https://doi.org/10.1016/j.neuron.2019.05.002
10. Taoufiq Z et al (2020) Hidden proteome of synaptic vesicles in the mammalian brain. Proc Natl Acad Sci USA 117(52):33586–33596. https://doi.org/10.1073/pnas.2011870117
11. Lam SS et al (2015) Directed evolution of APEX2 for electron microscopy and proximity labeling. Nat Methods 12(1):51–54. https://doi.org/10.1038/nmeth.3179
12. Rafiee MR et al (2020) Protease-resistant streptavidin for interaction proteomics. Mol Syst Biol 16(5):e9370. https://doi.org/10.15252/msb.20199370
13. Wisniewski JR, Zougman A, Nagaraj N, Mann M (2009) Universal sample preparation method for proteome analysis. Nat Methods 6(5):359–362. https://doi.org/10.1038/nmeth.1322

Chapter 8

Monitoring Synapses via Trans-synaptic GFP Complementation

Theodoros Tsetsenis

Abstract

Over the last years, the analysis of synaptic connectivity in the mammalian brain has been accelerated by the use of techniques combining electrophysiology, light microscopy, viral tracing, and genetic manipulations in animal models. Of particular interest are methods that aim to label synapses by tethering complementary split GFP fragments in opposing sites of the synaptic cleft. Here, I describe SynView, a method for monitoring synapse formation based on GFP complementation and provide a detailed protocol for use in neuronal cultures from mouse hippocampus.

Key words SynView, Neurexin, Neuroligin, Split-GFP, Synapse formation

1 Introduction

A major challenge in neuroscience research has always been the mapping of synaptic connectivity of the complex neuronal networks in the mammalian brain. Toward this goal, many techniques have been developed over the last years with the aim to create links between neuronal circuitry and behavior. These range from high-throughput electron microscopy methods [1] to viral tracing strategies [2–4]. While the utilization of these approaches has managed to dissect a number of neural circuits, they are not designed to provide functional information regarding structural synaptic plasticity, which is crucial to understanding how the brain controls complex neural processes. To achieve this, we need methods that can enable the direct visualization of synapses in real time.

There is an integral physical interaction that occurs across the synapse, which is mediated by synaptic cell adhesion molecules and is one of the fundamental events during synaptogenesis. Among the class of synaptic cell adhesion molecules, the trans-synaptic interaction between the presynaptic neurexins and the postsynaptic neuroligins is one of the strongest and best characterized [5]. Several

Tolga Soykan and Alexandros Poulopoulos (eds.), *Synapse Development: Methods and Protocols*, Methods in Molecular Biology, vol. 2910, https://doi.org/10.1007/978-1-0716-4446-1_8,

studies have attempted to take advantage of the trans-synaptic interaction of neuroligins and neurexins and develop tools for fluorescent tagging of synapses using split-GFP approaches [6–9]. Variations of these methodologies featuring different fluorescent proteins have also been created, enabling the differentiation of distinct synaptic circuits [10, 11]. However, the major concern with all these approaches is that they may not actually report a physiological interaction of a trans-synaptic cell-adhesion complex, but instead monitor the close approximation of two membranes at any location, not only in synaptic specializations; the only exception being activity-dependent methodologies like X-RASP [11].

In order to overcome the above-mentioned limitations, we have developed SynView [12], an alternative method for monitoring synapse formation. In this approach, we have generated novel neurexin-1β and neuroligin-1 fusion proteins with complementary "split" GFP moieties positioned in such a fashion that binding of neurexin-1β to neuroligin-1 permits GFP reconstitution without severely changing their binding affinities. To achieve this, we based the design of all fusions on the atomic structure of the neurexin-1β/neuroligin-1 complex that was previously described [13, 14]. According to this model and differently from prior similar attempts, we inserted split-GFP fragments into neurexin-1β and neuroligin-1 specifically at positions that neither impair their normal folding nor impede their interactions. Moreover, based on our design [12], the split-GFP moieties would come into close enough proximity to reconstitute GFP fluorescence only upon neurexin/neuroligin binding.

Using trans-cellular reconstitution of GFP-fluorescence as an assay, we have successfully validated the SynView methodology and demonstrated that neurexin-1β forms a trans-synaptic complex with neuroligin-1 and that this interaction can be used to label synapses in a specific fashion in vivo. Here, I provide a detailed step-by-step protocol for use of the SynView approach to label synapses in cultured mouse hippocampal neurons.

2 Materials

2.1 Equipment

1. Mammalian culture hood.
2. 5% CO_2 incubator.
3. Confocal microscope.

2.2 Lentivirus Production

1. HEK293T cells (ATCC, CRL-3216).
2. Cell Line Medium: 10% Fetal Bovine Serum in Dulbecco's Modified Eagle Medium.
3. pCMV-VSV-G (Plasmid #8454, Addgene).

4. pMDLg/pRRE (Plasmid #12251, Addgene).
5. pRSV-Rev (Plasmid #12253, Addgene).
6. Lipofection reagent: e.g., X-tremeGENE HP DNA Transfection Reagent (Roche).

2.3 Primary Hippocampal Culture

1. Basic Culture Medium: 0.5% (w/v) glucose, 0.2 mg/mL transferrin in Minimum Essential Medium (MEM), filter and store at 4 °C.
2. Plating Medium: 10% Fetal Bovine Serum, 2 mM L-Glutamine, 0.025 mg/mL Insulin in Basic Culture Medium. Filter and store at 4 °C. Expires after 1 month.
3. Growth Medium: 5% Fetal Bovine Serum, 0.5 mM L-Glutamine, 1% (v/v) B-27 supplement (Gibco) in Basic Culture Medium. Filter and store at 4 °C. Expires after 1 month.
4. 4 ARA-C Medium: 4 μM Arabionside (Ara-C) in Growth Medium.
5. Hank's Balanced Salt Solution (HBSS): 350 mg/L $NaHCO_3$, 1 mM HEPES in standard Hank's Solution without calcium or magnesium (Sigma), pH with NaOH to 7.3–7.4.
6. Matrigel: 1:50 Matrigel® in sterile MEM, store at 4 °C.
7. Papain Solution: 10 U/mL papain, 1 μM $CaCl_2$, 0.5 μM EDTA in HBSS.
8. DNase Solution: 50 mg/mL DNase I in water. Aliquot and store at −20 °C.
9. Calcium Phosphate Precipitation Mammalian Transfection Reagents or kit.
10. Circular glass coverslips No 1.5, 12 mm diameter.

3 Methods

A timeline for a typical SynView experiment is illustrated in Fig. 1.

3.1 Preparation of Lentiviruses Expressing Nrx1β-GFP1-10^{S2}

All procedures for preparing and handling lentiviruses should be performed in Biological Safety Level 2 (BSL-2) environments. Make sure that BSL-2 work practices and personal protective equipment are used at all times.

1. The day before transfection, seed HEK 293T cells in 6-well plates (*see* **Note 1**). Grow cells in Cell Line Medium. One fully confluent T75 flask can be used to make four 6-well plates.
2. The next day start the transfection procedure when HEK 293T cells have reached 80% confluence. Replace the medium with 1.5 mL of MEM for each well.

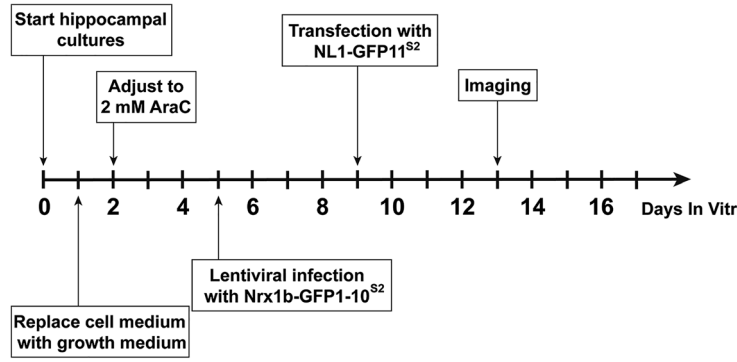

Fig. 1 Experimental timeline for the SynView approach

3. For every 6-well plate prepare the following mix. In a tube containing 1.2 mL of MEM add the following DNA plasmids and mix:

   6 μg pCMV-VSV-G plasmid

   6 μg pMDLg/pRRE plasmid

   6 μg pRSV-Rev plasmid

   12 μg FUW-Nrx1β-GFP1-10^{S2}

4. Add 90 μL of X-tremeGENE HP DNA Transfection Reagent (*see* **Note 2**) and mix thoroughly.
5. Incubate the transfection mix at room temperature for 20 min.
6. Add 200 μL of the transfection mix drop-wise on each well of HEK 293T cells. Return plates in the incubator for 48 h.
7. Collect and pool the supernatant from all wells and centrifuge at 1000 g for 5 min to precipitate any cells and debris.
8. Use immediately to infect primary hippocampal neurons at Day In Vitro 5 (DIV5) or aliquot and freeze at −80 °C (*see* **Note 3**).

3.2 Primary Culture of Hippocampal Neurons

1. Place autoclaved glass coverslips in each of the middle 12 wells of a 24-well plate. Apply 150 μL of Matrigel on each coverslip. Incubate at 37 °C for at least 30 min.
2. Aliquot 10–14 mL of cold HBSS into a 15 mL conical tube and place on ice (*see* **Note 4**).
3. Prepare the papain solution and keep warm at 37 °C. Prepare 10 mL for every 15 mL conical tube of HBSS.
4. Using sterile techniques, dissect the hippocampi from newborn (P0–P1) mouse pups (*see* **Note 5**). Collect 4 hippocampi in one 15 mL tube of cold HBSS on ice.
5. Aspirate HBSS from hippocampi and wash once with 14 mL of ice-cold HBSS.

6. Aspirate HBSS and filter 10 mL of Papain Solution using a 0.2 μm syringe filter into the tube. Incubate for 20 min at 37 °C water bath.
7. Remove papain and wash hippocampi twice with 10–12 mL Plating Medium.
8. After the second wash, add 1 mL of Plating Medium and triturate using a 1 mL pipette tip, until no tissue clumps are visually present. Add another 12 mL of Plating medium and mix.
9. Count cell density in a hemocytometer and adjust to 75000 cells/mL.
10. Take plates out of the incubator and aspirate Matrigel from all coverslips in each 24-well plate.
11. Add 1 mL of the neuronal cell suspension in each well. Return plates to the incubator.
12. 12 h after initial plating remove 900 μL of plating medium from each well and replace it with Growth Medium.
13. 48 h after plating (DIV2) remove 500 μL medium and replace with 4 ARA-C Medium (*see* **Note 6**). The cultures are now ready for lentiviral infection at DIV5.
14. When cultures reach DIV5, remove 300 μL of medium and replace them with Lentiviral Medium as prepared in Subheading 3.1.

3.3 Transfection of Primary Neuronal Cultures with NL1-GFP11^{S2} and Imaging

1. At DIV9, remove selected coverslips containing infected cultured neurons, immerse briefly in MEM and transfer in a new 24-well plate containing 500 μL of prewarmed MEM in each well. Return both the original and the new plate to the incubator (5% CO_2).
2. For each coverslip prepare in 2 separate tubes the following solutions using standard Calcium Phosphate Precipitation Transfection reagents (or commercially available reagents, e.g., Clontech CalPhos Mammalian Transfection Kit):

   Solution A 2 μg FUW-NL1-GFP11^{S2} plasmid

   3.1 μL 2 M $CaCl_2$

   Sterile H_2O to adjust total volume to 25 μL

   Solution B 25 μL 2X HEPES-Buffered Saline
3. Prepare the DNA–Ca_2PO4 precipitate by mixing solution A with solution B. Add about 1/8 volume of solution A at a time into solution B by quickly pipetting several times and gently vortexing at 600 rpm for 2–3 s.
4. Incubate the mixture at room temperature for 15–20 min without any further mixing to allow formation of fine particles

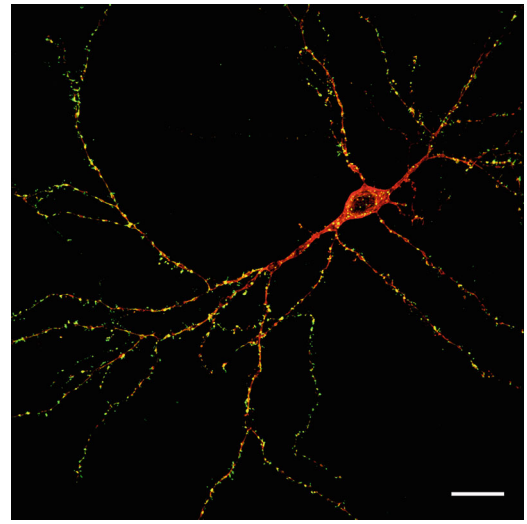

Fig. 2 Confocal image of a hippocampal neuron in culture using the SynView approach. Reconstituted split-GFP molecules (in green) identify positions of trans-synaptic neuroligin-1 bound to neurexin-1β that represent synaptic connections. Scale bar, 10 μm

of precipitate. Overmixing will cause the formation of large clusters of precipitate and decrease transfection efficiency.

5. Add the DNA–Ca-phosphate suspension solution drop-wise to each coverslip (50 μL per coverslip).
6. Incubate cells with the precipitate for 15–20 min in a 5% CO_2 incubator at 37 °C (*see* **Note 7**).
7. After incubation, transfer coverslips to new wells containing 1 ml HBSS which was pre-equilibrated in a 5% CO_2 incubator at 37 °C. Return coverslips to the incubator and incubate from 1 to 5 min until no clusters of precipitate are visible under the microscope (*see* **Note 8**).
8. Transfer the transfected coverslips back to their original wells containing the original neuronal culture medium.
9. The SynView signal appears after 2–3 days as punctate green fluorescence on the transfected neurons (Fig. 2). After this point, neurons can be imaged either live or fixed under a confocal microscope (*see* **Note 9**). The SynView signal is compatible with immunocytochemistry and can be combined with counterstaining using antibodies against synaptic proteins.

4 Notes

1. We have routinely observed that transfection was more efficient when HEK cells were seeded either in 6-well plates or 10-cm

culture dishes. Growth area is comparable in either case and no adjustments are necessary (6 wells = 10-cm dish). Generally, avoid transfection in culture flasks.

2. The current protocol was optimized based on the use of FUGENE6 or X-tremeGENE HP DNA Transfection Reagent as a transfection method for lentiviral production. Use of alternative methods like calcium phosphate will require troubleshooting as they don't end up producing robust final results and are not recommended.
3. When using non-concentrated lentiviral preparations, best results are obtained when infection is performed using freshly made virus. Aliquoting and storing the lentiviral prep at −80 °C will result in a decrease of the infectious titer. However, if virus production is done in bulk for use in multiple experiments, one freeze-thaw cycle of the virus can be performed. Use of concentrated lentiviral preparations of Nrx1-β-GFP1-10^{S2} has not produced robust results in our hands.
4. The volumes in this protocol refer to a hippocampal culture preparation of 12 wells of a 24-well dish. For larger preparations, adjust volumes accordingly.
5. Hippocampi should be collected from newborn mouse pups up to 1 day of age. Preparations from older pups do not usually result in healthy cultures and neuronal viability is compromised. Perform the dissections fast at room temperature and collect and keep the hippocampi on ice until the whole procedure is finished.
6. ARA-C is an inhibitor of glial cell growth and the timing of the addition of 4 ARA-C should be carefully chosen. If added too soon, this will prevent the glial layer that supports and nourishes neurons to be fully formed. However, if added very late, this will allow glial cells to overtake the culture area in expense of neuronal growth. In both cases, neuronal health and viability will be severely compromised. Cultures should be monitored carefully 24 h after addition of Growth Medium to observe the formation of the glial layer on the coverslip surface, which will indicate the exact time point for switching to ARA-C Medium.
7. Incubation times greater than 20 min result in increased neuronal death in the culture. This is due to toxicity caused by the calcium phosphate. Incubation times between 15 and 20 min result in sufficient number of transfected hippocampal neurons.
8. It is important to ensure that the precipitate is completely dissolved, as it can affect neuronal survival. Repeat the HBSS wash if any clusters remain visible under the microscope.

9. For imaging of fixed cells, perform fixation using electron microscopy grade 4% paraformaldehyde. Avoid using methanol or methanol-containing fixatives as they can cause quenching of the GFP fluorescence and reduce or abolish the SynView signal.

References

1. Helmstaedter M, Briggman KL, Turaga SC, Jain V, Seung HS, Denk W (2013) Connectomic reconstruction of the inner plexiform layer in the mouse retina. Nature 500:168–174
2. Beier KT, Steinberg EE, DeLoach KE, Xie S, Miyamichi K, Schwarz L et al (2015) Circuit architecture of VTA dopamine neurons revealed by systematic input-output mapping. Cell 162:622–634
3. Callaway EM, Luo L (2015) Monosynaptic circuit tracing with glycoprotein-deleted rabies viruses. J Neurosci 35:8979–8985
4. Wickersham IR, Lyon DC, Barnard RJ, Mori T, Finke S, Conzelmann KK et al (2007) Monosynaptic restriction of transsynaptic tracing from single, genetically targeted neurons. Neuron 53:639–647
5. Sudhof TC (2008) Neuroligins and neurexins link synaptic function to cognitive disease. Nature 455:903–911
6. Feinberg EH, Vanhoven MK, Bendesky A, Wang G, Fetter RD, Shen K, Bargmann CI (2008) GFP Reconstitution Across Synaptic Partners (GRASP) defines cell contacts and synapses in living nervous systems. Neuron 57:353–363
7. Kim J, Zhao T, Petralia RS, Yu Y, Peng H, Myers E, Magee JC (2011) mGRASP enables mapping mammalian synaptic connectivity with light microscopy. Nat Methods 9:96–102
8. Shearin HK, Quinn CD, Mackin RD, Macdonald IS, Stowers RS (2018) t-GRASP, a targeted GRASP for assessing neuronal connectivity. J Neurosci Methods 306:94–102
9. Yamagata M, Sanes JR (2012) Transgenic strategy for identifying synaptic connections in mice by fluorescence complementation (GRASP). Front Mol Neurosci 5:18
10. Li Y, Guo A, Li H (2016) CRASP: CFP reconstitution across synaptic partners. Biochem Biophys Res Commun 469:352–356
11. Macpherson LJ, Zaharieva EE, Kearney PJ, Alpert MH, Lin TY, Turan Z et al (2015) Dynamic labelling of neural connections in multiple colours by trans-synaptic fluorescence complementation. Nat Commun 6:10024
12. Tsetsenis T, Boucard AA, Arac D, Brunger AT, Sudhof TC (2014) Direct visualization of trans-synaptic neurexin-neuroligin interactions during synapse formation. J Neurosci 34: 15083–15096
13. Arac D, Boucard AA, Ozkan E, Strop P, Newell E, Sudhof TC, Brunger AT (2007) Structures of neuroligin-1 and the neuroligin-1/neurexin-1 beta complex reveal specific protein-protein and protein-Ca^{2+} interactions. Neuron 56:992–1003
14. Ko J, Zhang C, Arac D, Boucard AA, Brunger AT, Sudhof TC (2009) Neuroligin-1 performs neurexin-dependent and neurexin-independent functions in synapse validation. EMBO J 28:3244–3255

Chapter 9

Imaging Synapse Ultrastructure and Organization with STED Microscopy

Marta Maglione and Stephan J. Sigrist

Abstract

Determining the localization of proteins within a cell and their possible interactions is highly relevant to understand their functionality. Nevertheless, subcellular structures of interest in neurobiology, most importantly synapses with their pre- and postsynaptic compartments, are usually smaller than the resolution limit of conventional light microscopy. Indeed, diffraction of light limits to roughly half of the wavelength of light the resolution of a conventional light microscope. In this regard, super-resolution light microscopy (SRLM) techniques have emerged, achieving even more than ten times the resolution of conventional light microscopy, thus allowing to resolve subsynaptic structures also in situ. Importantly, stimulated emission depletion (STED) microscopy has been extensively used to image in situ the nanoscale organization of presynaptic compartments, such as the area of the presynaptic plasma membrane where synaptic vesicles fuse to release neurotransmitters, the so-called active zone. In this article, we outline a method to determine the localization of active zone scaffolding key players relative to voltage-gated calcium channels within the presynaptic active zone by time-gated STED (gSTED) microscopy in situ.

Key words gSTED, Super-resolution, Brain slices, Synapse, Mossy fiber, Active zone, Cav2.1, RIM1

1 Introduction

Chemical synapses are highly specialized cell-cell contacts, composed of a presynaptic and a postsynaptic compartment, whose size is typically smaller than few hundred nanometers and thereby below the resolution limit of a conventional light microscope [1, 2]. At the presynapse, a meshwork of proteins, the so-called cytomatrix of the active zone (CAZ), assembles at the plasma membrane where synaptic vesicle fuse to release neurotransmitter [3]. At excitatory synapses, the postsynaptic compartment, which senses released neurotransmitters, is characterized by an electron-dense postsynaptic density. Notably, CAZ key components tether

Tolga Soykan and Alexandros Poulopoulos (eds.), *Synapse Development: Methods and Protocols*, Methods in Molecular Biology, vol. 2910, https://doi.org/10.1007/978-1-0716-4446-1_9,

synaptic vesicles (SV), driving them to docking and fusion sites, and localize voltage-gated Ca^{2+} channels in close proximity to SV release sites, thereby shaping neurotransmission [3–5].

Electron microscopy allows examining fine structures at the nanoscale and has been the method of choice used to investigate synaptic components. However, a drawback of this technique is its inability to reveal the identity of the structures and protein localization. Immunoelectron microscopy, by labeling target proteins with gold-conjugated antibodies, addressed this issue. Nevertheless, these stainings are demanding in terms of sample preparation and are affected by rather low labeling densities [6]. Light microscopy techniques are less challenging regarding tissue preparation and easily allow to visualize several proteins at once by multichannel acquisition. However, due to diffraction of light, the optical resolution of conventional light microscopy is limited to few hundred nanometers, leaving unresolved subcellular structures critical to neuronal biology. Over the past decades, several super-resolution light microscopy techniques emerged, allowing to drastically improve resolution even more than 10 times the resolution of conventional light microscopy [7–12], thus revealing the nanoscale architecture of presynaptic and postsynaptic compartments [13, 14].

Pioneer work applying stimulated emission depletion (STED) microscopy at *Drosophila* neuromuscular junctions (NMJs) deciphered how the ELKS family member Bruchpilot (BRP), a core CAZ scaffold protein, organizes CAZ nanotopology [15–17] and identified RIM-Binding Protein (RIM-BP) as another key CAZ component, essential for Ca^{2+} channels clustering [18]. STED microscopy has been successfully applied to *Drosophila* whole mount brains and mammalian brain slices, revealing a generic rule underlying presynaptic architectures [19–24].

In this chapter, we describe how to perform triple channel time-gated STED (gSTED) imaging of synaptic markers in situ, on shock frozen brain tissue, and how to retrieve distances between clusters formed by the active zone protein RIM1 and the P/Q type Ca^{2+} channel subunit Cav2.1 at hippocampal synapses. This method allows to reduce shock freezing artifacts linked to too slow freezing, while preserving antigenicity thereby providing flexibility in the application of primary antibodies targeting CAZ proteins, which often fail to work on tissue fixed by conventional intracardial perfusion. With this method, we previously demonstrated that mammalian RIM-BP2 finetunes Ca^{2+} channel localization at the CAZ of hippocampal CA3-CA1 synapses [22], while at Mossy Fiber-CA3 (MF-CA3) synapses is required for the recruitment of the SV priming factor Munc13-1 at the CAZ [23].

2 Materials

2.1 Preparation of Sagittal Brain Slices

1. Dry ice block (2–3 cm thick) and dry ice pellet.
2. Aluminum foil.
3. Styrofoam box.
4. Spoon for dry ice powder.
5. Sharp razor blade.
6. Brain dissection tools.
7. 50 mL Falcon tubes (for storage).
8. Tissue Tek O.C.T Compound (e.g., Sakura).
9. Camel hair brush.
10. Superfrost Plus Gold coated glass slides (25 × 75 mm; e.g., Roth).
11. Cryostat.

2.2 Immunostaining of Synaptic Markers

1. Glass jar for slides.
2. PAP pen for immunostainings (e.g., Merck).
3. 0.1 M Phosphate Buffer (PB), pH 7.4.
4. 4% PFA in 0.1 M PB, pH 7.4.
5. 20 mM Glycine in 0.1 M PB, pH 7.4 (for quenching fluorescence).
6. 10% Normal Goat Serum (NGS), 0.3% TritonX-100 (TX-100) in 0.1 M PB, pH 7.4 (for blocking).
7. 0.3% TX-100 in 0.1 M PB (for washing).
8. 5% NGS, 0.3% TX-100 in 0.1 M PB, pH 7.4 (for antibody incubation).
9. Goat Fab fragments anti-mouse IgG.
10. Rabbit anti Cav2.1 (Synaptic Systems, #152 203) 1:500.
    Guinea Pig anti Homer1 (Synaptic Systems, #160-004) 1:200.
    Mouse anti RIM1 (BD Pharmingen, #610906) 1:200 (*see* **Note 1**).
11. Goat anti Rabbit ATTO647N 1:100 (Active Motif, #15048).
    Goat anti Guinea Pig AF594 1:200 (Invitrogen, #A-11076).
    Goat anti Mouse AF488 1:200 (Invitrogen #A-11029).
12. Kim-wipe (Kimtech Science).
13. High refractive index mounting medium (Prolong Gold, Invitrogen or Mowiol, Sigma-Aldrich).
14. High-precision coverslips 1.5H (e.g., Roth).

2.3 gSTED Imaging In Situ

1. Time-gated STED (gSTED) microscope (Leica Microsystems SP8 TCS STED 3X or Abberior Instruments STED Expert line) equipped with continuous 592 nm/pulsed 595 nm and pulsed 775 nm depletion lasers.
2. Pulsed white light laser or pulsed laser lines at appropriate wavelengths (e.g. 488 nm, 561 nm, 640 nm).
3. Hybrid Detectors (Leica Microsystems SP8 TCS 3X) or Avalanche photodiode detectors in photon counting mode (Abberior Instruments STED Expert line).
4. LED illumination (488 nm, 561 nm) or similar and appropriate filter set (FITC, AF488/Cy3, AF594).
5. 100× oil immersion objective, NA 1.4.
6. 20× oil immersion objective, NA 0.8.

2.4 Deconvolution and Analysis

1. Deconvolution software (SVI Huygens Professional or Abberior Instruments Imspector).
2. ImageJ software (NIH; http://imagej.nih.gov/ij/).

3 Methods

3.1 Preparation of Sagittal Brain Slices

3.1.1 Dissection

1. Just before the dissection starts, prepare two small (3 cm × 3 cm) pieces of aluminum foil and prepare fine dry ice powder from a dry ice pellet. Store the dry ice powder in a styrofoam box. Place the dry ice block in the styrofoam box in close vicinity to the dissection area.
2. Sacrifice the mouse according to the veterinary office policy of your institute. Disinfect the animal head by spraying with 70–90% solution of ethanol and decapitate.
3. Remove the brain and place it on the small aluminum foil.
4. With a sharp razor blade divide the two brain hemispheres and place each hemisphere inner side down on one aluminum foil.
5. Place the aluminum foils carrying the brain hemispheres on a 2–3 cm thick block of dry ice and cover each hemisphere with dry ice powder (*see* **Note 2**).
6. Freeze for 2 min.
7. Store both brain hemispheres, wrapped in the aluminum foil, in a 50 mL Falcon tube (to reduce freeze-drying) at −80 °C until sectioning. Brain tissue can be stored up to 1 year at −80 °C (*see* **Note 3**).

3.1.2 Sectioning

1. Before starting sectioning at the cryostat, adjust the chamber and knife temperature to optimize cutting. Too low temperature will result in curled or cracked slices, too high temperature

will let the slice stick to the knife or glass plate. In this protocol the chamber and knife temperature used were about −14 °C/−13 °C. Take the brain hemisphere out of the −80 °C freezer and store in dry ice for 30 min before cutting. At the same time fix the knife blade and let bring to temperature.

2. When the cryostat chamber reached the set temperature, put the brain hemisphere to be cut, still wrapped in aluminum foil, into the chamber and leave for 30 min to let the brain adjust to the chamber temperature.
3. On a tissue holder prepare a layer of Tissue Tek O.C.T Compound and let freeze.
4. Fix the brain hemisphere with a drop Tissue Tek O.C.T Compound on the chuck covered with Tissue Tek O.C.T Compound, with inner side facing on top for sagittal sectioning. Wait until the Tissue Tek O.C.T Compound is solidified (*see* **Note 4**).
5. Orient the chuck to keep the brain hemisphere in sagittal view. Start trimming and adjust chamber and knife temperature (±5 °C) to obtain flat slices. When the hippocampal formation is visible set slice thickness to 10 μm and start collecting sagittal slices on a warm coated glass slide. A camel hair brush can help to guide the slices over the knife blade, if working without glass plate. Keep slices at room temperature (RT) for 30 min and store at −20 °C or immediately fix with fixative of choice (here 4% PFA, 10 min RT). For longer storage keep slices at −80 °C (up to 1 year). Before starting the fixation and staining steps encircle the brain sections with a hydrophobic barrier using a PAP pen, to reduce the amount of solutions required.

3.2 Immunostaining for Pre- and Postsynaptic Markers

1. If slices were previously fixed, warm slides to RT and rehydrate slices in 0.1 M PB, pH 7.4 for 5–10 min.
2. If slices were unfixed proceed with fixation with 4% PFA in 0.1 M PB, pH 7.4, 10 min RT.
3. Following fixation, wash sections 3 × 15 min with 20 mM Glycine in 0.1 M PB, pH 7.4, in a glass jar, to quench fixative-induced fluorescence.
4. Block non-specific binding/Permeabilize 3 h at RT with 10% NGS, 0.3% TritonX-100 (TX-100) in 0.1 M PB, pH 7.4 in a dark humidified chamber (*see* **Notes 5** and **6**).
5. To avoid binding of fluorophore-conjugated anti-mouse IgGs to endogenous mouse IgGs, block with Goat Fab fragments anti-mouse IgG 1:10 in 0.1 M PB, 1 h RT.
6. Rinse briefly 3× with 0.3% TX-100 in 0.1 M PB.

7. Incubate sections with primary antibodies in 5% NGS, 0.3% TX-100 in 0.1 M PB, pH 7.4, o/n at 4 °C, in a dark humidified chamber to avoid sections drying.
8. Wash sections for 3 h every 20 min in a glass jar, at RT, with 0.3% TX-100 in 0.1 M PB, pH 7.4.
9. Incubate sections with secondary antibodies in 5% NGS, 0.3% TX-100 in 0.1 M PB, pH 7.4, 2 h RT, in a dark humidified chamber. To avoid dye aggregates, centrifuge the solution containing the secondary antibodies for 30 min at 13,000 rpm, at 4 °C, beforehand.
10. Wash sections 4 × 15 min, RT with 0.1 M PB, pH 7.4 in a glass jar.
11. Let briefly dry the brain sections and remove excess buffer with a Kim-wipe. Mount on high precision coverslips (#1.5, LH25.1 Roth) with Prolong Gold. Cure 24 h at RT and then store at 4 °C until imaging (*see* **Note 7**).

3.3 gSTED Imaging In Situ

1. Place the slide under the gSTED microscope with a 20× lens and find the region of interest in widefield fluorescence mode. In this protocol, the hippocampal CA3 stratum lucidum, where mossy fibers-CA3 synapses are located, was imaged.
2. Switch to 100× lens and scan in confocal mode a large field of view (e.g., 75 μm × 75 μm) with low laser intensity and large pixel size (e.g., 200 nm) to find synapses of interest. Scan channels sequentially and adjust spectral detection for each dye to avoid dye crosstalk. Adjust laser intensity for each channel in order to saturate a minimal amount of pixels.
3. For 2D gSTED imaging, set the field of view to 10 μm × 10 μm or 20 μm × 20 μm and pixel size to 20–25 nm, according to Nyquist criteria and the lateral resolution achieved with the gSTED microscope. Lower scan speed and set line accumulation to, e.g., 10 lines. For each channel, adjust excitation laser power to approximately twofold the power used in confocal mode. Set time-gated detection to about 750 ps, width 8 ns. Adjust the power of the STED laser. To find the appropriate power of the STED laser and to monitor STED effect, scan live in confocal mode and switch on/off the STED laser. Perform a sequential 2D confocal and gSTED image (*see* **Notes 8** and **9**).

3.4 Deconvolution and Analysis

1. Deconvolve 2D gSTED images with Huygens Professional software (SVI) or Imspector software (Abberior Instruments) with theoretical point spread function (PSF) automatically computed according to microscope parameters or estimated PSF generated with a 2D Lorentz function, respectively (*see* **Notes 10–13**).

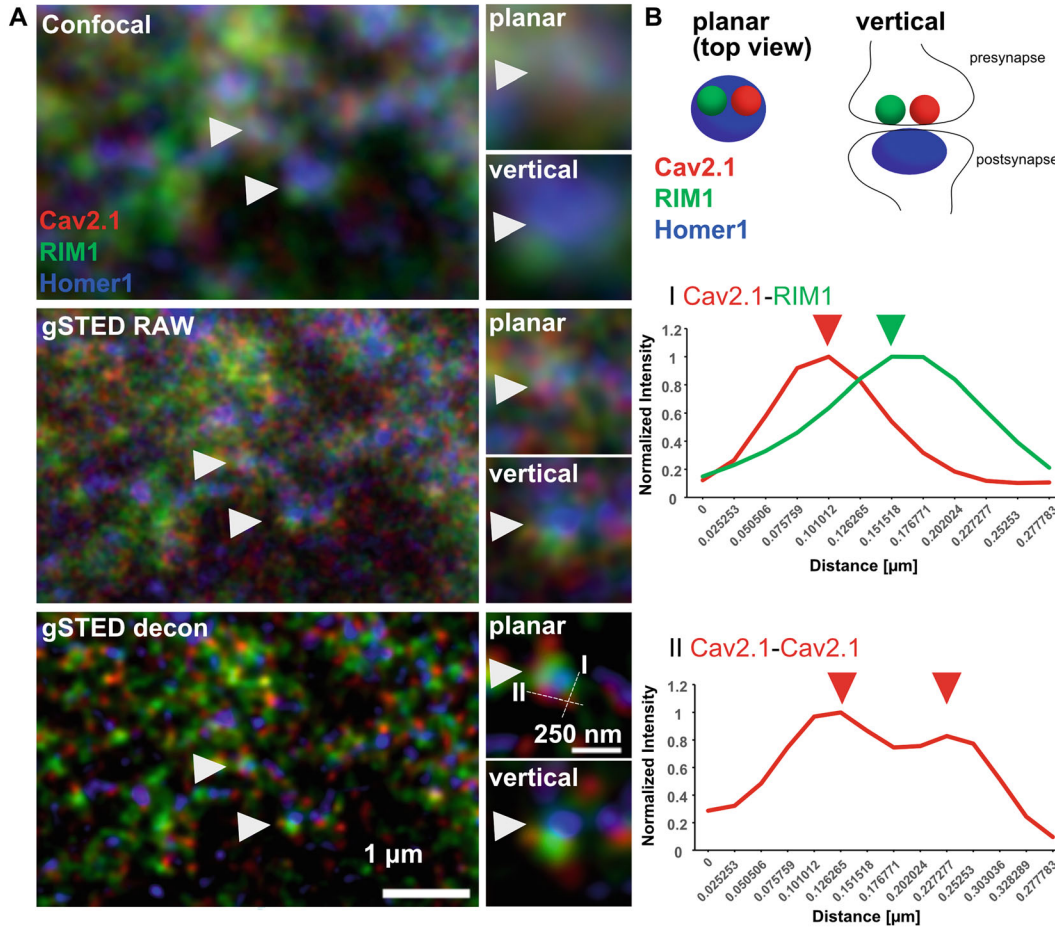

Fig. 1 Three-channel in situ gSTED imaging of Cav2.1, RIM1, and Homer1 at hippocampal MF synapses and analysis of their peak-to-peak distances. (**a**) Confocal (upper left), gSTED raw (middle left), and gSTED deconvolved (lower left) images of Cav2.1, RIM1, and Homer1 at MF synapses and crops of synapses in planar or vertical view, relative to Homer1 clusters. Images were acquired with a gSTED microscope equipped with continuous wave 592 nm and pulsed 775 nm STED lasers. (**b**) Cartoon representing Cav2.1 and RIM1 clusters oriented in planar and vertical view relative to Homer1 clusters. (**b** I) Peak-to-peak distance of Cav2.1 relative to a RIM1 cluster at a planar synapse. (**b** II) Peak-to-peak distance between two adjacent Cav2.1 clusters at a planar synapse. Peak-to-peak distances were retrieved by line profile measurements. Line profile thickness was set to ~250 nm (10 pixels). For display, intensity in each channel was normalized to its maximum. For display, crops are rescaled

2. Open deconvolved 2D gSTED images in ImageJ (NIH) and merge the corresponding channels in a composite. Adjust brightness and contrast for each channel without clicking apply, to better visualize synapses in the correct orientation.
3. Quantify synapses where Cav2.1 and RIM1 are opposed to a given Homer1 cluster, thereby belonging to the same active zone, oriented in planar or vertical view relative to Homer1 clusters and with similar brightness, indicating that they are in the same focal plane (Fig. 1a, b).

4. With the line tool draw a straight line (thickness 10 pixels) across a given Cav2.1 and RIM1 cluster, in parallel to the Homer1 cluster and retrieve the position of the intensity peak across the line with the plot profile tool (Analyze/plot profile). For multi-channel images the following ImageJ macro can be used: (Macro_plot_lineprofile_multicolor from Kees Straatman, University of Leicester, Leicester, UK). Export intensity values from individual synapses to Excel to retrieve Cav2.1-RIM1 peak-to-peak distances (Fig. 1bI). A SciPy code to automatically retrieve distances has been made available via Github (Gimber, 2019; copy archived at https://github.com/elifesciences-publications/LineProfileAnalysisWorkflow).
5. As described above, also inter-Cav2.1 cluster distances can be retrieved (Fig. 1bII).

4 Notes

1. The Mouse anti-RIM1 antibody (BD Pharmingen, #610906) used in this protocol has been discontinued. A recommended alternative, to test beforehand, is the Rabbit anti-RIM1 antibody produced by Synaptic Systems (#140 003), which is knock-out verified and validated for immunocytochemistry and immunohistochemistry.
2. This freezing procedure allows to minimize shock freezing artifacts into the tissue due to too slow freezing. Using dry ice pellet to freeze the brain tissue is not recommended, this does not provide an even freezing and it is not fast enough, causing freezing artifacts.
3. To avoid freezing artifacts, never freeze and thaw the frozen brain tissue.
4. To avoid freezing artifacts and breakage of the brain slices during cutting, do not embed the full hemisphere in Tissue Tek O.C.T Compound.
5. It is of outmost importance that the sections do not dry during the whole immunostaining. The dark chamber can be humidified with wet paper on its inner sides.
6. To block unspecific binding use animal serum obtained from the same species of the host of your secondary antibodies.
7. Prolong Gold increases its refractive index in time. To reduce optical aberrations due to refractive index mismatch and to optimize imaging, it is necessary to let Prolong Gold cure for 5 days before measurements. At the same time, imaging should be done within 1 week from mounting, to ensure maximal fluorescence of the dye.

8. If gSTED images are not well resolved or their intensity is too weak and signal-to-noise ratio too low, increase laser intensity, line accumulation, and/or decrease time-gated detection. If this is not sufficient, increase secondary antibody concentration in the next immunostaining.
9. To monitor and avoid possible crosstalk, it is recommended to image single stained slices for each dye used. Adjusted settings should then be used for triple-channel imaging.
10. Deconvolution of gSTED images drastically improves signal-to-noise (SNR) ratio, removing imaging noise and is therefore recommended for peak-to-peak distance measurements.
11. Iterative deconvolution algorithms alter pixel intensity non-linearly, thereby deconvolved images cannot be used for densitometric measurements. Nevertheless, peak-to-peak distance measurements can be performed reliably to retrieve distances between particles.
12. With Huygens Professional software (SVI), for more accurate image deconvolution and better estimation of the theoretical point spread function, is advisable to acquire a small z-stack of at least 3 optical slices with optical thickness of about 150 nm. For Imspector-based deconvolution the full-width half maximum of the PSF needs to be measured beforehand. This can be done by measuring nanobeads with size below the expected resolution with the same settings used for sample acquisition.
13. Iterative algorithms, e.g., like Richardson-Lucy deconvolution, often give better results for in situ gSTED images. However always check deconvolved images for potential deconvolution artifacts, which can be detected as punctuated noise pattern in the image background.

References

1. Schikorski T, Stevens CF (1997) Quantitative ultrastructural analysis of hippocampal excitatory synapses. J Neurosci 17(15):5858–5867
2. Maglione M, Sigrist SJ (2013) Seeing the forest tree by tree: super-resolution light microscopy meets the neurosciences. Nat Neurosci 16(7):790–797. https://doi.org/10.1038/nn.3403
3. Zhai RG, Bellen HJ (2004) The architecture of the active zone in the presynaptic nerve terminal. Physiology (Bethesda) 19:262–270. https://doi.org/10.1152/physiol.00014.2004
4. Ackermann F, Waites CL, Garner CC (2015) Presynaptic active zones in invertebrates and vertebrates. EMBO Rep 16(8):923–938. https://doi.org/10.15252/embr.201540434
5. Szule JA et al (2012) Regulation of synaptic vesicle docking by different classes of macromolecules in active zone material. PLoS One 7(3):e33333. https://doi.org/10.1371/journal.pone.0033333
6. Reshetniak S, Rizzoli SO (2019) Interrogating synaptic architecture: approaches for labeling organelles and cytoskeleton components. Front Synaptic Neurosci 11:23. https://doi.org/10.3389/fnsyn.2019.00023
7. Hell SW (2007) Far-field optical nanoscopy. Science 316(5828):1153–1158. https://doi.org/10.1126/science.1137395
8. Hell SW, Wichmann J (1994) Breaking the diffraction resolution limit by stimulated emission: stimulated-emission-depletion

fluorescence microscopy. Opt Lett 19(11): 780–782. https://doi.org/10.1364/ol.19.000780

9. Gustafsson MG (2000) Surpassing the lateral resolution limit by a factor of two using structured illumination microscopy. J Microsc 198(Pt 2):82–87. https://doi.org/10.1046/j.1365-2818.2000.00710.x
10. Betzig E et al (2006) Imaging intracellular fluorescent proteins at nanometer resolution. Science 313(5793):1642–1645. https://doi.org/10.1126/science.1127344
11. Rust MJ, Bates M, Zhuang X (2006) Sub-diffraction-limit imaging by stochastic optical reconstruction microscopy (STORM). Nat Methods 3(10):793–795. https://doi.org/10.1038/nmeth929
12. Balzarotti F et al (2017) Nanometer resolution imaging and tracking of fluorescent molecules with minimal photon fluxes. Science 355(6325):606–612. https://doi.org/10.1126/science.aak9913
13. Hruska M et al (2018) Synaptic nanomodules underlie the organization and plasticity of spine synapses. Nat Neurosci 21(5):671–682. https://doi.org/10.1038/s41593-018-0138-9
14. Dani A et al (2010) Superresolution imaging of chemical synapses in the brain. Neuron 68(5): 843–856. https://doi.org/10.1016/j.neuron.2010.11.021
15. Kittel RJ et al (2006) Bruchpilot promotes active zone assembly, Ca2+ channel clustering, and vesicle release. Science 312(5776): 1051–1054. https://doi.org/10.1126/science.1126308
16. Wagh DA et al (2006) Bruchpilot, a protein with homology to ELKS/CAST, is required for structural integrity and function of synaptic active zones in Drosophila (vol 49, pg 833, 2006). Neuron 51(2):275–275. https://doi.org/10.1016/j.neuron.2006.06.022
17. Fouquet W et al (2009) Maturation of active zone assembly by Drosophila Bruchpilot. J Cell Biol 186(1):129–145. https://doi.org/10.1083/jcb.200812150
18. Liu KSY et al (2011) RIM-binding protein, a central part of the active zone, is essential for neurotransmitter release. Science 334(6062): 1565–1569. https://doi.org/10.1126/science.1212991
19. Fulterer A et al (2018) Active zone scaffold protein ratios tune functional diversity across brain synapses. Cell Rep 23(5):1259–1274. https://doi.org/10.1016/j.celrep.2018.03.126
20. Woitkuhn J et al (2020) The Unc13A isoform is important for phasic release and olfactory memory formation at mushroom body synapses. J Neurogenet 34(1):106–114. https://doi.org/10.1080/01677063.2019.1710146
21. Pooryasin A et al (2021) Unc13A and Unc13B contribute to the decoding of distinct sensory information in Drosophila. Nat Commun 12(1). https://doi.org/10.1038/s41467-021-22180-6
22. Grauel MK et al (2016) RIM-binding protein 2 regulates release probability by fine-tuning calcium channel localization at murine hippocampal synapses. Proc Natl Acad Sci USA 113(41):11615–11620. https://doi.org/10.1073/pnas.1605256113
23. Brockmann MM et al (2019) RIM-BP2 primes synaptic vesicles via recruitment of Munc13-1 at hippocampal mossy fiber synapses. elife 8. https://doi.org/10.7554/eLife.43243
24. Holderith N, Heredi J, Kis V, Nusser Z (2020) A high-resolution method for quantitative molecular analysis of functionally characterized individual synapses. Cell Rep 32(4):107968. https://doi.org/10.1016/j.celrep.2020.107968

Chapter 10

Photomarking Relocalization Technique for Correlated Two-Photon and Electron Microscopy Imaging of Single Stimulated Synapses

Miquel Bosch, Jorge Castro, Mriganka Sur, and Yasunori Hayashi

Abstract

Synapses learn and remember by persistent modifications of their internal structures and composition but, due to their small size, it is difficult to observe these changes at the ultrastructural level in real time. Two-photon fluorescence microscopy (2PM) allows time-course live imaging of individual synapses but lacks ultrastructural resolution. Electron microscopy (EM) allows the ultrastructural imaging of subcellular components but cannot detect fluorescence and lacks temporal resolution. Here we describe a combination of procedures designed to achieve the correlated imaging of the same individual synapse under both 2PM and EM. This technique permits the selective stimulation and live imaging of a single dendritic spine and the subsequent localization of the same spine in EM ultrathin serial sections. Landmarks created through a photomarking method based on the 2-photon-induced precipitation of an electrodense compound are used to unequivocally localize the stimulated synapse. This technique was developed to image, for the first time, the ultrastructure of the postsynaptic density in which long-term potentiation was selectively induced just seconds or minutes before, but it can be applied for the study of any biological process that requires the precise relocalization of micron-wide structures for their correlated imaging with 2PM and EM.

Key words Correlated imaging, Time-lapse live two-photon fluorescence microscopy, Serial-section transmission electron microscopy, Dendritic spine, Synapse, Postsynaptic density, Photomarking, Photoetching, Photobranding, DAB

1 Introduction

Synaptic plasticity has been extensively studied because it is considered the molecular basis for learning and memory. Synapses change over time in an experience-dependent manner, both functionally and structurally [1]. These changes can be studied in vivo or ex vivo by introducing fluorescent markers (such as GFP) and longitudinally imaging synapses and dendritic spines in real time with

Authors Miquel Bosch and Jorge Castro have contributed equally to this chapter.

Tolga Soykan and Alexandros Poulopoulos (eds.), *Synapse Development: Methods and Protocols*, Methods in Molecular Biology, vol. 2910, https://doi.org/10.1007/978-1-0716-4446-1_10,

confocal or 2-photon fluorescence microscopy (2PM). In addition to imaging, 2-photon lasers can be used to selectively stimulate individual synapses via photochemical reactions such as glutamate uncaging [2, 3]. However, light microcopy has an inherent limitation that prevents observing structural features below the light diffraction limit. Super-resolution and expansion microscopy techniques can nowadays overcome this limitation and are able to reach nanoscale resolutions in fixed or living cells [4–8]. Electron microscopy (EM) is more powerful in this sense as it can reach ultrastructural imaging with higher spatial resolution in the order of 0.1–0.2 nanometers, and reduced structural alterations compared to expansion microscopy. EM is ideal to detect and analyze synapses, including postsynaptic, presynaptic, and extrasynaptic substructures in unaltered tissue [9, 10]. For this reason, it is used for brain connectivity mapping projects [11]. However, EM has some critical limitations: it requires sample fixation, thus making impossible live time-course imaging of plastic changes, and it cannot detect fluorescence, thus precluding an easy relocalization of the selected neuron or synapses under study.

We developed a powerful methodological approach that bypasses these limitations to allow the correlated imaging of the same specific synapse with both 2PM and transmission EM (TEM) [12]. We combined several procedures in a way that permits: (1) the selective stimulation of a single dendritic spine (*via* glutamate uncaging), (2) the longitudinal observation of the plastic changes occurring in that spine (*via* 2PM), (3) the unequivocal localization of the same spine within ultrathin sections (*via* 2-photon-induced photomarking), and (4) the 3D reconstruction and analysis of the ultrastructural changes that selectively occurred in that spine (*via* serial section TEM—ssTEM). The key point is the photomarking step, which is based on the 2-photon-induced precipitation of an electrodense compound, diaminobenzidine (DAB), that generates precise fiducial landmarks visible under both 2PM and EM imaging [12–15]. These landmarks are fine lines, one or a few microns wide, which can be drawn in any region of the tissue following any useful spatial pattern. In this case, they are drawn to flank the selected dendrite and to point to the stimulated spines. After localizing these lines on ssTEM images, it is possible to unambiguously identify the same synapses that were previously stimulated and imaged with 2PM. Two-photon precipitation of DAB was previously used to relocalize single neurons [13] and we adapted it to relocalize single synapses after long-term potentiation (LTP) was selectively induced in that spine and structural changes visualized with 2PM [12, 16, 17]. An almost identical method was developed in parallel to us, named near-infrared branding (NIRB) technique, which proved to similarly localize dendritic spines and axons in both optical and EM imaging [14]. Other methods have been used to correlate optical imaging of individually labeled neurons,

dendrites, or synapses with EM imaging [15]. However, some of these methods, such as biocytin detection [18], GFP immunostaining [19–22], GFP photo-oxidation [23, 24], or photoconversion of organic fluorescent dyes [25], suffer from the problem that the spine gets obscured by the precipitate, precluding a clear visualization of the internal subcellular structures such as the PSD. Other approaches can solve this problem but are not suitable for single synapse relocalization in thick tissue. For example, the use of endogenous landmarks, such as blood vessel patterns, is useful to re-identify neurons or groups of neurons [26, 27] but such landmarks are hard to find at microscale resolution. On the other hand, introduction of exogenous fiducial marks such as fluorescent beads [28], or the use of nanoprobes, such as gold nanorods [29], fluorescent nanoparticles (quantum dots, nanodiamonds, FluoNanogold) [15], are difficult to carry out in thick tissues like organotypical slice cultures or in vivo. We had to overcome these problems, since our goal was to image changes in PSD ultrastructure just seconds or minutes after LTP was induced in a single synapse in a hippocampal slice. Plastic changes in PSD morphology had been previously observed with EM after the classic electrical induction of LTP in multiple synapses [30, 31] but not after single-synapse LTP. Using our method, we discovered that the structural plasticity of the spine and the PSD are not synchronized during LTP: PSD enlargement is 1 h delayed compared to spine enlargement [12, 22, 32]. The same photomarking technique has recently been employed to correlate in vivo 2PM imaging with different types of EM to study, for example: cortical pyramidal neuron dendrites and spines [33–35], interneuron spines [36], cortical oligodendrocytes [37], cortical myelinated axons [38], and macaque retina [39]. This method can easily be extended beyond synapse biology and used for the study of any biological process that requires precise relocalization of micron-wide structures for their correlated imaging with live 2PM and EM.

2 Materials

2.1 Hippocampal Slices

Organotypic hippocampal slice culture is a particularly useful experimental approach for studying synaptic plasticity. In this preparation, neurons mature in a relatively similar way as they do in vivo [40–44], and the local hippocampal synaptic circuitry is largely preserved [45, 46]. Acute slices from adult or adolescent transgenic mice expressing fluorescent proteins (e.g., Thy1-YFP mice) are more similar to the intact brain, but the organotypic preparation allows for a more versatile genetic manipulation, since it is easier and faster to transfect any kind of gene or combination of genes using biolistic, viral or electroporation methods [47, 48]. Hippocampal slice cultures are typically prepared from rat (e.g., SD) or

mouse (e.g., C57/BL6) pups of both sexes, at postnatal day 6–8 (P6–8; *see* **Note 1**). Slice cultures can also be prepared from other brain regions, such as cortex, striatum, cerebellum, thalamus, brainstem, etc. [49–52].

2.2 Plasmids Expressing Fluorescent Proteins

In order to longitudinally visualize dendritic spines or synaptic components in a living neuron using 2PM, it is necessary to introduce a source of fluorescence into the cell, for example, a plasmid expressing a fluorescent protein, either alone or as a fusion protein. For time-course imaging of spine morphological changes, expression of a stable, small, and soluble marker such as EGFP is sufficient. DsRed2 is a good choice if a red-emitting marker is needed (*see* **Note 2**). Fluorescent proteins fused to naturally localized endogenous molecules can be used to target specific cell locations (*see* **Note 2**). To target the synapse or the PSD, for example, we express fluorescently-labeled Homer1b, since exogenous overexpression of this protein does not alter normal synaptic physiology and Homer 1b exhibits relatively rapid synaptic turn-over, which prevents loss of signal by photobleaching [53, 54]. We routinely use CMV promoter for expression of most genes, or CAG if we need stronger expression.

2.3 Two-Photon Microscope Setup

Time-lapse fluorescence imaging can be carried out with a 1-photon confocal scanning microscope or a 2-photon microscope. Two-photon is recommended for in vivo imaging or in the case of thick tissue such as brain slices, and especially in the case of photochemical reactions such as glutamate uncaging. The best way to perform experiments involving simultaneous imaging and stimulation of single spines by glutamate uncaging is to combine two mode-locked femtosecond-pulse Ti:sapphire lasers, one for imaging and one for uncaging (*see* **Note 3**). This expensive equipment can be purchased from several vendors, or can be custom-made provided that the adequate knowledge and equipment are possessed [55–58]. Two-photon imaging in slices is typically performed with the laser tuned between 860 and 980 nm, being 910–930 nm the optimum wavelength to excite both green and red fluorophores (such as EGFP and DsRed2). Glutamate uncaging is usually triggered with the same or a second laser tuned at 710–730 nm. Two-photon and 1-photon lasers can be further combined to perform more complex experiments (*see* **Note 3**).

Use a microscope (preferably upright) equipped with a 10× (0.3 NA) and a 60× (0.9–1.1 NA, water immersion if upright) objective lenses. The microscope chamber must have a set of inlets installed to constantly perfuse artificial cerebrospinal fluid (ASCF) aerated with 95% O_2/5% CO_2 (carbogen). As these caged compounds are generally expensive, we recommend recirculating the same solution and using the minimum volume of liquid (e.g., 5–15 mL). This recirculation can be done using a peristaltic pump

located close to the stage. It is important to carefully set up the perfusion system to ensure that the level of liquid in the chamber is always constant (*see* **Note 4**).

For such a small volume of recirculating solution, evaporation can become a problem in experiments of long duration. It is convenient to check how severe this problem is in each particular setup. A good solution to prevent evaporation is to cover the chamber with some sort of plastic shield or wet hard paper during the experiment. It is also useful to introduce humidity into the carbogen by bubbling it first through water before bubbling into the ACSF. For experiments lasting several hours, it might still be necessary to add double-distilled (dd) water several times to compensate for the increase in osmolality. Pilot experiments must be carried out to measure the rate of evaporation and to determine how much water to add, and how often (*see* **Note 5**).

2.4 Solutions for Slice Preparation, 2-Photon Imaging and Photomarking

1. Culture Medium: Modified Eagle's Medium (MEM) with 20% horse serum, 27 mM D-glucose, 6 mM $NaHCO_3$, 2 mM $CaCl_2$, 2 mM $MgSO_4$, 30 mM HEPES, 0.01 % ascorbic acid, and 1 μg/mL insulin. Adjust pH to 7.3 and osmolality to 300–320 mOsm/L (*see* **Note 6**). We usually do not add antibiotics. Sterilize by filtering through a 0.22 μm filter and keep at 4 °C no longer than 4 weeks.
2. Dissection Solution: 2.5 mM KCl, 26 mM $NaHCO_3$, 1 mM NaH_2PO_4, 11 mM glucose, 238 mM sucrose, 1 mM $CaCl_2$, and 5 mM $MgCl_2$ in dd water. Prepare fresh or from partial 10× stock solution (*see* **Note 7**). Bubble with carbogen for 20 min. Use it ice-cold or, optionally, place it at −80 °C for ~10 min or at −20 °C for ~35 min until it acquires a slush-like consistency.
3. Magnesium-free ACSF: 119 mM NaCl, 2.5 mM KCl, 26.2 mM $NaHCO_3$, 1 mM NaH_2PO_4 11 mM glucose, 3 mM $CaCl_2$, 1 μM tetrodotoxin (TTX), and 50 μM picrotoxin in dd water. Prepare fresh or from a partial 10× stock solution (*see* **Note 8**). Bubble with carbogen for 20 min. Occasionally, check that osmolality is in the range of 320 ± 20 mOsm/L.
4. Uncaging ACSF: 2.5 mM 4-methoxy-7-nitroindolinyl (MNI)-L-glutamate (caged glutamate) in Mg-free ACSF. The concentration of caged glutamate can vary depending on the efficiency of the system and the budget of the researcher (typically 2–6 mM). This compound is expensive, so we recommend testing the intensity and duration of the uncaging laser that triggers the desired stimulation using the minimum concentration of this compound (*see* **Note 27**). Keep this compound under darkness and prepare this solution with minimum ambient light and maximum protection from UV light (*see* **Note 26**).

5. Fixative Solution: 2% (w/v) paraformaldehyde (PFA), 2% (w/v) glutaraldehyde (GA) in 0.1 M Phosphate Buffer (PB) pH 7.4 (*see* **Note 9**). Make it fresh every day before fixation, using dedicated glassware and plasticware. Keep at room temperature (r.t). This solution, as well as PFA and GA, are highly toxic and so the appropriate protection must be used.
6. Photomarking Solution: 7 mM 3,3′-diaminobenzidine (DAB) in ice-cold 0.1 M Tris-HCl buffer. Adjust pH to 7.4 and cool on ice. Filter with a syringe filter (0.2 μm pore size) to remove debris. This solution must be made fresh and pH should be rechecked just before the experiment. DAB is a carcinogen and must be handled and disposed of appropriately.

2.5 Solutions for Electron Microscopy

1-. Osmium Tetroxide Solution: 1% osmium tetroxide (OsO_4) in 0.1 M PB (prepared from a pre-made 2% stock solution). Osmium tetroxide is volatile and extremely toxic in contact with skin and mucosae. Prepare this solution carefully using glassware, under the fume hood to avoid inhalation, and with two layers of latex/nitrile gloves to avoid skin exposure.

2-. Osmium Tetroxide/Potassium Ferrocyanide Solution: 1.5% (w/v) potassium ferrocyanide ($K_4Fe(CN)_6{\cdot}3H_2O$) in Osmium Tetroxide Solution.

3-. Toluidine Blue Solution: 1% (w/v) toluidine blue in dd water. Filter with a syringe filter.

4-. Durcupan Epoxy Resin: 10 parts of component A, 10 parts of component B, 0.3 parts of component C, and 0.2 parts of component D (by volume; ratios may be optimized). Durcupan must be prepared quite in advance before use. It is better to prepare it in a previously dehumidified hood (use Drierite® or a dehumidifier). In order to obtain a hard resin that will not brittle during sectioning, we recommend the proportions above, added in the same order (*see* **Note 10**). Durcupan is toxic and so the appropriate protection measures must be taken.

5-. Uranyl Acetate Solution: 1% uranyl acetate in dd water. Filter it through a 0.22 μm disc filter. Uranyl acetate is light-sensitive; keep in darkness at 4 °C. All glass equipment that has been in contact with uranyl acetate should be separated from other labware.

6-. Lead Citrate Solution: 3 mM lead citrate, 0.1 N NaOH in degasified dd water. Because CO_2 can precipitate lead in the form of $PbCO_3$, it is necessary to prepare degasified water (CO_2-free) by boiling dd water for 30 min and storing it in an airtight container. All material in contact with lead citrate must be made of plastic.

2.6 Pioloform Slotted Grids

To maximize the viewable area in the serial sections, use grids with oval slots of 1 mm wide by 2 mm long. To support the sections, coat the grids with pioloform (stronger than formvar) or purchase factory-coated grids, which give a highly homogenous and reproducible film thickness.

3 Methods

The complete protocol is a combination of different techniques with multiple steps each: (1) Preparation of hippocampal slice cultures; (2) Transfection of slices with fluorescent markers; (3) Two-photon imaging and stimulation of single dendritic spines; (4) Fixation of the sample; (5) Creation of landmarks by the photomarking procedure; (6) Processing of the sample for EM; (7) Serial section cutting; (8) EM imaging of the sections; (9) Relocalization and 3D reconstruction of the stimulated spines.

In this section, we will only describe in detail the steps that contain crucial or novel methodologies (steps 3, 4, 5, 9). We will provide some useful basic information but will not describe the other steps in detail (steps 1, 2, 6, 7, 8), as methods are reported in detail in this volume and elsewhere (references below).

3.1 Preparation of Hippocampal Slice Cultures

Slices of 350–400 μm thickness are prepared from P6–8 rat (or other species such as mouse, ferret…) hippocampi using a McIlwain tissue chopper, and cultured at 35 °C on interface membranes for 1–4 weeks (*see* **Notes 11** and **12**). Follow the preparation method used by Bosch and colleagues (2014) [12, 59], originally developed by Stoppini and colleagues in 1991 [60] based on previous works [43, 61], and technically described in detail elsewhere [62–64]. The experiment is typically carried out at 7–15 days in vitro (DIV), usually 2–4 DIV after gene transfection (to allow for fluorescent protein expression).

3.2 Gene Transfer into Slices

Our preferred method for transfection of plasmids expressing fluorescent proteins is biological ballistics (biolistics, gene gun) [65]. It is easy, rapid, and highly reproducible, and generates well-isolated transfected cells, with minimum background noise. Compared with other methods, it facilitates the expression of more than one protein by combining several plasmids in the same bullet. It also allows the simultaneous downregulation of endogenous proteins (by including a shRNA expression vector), thereby facilitating replacement approaches. Follow the instructions provided by the manufacturer and/or those described in [64, 66, 67]. Assess the quality of slices after ~5 DIV (*see* **Note 13**). Plasmids are typically transfected no earlier than 5 DIV and no later than 15 DIV (*see* **Note 14**). Allow a minimum of 2 days for the expression of exogenous proteins. Some proteins may need > 4 days to reach

the necessary degree of expression for comfortable imaging. On the other hand, if higher number of transfected cells is needed, or higher spatial accuracy is required (i.e., if a specific region of hippocampus has to be selectively targeted, e.g., only CA3), viral infection is a better choice [47, 68, 69]. This method however may result in too many fluorescent cells, thus making it hard to find an isolated dendrite with dark background. Single-cell electroporation and photo-transfection are excellent alternative methods in which one cell can be specifically selected and transfected [70–73], but are much more time-consuming. Additionally, instead of a genetic marker, it is possible to stain the cell by particle-mediated introduction of a lipophilic dye (e.g., DiOlistics) or to fill the cell with a fluorescent organic dye through a pipette, if one is patching the neuron for electrophysiological recording (*see* **Note 15**).

3.3 Two-Photon Imaging and Single-Synapse Stimulation

1. Start the experiment by turning the lasers on to warm the whole system up (*see* **Note 16**). Because stimulation of single synapses requires a high degree of precision, the 910 nm imaging laser and the 720 nm uncaging laser must be aligned daily (with an error of < 50 nm). This alignment can be performed using 0.5 μm diameter (Ø) fluorescent beads. Beads are simultaneously or sequentially imaged with both lasers and the light path of each laser must be adjusted so that both images overlap as much as possible (*see* Fig. 1a–f). It is useful to further check the alignment by selecting a group of several beads clustered together and use the uncaging beam to bleach one of them. If lasers are well aligned and reach the sample with the correct precision, only the selected bead should be bleached out but not the neighboring ones (Fig. 1g–i) (*see* **Note 17**).
2. Prepare the Mg-free ACSF (as described in the Subheading 2; *see* **Note 8**) and the Fixative Solution. Turn on the peristaltic pump and start the Mg-free ACSF perfusion, usually at 2–4 mL/min, while constantly aerating with carbogen. Make sure the chamber's liquid level is constant (*see* **Note 4**). It is not necessary to recirculate the same solution at this point, as the caged glutamate is still not present: outflow solution can be discarded and inflow solution can be fresh. Turn on the temperature controller and set it at the desired value (we usually set it at 30 °C, although efficient LTP and spine enlargement can be achieved at 23–35 °C).
3. When the microscope setup is ready and all conditions are stable (temperature, perfusion flow, laser power, and alignment…) select the appropriate sample to be placed in the chamber (*see* **Note 18**). Pick up one membrane insert from the well and put it on the cover of a Petri dish (*see* **Notes 19** and **20**). Quickly, cut a piece of the membrane containing the slices with a surgical scalpel (*see* **Note 11** and **12**). Cut it in an

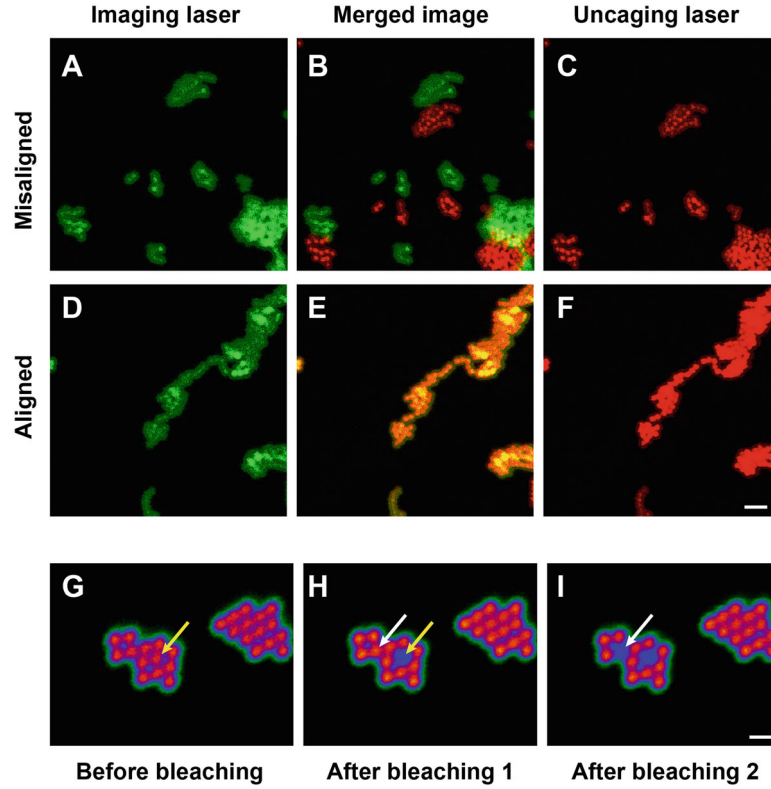

Fig. 1 Laser alignment with fluorescent beads. (**a**–**f**) Fluorescent beads of 0.5 μm Ø are used to align the imaging laser with the uncaging laser. Beads are imaged with the imaging laser (**a**, **d**) and, simultaneously or sequentially, they are imaged with the uncaging laser (**c**, **f**). Both images are merged (**b**, **e**) and, if they do not completely overlap (**b**, example of large misalignment), the mirrors that bring the lasers into the microscope must be adjusted until both images match as perfectly as possible (**e**, good alignment). Scale bar in **a**–**f**, 2 μm. (**g**–**i**) Alignment can be further confirmed by imaging a cluster of fluorescent beads (**g**) and using the uncaging laser to bleach one single bead (**h**; yellow arrow) and then, for instance, another one (**i**; white arrow). Scale bar in (**g**–**i**), 1 μm. Images are pseudocolored for presentation purposes

irregular shape (rectangular or trapezoidal), in order to be able to later identify the position and the orientation of the selected neuron within the slice and within the piece of membrane. Additionally, cut a small dent in one corner of the membrane to further break symmetry and to identify which side is up and which down (*see* **Note 21**).

4. Put the membrane in the chamber and use a holder to immobilize the membrane (*see* **Note 22**). Use epifluorescence illumination through the 10× objective lens to search for a good transfected pyramidal neuron to image. A good neuron is one with a moderate level of fluorescence expression and typical

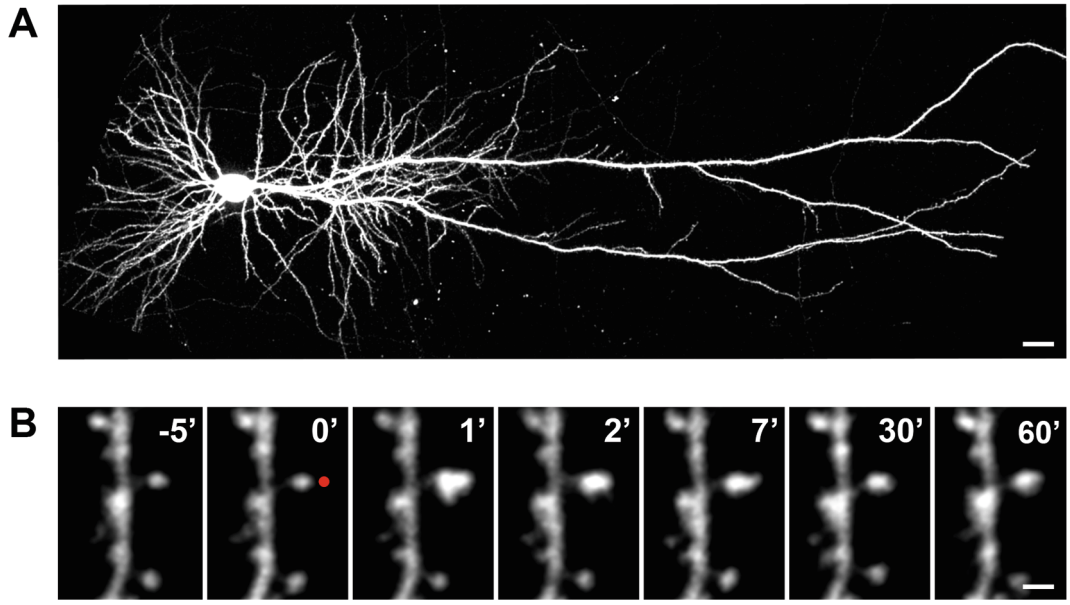

Fig. 2 Neuronal morphology and spine structural plasticity. (**a**) Example of a hippocampal CA1 pyramidal neuron from an organotypic slice culture, transfected with DsRed2. Scale bar, 10 μm. (**b**) Time-lapse 2-photon imaging of the persistent enlargement of a dendritic spine after induction of long-term potentiation by 2-photon glutamate uncaging. Red dot: position of the uncaging laser. Time stamp in minutes after stimulation. Scale bar, 1 μm

healthy morphology: long straight dendrites, normal spine density, and normal basal and apical dendritic tree with multiple branches (see example in Fig. 2a). Avoid cells with signs of unhealthy conditions, such as dendritic blebbing, wavy dendrites, small or few spines, or fluorescent aggregates.

5. Incubate the slices for some time (5–60 min, typically 20 min, but this must be tested empirically) to stabilize some parameters (temperature, metabolism, mechanical drifts due to overall changes of slice shape…). These parameters might change during the first minutes of imaging or recording but usually stabilize soon thereafter (*see* **Note 23**). Change the objective lens to the 60× to carry out the subsequent imaging and stimulation.
6. Choose a segment of a dendrite running parallel to the imaging plane, which in turn will be parallel to the bottom surface of the slice, since the slice is sitting flat on the chamber surface. This will increase the chance of the ultrathin sections being cut as parallel as possible to the dendrite and, therefore, will minimize the number of sections later required to reconstruct the whole dendrite with all the selected spines. It is also advisable to select a dendrite close to the upper slice surface to accelerate the cutting process. We choose segments of primary or secondary

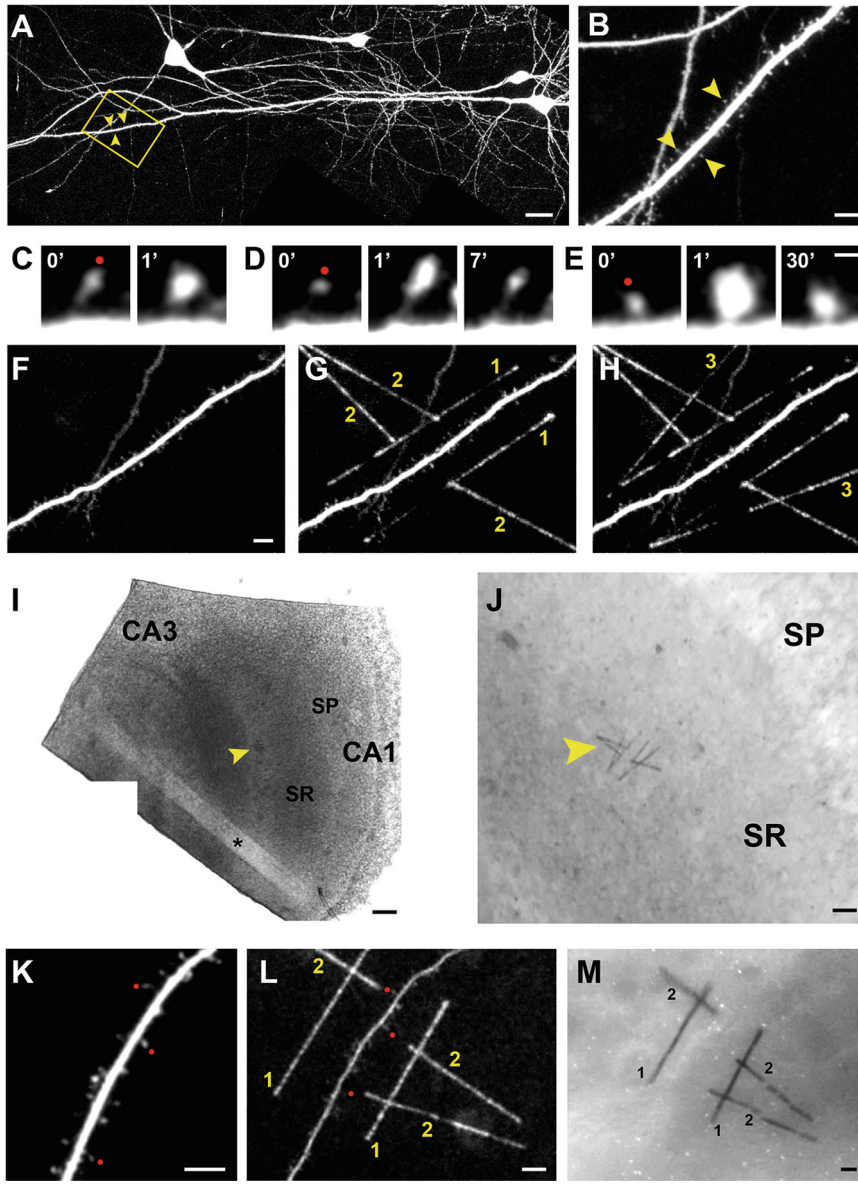

Fig. 3 Generation of landmarks by 2-photon photomarking. (**a**) Two-photon collage image of live hippocampal neurons in an organotypic slice culture. A straight and superficial segment of the dendrite of a pyramidal neuron is selected for the experiment. The yellow square highlights the region shown in (**b**). Scale bar, 25 μm. (**b**) Three spines (labeled with arrowheads in **a** and **b**) from the selected dendritic segment (yellow square in **a**) are chosen to be stimulated at different time points. Scale bar, 5 μm. (**c**–**e**) Two-photon time course live imaging of the spine head enlargement of the 3 stimulated spines at 1 min (**c**), 1–7 min (**d**), and 1–30 min (**e**) after induction of LTP. Red dot: position of the uncaging laser. Scale bar, 1 μm. (**f**) Two-photon image of the same dendritic segment after fixation. Scale bar, 5 μm. (**g**) Landmarks created by 2-photon precipitation of DAB in straight fine lines. Two lines flanking the dendrite (labeled as "1") are initially drawn and 3 semi-perpendicular lines pointing to the stimulated spines (labeled as "2") are subsequently drawn. (**h**) Additional lines are created several microns above (labeled as "3"). (**i**) Piece of a fixed hippocampal slice visualized under bright field. Arrowhead points to the DAB landmarks. *SP* stratum pyramidale; *SR* stratum radiatum. Asterisk

dendrites from the distal part of the main apical dendrite of CA1 pyramidal neurons, which we have found to have long (20–40 μm) and straight segments that run parallel to the imaging plane (*see* Figs. 2a and 3a). Choose one or several dendritic spines of medium-size diameter to stimulate (*see* **Note 24**). We typically choose small mushroom-type spines, with a clear head and neck (no stubby, no filopodia, no big spines; *see* Figs. 2b and 3c–e). We target 3 spines in each experiment, separated at least by >10 μm, and stimulate them sequentially, in intervals no shorter than 10 min between them (*see* Fig. 3b–e, k; *see* **Note 25**).

7. Imaging parameters must be optimized depending on the type of experiment, type of sample, type of fluorescent gene expressed, etc. We found the following to be good parameters for time-course imaging of EGFP-transfected neurons: use the 60× objective lens and a digital zoom of around 10× to acquire a Z-series of 512 × 512-pixel XY-scanned images taken every 0.5–1 μm in depth (Z). Usually, 3–4 images are enough to reconstruct one spine in the Z-dimension, but it is advisable to take 7–15 images if you also want to acquire neighboring spines. Also, slow drift in the X, Y, or Z dimension is common during long experiments and so it might be necessary to adjust the XYZ positions regularly. Time-course imaging requires good signal stability. Photobleaching and phototoxicity are common problems, especially with fusion proteins of slower dynamics than free EGFP. Therefore, it is important to reduce laser intensity, exposure, dwell time, number of images taken, etc., and to enhance sensitivity by increasing photomultiplier tube (PMT) voltage as much as possible to minimize photodamage, even though image quality is reduced.

8. Stimulation of single spines has been performed by several methods, of which 2-photon-induced uncaging of caged glutamate is the most selective and efficient [2, 3]. Several laboratories have reported induction of LTP in single spines [12, 67, 74–78] and a few laboratories have reported induction of long-term depression (LTD) in single spines by glutamate uncaging [78–82]. We usually induce LTP using uncaging pulses of 1 msec of duration, repeated at 1 Hz for 1 min, in Mg-free

Fig. 3 (continued) marks a wound made by the holder. Scale bar, 0.2 mm. (**j**) Arrowhead points to the same DAB landmarks (as in **h**) visualized under bright field at higher magnification. Scale bar, 25 μm. (**k**–**m**) Another example of the photomarking procedure on a different sample. (**k**) Two-photon live image of a dendritic segment. Three spines are also stimulated (red dots). (**l**) Two-photon image of the same dendrite after fixation and photomarking. Lines flanking the dendrite (labeled as "1") and semi-perpendicular lines (labeled as "2") pointing to the stimulated spines (red dots) are visible. (**m**) Same region under bright field where the flanking ("1") and the semi-perpendicular ("2") DAB landmarks are visible. Scale bar in (**k**), 5 μm; in (**l**, **m**), 10 μm

ACSF containing MNI-glutamate, TTX, and picrotoxin (*see* Subheading 2). We first recirculate the Mg-free solution (without caged glutamate) while we place the slice into the imaging chamber, search for the neuron, and select the spines to be stimulated.

9. Once this is done, we prepare the Uncaging ACSF and switch the tubes to the reservoir containing this Uncaging ACSF, avoiding any dilution of the solution or calculating and taking into account the expected dilution of the caged glutamate. At this point, recirculate the same solution constantly by returning the outflow liquid to the tube containing the bubbling Uncaging solution. However, you can search for the neuron and spines using epifluorescence with the caged glutamate in the solution with no evident unwanted uncaging, provided the use of the correct fluorescence filter (typical GFP filters block the UV range of absorption of caged glutamate), avoiding UV light, keeping ambient room light to a minimum and/or using red or UV-filtered ambient light (*see* **Note 26**). It is possible, therefore, to replace the samples and perform several sequential experiments using the same Uncaging ACSF.
10. Laser intensity and pulse duration have to be adjusted for each microscope and for any given concentration of caged glutamate (*see* **Note 27**). Aim the laser close to the tip of the spine but not on top. As the 2-photon diffraction limit (NA 1.0 lens at 720 nm) is 0.62 μm Ø, it is best to shoot ~0.3 μm away from the spine tip (*see* red dot in Figs. 2b and 3c–e) to avoid direct artefactual excitation of the spine by the light. For 3–5 mM MNI-Glutamate we typically use 3–6 mW of laser power, measured after the objective lens (30–60 mW measured at the back aperture, before the lens). At these intensities, we obtain averaged excitatory postsynaptic currents (EPSC) of ~5 pA with 1 ms pulses (*see* **Note 28**). Take baseline images for the first spine (usually every 1–5 min; *see* **Note 29**), confirm that the size of the spine is stable (*see* **Note 30**), induce LTP as described, and take subsequent time-course images, confirming that the spine has been persistently enlarged.
11. If stimulating several spines, move to the second spine, repeat the process, then to the third spine, etc. Record the position of each spine within the dendrite so that you can come back and image the second or third spine in an interleaved way. It is desirable to draw a schematic sketch of the neuron, the dendrite, and the position of each spine for later identification. If different spines have been stimulated sequentially at different time points, at the moment of fixation you will obtain spines potentiated for different periods (*see* Fig. 3c–e).

3.4 Fixation

1. The Fixative Solution must be prepared fresh each day and kept at r.t. After acquisition of the last image of the last stimulated spine, quickly turn on the red light (*see* **Note 26**), raise the objective lens, remove the plastic cover that prevents dehydration, pick up the membrane with tweezers and dip it immediately in Fixative Solution (in a beaker or a 6-multiwell plate).
2. Shake the beaker manually or with a mechanical shaker for 5 min at r.t. to accelerate the penetration of the fixative into the tissue. Put it in a shaker at r.t. for 90 min and then at 4 °C for a minimum of 12 h, always shielded from light.

3.5 Two-Photon-Mediated DAB Photo-Marking

1. Rinse slices thoroughly in 0.1 M PB 4–5 times and transfer them back to the 2-photon microscope chamber. Since the photomarking step requires the use of toxic dirty compounds (PFA/GA-fixed tissue and DAB), we recommend using a different dedicated set of objective lenses, chambers, perfusion tubes, and tweezers exclusively for these steps. Use the asymmetric shape or the dented mark to place the membrane in the appropriate upright position.
2. Prepare the ice-cold DAB solution just before its use (*see* Subheading 2). Perfuse continuously with the solution, aerated with pure oxygen (*see* **Note 31**). Use the epifluorescence light to localize the stimulated spines (*see* **Note 32**; *see* Fig. 3f).
3. Photoprecipitate the DAB creating fiducial patterns (see below) by line-scanning the tissue with the 720 nm 2-photon laser using line-scan mode. Other wavelengths have been also used (e.g., 910 nm; [14]). We could not achieve photoprecipitation using a 1-photon 488 nm confocal laser (*see* **Note 33**). As the DAB precipitate is also fluorescent, you should be able to see both the dendrite and the lines in the same image at 910 nm excitation (*see* Fig. 3g–h, l). The laser intensity and dwell time have to be adjusted for each sample, as photomarking efficacy can vary between experiments. Typically, laser power can be 15–25 mW as measured after the objective lens (150 and 250 mW measured at the back aperture, before the objective lens), with laser irradiation times around 15–60 s. It is recommended to perform a quick test in the same sample, selecting a similar region at the same depth but several μm away from the selected dendrite, and draw several lines at increasing laser intensities and/or dwell times in order to determine which intensity and time creates the best marks, with good autofluorescence signal (not too faint, not too thick). When carefully drawing the lines at the selected region using the chosen laser intensity, it might be necessary to overwrite the same line 2–3 times, if the first-pass result is too faint. Too much laser intensity or too many rounds of photoprecipitation might result in too much electrodense signal and/or burning and destroying the tissue.

4. Different linear patterns can be drawn for use as landmarks for later identification of the dendrite and spines. We usually draw two lines (e.g., of 40–80 μm long), parallel to the dendrite and as equidistant to the dendrite as possible (e.g., 15 μm away; *see* Fig. 3g, l). Measure (on the computer screen, approximately) the length of the line marks, the width, the distance of each one to the dendrite, etc. Save an image of these lines and the dendrite (*see* **Note 34**).
5. Next, draw several lines, perpendicular or semiperpendicular to the dendrite, starting ~40–60 μm away from the dendrite, and pointing to the selected spine but without reaching it, i.e., finishing 8–15 μm away from the spine, to avoid photoprecipitating on top of the spine. If you have stimulated 3 spines, draw 3 lines in an asymmetric pattern (e.g., each one with a different angle with respect to the dendrite; *see* Fig. 3g, l), which will greatly facilitate their unequivocal identification. Save another image and/or measure the length, angle, etc., and write down how precise the line points to the spine by extrapolation (*see* **Note 35**). These pictures and values are important to later compare the pattern of electrodense marks in the EM images to find the dendrite and spines in the absence of fluorescent signal.
6. Finally, move the focal point several microns above the dendrite (e.g., 3–4 μm) and add two more lines, drawn again in any asymmetric pattern that will help its identification (*see* Fig. 3h). These extra upper lines will be very useful in the process of sample sectioning. All these crossing lines are just examples of landmark patterns that we successfully used in our experiments, but any other geometric patterns that the experimenter finds useful can be applied (e.g., squares or rectangles [14, 34]).

3.6 Sample Processing for EM

1. Rinse the membranes in 0.1 M PB several times at r.t.
2. Detach the selected slice from the membrane with a scalpel blade slowly and carefully, avoiding any damage to the sample. It is critical to mark the slice with an asymmetric cut in one or two corners to effectively differentiate the top from the bottom side of the section at later steps.
3. At this point it is convenient to process several slices at the same time in 4 mL amber vials. Use plastic pipettes to remove liquid and use glass hooks to transfer slices between vials. Transfer slices to Osmium Tetroxide/Potassium Ferrocyanide solution and incubate for 30 min at 4 °C in a rotator (*see* **Note 36**).
4. Rinse the slices 4 times for 5 min in PB at 4 °C and transfer them to the Osmium Tetroxide Solution for an additional 30 min at 4 °C.

5. Transfer slices to new vials and start the dehydration process by rinsing them in alcohol solutions at incremental concentrations: rinse twice for 5 min in 30% ethanol. Repeat with 50% ethanol, then 70% ethanol, then 90% ethanol. Rinse once in 95% ethanol for 10 min and twice in 100% ethanol for 10 min.
6. Rinse twice in propylene oxide for 10 min.
7. Transfer the slices to a 1:1 mix of fresh Durcupan Epoxy Resin and propylene oxide, and incubate them in the rotator overnight at r.t.
8. Transfer the slices into fresh Durcupan and incubate for 4 more hours in the rotator at r.t.
9. Start the process of flat-embedding the samples between two sheets of poly-chloro-tri-fluoro-ethylene (PCTFE) film (e.g., ACLAR®) with new fresh Durcupan resin. Put the slices between the plastic films and use scale calibrating weights (20–50 g) to deliver pressure. Carefully eliminate all bubbles.
10. Heat the samples in an oven at 57 °C and cure them for 2 days.
11. Remove the PCTFE film attached to the bottom side of the slice (the one furthest from the photomarked region) and glue that side with epoxy glue onto cylinders made of Durcupan. These cylinders can be made using standard BEEM cylinder molds. The top side of the section (the one closer to the photomarked region) should be facing up. This orientation is important to minimize the amount of resin we will have to remove during coarse sectioning with the glass knife. More detailed protocols on sample processing for TEM imaging can be found in Bozzola and Rusell (1999) [83].

3.7 Cutting Ultrathin Serial Sections

1. Start by manually trimming the block to create a trapezoid with parallel borders using an oil-free razor. Due to their stiffness and sharpness, we prefer single-edge razors over double-edge safety razors.
2. In order to have perfect parallel top and bottom sides with smooth slopping surfaces in the trapezoid, continue trimming in an ultramicrotome using the angled sides of a 45° Cryotrim diamond knife at a 2–3° attack angle [84]. Our block faces are typically ~400–500 μm wide and ~500–700 μm long to cover as much of the targeted area as possible.
3. Cut semi-thin sections (500 nm) with a glass knife and stain them with Toluidine Blue Solution until the two upper lines of DAB marks appear (*see* Fig. 4a).
4. At this point, initiate the ultrathin serial sectioning of the sample at 60–70 nm thickness. To minimize compression, use a 35° diamond knife and try to section using attack angles of ~4°. Sections should come in a straight ribbon but, in our

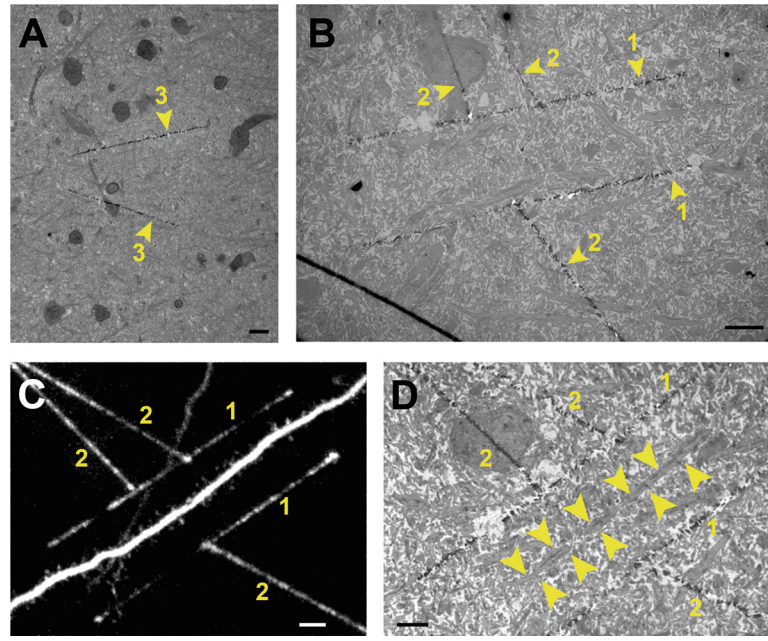

Fig. 4 Relocalization of landmarks in serial section TEM images. (**a**) Electron micrograph of the region shown in Fig. 3a–j where the 2 upper landmarks are visible (arrowheads labeled as "3"; same as those visible in 3H labeled as "3"). The appearance of these landmarks during cutting semi-thin sections announces the moment to start cutting ultrathin sections. Scale bar, 10 μm. (**b**) Electron micrograph of the same region, 3–4 μm deeper, where the next landmarks are visible, the ones parallel to the selected dendrite (arrowheads labeled as "1") and the ones semiperpendicular to the dendrite pointing to the stimulated spines (arrowheads labeled as "2"). Scale bar, 10 μm. (**c**) Two-photon image of the selected region (also shown in Fig. 3g) where the fluorescence of the dendritic DsRed2 and the DAB landmarks are visible, to be compared to D. Scale bar, 10 μm. (**d**) Electron micrograph of the selected region, where the electrodense signal of the DAB landmarks is visible. The selected dendrite is delimited with arrowheads. Scale bar, 10 μm

experience, anything longer than 15–20 sections will be hard to handle in the diamond knife boat. The best sectioning can be obtained by programming the optimal cutting speed at 0.8–1 mm/second (*see* **Note 37**). Use an eyelash manipulator (eyelash attached to a brush handle) to split the ribbon into groups of 5–7 sections.

5. Mount sections onto Pioloform-coated slotted grids (*see* Subheading 2) using a high-angle insertion of the grid in the boat and with the grid-slot parallel to the ribbon. Gently pull the grid up to prevent excessive shearing force on the ribbon.
6. Dry the grids. We recommend using absorbent paper points instead of letting the grids air dry, as the sections could get dispersed. After the sections are completely dried, proceed with staining.

7. For staining, put several drops of Uranyl Acetate Solution (*see* Subheading 2; *see* **Note 38**), one per grid, on top of a Petri dish covered with parafilm. Place the grid face down on top of the drop so the sections are in direct contact with the solution. Stain for 1 min and then rinse by letting 6–8 drops of dd water run over the tweezers (we found this method less perturbing for the sections than immersing the grids into beakers).
8. After completely drying the grids, repeat the same procedure with the Lead Citrate Solution (*see* Subheading 2), always minimizing the contact of this solution with CO_2 (*see* **Note 39**). Rinse the grids with CO_2-free dd water using the same method used with the uranyl acetate solution. A more detailed protocol on serial sectioning for ssTEM can be found in Harris and colleagues (2006) [84], *basic techniques for TEM* in Hayat (1985), and *three-dimensional electron microscopy* in Muller-Reichert and Pigino (2019) [85, 86].

3.8 Relocalization of the Dendrite in Serial Section Transmission EM

1. Load the grids on the sample holder and image them with the transmission electron microscope with a filament tension of 100 kV and at low magnification (×3000) [87].
2. Search for the electrodense DAB landmarks in all serial sections following an established order. Each grid and section must be sequentially numbered. Try to search the landmarks on the grids located in the middle of the sectioning sequence first. If the cutting and sectioning process has been successfully done in a parallel fashion with respect to the dendrite, very few sections should include most of the DAB lines (*see* Fig. 4b). If not totally parallel, the DAB lines will appear as small traces over many sections, which will make the relocalization more difficult, though not impossible. Once the landmarks are localized, start collecting mid-magnification images (×5000–8000) and draw an approximate map of these lines.
3. Localize the two lines that flank the dendrite in parallel and search for the dendrite that best matches the expected position of the selected dendrite, which should be situated at equal distance from these two flanking lines and at the same depth (*see* Fig. 4c, d). At this point, it is not necessary to completely identify the stimulated spines but should have a good guess as to which one is the selected dendrite by thoroughly comparing these mid-magnification images (Fig. 4d) with the previous 2-photon images (Fig. 4c) of the same region (*see* **Note 40**).
4. Once confident of the identification of the dendrite, search for the semi-perpendicular lines pointing to the spines and use them to find the regions where the stimulated spines are expected to be located. Start collecting images of those regions at high magnification (×23000) in all the sections. Collect

them in a way that builds a virtual cube containing the stimulated spines and the dendrite (i.e., a 3D stack volume comprising several sections above and below the expected position of the spines). This cube will also include several unstimulated neighboring spines. The best method to prevent missing spots is a meander sampling, i.e., taking pictures uniformly spaced in a grid pattern. For that purpose, it is helpful to use the EM stage position display and to set a consecutive numbering scheme (section number, row, and image within the row) to help during the photo-stitching step.

3.9 Morphometric 3D Reconstruction and Analysis of Spines

1. Use the automated stitching function of an image processing program (e.g., the Photomerge function in Photoshop) to stitch together all the regions imaged from the same section to create a collage image in 2D.
2. Combine these collage images from different sections to create the 3D stack volume of the whole selected dendrite containing all the stimulated spines and several neighboring spines. If stimulated spines are too far away from each other, build separated 3D stack volumes for each of the selected regions.
3. To perform image alignment, reconstruction, and analysis, we used the Reconstruct software package (http://synapses.clm.utexas.edu/synapseweb/software-0) [88] but newer programs that combine automatic profile segmentation, reconstruction, and analysis with improved 3D visualization tools are also recommended [89]. Perform an initial rough reconstruction to see the overall shape of the dendrite and compare it to the 2-photon fluorescent images. If the dendrite has any feature that permits its identification, such as a turn, a point of branching, a group of spines, a non-spiny region, etc., try to match this feature between the fluorescence and the reconstructed EM images (Fig. 5). At this point, you must be quite confident that you have correctly identified the dendrite of interest.
4. Proceed to reconstruct all the spines that reside in the regions that have been imaged and stitched, in a blind fashion, i.e., before determining whether they are stimulated or unstimulated (*see* Fig. 5a–d). We focused and reconstructed the same type of stimulated or control spines, i.e., thin or mushroom spines, but not stubby or filopodia (*see* Fig. 5a, d–g). Reconstructions should include the dendritic shaft, as well as any other features of interest, such as the PSD, endoplasmic reticulum, presynaptic boutons, etc. (*see* Fig. 5a, e–g).
5. Localize the DAB landmarks that point to the stimulated spines and identify those spines from the set of reconstructed spines (*see* Fig. 5c, d). It is convenient to measure the relative distances of these spines to the neighboring spines or other features of

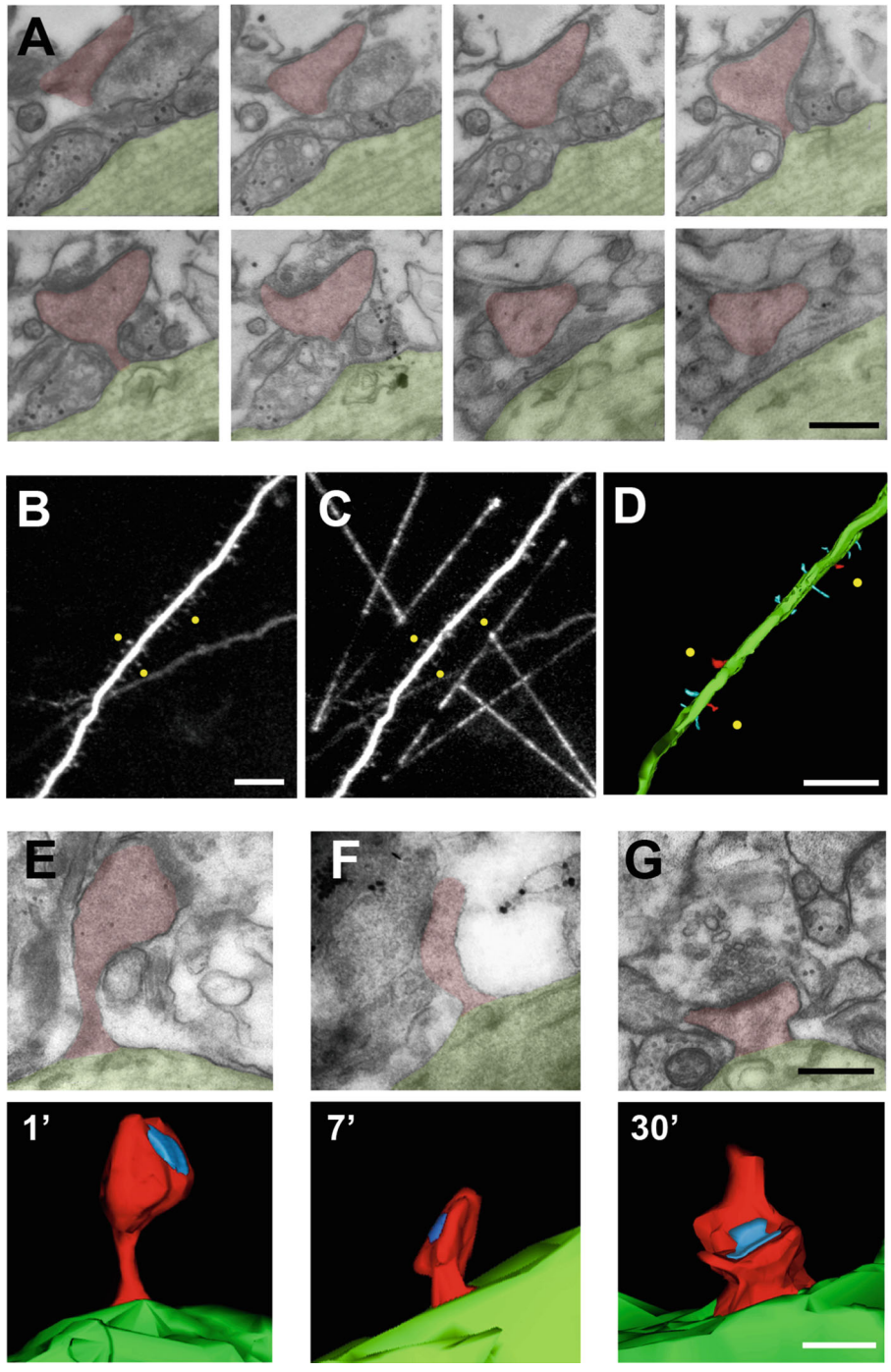

Fig. 5 Reconstruction of the dendrite and stimulated spines in 3D. (**a**) Example of a dendritic spine reconstructed from serial section EM images. Red, spine head and neck area; green, dendrite area. Scale bar, 0.5 μm. (**b**–**d**) Reconstruction of the whole selected dendrite. (**b**) Two-photon image of the dendrite after fixation (same as Fig. 3f, for comparison with 5D). Stimulated spines are highlighted with yellow dots. Scale bar, 10 μm (**c**) Two-photon image of the dendrite after photomarking (same as Fig. 3h, for comparison with 5D). (**d**) Reconstruction in 3D of the dendrite (green), stimulated spines (red), and unstimulated spines (blue).

the dendritic shaft (turns, branching points…) and compare them to the fluorescence images. It may turn out to be impossible to unequivocally identify the stimulated spines, because they have disappeared, or because it is hard to decide between two spines. In this case, discard this spine from the study because the power of this experimental technique relies on the possibility to unequivocally identify the spines under both 2-photon and electron microscopy, and compare stimulated versus unstimulated synapses with certainty, thus avoiding any reliance on mixed population statistics.

6. Use the Reconstruct software package [88] to measure all desired parameters in each section (length and area of spine head, spine neck, PSD, endoplasmic reticulum, mitochondria, presynaptic bouton, vesicles, etc.) and use them to calculate the desired final 3D volumes and areas (*see* Fig. 5e–g). Recent developments in convolutional neuronal networks (CNNs) provide open-source programs that automatically segment and reconstruct EM images [90].

4 Notes

1. Viable slices can be prepared from pups as young as P1, but they are less mature in terms of morphological, functional, and circuitry development. Pups older than P8 yield more mature slices but are more fragile in terms of survival and less easy to transfect.
2. Red fluorescent proteins are better excited with longer 2-photon excitation wavelengths (900–1100 nm), which offers lower resolution but deeper tissue penetration. DsRed2 is bright, stable, and well-expressed, but its tetrameric structure makes it inappropriate for fusion proteins, as there is the risk of forming aggregates. GFP can also form weak dimers. For these reasons, mCherry and monomeric-GFP are better options in the case of fusion proteins.
3. It is possible to use a single 2-photon laser for sequential, not simultaneous, imaging and uncaging, by changing the wavelength back and forth between 910 nm (imaging) and 720 nm (uncaging). Another option is to use one 720 nm 2-photon laser for uncaging and a 488 nm 1-photon laser for simultaneous imaging. Many other experimental approaches are

Fig. 5 (continued) Scale bar, 5 μm. (**e**–**g**) Reconstruction of the stimulated spines shown in Fig. 3c–e. (**e**) EM image and 3D reconstruction of a spine stimulated 1 min before fixation. Green, dendritic shaft; Red, spine; Blue, PSD. (**f**) Spine stimulated 7 min before fixation. (**g**) Spine stimulated 30 min before fixation. Scale bar, 0.5 μm

possible with two combined 2-photon lasers (or changing wavelengths of one 2-photon laser) and one (or more) 1-photon lasers. It is possible then to perform different compatible photochemical reactions while imaging at the same time. For example, you can use: (1) an 820 nm laser to photoactivate photoswitchable proteins in one spine (e.g., to measure turnover of PAGFP-labeled proteins), (2) a 720 nm laser to photostimulate the same spine by glutamate uncaging (to trigger plastic changes) while (3) using a 488 nm laser to simultaneously image the same spine (e.g., *see* Fig. 4 in Bosch et al. 2014 [12]) In the case of 1-photon confocal imaging, always choose a dendrite close to the slice surface.

4. Avoid mechanical vibrations (and electrical noise if combining with electrophysiological recordings). Avoid fluctuations of the level of liquid in the chamber, especially the extreme cases of drying out the chamber or spilling liquid out of the chamber (which can damage the lower optical components of the microscope). A constant level in the chamber can be achieved by forcing the outflow rate to be faster than the inflow rate. For example, use the pump to remove the liquid from the chamber and elevate it to the reservoir and let gravity return it to the chamber; or use a higher flow speed for outflow than inflow; or if using the same pump and thus the same speed, use a softer plastic tube (or wider internal diameter) for the outflow and a harder plastic tube (or narrower internal diameter) for the inflow, thus facilitating the pump to more easily displace the liquid through the outflow tube. Check that the pump and tubes are correctly installed and in good condition every day, as this is a common source of problems. Avoid precipitation of salt from ACSF, especially on objective lenses. Recirculate dd water at the end of the day to thoroughly wash all tubes, chambers, and objectives lenses that have been in contact with ACSF or any solution. Recirculate disinfectant solution often (monthly), and replace the tubes with new ones as soon as any sign of deterioration appears.
5. Measure osmolality every 30 min and determine when it increases significantly. In our setup we could perform 1.5–2 h long experiments without any major increase in osmolality. For longer experiments, we usually kept a constant osmolality by adding ~100–200 μL of dd water every 1 h, approximately, to the 10–15 mL of recirculating solution.
6. We recommend testing several batches of horse serum, selecting the one that gives better survival, slice quality, synaptic plasticity, etc., and purchasing large quantities of that batch. Adjust medium pH to 7.3 by adding consecutive small amounts of 10 M NaOH. Typically, up to ~100–200 μL of 10 M NaOH are needed to increase pH from around ~6.9 up

to 7.3 in 0.5 L of culture medium. Adjust osmolality by adding dd water, even though the concentration of all components might be reduced below the suggested values. Osmolality is more important than the final concentration of these components. Typically, consecutive small amounts of dd water, up to a final volume of ~90–120 mL, are added to reach 300–320 mOsm/L in an initial 0.5 L of medium.

7. Prepare a 10× partial stock solution: 25 mM KCl, 260 mM $NaHCO_3$, 10 mM NaH_2PO_4, and 110 mM glucose. Filter and keep at 4 °C. Before dissection, dilute it 10 times with dd water, and add 238 mM sucrose, 1 mM $CaCl_2$, and 5 mM $MgCl_2$.
8. Prepare a Ca-free Mg-free 10× ACSF stock solution in dd water with 1190 mM NaCl, 25 mM KCl, 260 mM $NaHCO_3$, 10 mM NaH_2PO_4, and 110 mM glucose. Filter and keep at 4 °C. On the day of the experiment, dilute 10 times with dd water, bubble with carbogen for 20 min, and add 3 mM $CaCl_2$. Just before its use, add 1 μM TTX and 50 μM picrotoxin. TTX is added to block the spontaneous neuronal activity that would otherwise increase too much due to the lack of Mg. Prepare a stock solution of 1 mM TTX using TTX-citrate or dissolving TTX in 0.1 M sodium citrate or acetate buffer at pH 4.8. Picrotoxin is optional in case you also want to block GABAergic transmission.
9. First prepare 4% EM-grade PFA solution (w/v) in 0.2 M PB. Dissolve it by heating at 55 °C and slightly raising the pH with a few drops of 1 M NaOH. Filter and let cool down to room temperature (r.t.). Mix this solution with a pre-made stock solution of 10% GA and dd water with these proportions (4% PFA:10% GA:dd water; 10:4:6). Adjust pH to 7.4.
10. Because of their viscosity, add components A and B by directly pouring them in a beaker thoroughly cleaned with acetone that will only be used for this purpose. For the less viscous components C and D, use plastic disposable pipettes. Use a scale to measure the quantities and mix thoroughly with a perfectly cleaned glass rod. Transfer to a vacuum bell jar and proceed to degasify the mix. When applying vacuum, one should see major bubbles that disappear after a few minutes and a small film of foam in the interphase between Durcupan and air. Use 10 mL syringes to take the resin, avoiding the foamy interphase. Wrap the syringes in parafilm and store in the fridge in a dark compartment to prevent further polymerization. The remaining foamy resin can be used to prepare the 1:1 mix of propylene oxide and resin.
11. Slices are usually cultured on top of semi-permeable (0.4 μm pore) membrane inserts (Millipore) in 6-well plates. Some money can be saved by culturing the slices on top of

already-cut pieces of Biopore Millicell hydrophilic polytetrafluoroethylene membrane placed onto these membrane inserts. Membrane inserts can then be recycled by re-sterilization with washes of ethanol, 10% acetic acid, water, ethanol, and drying at UV [64]. Another economical alternative is to use Omnipore (Millipore) membranes [63].

12. It is convenient to culture 4 slices in each well, placed close to each other in the center of the well (to facilitate the transfection by gene gun), but without touching each other. Culturing more than 4 slices per well would consume medium nutrients too fast. Less than 4 slices is possible but then more wells and medium will be required, making the experiment more expensive.
13. Assess the quality of slices by DIV 5 by confirming that: (1) microglia has cleared and the slice become transparent, with no dark spots; (2) hippocampal subregions (CA1, CA3, Dentate Gyrus) are clearly visible, and (3) CA3 thickness is comparable to CA1 thickness (CA3 large neurons are more vulnerable to damage).
14. Dead surface neurons will disappear over the first days of culturing and glial response will decrease after that. Transfection of slices too early may result in many unwanted transfected cells: dying neurons or glial cells. On the other hand, efficiency of transfection decreases with time: one will need to prepare and transfect many more slices to have good chances of finding the appropriate fluorescent neuron.
15. If the neuron is whole-cell patched, long-term experiments might be precluded because of the dilution of cellular components into the pipette solution. Some extra experimental conditions might be necessary. For instance, maintenance of spine enlargement after LTP induction during whole-cell patch clamp requires adding 5 μM actin monomers to the pipette [91].
16. Empirically determine how long it takes for the system to reach stable conditions (temperature, etc.) by measuring laser power at final point (chamber) and by checking laser alignment. It can vary from a few minutes to a few hours.
17. This checking point is also useful to confirm the lasers are well aligned in the Z dimension. Try to change the position of the objective lens by focusing on several points along the Z dimension and confirm that maximum bleaching is achieved when the bead is well focused. If maximum bleaching is shifted and occurs at another z position, you can fix that by a major realignment of all optical components, or you can introduce the same Z shift when uncaging the dendritic spine.

18. It is possible to prepare the Uncaging ACSF at this point and recirculate it in the system before placing the sample (*see* also **Note 26**). We recommend, however, keeping the working Mg-free ACSF, place the sample, and replace the solution later with Uncaging ACSF.
19. It can sometimes be useful to check the location of fluorescent cells with an epifluorescence microscope before cutting out the membrane from the culture dish, in order to know which well and which slice might contain well-transfected neurons. Alternatively, one can prepare a high number of wells with enough slices. Just cut out a piece of membrane containing the 4 slices, put it in the chamber and look for the appropriate neuron. By chance, after checking several slices, it is usually possible to find one slice with an appropriate neuron in the appropriate region expressing the appropriate level of fluorescence signals.
20. Minimize the time that the slices are out of the incubator or out of the imaging chamber. Thus, it is worthwhile to have a small incubator next to the microscope in which to store the plates on the imaging day, also to avoid disturbing the remaining cultures in the main incubator.
21. Take notes of the shape of the membrane piece, the position of the slice and the position and orientation of the neuron. It will be necessary to know later where to start looking for the landmarks.
22. Slice holders can be purchased or custom-made. Bend a 1 mm Ø platinum wire and make a ~10–14 mm Ø semi-circle or U-shape. Cut the vertical strings of a nylon mesh (e.g., stockings) and keep the horizontal ones. Glue the nylon strings on the two sides of the metal semi-circle so that ~5 strings cross it, and cut the ends.
23. Some metabolic parameters, such as neuronal protein synthesis rate, might need >3 h of preincubation at 32 °C [92, 93] to reach a true stable state.
24. If you choose a secondary dendrite or the distal part of the main dendrite, the diameter of the dendrite will be smaller and the spine will be easier to image.
25. This way, you can have 3 stimulated spines in the same sample and thus reduce the number of samples to process by a factor of 3. However, if spines are too close in space or stimulated too close in time, you may induce metaplastic interactions [75].
26. Keep the caged glutamate under dark conditions. Prepare the Uncaging ACSF under the minimum illumination possible. It is useful to use a red light bulb or LED to illuminate the room or inside the microscope dark box, when needed, and to keep the chamber and the circulating uncaging solution covered all

the times (with black curtains or yellow cellophane or UV filters) to protect it from ambient light, computer monitors, etc. If neurons start deteriorating just after the addition of caged glutamate, it could mean the batch is contaminated with free glutamate. This rarely happens and it can be detected by standard amino acid analysis.

27. We recommend performing pilot experiments where simultaneous intracellular recordings are made together with 2-photon imaging. In these pilot experiments, one wants to adjust the caged glutamate concentration, laser intensity, and pulse duration to obtain an averaged EPSC response within a range similar to mini EPSCs [12, 45, 54]. Once this is firmly established, subsequent imaging experiments can be performed without simultaneous recordings, which are highly time-consuming and preclude long-term experiments.
28. The efficiency of uncaging depends on the depth in the tissue and on the type of neuron. Therefore, this laser intensity value can be further adjusted for each neuron and for each depth by selecting a test spine, located in the same neuron and at a similar depth but in another dendrite or away from the selected region where the experimental spines will be stimulated, and inducing LTP to obtain a peak increase in spine volume of around 200–300% in the first 1–2 min and a subsequent sustained increase in spine volume of 50–100% for at least 10 min (*see* Figs. 2b and 3c–e) [12].
29. Neurons transfected with EGFP, DsRed2, or any free soluble fluorescent protein, are less susceptible to bleaching, and so one can take images more often than when using slow-dynamics synaptic fusion proteins as markers (e.g., EGFP-PSD-95). Typically, one can take an image every 1–5 min if the total experiment lasts for 30–60 min, or every 10–30 min if the experiment lasts for hours.
30. A variation of 10–20% of spine head volume between consecutive images is typical in these experiments using Mg-free solutions, possibly due to the endogenous plasticity of spines, and to a lesser extent, also due to technical variations of the microscopic imaging.
31. Do not bubble with carbogen, as the CO_2 will decrease pH and will prevent DAB photoprecipitation. Do not expose fixed slices to hostile conditions that could erase the fluorescence signal, such as drastic changes in pH or strong photobleaching illumination.
32. A decrease in fluorescence signal is expected after the fixation step. A small degree of morphological distortion is also expected. Dendrites might look a little bit wavy and some blebbing may appear. Spine morphology should look as it was

in the last live image. This distortion, if it happens, should not preclude a valid comparison between stimulated and control spines, since it should homogeneously affect all of them. However, if the neuron looks unhealthy (too much blebbing, dendrites that are too curvy) and/or the spines look too distorted or disappear, it means the fixation step has not been quick or strong enough. We recommend discarding such samples.

33. This photoprecipitation can be done in any region of the tissue and is probably achieved by the light-dependent generation of free radicals from endogenous intracellular oxidizable molecules. Photoprecipitation seems to occur more efficiently in regions that resemble the cell nuclei (*see* Fig. 3l).
34. Do not take many images and do not use high intensity of imaging laser, as bleaching is now a more significant problem because the sample and the fluorescent proteins are now fixed.
35. It is rather difficult to draw the lines pointing exactly to the spine. And it is actually not totally necessary. So, if the line points not exactly to the spine but X μm away, we will just have to search for the spine -X μm away from the line on the EM images.
36. Osmium tetroxide solutions are highly susceptible to contaminants and easily reduced by light, so even if using amber vials, cover them with aluminum foil. Any solution that develops a black clouding or deposits, should be discarded and a fresh solution should be made.
37. It is important to prevent vibrations and air drafts that may interfere with the sectioning process by having the ultramicrotome set up in an enclosed area and minimizing movement around it. It is also important to minimize the levels of static by keeping a humid atmosphere with a humidifier.
38. Use a syringe covered with aluminum foil attached to a 0.22 μm disc filter to drop the Uranyl Acetate Solution. Always discard the first drop.
39. To obtain a CO_2-free environment, wrap the rim of the Petri dish with kimwipes soaked in 1 N NaOH solution and add some NaOH pellets. It is also critical to reduce breathing when handling the grids and wear a surgical mask while staining to prevent exposure of the samples to exhaled CO_2.
40. While taking the EM images, it is convenient to simultaneously look at printed copies of the 2-photon fluorescence images of the selected region (or display them on a monitor) and constantly compare the pattern of landmarks to confirm you are in the correct region and correct depth.

Acknowledgments

We thank Kensuke Futai, Kenichi Okamoto, Eva Rojo, and Andrea Santuy for helpful suggestions. This work was originally supported by a "Beatriu de Pinós" fellowship (AGAUR, "Generalitat de Catalunya"), the FRAXA Foundation, a Marie Curie Reintegration Grant (H2020-MSCA-IF) (to M.B.), the "Fundación Caja Madrid" (to J.C.), the Anne Punzak Marcus Fund (to M.S.), RIKEN, an NIH grant (R01DA17310), a Grant-in-Aid for Scientific Research (A) (JP20240032), and a Grant-in-Aid for Scientific Research on Innovative Area "Foundation of Synapse and Neurocircuit Pathology" (JP22110006) from the Ministry of Education, Culture, Sports, Science and Technology of Japan, the Human Frontier Science Program (RGP0022/2013), and The Key Recruitment Program of High-end Foreign Experts of the Administration of Foreign Experts Affairs of Guangdong Province (to Y. H). Conflict of interest statement: Y.H. is partly supported by Takeda Pharmaceutical Co. Ltd. and Fujitsu Laboratories.

References

1. Bosch M, Hayashi Y (2011) Structural plasticity of dendritic spines. Curr Opin Neurobiol 22:1–6
2. Matsuzaki M, Ellis-Davies GC, Nemoto T et al (2001) Dendritic spine geometry is critical for AMPA receptor expression in hippocampal CA1 pyramidal neurons. Nat Neurosci 4: 1086–1092
3. Ellis-Davies GC (2020) Useful caged compounds for cell physiology. Acc Chem Res 53: 1593–1604
4. Zhuang Y, Shi X (2023) Expansion microscopy: a chemical approach for super-resolution microscopy. Curr Opin Struct Biol 81:102614
5. Tønnesen J, Nägerl UV (2013) Superresolution imaging for neuroscience. Exp Neurol 242:33–40
6. Chéreau R, Tønnesen J, Nägerl UV (2015) STED microscopy for nanoscale imaging in living brain slices. Methods 88:57–66
7. Sigrist SJ, Sabatini BL (2012) Optical superresolution microscopy in neurobiology. Curr Opin Neurobiol 22:86–93
8. Fuhrmann M, Gockel N, Arizono M et al (2022) Super-resolution microscopy opens new doors to life at the nanoscale. J Neurosci 42:8488–8497
9. Harris KM, Weinberg RJ (2012) Ultrastructure of synapses in the mammalian brain. Cold Spring Harb Perspect Biol 4:a005587
10. Craig CH, Kandel ER, Harris KM (2015) Structural components of synaptic plasticity and memory consolidation. Cold Spring Harb Perspect Biol 7:a021758
11. Swanson LW, Lichtman JF (2016) From cajal to connectome and beyond. Annu Rev Neurosci 39:197–216
12. Bosch M, Castro J, Saneyoshi T et al (2014) Structural and molecular remodeling of dendritic spine substructures during long-term potentiation. Neuron 82:444–459J
13. Tanaka I (2005) Number and density of AMPA receptors in single synapses in immature cerebellum. J Neurosci 25:799–807
14. Bishop D, Nikić I, Brinkoetter M et al (2011) Near-infrared branding efficiently correlates light and electron microscopy. Nat Methods 8:568–570
15. Iwasaki H, Ichinose S, Tajika Y et al (2022) Recent technological advances in correlative light and electron microscopy for the comprehensive analysis of neural circuits. Front Neuroanat 16:1061078
16. Castro J, Bosch M, Hayashi Y et al (2009) Ultrastructural reorganization after long-term potentiation at a single dendritic spine. Poster communication at Neuroscience Meeting, Society for Neuroscience, Chicago
17. Bosch M, Castro J, Narayanan R et al (2009) Structural and molecular reorganization of a single dendritic spine during long-term

potentiation. Poster communication at Neuroscience Meeting, Society for Neuroscience, Chicago

18. Nägerl UV, Köstinger G, Anderson JC et al (2007) Protracted synaptogenesis after activity-dependent spinogenesis in hippocampal neurons. J Neurosci 27:8149–8156
19. Zito K, Knott G, Shepherd GMG et al (2004) Induction of spine growth and synapse formation by regulation of the spine actin cytoskeleton. Neuron 44:321–334
20. Knott GW, Holtmaat A, Trachtenberg JT et al (2009) A protocol for preparing GFP-labeled neurons previously imaged in vivo and in slice preparations for light and electron microscopic analysis. Nat Protoc 4:1145–1156
21. Chen JL, Lin WC, Cha JW et al (2011) Structural basis for the role of inhibition in facilitating adult brain plasticity. Nat Neurosci 14: 587–594
22. Sun Y, Smirnov M, Kamasawa N et al (2021) Rapid ultrastructural changes in the PSD and surrounding membrane after induction of structural LTP in single dendritic spines. J Neurosci 41:7003–7014
23. Monosov EZ, Wenzel TJ, Lüers GH et al (1996) Labeling of peroxisomes with green fluorescent protein in living P. pastoris cells. J Histochem Cytochem 44:189–581
24. Grabenbauer M, Geerts WJC, Fernadez-Rodriguez J et al (2005) Correlative microscopy and electron tomography of GFP through photooxidation. Nat Methods 2:857–862
25. Nikonenko I, Boda B, Alberi S et al (2005) Application of photoconversion technique for correlated confocal and ultrastructural studies in organotypic slice cultures. Microsc Res Tech 68:90–96
26. Bock DD, Lee W-CA, Kerlin AM et al (2011) Network anatomy and in vivo physiology of visual cortical neurons. Nature 471:177–182
27. Briggman KL, Helmstaedter M, Denk W (2011) Wiring specificity in the direction-selectivity circuit of the retina. Nature 471: 183–188
28. Watanabe S, Punge A, Hollopeter G et al (2011) Protein localization in electron micrographs using fluorescence nanoscopy. Nat Methods 8:80–84
29. Sochacki KA, Shtengel G, van Engelenburg SB et al (2014) Correlative super-resolution fluorescence and metal-replica transmission electron microscopy. Nat Methods 11:305–308
30. Desmond NL, Levy WB (1986) Changes in the postsynaptic density with long-term potentiation in the dentate gyrus. J Comp Neurol 253: 476–482
31. Ostroff LE, Fiala JC, Allwardt B et al (2002) Polyribosomes redistribute from dendritic shafts into spines with enlarged synapses during LTP in developing rat hippocampal slices. Neuron 35:535–545
32. Meyer D, Bonhoeffer T, Scheuss V (2014) Balance and stability of synaptic structures during synaptic plasticity. Neuron 82:430–443
33. Blazquez-Llorca L, Hummel E, Zimmerman H et al (2015) Correlation of two-photon in vivo imaging and FIB/SEM microscopy. J Microsc 259:129–136
34. Maco B, Cantoni M, Holtmaat A et al (2014) Semiautomated correlative 3D electron microscopy of in vivo-imaged axons and dendrites. Nat Protoc 9:1354–1366
35. Gemin O, Serna P, Zamith J et al (2021) Unique properties of dually innervated dendritic spines in pyramidal neurons of the somatosensory cortex uncovered by 3D correlative light and electron microscopy. PLoS Biol 19:e3001375
36. Georgiu C, Kehayas V, Lee KS et al (2022) A subpopulation of cortical VIP-expressing interneurons with highly dynamic spines. Commun Biol 5:352
37. Palhol JSC, Balia M, Sánchez-Román Terán F et al (2023) Direct association with the vascular basement membrane is a frequent feature of myelinating oligodendrocytes in the neocortex. Fluids Barriers CNS 20:24
38. Bacmeister CM, Huang R, Osso LA et al (2022) Motor learning drives dynamic patterns of intermittent myelination on learning-activated axons. Nat Neurosci 25:1300–1313
39. Kim YJ, Peterson BB, Crook JD et al (2022) Origins of direction selectivity in the primate retina. Nat Commun 13:2862
40. Buchs PA, Stoppini L, Muller D (1993) Structural modifications associated with synaptic development in area CA1 of rat hippocampal organotypic cultures. Dev Brain Res 71:81–91
41. Collin C, Miyaguchi K, Segal M (1997) Dendritic spine density and LTP induction in cultured hippocampal slices. J Neurophysiol 77:1614–1623
42. Zafirov S, Heimrich B, Frotscher M (1994) Dendritic development of dentate granule cells in the absence of their specific extrinsic afferents. J Comp Neurol 345:472–480
43. Gähwiler B (1997) Organotypic slice cultures: a technique has come of age. Trends Neurosci 20:471–477
44. Muller D, Buchs PA, Stoppini L (1993) Time course of synaptic development in hippocampal organotypic cultures. Dev Brain Res 71:93–100

45. A. De Simoni, C.B. Griesinger, and F. a Edwards (2003) Development of rat CA1 neurones in acute versus organotypic slices: role of experience in synaptic morphology and activity. J Physiol 550, 135–147.
46. Debanne D, Guérineau NC, Gähwiler BH et al (1995) Physiology and pharmacology of unitary synaptic connections between pairs of cells in areas CA3 and CA1 of rat hippocampal slice cultures. J Neurophysiol 73:1282–1294
47. Washbourne P, McAllister AK (2002) Techniques for gene transfer into neurons. Curr Opin Neurobiol 12:566–573
48. Karra D, Dahm R (2010) Transfection techniques for neuronal cells. J Neurosci 30:6171–6177
49. Bolz J, Novak N, Götz M et al (1990) Formation of target-specific neuronal projections in organotypic slice cultures from rat visual cortex. Nature 346:359–362
50. Molnár Z, Blakemore C (1991) Lack of regional specificity for connections formed between thalamus and cortex in coculture. Nature 351:475–477
51. Seidl AH, Rubel EW (2010) A simple method for multiday imaging of slice cultures. Microsc Res Tech 73:37–44
52. Umeshima H, Hirano T, Kengaku M (2007) Microtubule-based nuclear movement occurs independently of centrosome positioning in migrating neurons. Proc Natl Acad Sci USA 104:16182–16187
53. Hayashi MK, Tang C, Verpelli C et al (2009) The postsynaptic density proteins homer and shank form a polymeric network structure. Cell 137:159–171
54. Sala C, Futai K, Yamamoto K et al (2003) Inhibition of dendritic spine morphogenesis and synaptic transmission by activity-inducible protein Homer1a. J Neurosci 23:6327–6337
55. Nikolenko V, Nemet B, Yuste R (2003) A two-photon and second-harmonic microscope. Methods 30:3–15
56. Majewska A, Yiu G, Yuste R (2000) A custom-made two-photon microscope and deconvolution system. Pflugers Arch 441:398–408
57. Tsai PS, Nishimura N, Yoder EJ et al (2002) Principles, design and construction of a scanning microscope for in vitro and in vivo brain imaging. In: Frostig RD (ed) In vivo optical imaging of brain function. CRC Press, Boca Raton
58. Tsai PS, Kleinfeld D (2009) In vivo two-photon laser scanning microscopy with concurrent plasma-mediated ablation principles and hardware realization. In: Frostig RD (ed) In vivo optical imaging of brain function. CRC Press, Boca Raton, pp 59–115
59. Okamoto K-I, Nagai T, Miyawaki A et al (2004) Rapid and persistent modulation of actin dynamics regulates postsynaptic reorganization underlying bidirectional plasticity. Nat Neurosci 7:1104–1112
60. Stoppini L, Buchs P-A, Muller D (1991) A simple method for organotypic cultures of nervous tissue. J Neurosci Methods 37:173–182
61. Yamamoto N, Kurotani T, Toyama K (1989) Neural connections between the lateral geniculate nucleus and visual cortex in vitro. Science 245:192–194
62. Gogolla N, Galimberti I, DePaola V et al (2006) Preparation of organotypic hippocampal slice cultures for long-term live imaging. Nat Protoc 1:1165–1171
63. Koyama R, Muramatsu R, Sasaki T et al (2007) A low-cost method for brain slice cultures. J Pharmacol Sci 104:191–194
64. Soares C, Lee KFH, Cook D et al (2014) Patch-clamp methods and protocols 1183: 205–219
65. O'Brien JA, Lummis SCR (2006) Biolistic transfection of neuronal cultures using a hand-held gene gun. Nat Protoc 1:977–981
66. Woods G, Zito K (2008) Preparation of gene gun bullets and biolistic transfection of neurons in slice culture. J Vis Exp e675:3–6
67. Govindarajan A, Israely I, Huang SY et al (2011) The dendritic branch is the preferred integrative unit for protein synthesis-dependent LTP. Neuron 69:132–146
68. Ehrengruber MU, Hennou S, Bueler H et al (2001) Gene transfer into neurons from hippocampal slices: comparison of recombinant Semliki Forest Virus, adenovirus, adeno-associated virus, lentivirus, and measles virus. Mol Cell Neurosci 17:855–871
69. Malinow R, Hayashi Y, Maletic-Savatic M et al (2010) Introduction of green fluorescent protein (GFP) into hippocampal neurons through viral infection. Cold Spring Harbor Protoc: pdb.prot5406
70. Haas K, Sin W, Javaherian A et al (2001) Single-cell electroporation for gene transfer in vivo. Neuron 29:583–591
71. Pagès S, Cane M, Randall J et al (2015) Single cell electroporation for longitudinal imaging of synaptic structure and function in the adult mouse neocortex in vivo. Front Neuroanat 9: 36
72. Antkowiak M, Torres-Mapa ML, Witts EC et al (2013) Fast targeted gene transfection and optogenetic modification of single neurons

using femtosecond laser irradiation. Sci Rep 3: 3281

73. Barrett LE, Sul JY, Takano H et al (2006) Region-directed phototransfection reveals the functional significance of a dendritically synthesized transcription factor. Nat Methods 3:455–460
74. Matsuzaki M, Honkura N, Ellis-Davies GCR et al (2004) Structural basis of long-term potentiation in single dendritic spines. Nature 429:761–766
75. Harvey CD, Svoboda K (2007) Locally dynamic synaptic learning rules in pyramidal neuron dendrites. Nature 450:1195–1200
76. Steiner P, Higley MJ, Xu W et al (2008) Destabilization of the postsynaptic density by PSD-95 serine 73 phosphorylation inhibits spine growth and synaptic plasticity. Neuron 60:788–802
77. Lee S-JR, Escobedo-Lozoya Y, Szatmari EM et al (2009) Activation of CaMKII in single dendritic spines during long-term potentiation. Nature 458:299–304
78. Tazerart S, Mitchell DE, Miranda-Rottmann S et al (2020) A spike-timing-dependent plasticity rule for dendritic spines. Nat Commun 11: 4276
79. Oh WC, Hill TC, Zito K (2013) Synapse-specific and size-dependent mechanisms of spine structural plasticity accompanying synaptic weakening. Proc Natl Acad Sci USA 110: E305–E312
80. Holbro N, Grunditz A, Oertner TG (2009) Differential distribution of endoplasmic reticulum controls metabotropic signaling and plasticity at hippocampal synapses. Proc Natl Acad Sci USA 106:15055–15060
81. Hayama T, Noguchi J, Watanabe S et al (2013) GABA promotes the competitive selection of dendritic spines by controlling local Ca^{2+} signaling. Nat Neurosci 16:1409–1416
82. Noguchi J, Nagaoka A, Hayama T et al (2019) Bidirectional in vivo structural dendritic spine plasticity revealed by two-photon glutamate uncaging in the mouse neocortex. Sci Rep 16: 1409–1416
83. Bozzola J, Russell L (1999) Specimen preparation for transmission electron microscopy. In: Jones, Bartlett (eds) Electron microscopy, 2nd edn, pp 16–47
84. Harris KM, Perry E, Bourne J et al (2006) Uniform serial sectioning for transmission electron microscopy. J Neurosci 26:12101–12103
85. Hayat M (1985) Basic techniques for transmission electron microscopy. Cambridge University Press
86. Muller-Reichert T, Pigino G (2019) Three-dimensional electron microscopy, 1st edn. Academic
87. Williams D, Carter B (2009) Transmission electron microscopy: a textbook for materials science, 2ns edn. New York
88. Fiala JC (2005) Reconstruct: a free editor for serial section microscopy. J Microsc 218:52–61
89. Morales J, Alonso-Nanclares L, Rodriguez JR et al (2011) Espina: a tool for the automated segmentation and counting of synapses in large stacks of electron microscopy images. Front Neuroanat 5:18
90. Urakubo H, Bullman T, Kubota Y et al (2019) UNI-EM: an environment for deep neural network-based automated segmentation of neuronal electron microscopic images. Sci Rep 9:19413
91. Tanaka J-I, Horiike Y, Matsuzaki M et al (2008) Protein synthesis and neurotrophin-dependent structural plasticity of single dendritic spines. Science 319:1683–1687
92. Sajikumar S, Navakkode S, Frey JU (2005) Protein synthesis-dependent long-term functional plasticity: methods and techniques. Curr Opin Neurobiol 15:607–613
93. Osterweil EK, Krueger DD, Reinhold K et al (2010) Hypersensitivity to mGluR5 and ERK1/2 leads to excessive protein synthesis in the hippocampus of a mouse model of fragile X syndrome. J Neurosci 30:15616–15627

Part III

Mapping Synaptic Connectivity and Activity

Chapter 11

Image Analysis Routines for Quantification of Synaptic Density and Connectivity

Luca Della Santina and Mrinalini Hoon

Abstract

Fixed tissue analyses of synaptic density and connectivity rely on analyses of image stacks containing fluorescence signals. This chapter details image analysis routines that can be implemented to determine connectivity between labeled cell types and procedures for quantification of synaptic density across a tissue volume or specifically within a labeled cell of interest. The chapter details open-source software and practices that can be implemented for these analyses as well as considerations for validation of detected signals, estimation of background noise in images, and determination of non-specific detections.

Key words Fluorescence, Image analysis, Synaptic density, Synaptic connectivity

1 Introduction

Image analyses are central to assessments of cellular connectivity. For assessments of neural connectivity, the points of contact are synaptic appositions that are key to understanding the role of molecular organizers, the perturbations introduced by disease or degenerating conditions, and for assessing the success of regenerative strategies. These assessments are commonly done by analyses of fluorescent image stacks generated by confocal microscopy. Typically, immunohistochemical labeling of cellular processes or synaptic proteins is imaged across several planes in z-stacks that are then visualized in softwares such as ImageJ/Fiji, Imaris, or Amira for subsequent analyses. The principles of apposition estimation have been detailed previously [1] but this chapter focuses on the utilization of open-source software and tools for estimations of synaptic density and connectivity and the corresponding step-by-step analysis procedures.

Connectivity analyses can be carried out to determine contact between two cell types, to ascertain enrichment of synaptic proteins within a cell of interest or to determine appositions and correlations

Tolga Soykan and Alexandros Poulopoulos (eds.), *Synapse Development: Methods and Protocols*, Methods in Molecular Biology, vol. 2910, https://doi.org/10.1007/978-1-0716-4446-1_11,

between two sets of synaptic puncta. In this chapter, we will detail the analysis routines to gauge contact between two retinal neurons—a glutamatergic interneuron population labeled by the marker protein kinase C or PKC and a GABAergic interneuron (A17) labeled through intracellular dye filling (3.1.1). In 3.1.2 we will detail quantification of synaptic puncta within a cell of interest: excitatory postsynapses as labeled by the glutamatergic scaffolding protein PSD-95 within dendrites of a retinal ganglion cell (RGC). In 3.1.3 we will outline assessment of appositions between two types of synaptic puncta—inhibitory presynaptic (vesicular inhibitory amino acid transporter: VIAAT) and postsynaptic receptor ($GABA_A$ receptor) puncta in a section from striatal tissue. We will also outline the steps for assessment of appositions of puncta when one population resides within a cell of interest. The different approaches to estimating synaptic density and connectivity are summarized in Fig. 1a and can comprise:

- Cell to cell apposition (A17-PKC, Fig. 2): Contacts (appositions) between the membrane of two types of labeled neurons can be assessed by creating a binary mask of the labeled neurons. In this example a retinal A17 amacrine cell is labeled by cell filling from a patch pipette and immunolabeling for PKC was performed to identify the surrounding axons of rod bipolar cells. This approach allows the measurement of connectivity based on apposition between two cell types. A17 cells and PKC-labeled boutons are known to show appositions [2, 3].
- Puncta inside a cell of interest (PSD95 within RGC, Fig. 3): In this example, a specific cell of interest is labeled using biolistic transfection [4] of untagged CFP fluorescent protein, which is free to diffuse and fill the cytosol of the transfected neuron (an alpha retinal ganglion cell). Synaptic puncta were labeled by co-expression of a cmv-PSD95-YFP plasmid which upon expression accumulated the YFP-tagged PSD95 protein at glutamatergic postsynaptic sites [5, 6].
- Puncta apposition between synaptic markers ($GABA_A$ receptor and VIAAT in Striatum, Fig. 4): In this example immunolabeling is performed on a section of striatal tissue for inhibitory presynapses (VIAAT) and inhibitory postsynapses (labeled by performing immunostaining for the a3-subunit of $GABA_A$ receptors). Apposition is expected between these markers as $GABA_A$ receptor subunits and VIAAT label the two inhibitory synaptic compartments in the striatum [7].
- Punctum to puncta within cell apposition (PSD95 within RGC apposed to presynaptic marker CtBP2, Fig. 5): Here, appositions between PSD95 puncta within a RGC of interest (labeled in Fig. 3) and an immunolabeled marker of presynaptic ribbon synapses CtBP2, are quantified. Object-wise colocalization

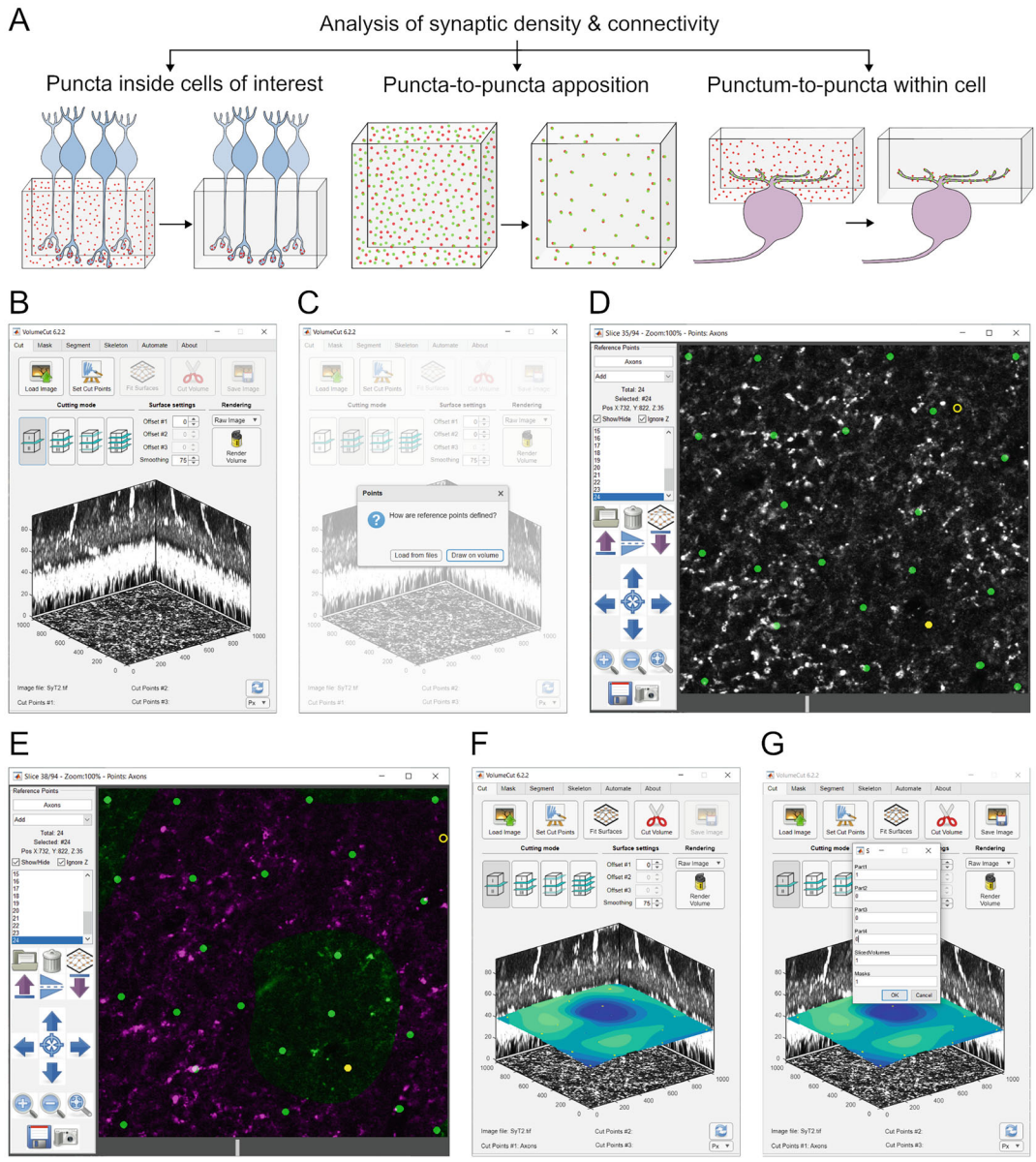

Fig. 1 Overview of analysis routines and volume segmentation along arbitrarily shaped surfaces using VolumeCut. (**a**) Schematic representation of different analysis routines that can be used for synaptic density and connectivity estimation. (**b**) Loaded image volume of retinal bipolar axons labeled by synaptotagmin 2 antibody. The main user interface shows the maximum intensity projections of the volume along the cardinal axes. (**c**) Selection or creation of fiducial points. (**d**) Manual annotation of fiducial points (green circles) over the image volume. (**e**) Online fitting of the volume along fiducial points, resulting in the image voxels annotated as above or below the surface (green vs purple) passing through fiducial points. (**f**) Best-fitting surface (shaded in blue/cyan) passing through user-defined fiducial points (yellow spots). (**g**) Selection of segmented volumes and binary masks to be saved

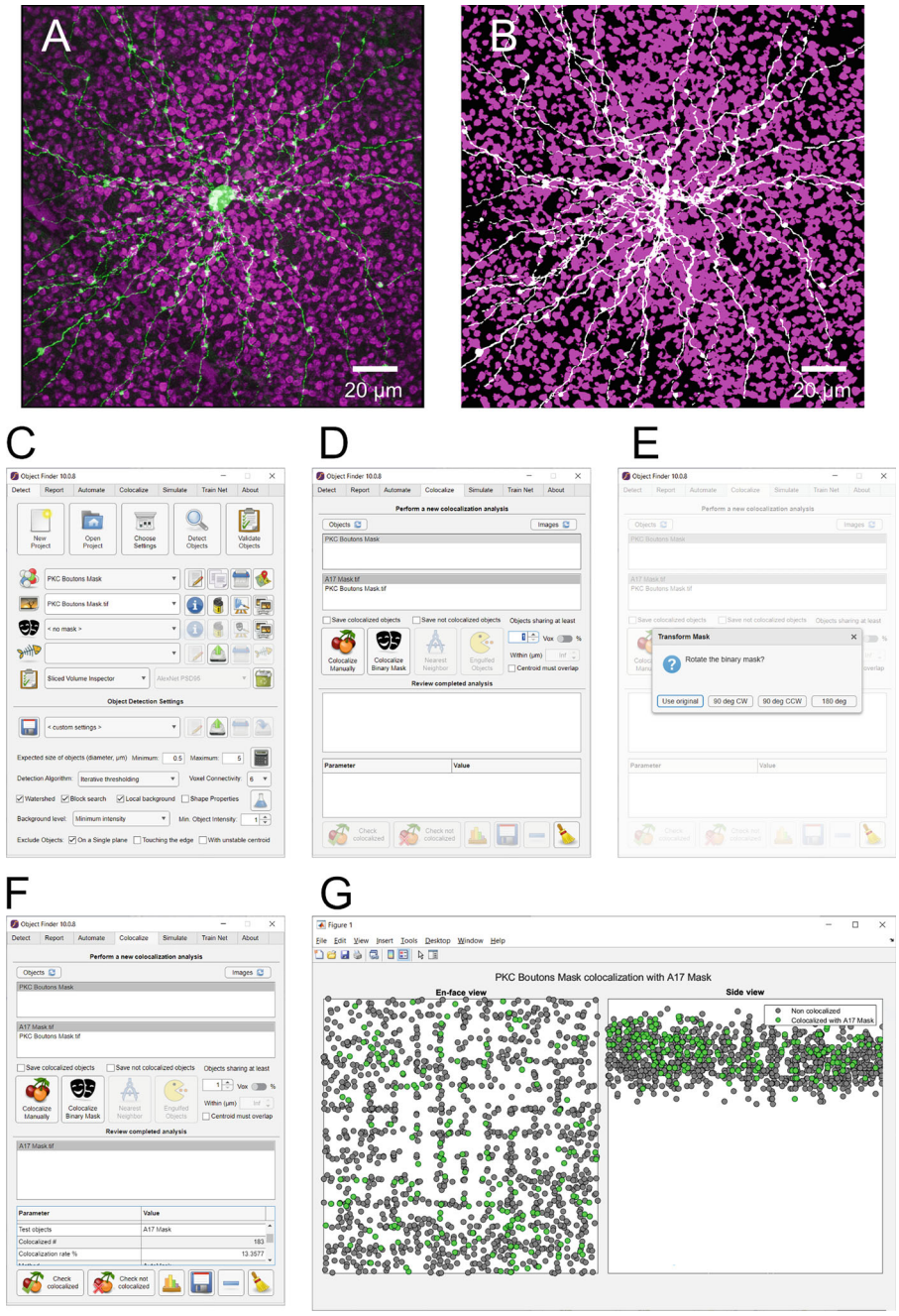

Fig. 2 Colocalization of objects between two masks. (**a**) Maximum intensity projection (top-down view) of an A17 retinal amacrine interneuron (fluorescently filled, green) and axonal boutons of rod bipolar cells (RBCs: immunolabeled, magenta). (**b**) Binary masks of the two channels (A17: white, RBC boutons: magenta). (**c**) Detection of RBCs boutons as object sets in ObjectFinder. (**d**) Colocalization analyses user interface. (**e**) Rotation of binary mask channel ("use original" for no rotation). (**f**) Results from the colocalization analyses. (**g**) Visual representation of the RBCs boutons apposed to the A17 cell (green circles) versus boutons that are not apposed (gray circles)

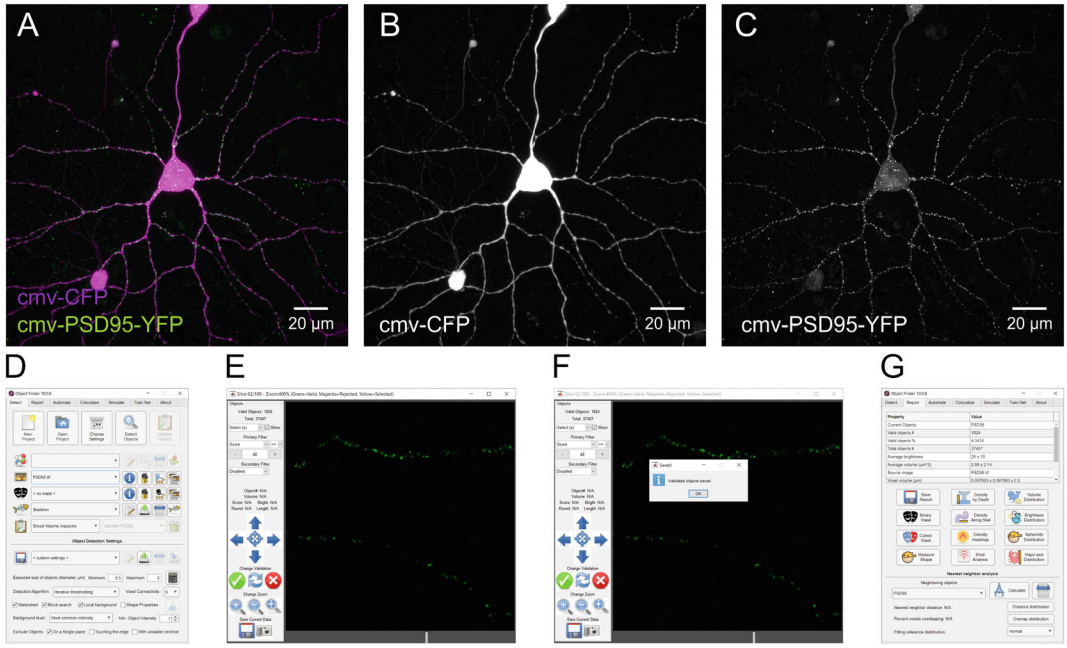

Fig. 3 Quantification of a synaptic marker in a 3D image stack with ObjectFinder. (**a**) Biolistically labeled retinal ganglion cell (RGC) in which two plasmids were transfected: cmv-CFP enabling cellular morphology visualization by filling of the cytosol (magenta) and cmv-PSD95-YFP enabling visualization of postsynaptic glutamatergic sites (green). (**b**) Individual cell fill channel (CFP). (**c**) Individual channel of the synaptic marker PSD95-YFP. (**d**) User interface for the detection of puncta in ObjectFinder. (**e**) User interface for visual inspection and validation of candidate puncta, showing valid objects in green and invalid objects in magenta. (**f**) Completed annotation of candidate puncta and storage of validation data. (**g**) Summary statistics for the detected set of puncta and user interface for plotting synaptic density and distribution statistics

analyses was used to determine apposition between the fluorescent signals of pre- and postsynaptic puncta. This approach allows delineation of ribbon vs ribbon-less synapses in the retinal inner plexiform/synaptic layer [8, 9].

2 Materials

For the image analysis routines outlined in this chapter, the following software and programs are recommended:

1. *Amira* (Thermo Fisher Scientific) for visualization of image stacks, generating 3D masks from image channels.
2. *Fiji/ImageJ* (NIH; open source) for visualization of image stacks and skeletonization of cellular processes (through simple neurite tracer).

   ImageJ: https://imagej.nih.gov/ij/index.html

   Fiji: https://fiji.sc/

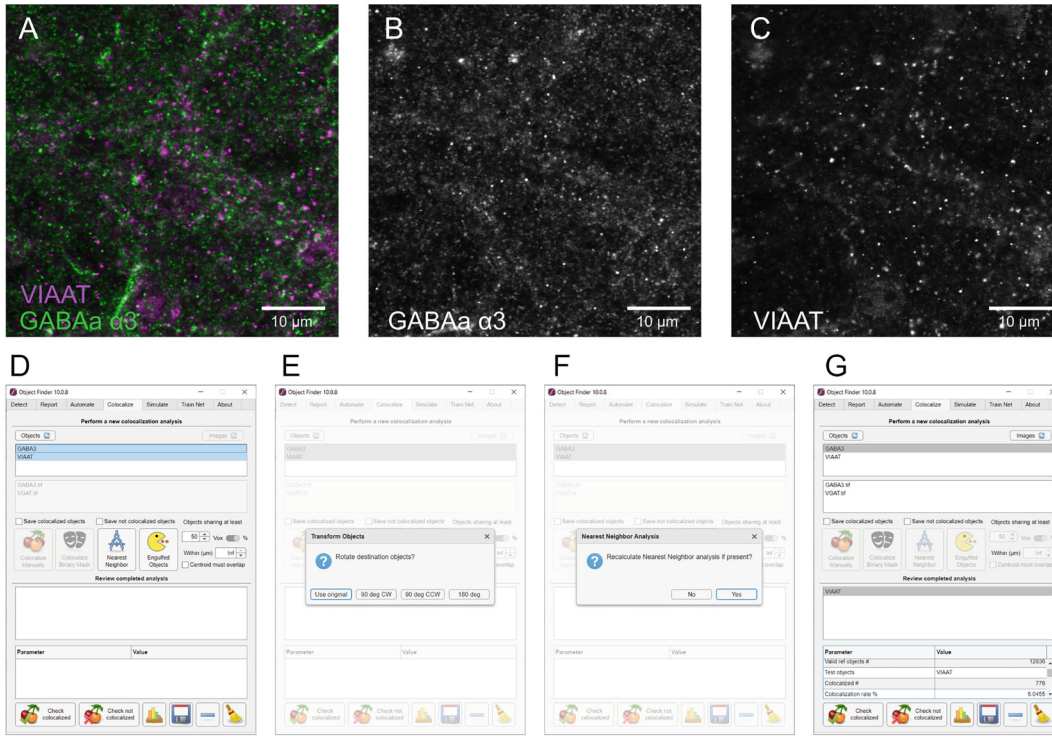

Fig. 4 Automatic colocalization analyses between two sets of puncta. Immunolabeling of a section of mouse striatal tissue for the inhibitory synaptic proteins VIAAT (magenta) and the a3-subunit of $GABA_A$ receptor ($GABA_A$a3: green). (**a**) Sample confocal plane showing the composite image. (**b**) Individual channel for the α3 subunit of $GABA_A$ receptor (**c**) Individual channel for VIAAT. (**d**) User interface for the colocalization analyses between these two sets of puncta. (**e**) Rotation of one set of puncta against the other set to determine random associations ("use original" to avoid rotation). (**f**) Recalculation of nearest neighbor statistics. (**g**) Results from the colocalization analyses

3. *Imaris* (Oxford Instruments) for optional skeletonization of cellular processes by creation of associated "filaments".
4. *MATLAB* (Mathworks) for running custom analyses software (ObjectFinder and VolumeCut).
5. *ObjectFinder* (open-source software) for puncta "dot" estimation, colocalization quantifications, and image estimations.

   https://lucadellasantina.github.io/ObjectFinder

   Version 10.0 was used for this chapter: https://doi.org/10.5281/zenodo.4767847
6. *VolumeCut* (open-source software) for masking specific synaptic layers.

   https://lucadellasantina.github.io/VolumeCut

   Version 6.3 was used for this chapter: https://doi.org/10.5281/zenodo.5048331

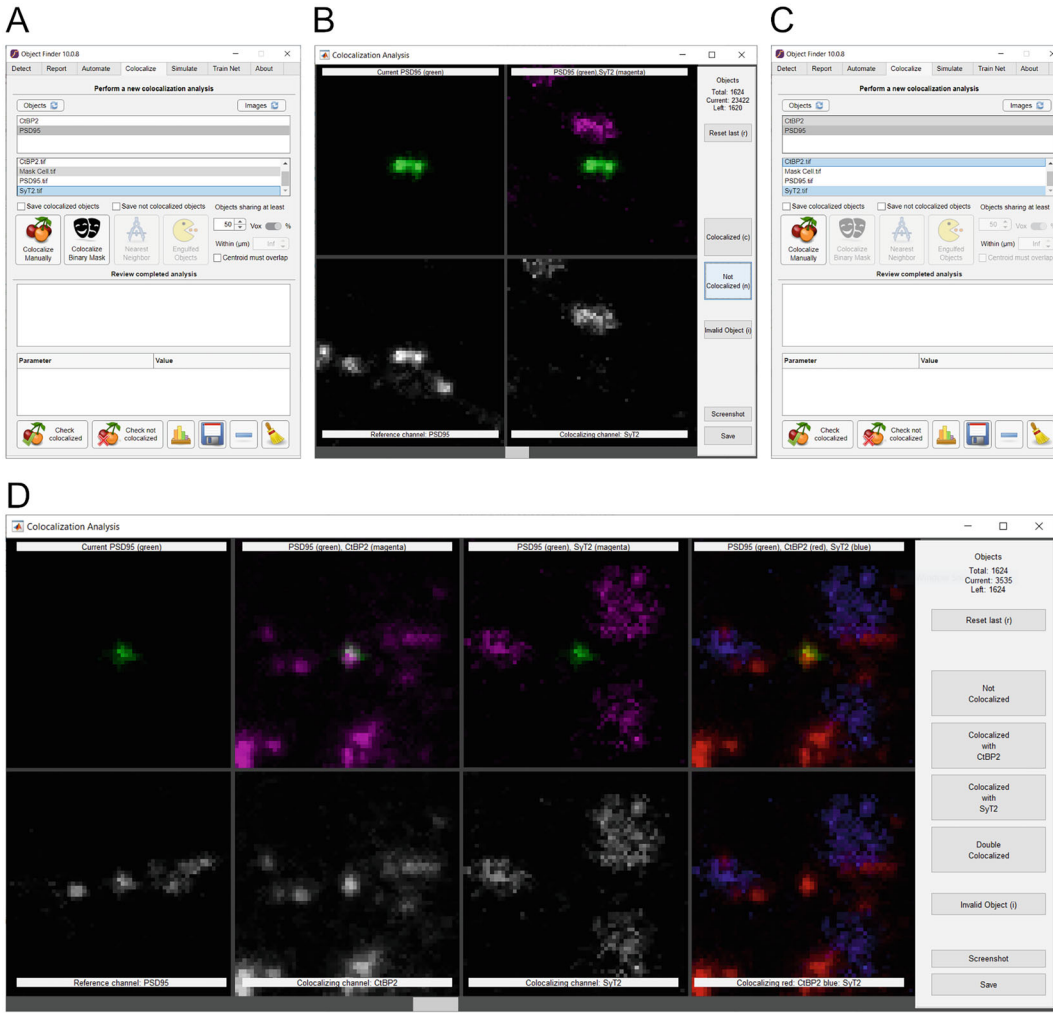

Fig. 5 Manual colocalization of puncta using raw fluorescent signals. (**a**) User interface for the manual colocalization of a set of puncta (e.g., PSD95) with an image stack labeling another puncta type (e.g., synaptotagmin 2: Syt2). (**b**) User interface presenting each individual PSD95 punctum (green) in a randomized manner to the user for manual assignment of colocalized vs non-colocalized status after comparing with the Syt2 image stack (magenta). (**c**) User interface for the manual colocalization of a set of puncta (e.g., PSD95) with two different image stacks (e.g., Syt2 and a ribbon presynaptic marker CtBP2). (**d**) User interface presenting each individual PSD95 punctum (green) in a randomized manner to the user for manual assignment of colocalized vs non-colocalized status after comparing with the two image stacks (SyT2 or CtBP2, magenta). Right-most panel shows the three signals overlaid (PSD95 in yellow, CtBP2 in red, SyT2 in blue)

3 Methods

Prior to following the outlined analysis routines, it is advisable to save the individual channels from a composite image stack as separate TIFF files. This can easily be done in ImageJ. ImageJ can also

be used to median filter the individual channels to eliminate the photomultiplier tube/detector noise commonly associated with images generated at the confocal microscope. Caution should be exercised when selecting the radius for median filtering (*see* **Note 1**) as a higher value can lead to image distortion [10].

3.1 Estimation of Synaptic Connectivity Through Signal Colocalization

3.1.1 Punctum-to-Cell/Layer Apposition

- *Cell volume masking via Amira:*

  To generate binary masks or labels that contain the signal of interest (cell or process of interest) in z-stacks that encompass several image planes, follow these steps after loading the image stack in the analyses software *Amira*.

  1. Import the image stack with the correct x-y and z resolution into Amira (*see* **Note 2**). These parameters can be gathered from the metadata of the image file.
  2. Select the channel containing the signal of interest that needs to be masked out. Amira generates "labels" that are 3D masks containing the cell or process of interest.
  3. To begin the segmentation process, select the image stack of interest and choose the "Label Field" option. This can be found under the search string "Edit New Label Field" and a new Label Field can be created for the channel of interest.
  4. Selecting a new Label Field will direct the user to the segmentation window (distinct from the project browser) where the raw image stack is visible and where the user can scroll through the z-planes to highlight regions of interest.
  5. To select a specific region of interest, a magic wand tool is accessible where a threshold can be set to select signals above a certain (background) level. An "all slices" option is also available which allows users to simultaneously select connected pixels across z-planes.
  6. When a region of interest is highlighted the "Add" button can be clicked to include the region into the mask/labels. There is also a "Subtract" button to remove regions from a specific mask or label.
  7. The brush tool can also be used to paint out or paint in regions into a mask/label. The width of the brush can be selected by the user.
  8. Once all regions have been incorporated into the mask, the user can save the labels file from the main projects browser.

  Additional manual fine-tuning of the segmentation process can be applied as discussed in **Note 3**.

- *Synaptic layer volume masking* (*using VolumeCut*, Fig. 1):

  Synapses in the CNS are typically located in synaptic layers, which are usually non-flat surfaces due to the curvature of the

enclosing tissue (e.g., due to the retinal curvature or due to the gyri and sulci of the brain), or sometimes due to tissue handling and fixation before imaging. Therefore, the user would need to define a subvolume within the acquired image stack, in order to restrict the search for synapses and to calculate metrics such as synaptic density, which are dependent on precise segmentation of the volume of interest. Segmentation of a volume of interest can be accomplished using the open-source software VolumeCut, by defining fiducial points along the borders of the synaptic layer, and thereafter by segmenting (cutting) the volume along the curved surface best fitting the user-defined fiducial points in three dimensions. The following steps outline the process:

1. Open VolumeCut from MATLAB.
2. Click "Open Image" and select the volume to segment (Fig. 1b).
3. Select from the main screen the cutting mode (cut along 1, 2, 3, or 4 surfaces, Fig. 1b second row of buttons).
4. Click "Set Cut Points" (Fig. 1b top row of buttons).
5. Click "Draw on Volume" to define fiducial points or "Load from files" if reusing previously defined points (Fig. 1c).
6. Navigate the volume using the mouse wheel and using left click, place fiducial points to perform the volume segmentation. The number of points required for an accurate segmentation depends on the size of the image and the curvature of the surface to cut. Usually, 20–30 fiducial points are sufficient to segment a synaptic layer border (Fig. 1d).
7. Click the surface fit button to preview the regions above/below (green/purple). When the fitting surface is satisfactory, save and close this screen (Fig. 1e).
8. Click "Fit Surfaces" to best fit a surface passing through the fiducial points (Fig. 1f, top row of buttons).
9. Click "Cut Volume" to perform the segmentation of the volume along the surface(s) (Fig. 1f, top row of buttons).
10. Click "Save Images" and choose which cut surfaces and binary masks to save (value = 1) or discard (value = 0) (Fig. 1g).

- *Overlap between binary masks using ObjectFinder* (Fig. 2):

  Once the volumes of the cells of interest have been segmented (using the previous two methods), binary masks can be analyzed for appositions of the labeled structures as a form of contact between the annotated neurons. To do so, the open-source software ObjectFinder can be used to determine the number and location of appositions. Typically, one image stack

is rotated relative to the other and appositions assessed to determine the rate of non-specific contacts. Outlined below are the analysis steps for determining the overlap between two sets of labeled neurons (Cell to Cell apposition):

1. Open ObjectFinder.
2. Click New Project.
3. Click Folder icon and select an empty folder that will host the project.
4. Click Add ("+") button to add each TIFF file for the two masks (here PKC boutons and A17 amacrine cell, Fig. 2b).
5. Click "Create" to create a new project based on these images.
6. Select the mask image containing smaller objects (PKC boutons, Fig. 2c second list box).
7. Select "Minimum Intensity" as Background Level (Fig. 2c Object Detection Settings).
8. Click Detect Objects (Fig. 2c, top row of buttons).
9. Go to "Colocalize" tab.
10. Select objects from the first list (PKC boutons, Fig. 2d top list).
11. Select mask to colocalize them with (A17 cell mask, Fig. 2d second list).
12. Click "Colocalize Binary Mask" (Fig. 2d buttons).
13. Select whether to rotate the colocalizing mask to estimate non-specific colocalization (Fig. 2e, select "use original" to calculate the empirical colocalization).
14. Select colocalization results from the bottom list to view colocalization rate (Fig. 2f, bottom list).
15. Click the "Plot" button (Fig. 2e, bottom row of buttons) to show the locations of apposed PKC boutons (Fig. 2g, green circles) versus un-apposed boutons (Fig. 2g, gray circles).

3.1.2 Punctum Within Cell of Interest

To detect synaptic puncta within a cell of interest in an image stack, the following process should be performed using the open-source softwares Fiji and ObjectFinder:

- *Image preparation for synapse quantification using Fiji and ObjectFinder:*

  This step uses Fiji to separate the image stack into individual color channels, to maximize the representation of pixel intensities within an 8-bit image range, and to save each channel as an individual 3D TIFF file to be recognized and used by ObjectFinder and assembled into an ObjectFinder project.

1. Open ImageJ.
2. Load image from microscope format.
3. Separate color channels into separate image stacks (Image -> Color -> Split Channels).
4. Apply median filtering to each image stack (Process -> Filter -> Median).
5. Adjust dynamic range of each image stack (Image -> Adjust -> Brightness/Contrast).
6. Convert each image stack to 8-bit (Image -> Type -> 8-bit).
7. Save each channel as a TIFF image stack.
8. Open ObjectFinder.
9. Click New Project.
10. Click Folder icon and select an empty folder that will host the project.
11. Click Add ("+") button to add each TIFF file.
12. Click Create.

- *Identification of objects in an image stack using ObjectFinder* (Fig. 3):

  This step makes use of ObjectFinder to detect candidate synapses among the signal present in the image stacks. Candidate synapses are represented as digital objects that can be further assessed for their morphological properties (e.g., shape, size, intensity) and used to quantify density of synapses in the tissue and apposition with other synaptic proteins.

  1. Select the image to analyze from list of images (Fig. 3d second listbox).
  2. Specify expected objects size range in object detection settings (Fig. 3d parameters at the bottom).
  3. Select a binary mask to restrict the search (Fig. 3d, third list, optional).
  4. Click Detect Objects (Fig. 3d top row of buttons).
  5. Repeat for each image stack to analyze.

- *Validation of candidate puncta from an object set using ObjectFinder* (Fig. 3):

  In this section, the user will further refine the set of candidate synapses by validating the synaptic candidates according to their appearance, size, and shape to generate a set of objects representing the synaptic proteins within the analyzed image stack.

1. Select the set of objects to validate from the list of available object sets (Fig. 3d, first list box).
2. Select validation method, default is "Sliced Volume Inspector" (Fig. 3d fifth list box).
3. Click "Validate Objects".
4. Use Sliced Volume Inspector to browse the volume. Valid objects are in green, rejected objects are in purple (Fig. 3e).
5. Add a threshold constraint to restrict the pool of valid objects (Fig. 3e left panel).
6. Further refine manually by selecting individual objects or groups of objects with the lasso tool (Fig. 3e).
7. Click save to store the current validation pool (Fig. 3f).
8. Repeat for each object set to validate.
9. Inspect object statistics using the "Report" tab (Fig. 3g).

3.1.3 Punctum-to-Punctum Apposition

In order to determine whether puncta from a fluorescently labeled synaptic protein are apposed or not to puncta of a different synaptic protein (e.g., presynaptic marker against a postsynaptic marker), colocalization analyses can be performed based on the fact that the signal from the fluorescent markers will overlap in space due to the close apposition of the two proteins. In order to do so, either completely automatic pairwise colocalization analyses based on nearest neighbor distance and overlap can be performed in ObjectFinder, or the user can perform manual colocalization analyses via visual inspection of each individual puncta against the colocalizing channel. The former is useful to optimize speed and reliability of the analyses, the latter is useful to generate a gold standard dataset to compare the automatic analyses against, or to train machine learning algorithms to perform the same task.

- *Automatic pairwise colocalization analyses between two sets of puncta* (Fig. 4):

  1. Open ObjectFinder.
  2. Load project and select the project's folder.
  3. Go to "Colocalize" tab.
  4. Select the first set to colocalize from the list of objects (Fig. 4d).
  5. Holding down "Ctrl", select the second object set to colocalize from the list.
  6. Determine the necessary threshold of voxels (absolute or as a percentage of the reference object size) to exceed to achieve colocalized status (Fig. 4d middle panel).

7. Determine whether colocalization can occur only within a given distance from the objects' centroids (Fig. 4d middle panel).
8. Click "Nearest neighbor" to perform colocalization analyses.
9. Select whether to rotate the colocalizing objects with respect to the reference objects (Fig. 4e).
10. Select whether to perform the nearest neighbor analyses. This step can be skipped by answering "no" in case the same analyses was performed previously or if the user wants to repeat the analyses using a different colocalization threshold value (Fig. 4f, choose yes for the analyses).
11. Review completed analyses (Fig. 4g, list at the bottom).
12. Save or plot colocalization analysis results (Fig. 4g buttons at the bottom).

- *Manual colocalization analyses between puncta and image stacks* (Fig. 5):

1. Open ObjectFinder.
2. Load project and select the project's folder.
3. Go to "Colocalize" tab.
4. Select the set of objects to colocalize from the list of objects (Fig. 5a, top list).
5. Select the image stack(s) to colocalize the objects from the list of images. Up to two colocalizing image stacks can be selected (Fig. 5a, select one image from the middle list for a two-way colocalization. Fig. 5c, select two images from the middle list for a three-way colocalization).
6. Click "Manual Colocalization" to start the colocalization interface (Fig. 5a).
7. A small substack centered on the current object will be presented (Fig. 5b, d).
8. Inspect the stack for each channel and make a manual determination whether the current object is colocalized or not colocalized with the image stack channel(s) (Fig. 5b, d, right panel of buttons).
9. Repeat for each object. Objects will be presented in a random order.
10. After completing all manual annotations, close the colocalization window.
11. Review completed analyses (Fig. 5a, c, bottom list).
12. Save or plot colocalization analysis results (Fig. 5a, c, buttons at the bottom).

3.1.4 Evaluation of Non-specific Apposition

When evaluating apposition between cells or between synaptic proteins, an important aspect of the analyses is to assess the amount of apposition that occurs just by chance in the tissue, or in other words, the amount of apposition that the two signals have just by virtue of coexisting in the same region of space. To do so, ObjectFinder can be used to either rotate one synaptic signal against the other synaptic protein, or to randomly shuffle the position of each detected synaptic protein in volume, and recalculate the apposition metric (i.e., pairwise colocalization amount between the two synaptic proteins).

- *Retaining the correlation structure within a single set of synaptic puncta:*

  Rotation of one set of puncta vs a binary mask (Fig. 6a–d):

  1. Load ObjectFinder.
  2. Open project containing the two sets of objects to test.
  3. Go to "Colocalize" tab.
  4. Select from the list of objects the objects to colocalize (Fig. 6b, top list).
  5. Select from the list of images the binary mask (Fig. 6b, middle list).
  6. Click "Binary Mask" (Fig. 6b).
  7. Choose the rotation amount (90° clockwise, 90° counterclockwise, 180°, Fig. 6c).
  8. Select the reference set of objects to review completed analyses (Fig. 6d).
  9. Save or plot colocalization analysis results (Fig. 6d, buttons at the bottom).

- *Losing the correlation structure within a single set of synaptic puncta:*

  Scrambling positions of puncta vs a binary mask (Fig. 6e–g):

  1. Load ObjectFinder.
  2. Open project containing the objects to test.
  3. Go to "Simulate" tab.
  4. Choose "Number of Iterations" that will scramble puncta (Fig. 6e).
  5. Choose "Overlap" as parameter to test after scrambling (Fig. 6e).
  6. Click "Mask" and select the binary mask from the list of images (Fig. 6e).
  7. Click "Simulate" to scramble puncta within the current set (Fig. 6f).

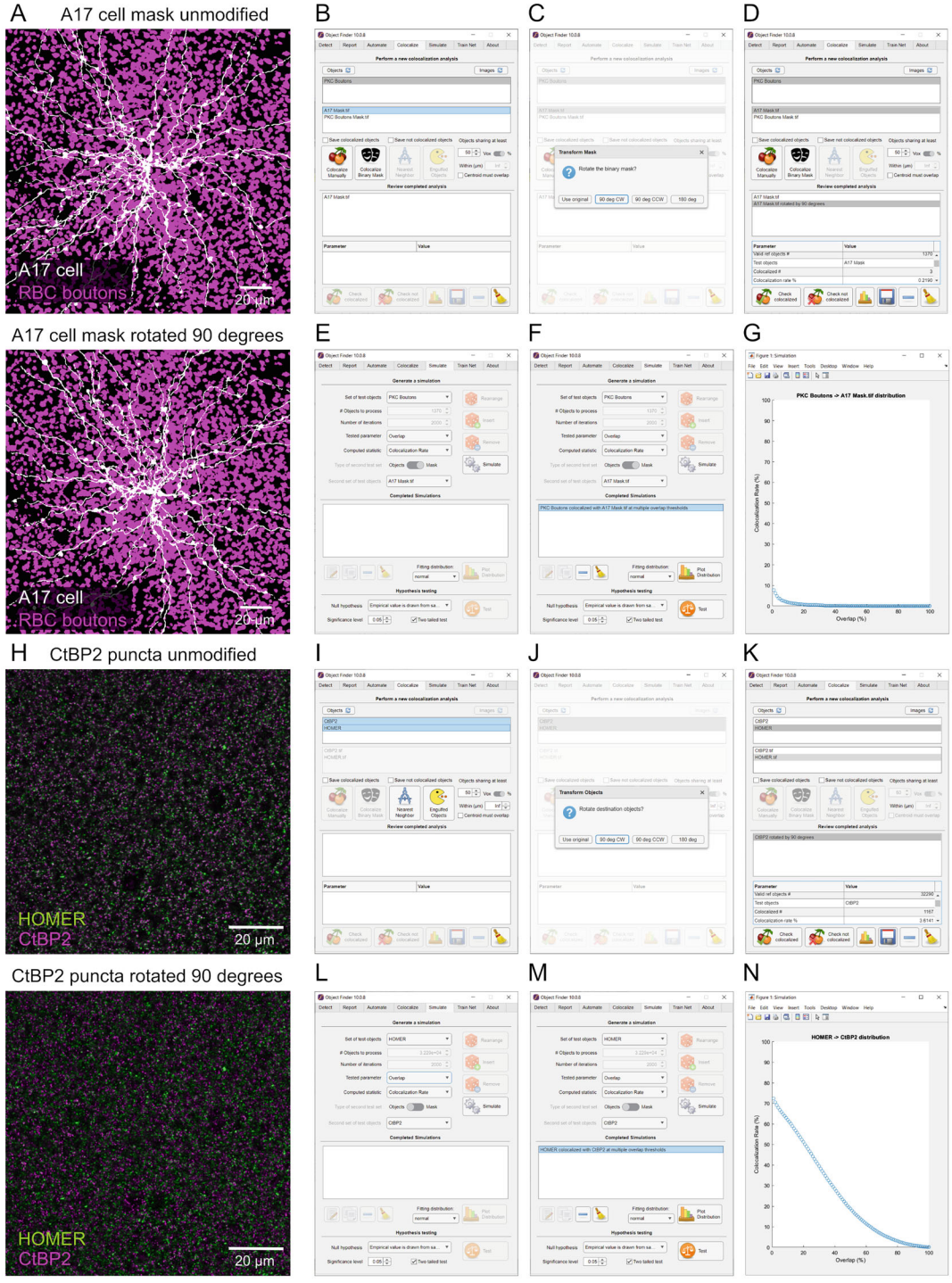

Fig. 6 Quantification of nonspecific apposition. (**a**) A17 amacrine cell mask (white) overlapping with RBC boutons (magenta) with the A17 cell channel either unmodified (top panel) or rotated 90° clockwise (bottom panel) to assess non-specific apposition with RBC boutons. (**b**) User interface for colocalization analyses. (**c**) User-selected rotation of the colocalizing mask. (**d**) Results of the colocalization analyses with rotated A17 cell

8. Review the completed simulation and test for statistical significance of the empirical distribution versus the simulated one (Fig. 6g).

- *Retaining the correlation structure within the two sets of synaptic puncta:*

  Rotation of one set of puncta vs the other puncta set (Fig. 6h):

  1. Load ObjectFinder.
  2. Open project containing the two sets of objects to test.
  3. Go to "Colocalize" tab.
  4. Select holding "Ctrl" the reference and test set of objects (Fig. 6i).
  5. Click "Nearest Neighbor" (Fig. 6i).
  6. Choose the rotation amount (no rotation, 90° clockwise, 90° counterclockwise, 180°, Fig. 6j).
  7. Select the reference set of objects to review completed analyses (Fig. 6k).
  8. Save or plot colocalization analysis results (Fig. 6k, buttons at the bottom).

- *Losing the correlation structure within the two sets of synaptic puncta:*

  Scrambling positions of puncta (Fig. 6l–n)

  1. Load ObjectFinder.
  2. Open project containing the objects to test.
  3. Go to "Simulate" tab (Fig. 6l).
  4. Choose "Number of Iterations" that will scramble puncta (Fig. 6l).
  5. Choose "Overlap" as parameter to test after scrambling (Fig. 6l).
  6. Choose the test set of colocalizing puncta (Fig. 6l).

Fig. 6 (continued) mask. (**e**) User interface for the simulation of random rearrangements of RBC boutons. (**f**) Results of the overlap with simulated randomized RBC boutons. (**g**) Plot of colocalization rate as a function of overlap threshold. (**h**) Retinal whole mount tissue immunolabeled for the postsynaptic marker Homer (green) and the presynaptic ribbon marker CtBP2 (magenta) with the CtBP2 channel either unmodified (top panel) or rotated 90° clockwise (bottom panel) to assess non-specific apposition between the two signals. (**i**) User interface for colocalization analyses. (**j**) User-selected rotation of the colocalizing mask. (**k**) Results of the colocalization analyses with rotated CtBP2 puncta. (**l**) User interface for the simulation of random rearrangement of Homer and CtBP2 puncta. (**m**) Results of the simulation of overlap with randomized CtBP2 puncta. (**n**) Plot of colocalization rate as a function of overlap threshold

7. Click "Simulate" to scramble puncta within the current set (Fig. 6m).
8. Review the completed simulation and test for statistical significance between the empirical distribution versus the simulated one (Fig. 6n).

3.2 Estimation of Synaptic Density

3.2.1 Puncta Detection Using ObjectFinder

This section provides an advanced guide to set the optimal parameters for synaptic detection using ObjectFinder. At the bottom of the "Detect" tab, users can specify the detection parameters for the algorithm:

1. Input the objects' diameter range using "Expected size of Objects".

   Input the minimum and maximum allowed object diameter values within the image volume. This parameter is critical for the algorithm to perform accurately and with maximum detection speed. The included calculator will help to determine the best settings for the objects you are expecting to detect.
2. Choose the appropriate "detection algorithm" (default is "Iterative thresholding").

   This parameter specifies the type of algorithm that ObjectFinder will use to detect candidate objects. "Iterative thresholding" is the most accurate algorithm used by default, whereas "Local thresholding" is a less accurate but faster algorithm. The latter is recommended to use only when one is expecting to detect object amounts in the order of billions or trillions.
3. Specify the number of "voxel connectivity" directions (default is 6).

   This parameter defines the number of directions in which ObjectFinder should look for connected voxels within the three-dimensional space. Available options are: 6 (ObjectFinder default, requires the two voxels to share a common face), 18 (voxels need to share a common face or edge to be considered connected), or 26 (ImageJ/Fiji default, voxels need to share either a common face, edge or corner to be considered connected).
4. Choose whether to apply "watershed segmentation" (default is enabled).

   This option is an additional step that splits candidate objects with multiple intensity peaks as individual objects using watershed segmentation. Doing so is useful if some of the synaptic proteins are apart from each other at distances close to the resolution limit of the imaging system.
5. Choose whether to "block search" (default is enabled).

   This function searches the entire volume by splitting it into smaller sub-volumes. When this option is selected, the local

background is computed, as opposed to calculating a global background level for the entire image volume when this option is unselected.

6. Choose the best method to estimate "background level". Defines which metric will be used to estimate the amount of background in the image volume.

   The available options (*see* **Note 4** for a detailed discussion) are: *Most common intensity*: Default option useful for most images, where the synaptic signal occupies less than half of the entire image volume. *Minimum Intensity*: Useful for very high signal-to-noise images such as binary masks or in situ hybridization experiments. *Standard Deviation*: Useful for images in which the synaptic signal occupies most of the image volume.

7. Set a "minimum object intensity" threshold (default is 1).

   This parameter specifies the number of times above background level from which the dimmest candidate objects can be detected.

8. Choose whether to estimate "shape properties" (default is disabled).

   Calculates shape properties of objects such as oblongness and major axis length.

9. Choose whether to remove objects present "on a single Z plane" (default is enabled).

   When enabled, this selection will remove all candidate objects that are spanning only across a single Z plane. A general rule of image acquisition is to oversample each object, i.e., acquire with a z-step size fine enough such that each synaptic punctum is represented by at least two or three optical panels. This option allows the user to remove noise events occurring on an individual z-plane.

10. Choose whether to remove objects "touching the edge" of the mask (default is disabled).

    When enabled, this selection will remove all candidate objects that are touching the edge of the mask used to limit the search volume.

11. Choose whether to remove objects with "unstable centroids" (default is disabled).

    When enabled, this selection will remove objects if their center of mass is not stable along Z. This option is useful for immunolabeling images in which there are significant amounts of sediments from the antibodies.

3.2.2 Reporting Synaptic Density Statistics Using ObjectFinder

Once synaptic proteins have been identified in the volume, several statistics can be reported to describe the image and compare populations such as treatment versus control conditions. The group of quantified synapses can be described by their density in space (e.g.,

average synaptic density) as well as their density along a dimension of interest, such as along the depth of the imaged sample (e.g., synaptic density in different synaptic layers) or along the path of the neurite of a cell of interest (e.g., density of glutamatergic input synapses on the dendritic arbor).

In ObjectFinder follow these steps to generate reports, which will all be saved in the "Results" folder:

1. Select the objects to generate reports from the "Detect" tab.
2. Click on the "Report" tab.
3. Click "Save report" (floppy disk icon) to store all general statistics shown. This will store general statistics of the objects displayed in a comma-separated-value file within the "Results" folder of the current project. In addition, the following specific plots can be generated for the set of objects.
4. Click the "Binary mask" button or the "Colored mask" to generate mask of the volume marking the voxels belonging to detected objects. In a binary mask, voxels belonging to detected objects are all marked in white. In a colored mask, voxels belonging to detected objects are marked with different colors, each object has a different color than its neighbors.
5. Click "Density By Depth" button to plot the density of objects as a function of Z depth in the volume (Fig. 7a).
6. Click "Density Along Skel" to plot the linear density of objects along the path of a skeleton (Fig. 7b).
7. Click "Density Heatmap" to plot linear density of objects in the form of a 2D heatmap (Fig. 7c).
8. Click "Sholl analysis" to plot the complexity profile of the dendritic arbor following the standard Sholl analyses procedure [11]—number of dendritic intersections within concentric circles spaced at defined distances from the center of the cell body (Fig. 7d).
9. Click "Volume distribution" to plot the distribution of volumes for all detected objects (Fig. 8a).
10. Click "Brightness distribution" to plot the distribution of average brightness for all detected objects (Fig. 8b).
11. Click "Sphericity distribution" to plot the distribution of oblongness, ranging from 1 (perfect sphere) to 0 (line), for all detected objects. Oblongness is calculated by comparing the lengths of the three major axes (Fig. 8c).
12. Click "Major axis distribution" to plot the distribution of major axis length for all detected objects, the objects' major axis is calculated by fitting an ellipsoid to each object (Fig. 8d).

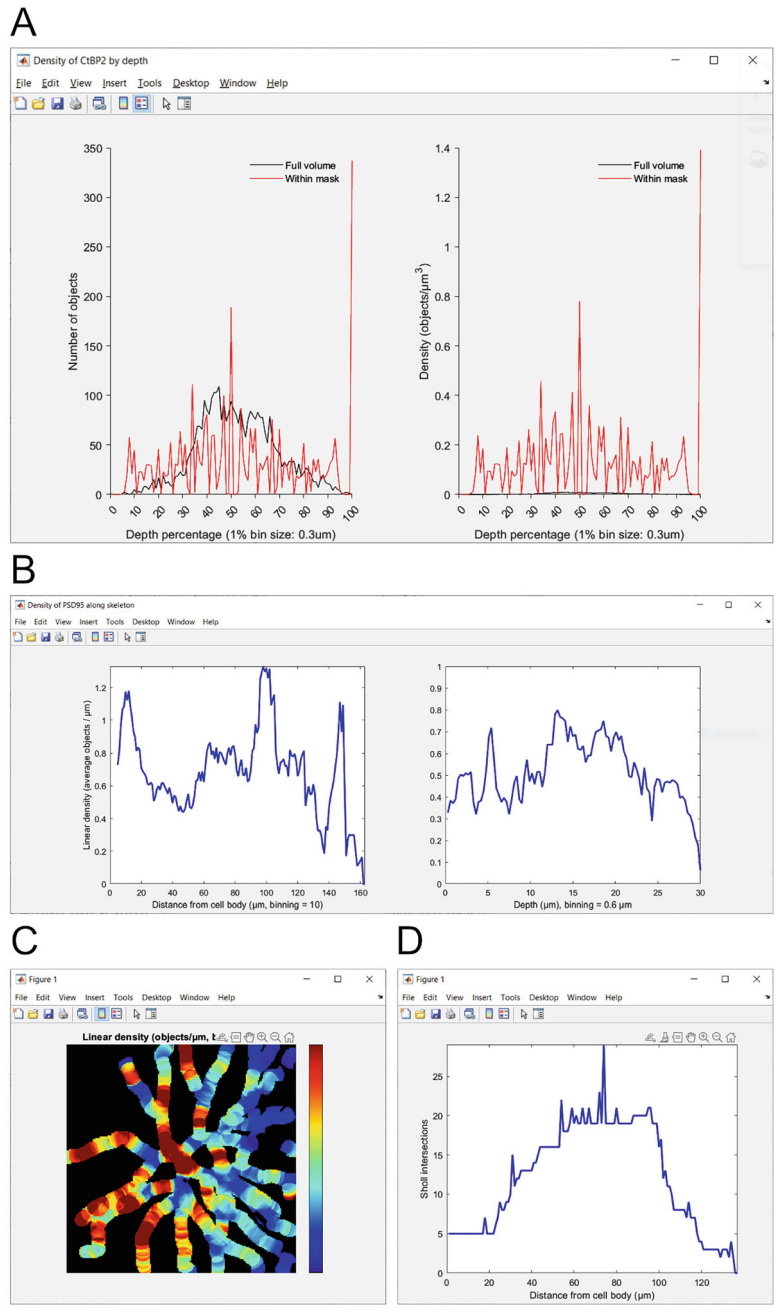

Fig. 7 Plotting aspects of synaptic density. (**a**) Plotting of synaptic density as a function of depth in the image volume (z-axis). The density of the detected synaptic protein is plotted against the depth of the whole image volume (black trace) or within the boundaries of an apposing binary mask (red trace showing CtBP2 apposed to a co-labeled retinal ganglion cell). (**b**) The density of the synaptic protein (PSD95) within a cell of interest is plotted along the path of the skeletonized dendrites of the neuron and linear density expressed as a function

4 Notes

This section covers common troubleshooting and optimizations associated with image preparation and object detection.

1. Median Filtering: In most microscopy images, a common source of noise is associated with the detector, e.g. the thermal noise of a photomultiplier tube for a classic confocal microscope system. The nature of this noise is random and therefore applying a simple digital median filter as a pre-processing step is usually sufficient to greatly reduce this type of noise. Caution needs to be taken in order to not create artifacts when applying median filters, in particular:
   - Avoid using a large kernel size, which would also reduce the signal in your image. A simple 3 × 3 kernel size is preferable as that will efficiently remove "salt and pepper" thermal noise while preserving the signal in your image.
   - Avoid using 3D median filtering, as most of the images are constructed by a stack of XY images, median filtering along the Z axis can thus create artifactual puncta.

     To apply a median filter to an image stack using Fiji:

   – Open your image stack.
   – Select "Process" from the menu followed by "Filters" and then "Median".
   – Specify 1 as pixel radius, this will result in a 3 × 3 median kernel.
   – Select "yes" when asked whether to process all images present in the stack.
2. Voxel size calibration: A critical step to ensure all calculations are to scale is to calibrate the voxel size in all image analysis programs used to prepare or analyze the image stacks. This is usually read automatically from the metadata associated with the raw image file, but it is good practice to double check and manually specify the correct voxel size in case it is missing. This is done at time of loading the image stack:

Fig. 7 (continued) of distance from the cell body (left panel) or depth within the volume (right panel). (**c**) Synaptic density heat-map of PSD95 within the labeled neuron, obtained by convolving the regional PSD95 density with a 5μm disk moving along the skeleton of the neuron of interest. (**d**) Sholl analyses of the dendritic skeleton used to represent synaptic protein density

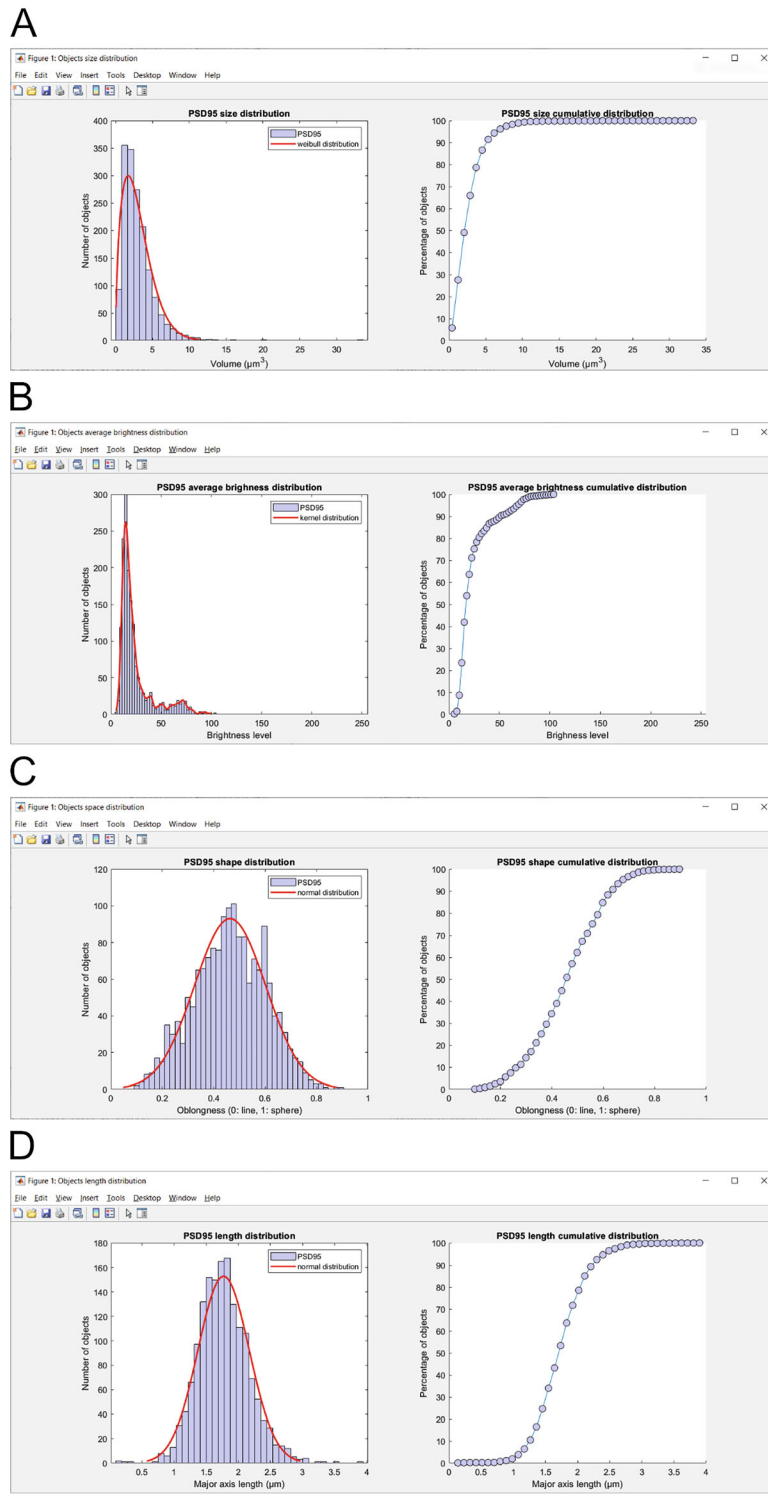

Fig. 8 Plotting distribution of synaptic properties. (**a**) Plotting of the distribution of PSD95 size histogram and cumulative distribution, together with best fit from Weibull distribution (red trace). (**b**) Plotting of the distribution of PSD95 puncta

- In Fiji, open the image stack and go to the "Image" menu then navigate to "Image properties" to define the voxel calibration.
- In Amira, when opening an image stack with the "open data" button, you will be asked in the "Image Read Parameters" window to specify the voxel size.
- In ObjectFinder, the voxel size will be automatically read from the TIF image file metadata. The user can check the current value using the "Image properties" button (blue info icon) next to the current image in the "Detect" section. If the voxel size is incorrect or missing, Fiji can be used to manually specify the correct value as described above).

3. Manual thresholding in Amira: Amira allows users to define manual thresholds to mask cellular processes which can be done specifically for each plane belonging to an image stack. This can be done through the "Label Field" option as discussed in 3.1.1. This feature can be very useful in case the automatic algorithm does not faithfully recognize the borders of the region of interest. Care should be taken to ensure that this technique of generating masks is stringent and strictly includes the signal representing the cell or process of interest. Selecting a lower threshold can lead to the inclusion of empty/dark pixels bordering the structure of interest and such diffuse masks will lead to erroneous over-estimations of connectivity when combined with downstream detection routines.

   The same process can be carried out to mask for a synaptic channel of interest. When a simple intensity threshold needs to be applied to isolate the signal of interest one can select the channel of interest and opt for the multi thresholding or "labelvoxel" option. This allows the user to define a specific intensity value that can serve as a threshold. The labels thus created will incorporate all signals above this threshold.

4. Signal-to-noise estimation for synaptic density quantification: Quantification of synapses in a noisy image, such as created by microscopy techniques, requires the signal-to-noise ratio to be sufficiently high to have an accurate estimation of the region occupied by each fluorescent synaptic protein against the image background. A critical step is the identification of noise in the image and quantification of noise levels across the 3D volume.

Fig. 8 (continued) brightness, defined as average brightness of the voxels belonging to each punctum. (**c**) Distribution of PSD95 roundness, ranging from 1 (perfect sphere) to 0 (perfect line). (**d**) Distribution of major axis lengths for all PSD95 puncta. All distributions can be fitted against standard statistical distributions (e.g., Normal, Poisson, Weibull, and more)

The two main components of noise arise from the method used to label the synapse and the method used to image the sample:

- Synaptic proteins can be labeled by fusing the protein of interest with a fluorescent protein (e.g., Biolistic transfection, viral transfection, or transgenic line). In this case, the noise levels are usually very low as the fluorescent protein is only produced within the cells expressing the transfected proteins. In such a situation, most of the background noise is due to autofluorescence of the tissue. Noise in these images can also be due to the fluorescent protein being trafficked to the synaptic site, thus producing a background fluorescence in the cytosol of the cell of interest lower in intensity from the signal at the synaptic locations, where the protein of interest is accumulated after trafficking is complete.
- Immunolabeling against synaptic proteins usually carries the highest amount of noise due to nonspecific binding of either primary or secondary antibodies with structures other than the protein of interest in the tissue. A characteristic of this noise is that it is structured and highly variable in different regions of the tissue sample. In addition, penetration of antibodies in the tissue is imperfect in nature, with lesser penetration and labeling amount as a function of tissue depth. These two components lead to variable signal-to-noise ratio across the image volume.
- Imaging synaptic proteins by microscopy techniques such as confocal microscopy and multi-photon microscopy introduces an additional noise component to the image due to thermal noise produced by the microscope detector. This type of noise, despite being very variable in amount due to the intrinsic noise of the detector and the chosen gain, is stochastic in nature and can be effectively minimized by averaging pixels during acquisition, or post-processing the acquired image with a median filter.

Given the different sources of noise that can be present in the image stack being analyzed, two main methods to quantify background noise levels can be used:

- Global estimation of background level. The entire image is assessed to determine either the lowest or the most common intensity value present in the image stack.
- Local estimation of background level. The image is divided into smaller sub-stacks and the local background level (absolute lowest level or most common value) computed for each sub-stack. This approach enables estimation of different background levels for parts of the image in which the labeling can have different amounts of noise.

Once the user has established whether to estimate noise globally versus locally in the image, the user will need to determine whether the most meaningful representation of background noise level is the lowest intensity, or the most common intensity found in the region of interest. The former is useful to quantify objects in binary masks, where noise level is zero, or in images where any non-zero level of intensity is meaningful, such as in RNAscope in situ hybridization [12] or quantum count of fluorescence. The latter is useful in most of the quantification of fluorescently labeled synaptic proteins, because the signal of interest, synaptic proteins, occupy a small fraction of the entire volume in the image stack, whereas the majority of the remaining voxel intensities are due to background.

Acknowledgments

This work was supported by NIH-NEI (EY007551 to UH Optometry Vison Core), NVIDIA corporation (L.D.S.), Glaucoma Research Foundation (L.D.S.), All May See Foundation (L.D.S.), by the McPherson Eye Research Institute's Rebecca Meyer Brown/Retina Research Foundation Professorship (to M.H.), and an unrestricted grant from the Research to Prevent Blindness, Inc. to UW Madison Department of Ophthalmology and Visual Sciences.

References

1. Hoon M, Sinha R, Okawa H (2017) Using fluorescent markers to estimate synaptic connectivity in situ. Methods Mol Biol 1538:293–320. https://doi.org/10.1007/978-1-4939-6688-2_20
2. Sinha R et al (2021) Transient expression of a GABA receptor subunit during early development is critical for inhibitory synapse maturation and function. Curr Biol 31(19): 4314–4326 e4315. https://doi.org/10.1016/j.cub.2021.07.059
3. Grimes WN et al (2014) Cross-synaptic synchrony and transmission of signal and noise across the mouse retina. elife 3:e03892. https://doi.org/10.7554/eLife.03892
4. Santina LD, Ou Y (2018) Biolistic labeling of retinal ganglion cells. Methods Mol Biol 1695: 161–170. https://doi.org/10.1007/978-1-4939-7407-8_14
5. Bleckert A et al (2013) Spatial relationships between GABAergic and glutamatergic synapses on the dendrites of distinct types of mouse retinal ganglion cells across development. PLoS One 8(7):e69612. https://doi.org/10.1371/journal.pone.0069612
6. Morgan JL, Schubert T, Wong RO (2008) Developmental patterning of glutamatergic synapses onto retinal ganglion cells. Neural Dev 3:8. https://doi.org/10.1186/1749-8104-3-8
7. Goffin D et al (2010) Dopamine-dependent tuning of striatal inhibitory synaptogenesis. J Neurosci 30(8):2935–2950. https://doi.org/10.1523/JNEUROSCI.4411-09.2010
8. Della Santina L et al (2021) Disassembly and rewiring of a mature converging excitatory circuit following injury. Cell Rep 36(5):109463. https://doi.org/10.1016/j.celrep.2021.109463
9. Okawa H et al (2019) Dynamic assembly of ribbon synapses and circuit maintenance in a vertebrate sensory system. Nat Commun 10(1):2167. https://doi.org/10.1038/s41467-019-10123-1

10. Wang YL (2007) Computational restoration of fluorescence images: noise reduction, deconvolution, and pattern recognition. Methods Cell Biol 81:435–445. https://doi.org/10.1016/S0091-679X(06)81020-4
11. Sholl DA (1953) Dendritic organization in the neurons of the visual and motor cortices of the cat. J Anat 87(4):387–406
12. Kiyama T, Mao CA (2020) Ultrasensitive RNAscope in situ hybridization system on embryonic and adult mouse retinas. Methods Mol Biol 2092:147–158. https://doi.org/10.1007/978-1-0716-0175-4_11

Chapter 12

Monosynaptic Tracing in Developing Circuits Using Modified Rabies Virus

Laura Cocas and Gloria Fernandez

Abstract

An attenuated rabies virus that expresses fluorescent protein has made it possible to analyze retrograde (presynaptic) monosynaptic connections in vivo. Combining attenuated rabies virus with a Cre-loxP-based system to target cells in a subtype-specific fashion, it is possible to examine neuronal input in vivo onto any class of neuron, in development and in the mature brain. We describe here the methods to amplify deletion mutant, pseudotyped rabies virus, selectively target cells of interest using genetic and viral approaches, as well as the stereotaxic procedures required to target neuronal subtypes of interest in vivo.

Key words Monosynaptic circuit tracing, Rabies virus, Neuronal circuit development, Viral amplification, Stereotaxic surgery

1 Introduction

Work from Callaway, Wickersham, and colleagues has revealed that monosynaptic circuit tracing using deletion-mutant rabies virus and clever targeting of the viral proteins necessary for infection and spread is a powerful tool to analyze precise circuits in vivo [1–4]. The approach relies on the ability to target neuronal subtypes in live animals, typically through the use of two helper viruses to deliver the viral proteins necessary for infection and spread, along with a third deletion mutant rabies virus that when complemented with the helper viruses can move retrograde to presynaptic partner cells [1, 2, 4–6]. Due to the long timelines required for the helper viruses to function prior to trans-synaptic labeling, these approaches are not useful for tracing early circuits in developmental studies. Further, low levels of fluorescent protein expression from helper virus can make it difficult to identify initially infected versus connected cells (unpublished observations and [7]).

We sought a method that would allow analysis throughout life, and that would be fast enough to allow short time windows for

Tolga Soykan and Alexandros Poulopoulos (eds.), *Synapse Development: Methods and Protocols*, Methods in Molecular Biology, vol. 2910, https://doi.org/10.1007/978-1-0716-4446-1_12,

analyses of developing circuits. After using one of the approaches below to target specific cells with G and TVA, as well as a fluorescent label, these mice are then injected with deletion mutant avian envelope protein pseudotyped rabies virus. Using any of these approaches, only the cells of interest are infected, and their presynaptic partner cells are retrogradely labeled, resulting in monosynaptic labeling of presynaptic cells and their postsynaptic partners. We describe here our current process to monosynaptically label neuronal circuits with rabies virus, including the amplification, pseudotyping, and ultracentrifugation of the virus, and the stereotaxic injection of both AAV and RabV virus. Amplification and pseudotyping of deletion mutant virus has been discussed in an excellent methods paper in detail; our methods here outline our modifications on the original approach[4]. General stereotaxic surgery has been extensively described previously. Here we outline our approach, modifying an existing protocol for stereotaxic injection of lentivirus[8]. We also discuss the main strategies for targeting viral proteins to cells of interest, using one of three approaches to express G and TVA in a cell subtype-specific fashion: (1) Cre/LoxP dependent cell targeting with transgenics, (2) Cre/tTA-dependent targeting with transgenics, or (3) helper virus-dependent Cre/-LoxP viral targeting.

2 Materials

2.1 Viral Amplification

1. Supplemented DMEM: Dulbecco's modified Eagle's medium high glucose, 10% heat-inactivated FBS, 1% glutamax, 1% penicillin/streptomycin.
2. 10 cm tissue culture plate.
3. Syringe Filters, 0.2 μm pore size.
4. 250 mL Stericup, 0.45 μm pore size.
5. 15 cm tissue culture plate.
6. Sucrose Solution: 20% sucrose in PBS. Filter-sterilize with 0.2 μm filter before use or storage. After filter sterilization, the solution can be stored at 4 °C indefinitely.
7. PBS (sterile).
8. Starting stock of RabV virus (available through Salk Viral Vector Core).
9. 3T3 cells.
10. BHK-19G cells [4].
11. BHK-EnvA cells [4].
12. 293T-TVA-800 cells (can be requested from Dr. John Young, jyoung@salk.edu).

13. Low temp/low CO_2 incubator: Standard cell culture incubator set to 35 °C and 3% CO_2.
14. Ultracentrifuge.
15. Swing rotor and buckets (e.g., Beckman SW28).
16. Polyallomer centrifuge tubes (e.g., Beckman, cat. no. 326823).

2.2 Delivery of G and TVA in a Cell-Type-Specific Manner

1. pAAV-synP-FLEX-splitTVA-EGFP-B19G (Addgene, plasmid #52473).
2. pTRE-Bi-G-TVA mice [9].
3. ROSA-tTA mice (Jackson, strain name; B6.Cg-*Gt(ROSA)26Sortm1(rtTA,EGFP)Nagy/*J).
4. ROSA-Ai14 mice (Jackson, strain name: B6;129S6-*Gt(ROSA)26Sortm14(CAG-tdTomato)Hze/*J).
5. ROSA-TVA-G mice (Jackson B6;129P2-*Gt(ROSA)26Sortm1(CAG RABVgp4,-TVA)Arenk/*J).

2.3 Stereotaxic Surgery Reagents

1. Stainless steel, 33 G hypodermic tubing (type 304), pre-cut to 34 mm.
2. Stainless steel, 26 G hypodermic tubing (type 304), pre-cut to 27 mm.
3. Polyethylene tubing, PE-20, 0.015″ (inner diameter) °ø 0.043″ (outer diameter).
4. Quick Setting Epoxy (Super Glue).
5. Stereotaxic alignment system base with mouse adaptor.
6. Alignment indicator.
7. Micro-manipulator with three axis, 1 μm resolution and digital display readout.
8. Centering microscope with 20× magnification.
9. Stereotaxic drill unit.
10. Dual cannula insertion tool (e.g., David Kopf, Model 1973).
11. Infusion pump (e.g., PHD 22/2000, Harvard Apparatus, Holliston, MA).
12. 70% Ethanol.
13. Sterile water.
14. Hair trimmer.
15. Electric heating pad.
16. Drill bit for stereotaxic drill, #85, 0.011″ diameter.
17. Tuberculin syringes with 26 G needle.
18. Betadine solution: 10% Povidone-iodine Topical Solution.
19. Bupivacaine: 0.25% Bupivacaine HCl (Sensocardine-MPF).

20. Isoflurane inhalation system: Isoflurane, isoflurane vaporizer, supply gas oxygen, supply gas regulator, flowmeter, induction chamber, tubing and valves, facemask and charcoal filter.
21. Veterinary ophthalmic ointment.
22. Cyanoacrylate tissue glue (e.g., Vetbond tissue adhesive, Henry Schein).
23. Cotton Tip applicators, 6″.
24. Hamilton gastight syringe, 10 μL; N; Gauge: 26 s; 2 in. (51 mm); Point style: 3 (e.g. Hamilton Model 80075).
25. Stainless steel utility scissors.
26. Adson forceps, straight, 12 cm.
27. Non-dissolvable sutures.

3 Methods

3.1 Production of Unpseudotyped Glycoprotein-Deficient Rabies Virus

1. Virus can be amplified by recovering from DNA, or amplifying from existing stocks, using either supernatant or ultracentrifuged stock. We will discuss here only the modifications of the amplification approach. For full details on the original methods, see [4] and updated methods [10].

3.1.1 Rabies Virus Amplification

1. Thaw BHK-19G cells and plate into Supplemented DMEM in 1 10 cm dish.
2. After cells have reached confluency (1–3 days later), split BHK-19G cells into 2 10 cm dishes so that cells will reach a confluency of 60% the following day.
3. In a Biosafety Level 2 (BSL-2) hood, infect cells with desired starting stock of RabV virus (RabV-GFP, RabV-mCherry, etc., initial aliquot stocks are usually 1–2 mL) (*see* **Note 1**). Pipette virus onto one 10 cm dish, and add Supplemented DMEM to a total volume of 8.5 mL. Once virus has been applied, return plate to low temp/low CO_2 incubator (set to 35 °C/3% CO_2). (Use the second 10 cm dish to amplify additional BHK-19G cells for subsequent steps.)
4. 5–6 h later, remove the virus and replace with 10 mL of Supplemented DMEM, and return to low temp/low CO_2 incubator.
5. Monitor infected neurons daily for confluence and fluorescence. When 90% of cells are fluorescent, the virus is ready to be passaged to new cells. If cells have not reached 90% fluorescence by day 5–6, but are confluent and becoming pyknotic or floating in the dish in large numbers, passage the virus rather than waiting for 90% infection.

6. Filter the viral supernatant and add the entire supplement to one new 15 cm dish with BHK-19G cells at 60% confluency.
7. Remove the viral supernatant 5–6 h later, replace with 20 mL fresh Supplemented DMEM.
8. Wait 5–6 days, until cells have reached 90% fluorescence or have become too confluent to continue to grow, as above.
9. When virus is ready, filter, and place 5 mL of viral supernatant and 13 mL of media onto new dishes, for a total of four 15 cm dishes producing virus.
10. Monitor infected neurons daily for confluence and fluorescence; when 90% of cells are fluorescent (or cells are overconfluent but not yet at 90% infection), remove supernatant, filter, and place 5 mL of viral supernatant onto 8 new dishes.
11. Extra filtered supernatant can be aliquoted and frozen in 5 mL cryotubes and stored at −80 °C.
12. 5–6 days later, when virus is ready, pool and filter supernatant from all 8 dishes for ultracentrifugation.

3.1.2 Virus Particle Concentration

1. To ultracentrifuge virus, insert plastic tubes into buckets for swinging rotor in a BSL-2 safety hood.
2. Place 25 mL of filtered supernatant into each of the 6 tubes. Gently add 5 mL of Sucrose Solution to the bottom of each tube containing supernatant.
3. Close and weigh buckets, weighing each pair of buckets and adjusting the volumes until each pair are balanced.
4. Decontaminate buckets before removing from hood.
5. Spin in an ultracentrifuge at 50,000 g for 2 h at 4 °C. If using a Beckman SW28 rotor, 20,000 RPM is the equivalent speed.
6. After centrifugation, in a BSL-2 hood, aspirate supernatant and pipette 100 μL sterile PBS onto pellet inside the plastic tube insert. Recap buckets, decontaminate, and place buckets on a shaker overnight at 1 HZ at 4 °C.
7. The following day, pool the virus from all 6 buckets, briefly vortex, briefly spin down in a tabletop centrifuge, and aliquot into 50 μL aliquots. Decontaminate tubes and store at −80 °C. Save 10 μL for titering virus.
8. Titer virus on 3T3 cells. Titer can be measured using flow cytometry or manual quantification, see [4] for discussion of differing titer techniques.

3.2 Production of EnvA-Pseudotyped Glycoprotein-Deficient Rabies Virus

1. Thaw BHK-EnvA cells and plate in a 10 cm dish.
2. When cells are 80% confluent, split cells and replate into three 15 cm dishes.

3. When two BHK-EnvA dishes have reached 80% confluency, combine cells from two dishes into 15 mL of medium, and replate 1ml of cells into each of 15 new 15 cm dishes with 20 mL of medium. (The goal is to have EnvA cells with 60% confluency within 24 h; this can generally be done by splitting one 15 cm plate 1:6).
4. Using the titer calculated on 3T3 cells above, infect 15 plates containing BHK-EnvA cells with the ultracentrifuged glycoprotein-deleted virus at a Multiplicity of Infection ratio (MOI) of 2.
5. Add 20 mL medium and store in the low temp/low CO_2 incubator.
6. The following day, aspirate the supernatant and wash cells 3× with 12 mL PBS. Carefully wash both bottom and sides of each dish, being careful not to disturb cells and adding the PBS and aspirating from the same area of the dish to minimize disturbing the cells (*see* **Note 3**).
7. Add 12 mL of fresh Supplemented DMEM. Monitor cells for fluorescence.
8. Two days after infection, aspirate the supernatant (the first supernatant is contaminated with parent unpseudotyped virus) and replace with 12.5 mL of fresh Supplemented DMEM. Cells should begin expressing fluorescence.
9. Three days after infection, the majority of EnvA cells should be expressing the viral fluorophore of interest. Pool supernatant from all 15 plates, filter, and pipette into rotor buckets as above.
10. Add 5 mL Sucrose Solution as above, and spin in an ultracentrifuge at 50,000 g for 2 h at 4 °C.
11. After centrifugation, in a BSL-2 hood, aspirate supernatant and pipette 100 μL sterile PBS onto pellet inside plastic tube insert. Recap buckets, decontaminate, and place buckets on a shaker overnight at 1 HZ at 4 °C.
12. The following day, pool the virus from all 6 buckets, briefly vortex, briefly spin down in a tabletop centrifuge, and aliquot into 10 or 20 μL aliquots (*see* **Note 4**).
13. Decontaminate tubes and store at −80 °C. Save 10 μL for titering virus.
14. Titer virus on TVA-800 cells and control 3T3 cells; EnvA pseudotyped virus should not infect 3T3 cells. Titer can be measured using flow cytometry or manual quantification, see [4] for discussion of differing titer techniques. Titers achieved using this approach range drastically between unpseudotyped and pseudotyped virus, from 2.9×10^5 to 1.6×10^{10}, see

[11]. If viral titer is low, or virus is contaminated with parent stock (3T3 cells are infected during titering) the pseudotyping process will have to be completed again, beginning at **step 4** (*see* **Note 5**).

3.3 Approaches to Target Cells of Interest with GRab and TVA Proteins Necessary for Monosynaptic Infection and Spread of Rabies Virus

We utilize one of three different approaches to selectively target cells of interest, depending upon the timing and the experimental design; each approach is outlined here.

Approach 1: We combine a cell-type-specific Cre driver mouse with a ROSA-G-TVA reporter mouse containing a floxed bicistronic construct coding for the avian envelope protein receptor (TVA) and the rabies glycoprotein (GRab), as well as a fluorescent reporter (e.g., ROSA-YFP) [12, 13]. This is especially useful for studying large populations of neurons, and is used for developmental studies, as helper virus use necessitates a 2-week delay in analysis.

Approach 2: We combine a cell-type-specific Cre line with a tetracycline-dependent mouse that expresses TVA and GRab (pTRE-Bi-G-TVA), requiring a tetracycline transactivator (ROSA-tTA) mouse and a fluorescent (e.g.) ROSA-YFP reporter mouse [9, 12, 14]. The tetracycline allows doxycycline-regulated control of GRab and TVA, and is useful for developmental studies, as AAV expression is too slow for short developmental time points.

Approach 3: We inject an AAV helper virus expressing GRab, TVA, and GFP. This virus contains the Addgene construct made by Ian Wickersham, pAAV-synP-FLEX-EGFP-B19G (Plasmid #59333). We use AAV produced by the UNC Vector Core; we use AAV serotype 8. The AAV must be injected at least 2 weeks prior to rabies virus injection [7] (*see* Fig. 1). This approach is very useful when labeling small numbers of neurons in adult brain, but requires careful targeting by re-injecting the same region with AAV and RabV at least 2 weeks apart (*see* **Note 2**).

3.4 Viral Injection Procedures

For viral tracing experiments, P12 and older Cre mice can be used on the stereotaxis frame. Younger animals require a custom-modified frame insert, available from Kopf. Viral proteins necessary for infection and spread (glycoprotein and TVA, the avian envelope protein receptor) can be delivered with any of the methods outlined above. Cre helper virus systems are discussed elsewhere [2, 15]. If using AAV virus, the AAV-Flex-G-TVA-GFP virus must be delivered at least 2 weeks prior to injection with EnvA pseudotyped glycoprotein-deleted virus ultracentrifuged as above. If using transgenics, the expression of G and TVA will be driven by the cell or tissue-specific Cre promoter and will therefore be dependent upon

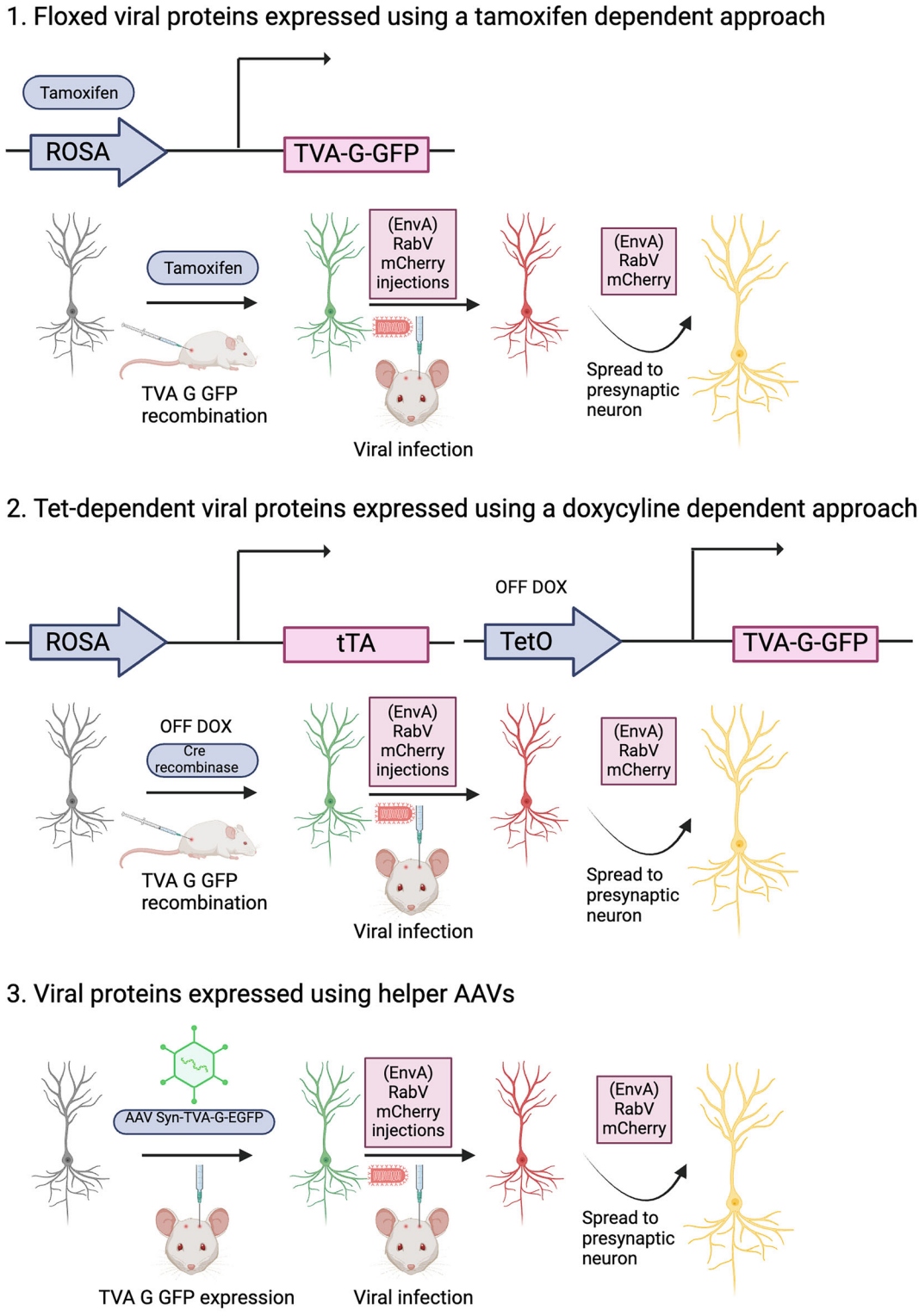

Fig. 1 Diagram illustrating three methods to target specific presynaptic connections in neurons in vivo use a modified deletion-mutation rabies virus. 1. Genetically regulated expression of TVA and G using a tissue-specific promoter-Cre mouse crossed to floxed ROSA-TVA-G and ROSA-GFP mice. Cre recombines and

the promoter of interest. If using AAV, volumes of 0.2–1 μL are appropriate, depending upon region-of-interest and the desired target size. Post injection, label bregma with black marker and vetbond to allow ease of targeting for surgery 2 weeks later. As the procedure is otherwise identical, stereotaxic surgery will be discussed for EnvA pseudotyped deletion mutant rabies virus that has been ultracentrifuged and titered above.

3.4.1 Injection Needle Preparation

1. Prepare injection needles at least 1 day prior to surgery. Briefly, lightly coat one 34 mm 33G stainless steel tube with epoxy, and then quickly insert the tube into one 27 mm 26G stainless steel tube, leaving approximately 5 mm of the 33G tube sticking out. The 33G contains a small thread inside; move back and forth briefly to keep the epoxy from clogging the needle but do not remove. Allow them to dry overnight.
2. The following day, use a ruler to bend 10 mm of the side opposite the 5 mL 33G overhang at a 90° angle, creating an L-shaped tube with a thin 5 mL overhang; this small overhang will be inserted directly into the brain.
3. Remove the thread and fit with a small piece of polyurethane tubing. Using a standard injection needle filled with water, inject water through the newly-made needle. If water is unable to flow, or if the needle leaks in between the two tubes, discard and replace the needle. If water flows through freely, it is ready for use.
4. Flush briefly with 70% ethanol and store in a 50 mL conical tube containing 70% ethanol; needles can be reused indefinitely.

Fig. 1 (continued) excises LoxP sites, allowing expression of GRab and TVA proteins postnatally. In these mice, cells of interest express the rabies glycoprotein GRab, and avian sarcoma virus leukosis receptor (ASLV) TVA proteins necessary for targeted infection and monosynaptic spread in a Cre-targeted subgroup of neurons. Viral infection via intracranial injection postnatally with SAD-ΔG-mCherry (EnvA) pseudotyped virus allows selective targeting in cells expressing both G and TVA proteins. MCherry-labeled virus spreads upstream to cells directly synaptically connected to virus-infected GRab- and TVA-expressing neurons of interest. 2. Doxycycline-dependent approach involves the use of tTA and TetO to regulate TVA-G-GFP expression. Off DOX state triggers Cre recombinase, making viral infection and spread to presynaptic neurons possible with EnvA-pseudotyped RabV mCherry virus. Genetically regulated expression of tTA (tissue-specific Cre; ROSA-tTA; ROSA-GFP) allows doxycycline-dependent control of GRab and TVA using the pTRE-Bi-G-TVA mouse line as well as a fluorescent reporter to label postsynaptic neurons. Infection and spread of SAD-ΔG-mCherry (EnvA) then labels presynaptically connected cell inputs. 3. Helper AAVs approach: Floxed, Cre-dependent GRab, TVA, and GFP are delivered with AAV-Flex helper virus. At least 2 weeks later, intracranial infection and spread of SAD-ΔG-mCherry (EnvA) labels postsynaptic cells and their presynaptic inputs

3.4.2 Stereotactic Injection

Virus should be handled according to institutional BSL-2 guidelines, and animal protocols followed for each institution's animal care and safety guidelines. The stereotaxis frame and surgery preparation and suturing area should be prepared for surgery. Tools should be sterilized prior to each injection, and the needle/injector prepared for injection.

1. Fit a gastight syringe with approximately 30 cm of polyethylene tubing. Attach the homemade needle from above to the opposite end of the polyethylene tubing.
2. Secure the needle into the dual cannula insertion tool by unscrewing the plastic cover and fitting the needle into the groove in the insertion tool. Replace the plastic cover and secure with the screw, making sure that the long side of the "L" of the needle containing the 33G 5 mL section is facing down; this is the side of the needle that will enter the brain.
3. Place the gastight syringe securely into the infusion pump, and remove the plunger.
4. Back fill the syringe with water using a 10 mL disposable tuberculin syringe. Ensure that the water flows continuously through the gastight syringe, polyethylene tubing, and needle and continue until there are no bubbles in the entire line; bubbles will prevent proper volume measurements during viral injection (*see* **Note 6**).
5. Replace the plunger, and gently pull the plunger until a 1 cm gap of air is present in the tubing next to the needle; this will ensure that when virus is added, it will not mix with the water in the tube.
6. The mouse should be anesthetized with isoflurane inhalation and the head shaved prior to surgery; the flow rate to initially anesthetize the mouse in the chamber should be between 3% and 5%; once the mouse is on the stereotaxic frame the flow rate is reduced to 1.5% (*see* **Note 7**).
7. Once unconscious, the mouse's tongue is gently placed to the side with blunt forceps and the bite bar inserted into the mouth; this will prevent gagging. The bite bar is secured into its holder on the stereotaxic frame, and the ear bars are placed inside each ear, and tightened until the head is secure. It is important to balance the ear bar distances between the left and right ears, and to ensure that the ear bars are placed anterior to the ear canals, just touching the zygomatic arch.
8. Once the mouse is secured onto the stereotaxic frame, the head can be prepared for surgery. Clean the skull with betadine and 100% ethanol, and then inject 100 μL Bupivacaine beneath the skin. Cover each eye with vet eye ointment.

9. Make an incision from the top of the skull near the nose to the base, just past lambda, and gently clean underneath the skin with a sterile cotton applicator.
10. Attach the microscope to the stereotaxic frame and determine the location of bregma and lambda.
11. Attach the alignment indicator to the frame. Gently lower the alignment indicator until it touches the skull and at least one of the two needles on the alignment indicator read zero. If both alignment needles do not reach zero, the X alignment is off, and will need to be adjusted. Loosen the screw on the M/L knob on the stereotaxic frame and adjust the tilt of the skull until both needles read 0. Then tighten the M/L knob, and raise the tool above the skull.
12. Loosen the knob on the alignment indicator, turning it 90° to determine the Z alignment. Lower the alignment indicator again until one of the alignment needles reach zero. If both needles are not at 0, loosen the screw on the A/P knob until the needles both read 0. Tighten the screw on the A/P knob and raise the alignment indicator above the skull.
13. Repeat the alignment of the X-axis as above; sometimes Z alignment will affect the original X alignment.
14. Once the X alignment is re-confirmed, remove the alignment indicator and replace with the microscope tool. Find bregma and set the digital manipulator to 0 in X and Y.
15. Remove the microscope, and replace with the drill tool, fitted with a 0.011″ diameter drill bit. Move the drill to the desired X and Y coordinates, which are visible on the digital manipulator.
16. Gently lower the drill onto the skull, and slowly drill a hole through the skull, being careful to stop as soon as the skull is pierced.
17. Clean the area with a cotton applicator. Remove the drill bit and replace with the cannula insertion tool. Raise the insertion tool so that there is at least a 1 cm gap between the tool and the skull.
18. Using the cap of a PCR tube, pipette 3 μL of (EnvA) pseudotyped deletion mutant G-deleted ultracentrifuged virus into the corner of the cap. Place the cap under the needle and lower the needle until it is touching the meniscus of the viral droplet. Gently pull the plunger of the syringe in the infusion pump to back fill the needle and polyethylene tube with virus; an air gap should remain between the virus and the water. Fill the tube with approximately 1μl of virus, taking care not to create any bubble in the virus in the tube. Return remaining virus to the original viral aliquot tube.

19. Set the plunger against the infusion pump, and set the infusion pump to inject at 5 μL/min to test the flow of the system. As soon as a droplet appears at the tip of the needle, stop the infusion pump, and reset the flow rate to 1 μL/min (*see* **Note 8**).
20. Choose a target volume of 100–500 nL, depending upon the area of interest. Mark the polyethylene tube at the edge of the virus with a permanent marker; this will help determine whether the virus is flowing properly during the injection.
21. Gently wipe off the needle with ethanol, and move the cannula insertion tool to the 0 point of the digital reader. This should be at bregma; lower the needle until it touches the skull at bregma, then press 0 and set to zero the Z-axis on the digital manipulator. Return to the original desired X and Y coordinates; this should be located directly over the drill hole.
22. Lower the needle through the hole into the brain until the desired depth is reached, then lower the needle an additional 0.1 μm, and raise the needle back to the desired depth. This will create a small space for the virus to flow and will prevent clogging.
23. Press start on the infusion pump, and monitor the virus movement, comparing the distance of the virus to the marker label to determine that the virus is flowing properly.
24. Once the pump has finished the injection (generally 2–5 min depending upon volume) wait an additional 10 min before beginning to raise the needle out of the brain; this will allow the virus to dissipate and will prevent it from being pulled back out with the needle retraction.
25. After 10 min, slowly raise the needle until it is outside of the brain; removing the needle should occur at an approximate rate of 0.3 μm/min.
26. Use forceps to suture the skull skin closed with non-dissolvable sutures (or as directed by institutionally approved protocol). 3–4 drops of vetbond placed over each suture will ensure that the sutures will stay closed.
27. Give mouse first buprenorphine dose (0.05–0.1 mg/kg). Return the mouse to a clean cage placed on a 37 °C heating pad, and allow to recover fully, giving mouse second buprenorphine dose (0.05–0.1 mg/kg) 4–6 h later (or as directed by institutionally approved protocol).
28. 5–14 days later, the mouse can be anesthetized and transcardially perfused, and the brain removed and prepared for histology (*see* **Note 9**). Representative images of synaptically connected cells labeled with viral circuit tracing using this approach are shown in Fig. 2.

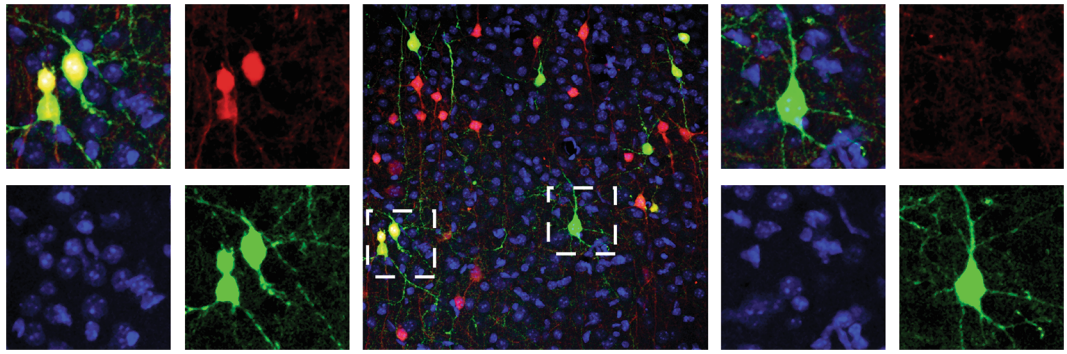

Fig. 2 Viral circuit tracing using genetic labeling of neurons for infection and spread. A composite image shows an example images of viral circuit tracing, showing fluorescently labeled neurons in a cerebral cortex tissue sample from mouse brain, via injection with Dlx5/6-Cre; ROSA-tTA; ROSA-Ai14; pTRE-Bi-G-TVA and pseudotyped (EnvA) SADΔGGFP, using Dlx5/6-Cre to target interneurons. The central image displays the green, red, and blue overlay image; postsynaptic Dlx5/6-lineage cells targeted with virus are red and green (yellow, expressing Tomato from ROSA locus and GFP from (EnvA) SADΔGGFP virus), and presynaptically connected neurons are labeled by (EnvA) SADΔGGFP only in green. High magnification optical section single color images on the left illustrate presynaptic interneurons; high magnification optical section single color images on the right illustrate synaptically connected neurons. White dashed boxes in the central image indicate areas of focus in the close-ups

4 Notes

1. Publication by the Wickersham lab outlines a fourth approach, a protocol using Cre-dependent helper viruses, to target Cre-labeled cells for viral circuit tracing [16]. Additionally, this group has examined the importance of helper virus concentrations in success for rabies viral spread, discussed in detail in [17].
2. The Salk Vector Core provides aliquots of ultracentrifuged unpseudotyped virus that can be used for amplification. If starting with a 10 μL ultracentrifuged aliquot from the Salk Vector Core, also begin with one 10 cm dish and amplify virus as outlined above. Supernatant stocks from this first amplification can be stored for future preps.
3. It is incredibly important to rinse the EnvA dishes for making EnvA pseudotyped virus carefully and thoroughly with PBS. Over washing results in cell loss; under washing results in contaminated stocks of unpseudotyped viral stock.
4. Viral stocks can be stored indefinitely at −80 °C. Avoid freeze-thaw of virus, which can result in lower titers.
5. If viral titers are lower than desired, and the viral MOI used to infect cells is already maximized at 2, it is possible to increase

titers by doubling the number of producer plates of virus and centrifuging serially, layering new supernatant over the first viral spin; remove supernatant after first spin and instead of adding PBS, replace with more filtered supernatant, and layer with Sucrose Solution.

6. It is important to avoid clogging the injection needle. If the needle clogs prior to injection, remove the virus and flush with water prior to continuing. Avoid clogging during the surgery by checking that viral flow is fluid prior to lowering the needle. Some bleeding may occur after the initial drilling through the skull; blot the drill site and ensure that bleeding has stopped prior to beginning the injection to avoid clogging the needle with blood during the lowering of the needle into the injection site.
7. In our hands, we find that isoflurane anesthesia is critical for consistent survival: we have also used Nembutal or Ketamine/Xylazine cocktails and find that the survival rates are lower, compared to isoflurane anesthesia alone.
8. The volume injected can range from 100 nL to 1 μL; it is important to inject slowly (1 μL/min) and allow recovery of at least 10 min before removing the needle to avoid tissue damage and to prevent the virus from moving along the retracting needle track during needle removal.
9. The number of cells that are targeted in vivo can be affected by several factors: (A) The efficiency of the Cre promoter and number of cells it targets; (B) The titer and volume of the AAV used; (C) The titer and volume of RabV. If large numbers of targeted cells are desired, genetic approaches to target cells with GRab and TVA yield larger numbers of initially infected cells. If fewer numbers of targeted cells are desired, AAV helper virus produces fewer initially infected cells. Using tamoxifen-dependent Cre lines can further decrease the number of cells targeted.

References

1. Wickersham IR, Lyon DC, Barnard RJ, Mori T, Finke S, Conzelmann KK, Young JA, Callaway EM (2007) Monosynaptic restriction of transsynaptic tracing from single, genetically targeted neurons. Neuron 53:639–647. https://doi.org/10.1016/j.neuron.2007.01.033. S0896-6273(07)00078-5 [pii]
2. Wall NR, Wickersham IR, Cetin A, De La Parra M, Callaway EM (2010) Monosynaptic circuit tracing in vivo through Cre-dependent targeting and complementation of modified rabies virus. Proc Natl Acad Sci USA 107: 21848–21853. https://doi.org/10.1073/pnas.1011756107
3. Larsen DD, Wickersham IR, Callaway EM (2007) Retrograde tracing with recombinant rabies virus reveals correlations between projection targets and dendritic architecture in layer 5 of mouse barrel cortex. Front Neural Circuits 1:5. https://doi.org/10.3389/neuro.04.005.2007
4. Wickersham IR, Finke S, Conzelmann KK, Callaway EM (2007) Retrograde neuronal tracing with a deletion-mutant rabies virus.

Nat Methods 4:47–49. https://doi.org/10.1038/nmeth999. nmeth999 [pii]

5. Sun Y, Nguyen AQ, Nguyen JP, Le L, Saur D, Choi J, Callaway EM, Xu X (2014) Cell-type-specific circuit connectivity of hippocampal CA1 revealed through cre-dependent rabies tracing. Cell Rep 7:269–280. https://doi.org/10.1016/j.celrep.2014.02.030
6. Marshel JH, Mori T, Nielsen KJ, Callaway EM (2010) Targeting single neuronal networks for gene expression and cell labeling in vivo. Neuron 67:562–574. https://doi.org/10.1016/j.neuron.2010.08.001
7. Kohara K, Pignatelli M, Rivest AJ, Jung H-Y, Kitamura T, Suh J, Frank D, Kajikawa K, Mise N, Obata Y, Wickersham IR, Tonegawa S (2014) Cell type-specific genetic and optogenetic tools reveal hippocampal CA2 circuits. Nat Neurosci 17:269–279. https://doi.org/10.1038/nn.3614
8. Lasek AW, Azouaou N (2010) Virus-delivered RNA interference in mouse brain to study addiction-related behaviors. Methods Mol Biol 602:283–298. https://doi.org/10.1007/978-1-60761-058-8_17
9. Weible AP, Schwarcz L, Wickersham IR, Deblander L, Wu H, Callaway EM, Seung HS, Kentros CG (2010) Transgenic targeting of recombinant rabies virus reveals monosynaptic connectivity of specific neurons. J Neurosci 30:16509–16513. https://doi.org/10.1523/JNEUROSCI.2442-10.2010. 30/49/16509 [pii]
10. Wickersham IR, Sullivan HA (2015) Rabies viral vectors for monosynaptic tracing and targeted transgene expression in neurons. Cold Spring Harb Protoc 2015(4):375–385. https://doi.org/10.1101/pdb.prot072389. PMID: 25834254
11. Osakada F, Mori T, Cetin AH, Marshel JH, Virgen B, Callaway EM (2011) New rabies virus variants for monitoring and manipulating activity and gene expression in defined neural circuits. Neuron 71:617–631. https://doi.org/10.1016/j.neuron.2012.03.019
12. Srinivas S, Watanabe T, Lin CS, William CM, Tanabe Y, Jessell TM, Costantini F (2001) Cre reporter strains produced by targeted insertion of EYFP and ECFP into the ROSA26 locus. BMC Dev Biol 1:4. https://doi.org/10.1186/1471-213X-1-4
13. Li Y, Stam FJ, Aimone JB, Goulding M, Callaway EM, Gage FH (2013) Molecular layer perforant path-associated cells contribute to feed-forward inhibition in the adult dentate gyrus. Proc Natl Acad Sci USA 110:9106–9111. https://doi.org/10.1073/pnas.1306912110
14. Wang L, Sharma K, Deng H-X, Siddique T, Grisotti G, Liu E, Roos RP (2008) Restricted expression of mutant SOD1 in spinal motor neurons and interneurons induces motor neuron pathology. Neurobiol Dis 29:400–408. https://doi.org/10.1016/j.nbd.2007.10.004
15. Miyamichi K, Amat F, Moussavi F, Wang C, Wickersham I, Wall NR, Taniguchi H, Tasic B, Huang ZJ, He Z, Callaway EM, Horowitz MA, Luo L (2010) Cortical representations of olfactory input by trans-synaptic tracing. Nature 472:191–196. https://doi.org/10.1038/nature09714. nature09714 [pii]
16. Lavin TK, Jin L, Wickersham IR (2019) Monosynaptic tracing: a step-by-step protocol. J Chem Neuroanat 102:101661. https://doi.org/10.1016/j.jchemneu.2019.101661. Epub 2019 Aug 10. PMID: 31408693
17. Lavin TK, Jin L, Lea NE, Wickersham IR (2020) Monosynaptic tracing success depends critically on helper virus concentrations. Front Synaptic Neurosci 12:6. https://doi.org/10.3389/fnsyn.2020.00006. PMID: 32116642; PMCID: PMC7033752

Chapter 13

Gene Knockout in the Developing Brain of Wild-Type Rodents by CRISPR In Utero Electroporation

Andrea J. Romanowski, Ryan R. Richardson, Celine Plachez, Reha S. Erzurumlu, and Alexandros Poulopoulos

Abstract

CRISPR/Cas9 constructs can be delivered by in utero electroporation to knock out a gene of interest in neurons of the developing brain in wild-type rodents. This approach allows for high-throughput genetic screening, circuit-specific gene knockout, and knockout cell phenotyping using sparse labeling within a wild-type in vivo context. Here we outline the methods and steps of designing guide RNAs in silico, cloning guide RNAs into plasmid backbones, and introducing these plasmids into the developing mouse cortex and hippocampus.

Key words CRISPR, Genome editing, In utero electroporation, Knockout, Brain development

1 Introduction

Neurodevelopmental disorders are often linked to mutations in genes that are expressed early in brain development. An alternative to using knockout animals produced through transgenic technologies is to genetically target cell types of interest directly in the developing brain of non-transgenic animals. This approach can be advantageous when time and throughput requirements do not allow the generation of mouse strains. Additionally, this approach can be a valuable alternative when germline strains and conditional strains are not viable or develop undesired systemic conditions. Targeted gene knockout in cells of wild-type animals has become experimentally feasible with the introduction of RNA-guided CRISPR/Cas nucleases as genome editing agents [1, 2]. In the developing brain, we and others have used CRISPR/Cas approaches for acutely knocking out a gene [3–5], knocking in a fusion protein or epitope tag [6], and editing single-nucleotide patient variants [7], all with cell-type specificity circumventing germline transmission breeding strategies.

Tolga Soykan and Alexandros Poulopoulos (eds.), *Synapse Development: Methods and Protocols*, Methods in Molecular Biology, vol. 2910, https://doi.org/10.1007/978-1-0716-4446-1_13,

Brain development occurs in phases over distinct time points, where progenitor cells give rise to specific neuron types. Progenitor cells typically line the ventricular system around which the central nervous system develops. We take advantage of the characteristic locations and developmental timing of distinct progenitor pools to target region-specific neuron subtypes using in utero electroporation [8–11]. In utero electroporation can deliver plasmid DNA to a subpopulation of progenitor cells by allowing it to enter the cells by the application of a transient electric field which enables negatively charged DNA injected into the ventricle to cross the cell membrane of progenitor cells lining the ventricle. Specific subsets of neurons can be targeted by selecting specific gestation times and by orientation of the electrode relative to the brain's surface. For example, cortical layer 2/3 excitatory neurons can be targeted at embryonic day (E) 15 when the electrode is positioned with the positive pole on the dorsal half of the brain, leading DNA injected in a lateral ventricle into progenitor cells of the dorsal pallium that give rise to cortical glutamatergic cells [10, 12, 13]. Conversely, injecting DNA into the lateral ventricle and orienting the electric field so that the positive pole faces the ventral surface, will lead DNA into the progenitor cells of the ventral pallium, which give rise to cortical GABAergic neurons [14, 15]. By targeting subpopulations of progenitor cells, in utero electroporation provides a technique to sparsely label neurons and introduce payloads via plasmids into neurons during early development.

Using in utero electroporation, we can introduce CRISPR/Cas9 constructs into progenitor cells, thereby producing a population of knockout cells in an otherwise wild-type brain. Cas9 is an RNA-guided nuclease from the clustered regularly interspaced short palindromic repeats (CRISPR) adaptive immunity discovered in microbes [16, 17]. Cas9 is guided by a short RNA sequence 20 nucleotides in length that is complementary to the target sequence directly upstream of a protospacer adjacent motif (PAM) sequence specific to the type of CRISPR system being used. In this protocol, we are using the system derived from *Streptococcus pyogenes* (spCas9 or Cas9) which uses a 5′-NGG PAM. Using a designed guide RNA (gRNA), Cas9 can be targeted to a specific gene locus and introduce a double-strand break in the DNA [18], which is subsequently repaired by cellular machinery in ways that lead to insertion or deletion of nucleotides (indels) anywhere from 25% to 95% of the time depending on the specific locus [19]. These indels often result in frame-shift mutations disrupting the Open Reading Frame (ORF) of the gene thereby resulting in protein products that are non-functional and typical of conventional knockout approaches. CRISPR/Cas9 has been used in many other contexts to create full knockout animal lines and cell-type specific knockouts. Combining CRISPR/cas9 and in utero electroporation is a powerful technique allowing for the knockout and labeling of a

sparse population of neurons of the same subtype, arising from the same progenitor pool. These neurons can then be studied in the context of a mostly wild-type environment which can circumvent lethal phenotypes of knockout lines, and without having to create transgenic lines for each gene.

The following describes how to design and clone gRNA plasmids, and introduce these plasmids into the developing rodent cortex via in utero electroporation to knockout a gene.

2 Materials

2.1 Design and Preparation of Plasmids

1. Plasmids:
   - P396 gRNA backbone plasmid (pJ2.U6<gRNA_scaffold, Addgene plasmid #226288).
   - A Cas9 plasmid with a promoter that expresses in the embryonic brain (i.e., CAG or EF1α promoters, e.g., Addgene plasmid #51142).
   - A fluorescent protein (FP) plasmid with a strong promoter that expresses in the embryonic brain (i.e., CAG promoter) to facilitate screening.
2. PCR tubes with caps.
3. Nuclease-free water (e.g., Invitrogen).
4. BbsI restriction enzyme (e.g., NEB BbsI-HF).
5. T4 DNA Ligase (e.g., NEB T4 DNA ligase).
6. Ligase Buffer (e.g., Promega T4 DNA ligase 10× buffer).
7. Chemically competent bacteria (e.g., One Shot TOP10, Thermofisher Scientific).
8. S.O.C media.
9. Autoclaved glass beads.
10. Carbenicillin or Ampicillin agar plates.
11. Autoclaved pipette tips or toothpicks.
12. Lysogeny broth (LB).
13. Ampicillin sodium salt, dissolved in sterile water to 100 mg/mL.
14. 14 mL round bottom tubes with caps.
15. Miniprep kit (e.g., Quick-DNA Miniprep Plus Kit, Zymo Research).
16. 1 L Erlenmeyer flask, autoclaved.
17. Midiprep kit (e.g., ZymoPURE Express Plasmid Midiprep Kit, Zymo Research).
18. 100% ethanol, molecular grade.

19. 3 M Sodium Acetate (pH 5.2), molecular grade (e.g., Thermofisher Scientific).
20. 1.5 mL Eppendorf tubes, autoclaved.
21. DNA Elution buffer (e.g., Zymo Research).
22. Thermocycler.
23. Heat block set to 42 °C.
24. Heat block set to 37 °C, shaking at 650 rpm.
25. Plate incubator set to 37 °C.
26. Shaking culture incubator set to 37 °C, shaking at 230 rpm.
27. Large centrifuge for midi prep.
28. Vacuum manifold.
29. Refrigerated microcentrifuge.
30. Spectrophotometer (e.g., NanoDrop One, Thermo Scientific).

2.2 In Utero Electroporation

1. E15 or E16 Timed-pregnant mice (e.g., CD1 from Charles River Laboratories).
2. Isoflurane.
3. Oxygen tank and regulator.
4. Isoflurane vaporizer system and induction chamber.
5. 0.1% filtered Fast green FCF in nuclease-free water.
6. Analgesic (e.g., Buprenorphine).
7. Sterile cotton tip applicators.
8. Sterile gauze (or equivalently press' N seal plastic wrap).
9. Hair removal cream (e.g., Veet).
10. Sterile disposable transfer pipettes.
11. Betadine surgical scrub.
12. Sterile surgical gloves.
13. Sterile bench pads.
14. 1/2 cc syringe with 27 G needle.
15. Parafilm.
16. 50 mL conical tubes.
17. Nylon monofilament reverse cutting 3/8 c 12 mm sutures.
18. Sterile 1× Phosphate Buffered Saline (PBS).
19. Alcohol antiseptic pads.
20. Glass capillary tubes, non-heparinized, diameter 1.1–1.2 mm (e.g., Fisherbrand).
21. Eye lubricant (e.g., Puralube Vet Ointment).
22. Electroporator (e.g., Electro Square Porator ECM 830).

23. Tweezertrodes (e.g., BTX company).
24. Water heat pad set to 37 °C (e.g., HTP-1500 heat therapy pump).
25. Dry block heater with 50 mL tube block, set to 40 °C (e.g., VWR, mini block heater).
26. Isoflurane vaporizerPipette puller (e.g., Narishige).
27. Pipette beveler (e.g., Narishige).
28. Dissecting microscope.
29. Sterile surgical scissors, medium and micro.
30. Sterile forceps, blunt and sharp.
31. Sterile suturing tools.
32. Aspirator tube assemblies for calibrated microcapillary (e.g., Sigma-Aldrich).
33. Red heat lamp.
34. Fluorescent stereoscope (e.g., Leica).

3 Methods

3.1 Design and Preparation of CRISPR Knockout Plasmids

In the following steps, we outline how to design and clone gRNAs that are needed to perform gene knockout using spCas9. Several online platforms, including benchling.com, indelphi.giffordlab.mit.edu [20], and CRISPOR.tefor.net [21], allow one to import the genomic sequence of a gene and design gRNAs for gene knockout. Predictions of precision and efficiency are provided to compare different gRNA options. Once gRNA target sequences have been selected, gRNA sequences can be synthesized or ordered using a nucleic acid synthesis provider, as such as those used commonly to synthesize oligos for PCR, and subcloned into a plasmid using common cloning protocols. Here we describe the process of producing gRNA constructs using Golden Gate Assembly (GGA), a method that allows for multiple inserts to be assembled into a vector backbone in one reaction by taking advantage of Type II restriction endonucleases that cleave DNA outside of the recognition sequence, leaving unique overhangs that allows for orderly assembly of multiple fragments [22, 23].

3.1.1 Preparation of Cas9 Plasmid and Guide RNA (gRNA) Backbone

1. Thaw plasmids: gRNA plasmid P396, Cas9 plasmid, and FP plasmid.
2. Add 1 mL of 100 mg/mL ampicillin to 1 L of autoclaved lysogeny broth (LB).
3. Prepare two flasks of 200 mL ampicillin LB (or other appropriate antibiotic) in 1 L Erlenmeyer flasks and inoculate one with the Cas9 plasmid and the other with the FP plasmid.

4. Inoculate 4 mL ampicillin LB in 14 mL round bottom tube with the gRNA backbone plasmid.
5. Incubate both at 37 °C in a large shaking culture incubator overnight (approx. 16–18 h).
6. Use a Midiprep kit to isolate the Cas9 and FP plasmids from the 1 L cultures.
7. Use a Miniprep kit to isolate the gRNA backbone plasmid from the 14 mL culture.

3.1.2 Designing and Cloning Guide RNA (gRNA)

1. Import the genomic sequence of the gene into software that enables genome sequence annotation, such as to Benchling in this example. In Benchling, click the add (+) button at the top of the left-hand menu. Hover over "DNA sequence" and select "import DNA sequence" option. Go to "import from database" tab. In search bar, enter gene name, NCBI accession number, ENSEMBL ID, etc., enter the genome to search, and click "search". Verify that the entry found is the correct entry. Select folder and click "import" (Fig. 1).
2. Find the exon that has the start codon with the first annotated amino acid (Methionine) and take note of the location for future reference.
3. Go to indelphi.giffordlab.mit.edu or equivalent in silico gRNA design webtool and click on "Gene Mode" tab (Fig. 2a).
4. Choose your reference genome species of choice, type your gene of interest into the search bar, and choose cell type (*see*

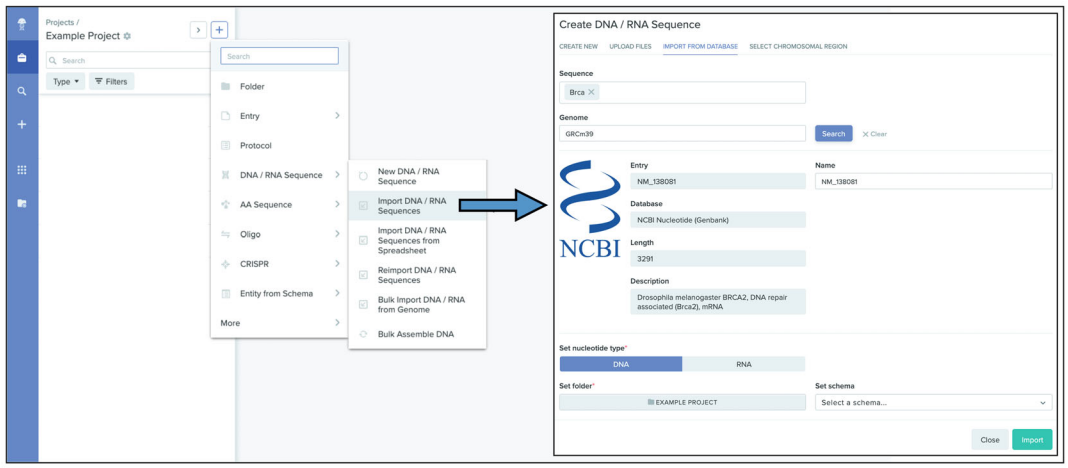

Fig. 1 Importing gene of interest into Benchling. Using Benchling, import the sequence of your gene of interest by clicking the plus sign button at the top right of the menu, when in a project folder. Click "import DNA/RNA sequence". Go to the "import from database" tab, and search for the gene name or NCBI accession name. Then click "import"

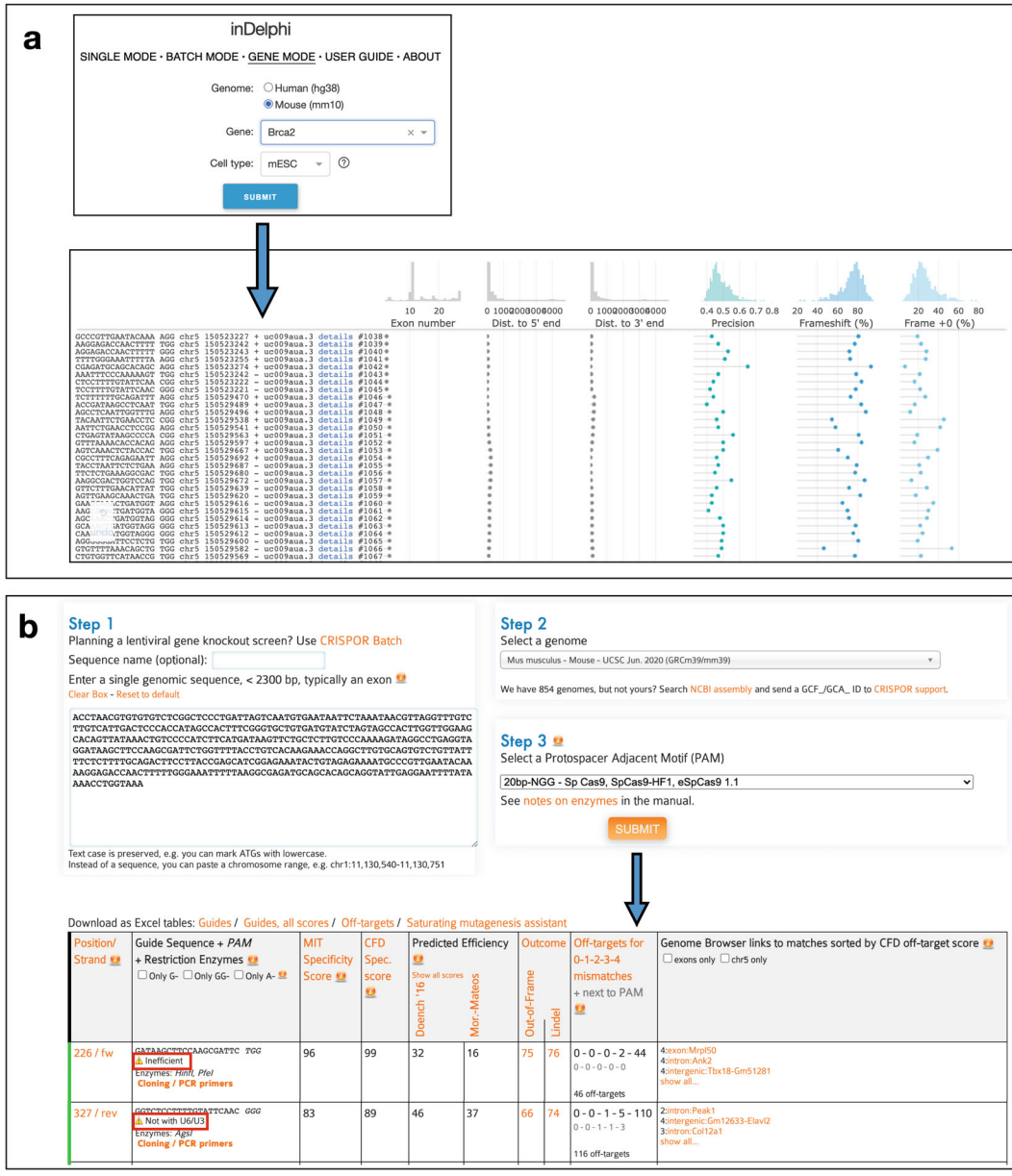

Fig. 2 Designing gRNAs using inDelphi and CRISPOR. (**a**) Go to the "Gene Mode" tape on inDelphi. Search for the gene of interest in the correct genome. Click "submit". The following page will show a large list of potential gRNAs. Take note of the sequence, precision rate, and frameshift percent. (**b**) Once you have identified a few gRNA sequences from inDelphi, double check them on CRISPOR. Enter the exon sequence from your gene, and select the genome. Click "submit". The following page will show a list of gRNAs. Search for the ones you found on inDelphi to get the predicted efficiency, off-target sites, and any restrictions. Some restrictions, like inefficient and not with U6/U3, are shown in red boxes

Note 1). Click submit. The results of the search will be a large list of potential gRNA sequences.

5. Choose 2–3 different gRNA sequences using the following criteria: (i) choose gRNAs that are located in an early exon that contains parts of the ORF, i.e., target the first exons after the start codon (*see* **Note 2**), (ii) choose gRNAs with high precision, meaning the target sequence is singular in the genome and the next closest sequence differs in as many nucleotide positions as possible, and (iii) choose gRNAs with high frameshift occurrence and low frame +0 occurrence (assessed in InDelphi).
6. Take note of the gRNA sequences that you have chosen by typing the sequence into an entry or annotating the genomic sequence on Benchling.
7. Go to CRISPOR.tefor.net to check cutting efficiency, off-targets, and specific cloning requirements for the gRNAs chosen from **step 5**. Enter the sequence of one of the exons where a gRNA targets in the box to the left (Fig. 2b).
8. Select the mouse genome and select the NGG protospacer adjacent motif (PAM) used for spCas9. Click submit.
9. Search for your chosen gRNA sequence and review any cloning requirements (*see* **Note 3**), predicted off-target sites (*see* **Note 4**), and predicted efficiency (*see* **Note 5**).
10. Once your gRNA selections have been checked using inDelphi and CRISPOR, you can finalize your selections and annotate your sequence on Benchling.
11. Copy the DNA sequence of your gRNA from the gene sequence and add to a blank entry and label as "sense strand" or "S/S". This is the forward sequence to your gRNA.
12. Go back to the annotated gRNA on the gene sequence and copy the reverse complement. To do this on Benchling, right click, hover over "copy special" and pick "Reverse Complement" to copy the reverse complement of the gRNA sequence. Add this to the same blank entry and label as "antisense strand" or "A/S". This is the reverse sequence to your gRNA.
13. Add BbsI restriction enzyme sticky-end overhangs onto each sequence. Add CACC to the beginning of the "sense strand" sequence and add CAAA to the beginning of the "antisense strand" sequence (*see* **Note 6**).
14. Order these gRNAs as custom DNA oligos from a nucleic acid synthesis provider (e.g., Integrated DNA Technologies (IDT)).
15. Once you have received the ordered oligos, dilute oligos to stock solutions of 100 μM using nuclease-free water.

16. Anneal oligos together by adding 1 μL of the 100 μM (approximately 750 ng) sense oligo stock solution, 1 μL of the 100 μM anti-sense oligo stock solution, and 7 μL nuclease-free water into a clean PCR tube. Mix gently.
17. Place the tube in a thermocycler and use the following program for slow annealing of the oligos:

    95 °C for 5 min

    Ramp down 0.1 °C per second to 25 °C

    Keep at 4–12 °C until next step
18. Prepare the Golden Gate Assembly (GGA) reaction by combining 2 μL annealed oligos from **step 17**, 20 Units BbsI, 1000 Units T4 Ligase, 100 ng gRNA plasmid backbone prepped in Subheading 3.1.1 (P396), 2 μL ligation buffer (Promega), and nuclease-free water up to 20 μL total volume in a clean PCR tube.
19. Run the GGA by putting the tube in the thermocycler using the following program:

    37 °C for 30 min

    37 °C for 3 min

    16 °C for 5 min

    Repeat **steps 2** & **3**, 15 times

    37 °C for 30 min

    65 °C for 20 min

    Hold at 12 °C
20. Transform ~2–2.5 μL GGA solution into competent bacteria (e.g., TOP10). Place the cells on ice for 30 min, heat shock bacteria by placing the tube in a 42 °C heat block for 30 s, then placing the tube back on ice for 2 min. Then add approximately 200 μL of SOC media to the tube, and place in a heat block at 37 °C for 30–60 min shaking at 650 rpm.
21. Plate on a carbenicillin or ampicillin plate using glass beads. Place the plate in an incubator at 37 °C overnight.
22. The next day, pick 2–3 different colonies from the plate to grow in small cultures overnight. To do this, take a sterile/autoclaved pipette tip or toothpick and pick up one bacterial colony (*see* **Note 7**), touch a separate labeled carbenicillin plate to document the specific colony chosen, and then swirl the toothpick into 4 mL of ampicillin lysogeny broth (LB) in a capped 14 mL tube. Place the touch plate in the incubator at 37 °C and the LB culture in a shaking incubator set to 37 °C, 230 rpm both for overnight.
23. The next day, take the cultures out of the shaking incubator and isolate the plasmid DNA using a miniprep kit.

24. Verify that the chosen colonies contain the correct plasmids via diagnostic restriction enzyme digests using the BbsI enzyme to confirm cloning sites have been removed (optional) and sequencing.
25. Inoculate a 200 mL LB ampicillin culture of the sequence-verified colony from the touch plate in a 1 L Erlenmeyer flask and place it the shaking incubator at 37 °C overnight.
26. The next day, take the culture out of the shaking incubator and isolate the plasmid DNA using a midiprep kit and check concentration and purity on a spectrophotometer (e.g., NanoDrop).
27. Ethanol-precipitate the gRNA and Cas9 plasmid DNA (from Subheading 3.1.1) by adding 600 μL 100% ethanol and 60 μL of 3 M Sodium Acetate to the eluted DNA, then centrifuge at 15,000 g, or max speed on a tabletop centrifuge for 20 min at 4 °C. Remove the supernatant from the white DNA pellet without disturbing the pellet. Let pellet air dry for 15 min, or put on a shaking heat block at 37 °C until dry.
28. Add enough elution buffer to make the final concentration of plasmid DNA around 4 μg/μL and confirm concentration using a spectrophotometer (e.g., NanoDrop).

3.2 In Utero Electroporation

In the following steps, we outline how to perform in utero electroporation in the developing mouse brain. This technique can also be performed on rats, with a few minor changes to the age of the embryo, equipment sizes, and electroporation parameters. This technique allows one to introduce plasmid DNA into the progenitor cells lining the ventricles of the developing rodent brain, and therefore tag specific populations of neurons. This chapter will go through the steps to target layer 2/3 intracortical neurons of the somatosensory cortex and pyramidal neurons in CA1/CA3 of the hippocampus.

3.2.1 Surgery Preparation

Mouse strain: Timed-pregnant CD1 female mice from Charles River Laboratories were used for their robust maternal behavior. However, it is an outbred strain, with less reliable DNA database sequence consistency. Therefore, it is recommended that gDNA of the gene of interest be sequenced prior to designing gRNAs.

1. Either breed or order timed-pregnant CD1 mice from Charles River Laboratories to be embryonic day 15 (E15) for layer 2/3 cortex or E16 for hippocampus electroporation (*see* **Note 8**).
2. Turn on heat pad to 37 °C, heat block to 40 °C, and electroporator.
3. Place two 50 mL conical tubes of sterile 1× PBS into the heat block to warm up for at least 15 min before the start of surgery.

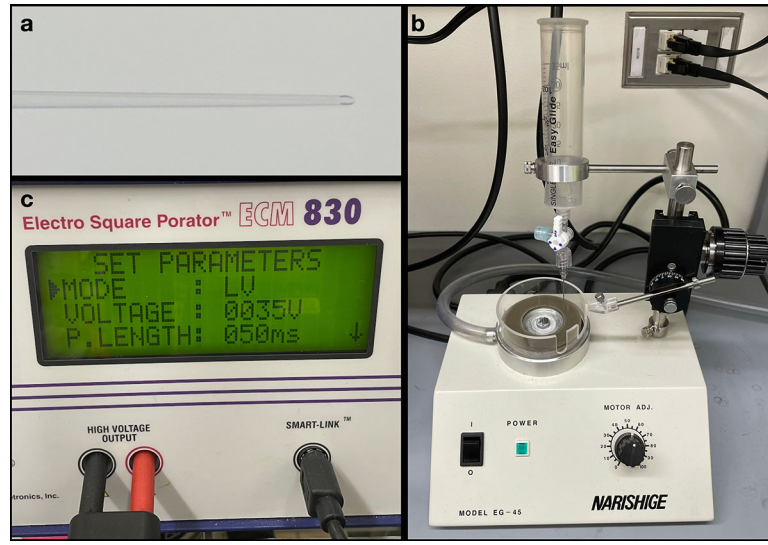

Fig. 3 Surgery preparations. (**a**) Glass capillary tubes were pulled to a point using a Narishige pipet puller. They were then beveled at a 30° angle with a larger opening. (**b**) Narishige rotating beveler set to 30° angle with a syringe above the diamond bit to drip distilled water throughout the grinding. (**c**) Electroporator has been set to the correct settings for cortical electroporation

4. Pull and bevel several glass capillary tubes to create glass micropipettes that have a rounded sharp point with a small opening at the end. These will be used to inject your DNA into the embryonic brains (*see* **Note 9**).
5. Use a beveler with a rotating diamond wheel and an angle-adjusting micropipette holder (Fig. 3b). Bevel the tip at a 30–35° angle with constant water flow to prevent chipping with wheel rotation at approx. 500–1200 rpm. Check under a stereoscope to make sure none have been broken or blocked (Fig. 3a).
6. Prepare a plasmid DNA mix for the surgery. Combine equal amounts of gRNA, Cas9, and FP plasmids to a total concentration of 4 μg/μL in elution buffer from the plasmid prep kit. Dilute fast green 1:10 in DNA mix. Make 10–20 μL total per pregnant animal.
7. Plug the tweezertrodes into the electroporator and set at the following parameters (Fig. 3c):

   Pulse Voltage: 35 V

   Pulse Length: 50 ms

   Number of Pulses: 4

   Interval Between Pulses: 1 s

8. Gather the sterile bench pad, sterile gauze, eye lubricant, sterile cotton tip applicators, alcohol antiseptic pads, parafilm, hair removal cream, sutures, beveled capillaries, aspirator, analgesic in 1/2 cc syringe with 27 G needle, and sterilized surgical tools.

3.2.2 In Utero Electroporation Surgery

All animals were treated in accordance with the regulations and guidelines of the Institutional Care and Use Committee of the University of Maryland School of Medicine and the NIH Guide for the Care and Use of Laboratory Animals (NIH Publications No. 80–23) revised 1996.

1. Prepare the mouse for surgery by placing it in the induction chamber at 3% isoflurane with 100% oxygen as the carrier until the animal's breathing has slowed to approximately 1 breath per second (approx. 3–5 min).
2. Remove the mouse from the induction chamber and place head in the nose cone with the animal on its stomach.
3. Give analgesic (e.g., Buprenorphine) and put eye lubricant on the eyes. Add more eye lubricant every 20 min during the surgery.
4. Flip the mouse onto its back and replace its head in the nose cone.
5. Prep the surgery site by swiping an alcohol wipe across the abdominal area.
6. Add a small amount of hair removal cream to the abdominal area, and create a small oval area in the lower abdomen (Fig. 4a).
7. Use a cotton tip applicator to spread the cream around the area until the hair is lifted.
8. Use 1× PBS and a Kim wipe to remove the excess hair and hair removal cream (*see* **Note 10**).
9. Once all of the hair is removed, apply a sterile alcohol pad and Betadine surgical scrub to sterilize the surgical area, repeating 3 times. Remove any residual Betadine scrub with sterile 1× PBS.
10. Cut a small hole in the sterile gauze that matches the size of the hairless area of the abdomen. Place the cut gauze around the area, and wet the edges with warm 1× PBS (*see* **Note 11**).
11. Verify that the mouse is under deep anesthesia with a toe pinch.
12. Make a 1 inch incision in the skin along the midline of the lower abdomen (*see* **Note 12**).
13. Use microscissors to cut away the connective tissue that connects the skin layer and the muscle layer below. This will aid in suturing.

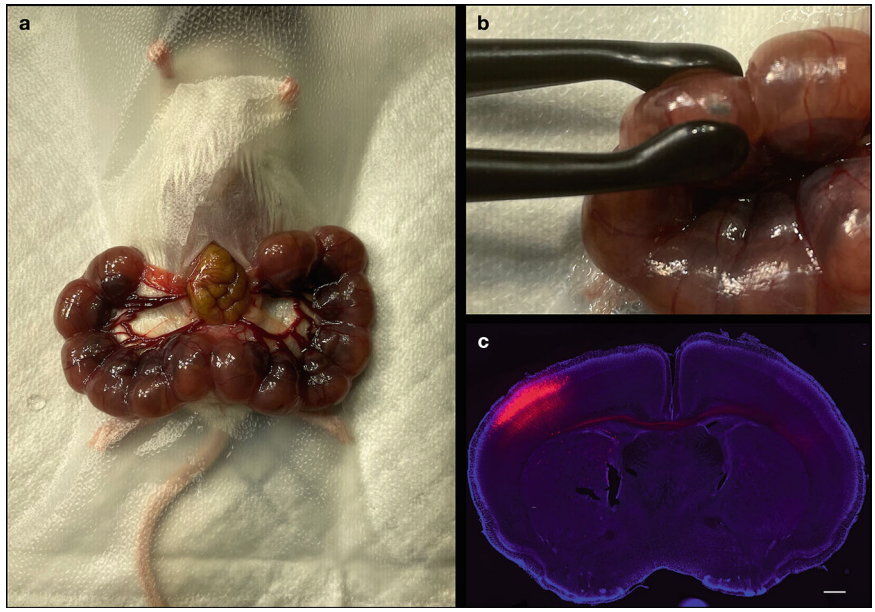

Fig. 4 In utero electroporation. (**a**) The uterine horn was exposed following a laparotomy. (**b**) Plasmid mix containing green dye was injected into the lateral ventricle of an E15 pup and tweezertrodes were placed on either side of the embryo's head, with the positive electrode on the same side as the injection, for a cortical electroporation. (**c**) A coronal section showing a positive cortical electroporation. Upper layer pyramidal neurons expressing red fluorescent protein (red) largely coexpress Cas9 and gRNAs to induce knockout of a gene. Their cell bodies are seen at the focus of the electroporated area (inset close up), while their axons can be seen projecting across the corpus callosum. Brain was perfused, sectioned at 80 μm, stained for RFP, and mounted using Fluoromount with DAPI. Scale bar 500 μm, inset 100 μm

14. Create a similar size incision along the midline of the muscle layer. Be careful not to cut too deep as the internal organs are pressed up against the muscle layer. Create a small hole first to lift the muscle away from the organs.
15. Now that the abdominal cavity has been opened, it is imperative to add warm sterile 1× PBS to the cavity every 2–3 min, or sooner if it looks dry.
16. Prepare your micropipette by placing the blunt end into the aspirator adapter. Aspirate any water that is left in your glass micropipette tip from beveling to prevent dilution of your DNA.
17. Pipette ~5 μL of your DNA mix onto a piece of parafilm.
18. Place the tip of the glass micropipette in the drop of DNA at a horizontal angle to prevent breaking the tip against the parafilm.
19. Suck up as much DNA as you can without introducing any air bubbles. Place the aspirator and needle safely aside.

20. With the blunt forceps, carefully grab at the node between two embryos and pull to remove the uterine horn from the abdominal cavity. Do not pull hard as you do not want to detach the uterine horn from the abdominal wall.
21. Pull on one side until you see a small knot of muscle that is attached to the abdominal wall. Repeat on the other side. Be cautious of the uterus that connects both sides of the uterine horn in the middle (Fig. 4a).
22. Wet with warm 1× PBS.
23. Wearing sterile gloves and using your fingers, carefully pick up one of the embryos in its amniotic sac. Note the orientation of the embryo. If you cannot see the top of the head, carefully palpate the embryo to rotate it in the sac. Be careful not to squeeze too hard as you might rupture the amniotic sac.
24. Once you have a clear view of the top of the head, locate the midline of the brain. On either side of this line are the lateral ventricles, often seen as dark shadows.
25. While holding the embryo with one hand, pick up your aspirator and glass micropipette. Poke the glass micropipette through the amniotic sac (*see* **Note 13**) and into the embryonic brain. Do not poke far into the brain, as the lateral ventricle is very shallow. Once you pierce through the edge of the brain, you are most likely in the ventricle.
26. Once you think your glass micropipette is in the lateral ventricle, blow through the aspirator at a slow steady pace. You should see blue dye filling up the ventricle (*see* **Note 14**). Fill the ventricle until you see a bright blue spot, this is approximately 0.75–1 μL (Fig. 4b).
27. Once you have filled the ventricle, while holding the embryo with one hand, put aside your aspirator and glass micropipette, and pick up the tweezertrode. To electroporate the cortex, place the positive electrode on the same side as the injection, and the negative electrode on the other side of the head. Both should be around the ear area (Fig. 4b). Lightly squeeze the head in between the tweezertrode without rupturing the amniotic sac (*see* **Note 15**). Once you are in the right position, start the electroporator and wait until all pulses are compete.
28. Remove the tweezertrodes, let go of the embryo, and wet with warm 1× PBS. To electroporate the hippocampus, reverse the positive and negative electrode positions.
29. Repeat **steps 23–28** on 3–6 other embryos, depending how many embryos are available (*see* **Note 16**).
30. Once you have completed all of your electroporations, carefully push the uterine horn back into the abdominal cavity using forceps to hold the skin/muscle back and your fingers to gently

push. Do not push with too much pressure as you can rupture the amniotic sac.

31. Once all embryos are back inside the abdominal cavity, fill it up with warm 1× PBS.
32. Suture the muscle layer and skin layer separately, using a continuous stitch.
33. Sterilize the incision with an alcohol pad.
34. Place the mouse back in its home cage, on its back under a red heat lamp.
35. Monitor the mouse for approximately 1 h to make sure it is not in pain and can move freely.
36. Continue to monitor the mouse daily until she gives birth, around E19–20.
37. Once the pups are born, screen them under a fluorescence stereoscope (*see* **Note 17**) non-invasively (*see* **Note 18**) by gently holding them at the focal distance and observing fluorescent protein signal to identify which pups have been successfully electroporated (*see* **Note 19**).

4 Notes

1. For rodent in utero electroporation, we will be using the mouse genome. If your cell type of interest is not listed in the menu, choose mESC if your cell type has no expected defects in DNA repair.
2. To check where the gRNA will cut, copy the gRNA sequence and search your gene sequence imported into Benchling. You can also annotate the Benchling sequence to save the gRNA sequence, by using the "Annotations" button on the right-hand menu of the sequence page.
3. Some gRNAs will indicate that they are inefficient or require a different promoter other than U6/U3. Choose gRNAs that do not have these warnings.
4. Choose gRNAs that do not have any off-targets with mismatches of 2 or less. Any gRNAs that have 3 or more mismatches with off-target sites are likely to be precise. Also check the MIT specificity score that is based on Hsu and colleagues [24]. The higher the score, the less likely there will be off-target effects.
5. The higher the efficiency score, the more likely there will be cleavage at that position in the genome. The predicted efficiency score is based off of two studies, the first being by Doench and colleagues [25] which uses Azimuth scores that

are based on data from cells, and recommended for gRNAs that use U6 as a promoter. The second score is from Moreno-Mateos and colleagues [26] which uses CrisprScan scores that are based on data from zebrafish embryos, and recommended for gRNAs that use T7 as a promoter.

6. If the gRNA sequence ends in T or A, add an additional C or G to increase cloning efficiency. Remember to add the corresponding G or C on the reverse strand to complement.
7. Be sure not to pick up more than one colony at a time, as this may result in a mixture of different plasmids. If the plate does not have singular colonies, take a sterile or autoclaved pipette tip or toothpick and streak it out on a separate carbenicillin plate to get single colonies. Then proceed to the next step.
8. Embryonic day zero is the morning that the vaginal plug is observed in mated female rodents. Also referred to as days post coitum (dpc).
9. Make sure that the opening is wide enough to be able to eject viscous liquid like your DNA mix, but not too wide as to damage the amniotic sac or brain of the embryo. We use an opening in the range of 50 μm. Also make sure that there are no chips or debris on the tip of the needle. Make 3–5 in total to have extra during the surgery in case you accidentally break one.
10. Be sure to avoid the ring of nipples around the abdomen, as you do not want to irritate them.
11. Wetting the surface of the gauze gives the embryos a warm and moist landing spot when we remove the uterine horn from the abdominal cavity.
12. Do not cut too low on the abdomen, as there is a large blood vessel that, if cut, can lead to death via exsanguination.
13. Do not hold the amniotic sac too tightly or when you poke your needle through, it will rupture.
14. Hold the needle as you would a pencil for good control of its location. If you do not see blue dye come out of the needle during the injection, take the needle out and try to blow out in the air. If nothing comes out, your needle is most likely blocked by brain matter, and you need to prepare a new one. This also means that you most likely inserted the needle too far into the embryonic brain.
15. You should see bubbles forming at the negative electrode and see the embryo twitch at each pulse. This shows that there was a good electrical field.
16. Do not electroporate the embryos closest to the abdominal wall or uterus on either side. The electrical pulses could cause

contractions and miscarriage. Do not electroporate more than 8 embryos in one dame, this could also cause miscarriages.

17. You can screen pups using a fluorescence stereoscope that has long working distance or other macroscopic fluorescence options like blue LED flashlight and orange filter glasses for GFP or corresponding LED and filter glasses got other FPs.
18. When using bicistronic plasmids that co-express Cas9 and FP, fluorescence is typically too weak to screen pups non-invasively. This may be due to reduced FP expression from the large bicistronic mRNA. To facilitate screening, we suggest to have Cas9 and FP on separate plasmids that are mixed and co-electroporated. However, if screening is not a problem, you may choose a single plasmid expressing both Cas9, an FP, as well as the gRNA cassette driven by a Pol III promoter like U6.
19. Some of the electroporated pups may not be born, as they may be resorbed before birth, or be stillborn. If this is the case, try to be gentler with your injection in your next surgery as you may have caused damage. Do not be discouraged, this surgery takes a lot of practice and patience.

References

1. Knott GJ, Doudna JA (2018) CRISPR-Cas guides the future of genetic engineering. Science 361:866–869
2. Tsuchida CA, Wasko KM, Hamilton JR et al (2024) Targeted nonviral delivery of genome editors in vivo. Proc Natl Acad Sci USA 121: e2307796121
3. Altas B, Tuffy LP, Patrizi A et al (2023) Region-specific phosphorylation determines neuroligin-3 localization to excitatory versus inhibitory synapses. Biol Psychiatry. https://doi.org/10.1016/j.biopsych.2023
4. Iffland PH, Everett ME, Cobb-Pitstick KM et al (2022) NPRL3 loss alters neuronal morphology, mTOR localization, cortical lamination, and seizure threshold. Brain 145(11): 3872–3885
5. Greig LC, Woodworth MB, Poulopoulos A et al (2024) BEAM: a combinatorial recombinase toolbox for binary gene expression and mosaic genetic analysis. Cell Rep 43:114650
6. Richardson RR, Steyert M, Khim SN et al (2023) Enhancing precision and efficiency of Cas9-mediated knockin through combinatorial fusions of DNA repair proteins. CRISPR J 6: 447–461
7. Robertson CD, Davis P, Richardson RR et al (2023) Rapid modeling of an ultra-rare epilepsy variant in wild-type mice by in utero prime editing. bioRxiv. https://doi.org/10.1101/2023.12.06.570164
8. Saito T, Nakatsuji N (2001) Efficient gene transfer into the embryonic mouse brain using in vivo electroporation. Dev Biol 240:237–246
9. Wang C, Mei L (2013) In utero electroporation in mice. Methods Mol Biol 1018:151–163
10. Poulopoulos A, Murphy AJ, Ozkan A et al (2019) Subcellular transcriptomes and proteomes of developing axon projections in the cerebral cortex. Nature 565:356–360
11. Blatt GJ, Brandenburg C, Poulopoulos A (2023) India ink to 3D imaging: the legacy of Dr. Deepak "Dee" N. Pandya and his influence on generations of neuroanatomists. J Comp Neurol 531:1875–1882
12. Tabata H, Nakajima K (2001) Efficient in utero gene transfer system to the developing mouse brain using electroporation: visualization of neuronal migration in the developing cortex. Neuroscience 103:865–872
13. Poulopoulos A, Davis P, Brandenburg C et al (2024) Symmetry in levels of axon-axon homophilic adhesion establishes topography in the corpus callosum and development of connectivity between brain hemispheres.

bioRxiv. https://doi.org/10.1101/2024.03.28.587108

14. Marín O, Rubenstein JL (2001) A long, remarkable journey: tangential migration in the telencephalon. Nat Rev Neurosci 2:780–790
15. Butt SJB, Fuccillo M, Nery S et al (2005) The temporal and spatial origins of cortical interneurons predict their physiological subtype. Neuron 48:591–604
16. Gasiunas G, Barrangou R, Horvath P et al (2012) Cas9-crRNA ribonucleoprotein complex mediates specific DNA cleavage for adaptive immunity in bacteria. Proc Natl Acad Sci USA 109:E2579–E2586
17. Jinek M, Chylinski K, Fonfara I et al (2012) A programmable dual-RNA-guided DNA endonuclease in adaptive bacterial immunity. Science 337:816–821
18. Ran FA, Hsu PD, Wright J et al (2013) Genome engineering using the CRISPR-Cas9 system. Nat Protoc 8:2281–2308
19. Brinkman EK, Chen T, Haas MD et al (2018) Kinetics and fidelity of the repair of Cas9-induced double-strand DNA breaks. Mol Cell 70:801–813.e6
20. Shen MW, Arbab M, Hsu JY et al (2018) Predictable and precise template-free CRISPR editing of pathogenic variants. Nature 563:646–651
21. Concordet J-P, Haeussler M (2018) CRISPOR: intuitive guide selection for CRISPR/Cas9 genome editing experiments and screens. Nucleic Acids Res 46:W242–W245
22. Engler C, Kandzia R, Marillonnet S (2008) A one pot, one step, precision cloning method with high throughput capability. PLoS One 3:e3647
23. Marillonnet S, Grützner R (2020) Synthetic DNA assembly using golden gate cloning and the hierarchical modular cloning pipeline. Curr Protoc Mol Biol 130:e115
24. Hsu PD, Scott DA, Weinstein JA et al (2013) DNA targeting specificity of RNA-guided Cas9 nucleases. Nat Biotechnol 31:827–832
25. Doench JG, Fusi N, Sullender M et al (2016) Optimized sgRNA design to maximize activity and minimize off-target effects of CRISPR-Cas9. Nat Biotechnol 34:184–191
26. Moreno-Mateos MA, Vejnar CE, Beaudoin J-D et al (2015) CRISPRscan: designing highly efficient sgRNAs for CRISPR-Cas9 targeting *in vivo*. Nat Methods 12:982–988

Chapter 14

Mapping Synaptic Activity at the Population and Cellular Levels with Genetically Encoded Voltage Indicators (GEVIs)

Younginha Jung, Ryuichi Nakajima, Sung Min Ahn, Nazarii Frankiv, Haeun Lee, Maesoon Im, Yoon-Kyu Song, and Bradley J. Baker

Abstract

In this chapter, we provide examples of using genetically encoded voltage indicators (GEVIs) to monitor neuronal intercellular communications at the population level (hippocampus of CA1 region) and individual cell level (retinal ganglion cells). Providing an optical readout for voltage transients, GEVIs enable the reporting of synaptic activity, both activation and inhibition, from chemical and electrical synapses. With the added flexibility of restricting expression of the GEVI to distinct cell types, GEVIs are becoming a powerful tool for interrogating neuronal activity.

Key words GEVIs, Voltage imaging, Neuronal activity, ArcLight, Calcium imaging, Hippocampal slice, Retinal ganglion cell

1 Introduction

The nervous system involves the coordination of multiple components to process sensory inputs, create memories, and elicit behavior. Voltage imaging can therefore be a powerful tool since it is a direct readout of membrane potential enabling the visualization of neuronal activity simultaneously from multiple locations [1, 2]. Depending on the optics in use, the investigator can visualize broad regional activity of multiple circuits, individual cellular components of a circuit, or even subcellular sections of a neuron. In addition, voltage imaging can optically report subthreshold potentials including inhibitory synaptic events. The supra- and subthreshold responses in conjunction with spatial and temporal resolution make voltage imaging a potentially powerful approach to analyze neuronal functions.

Authors Younginha Jung and Ryuichi Nakajima have contributed equally to this chapter.

Tolga Soykan and Alexandros Poulopoulos (eds.), *Synapse Development: Methods and Protocols*, Methods in Molecular Biology, vol. 2910, https://doi.org/10.1007/978-1-0716-4446-1_14,

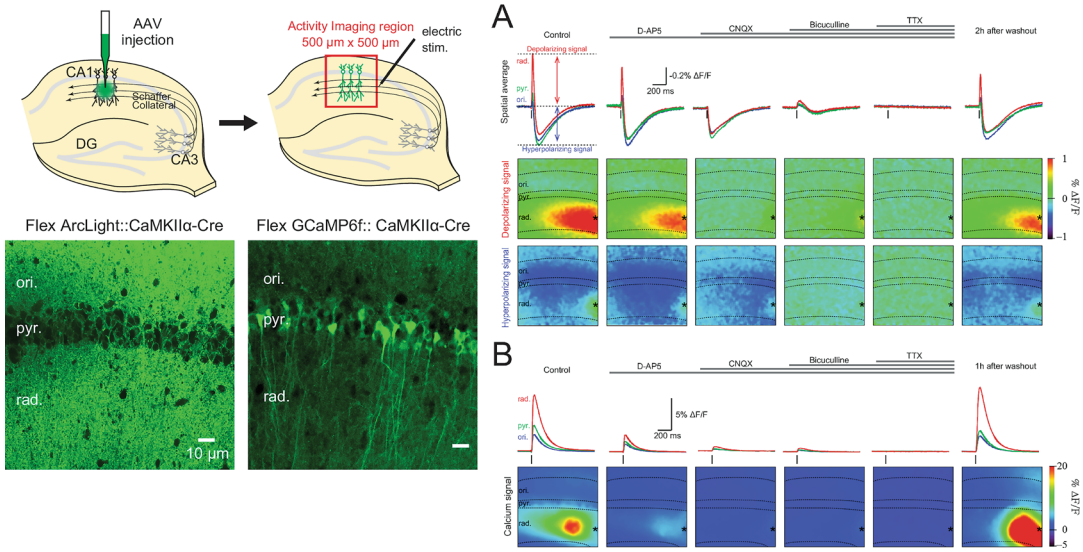

Fig. 1 Visualizing synaptic activity at the population level. An AAV containing floxed ArcLight (GEVI) or floxed GCaMP6f (GECI) was injected into the CA1 region of the hippocampus of CaMKII-Cre transgenic mouse line. The images below show the different expression patterns of the GEVI (left) and the GECI (right). Optical traces and heat maps (red—depolarization; blue—hyperpolarization) upon stimulation of the Schaffer Collateral axons from CA3 reveal activation in the radiatum for both the GEVI (top) and the GECI (bottom). However, only the GEVI optically reports the feedforward inhibition (heat map—blue region) in the oriens layer. (Modified from Nakajima and Baker, 2018 [7])

Historically, voltage imaging has relied primarily on dyes due to their high signal-to-noise ratio (SNR), rapid optical response (sub-millisecond), and ease of application [3, 4]. However, some brain regions are not easily accessible for dye staining, and those that are accessible result in the staining of all cells the dye contacts. In contrast, genetically encoded voltage indicators (GEVIs) are produced by the cell, enabling access to all brain regions. Furthermore, with the employment of cell-specific promoters, the expression of the GEVI can be restricted to a certain cell type [5] or even to a subcellular compartment of the cell (i.e., the soma [6]).

These advantages of a genetically encoded probe combined with the ability of imaging to interrogate multiple locations simultaneously enable the visualization of intercellular communications—the mapping of neuronal activity. In this section we will provide two types of examples, one at the population level where stimulation of the Schaffer collateral axons in the CA3 region of the hippocampus will mediate a response in CA1 pyramidal cells [7] and the second at the individual cell level depicting both chemical and electrical synaptic activities. As shown in Fig. 1, the response of the different layers in the CA1 region of the hippocampus can be quite varied. When the GEVI ArcLight [19] is expressed in CamKII^{+} cells in the CA1 region of the mouse hippocampus, a

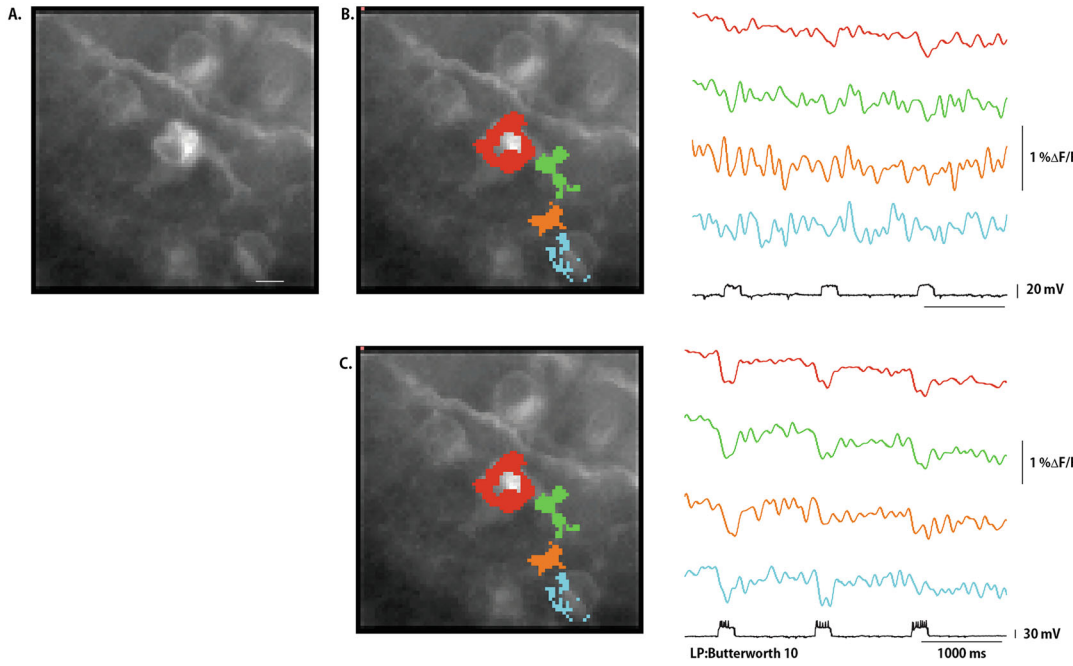

Fig. 2 Imaging intercellular communications at the cellular level. (**a**) Resting light intensity of retinal ganglion cells expressing the GEVI, Bongwoori-R3. (**b**) The cell in the center (red pixels) is under whole-cell current clamp. Low stimulation results in a small change in membrane potential that can only be observed in the soma. **(c)** Increasing the stimulation yields action potentials resulting in observable optical signals in the soma (red pixels), axon (green pixels), and neighboring cells (orange and blue pixels—modified from Jung et al., 2023 [10])

depolarizing signal (red pixels in the heat map) can be detected immediately upon stimulation of the Schaffer Collateral axons with the strongest signal in the Stratum radiatum. This is followed by a hyperpolarizing signal most intensely seen in the oriens layer (blue pixels in the heat map). Pharmacology can then be employed to further characterize the synaptic connections mediating the response (Fig. 1). Note that calcium imaging with GCaMP6f [8] yields a more robust optical signal compared to the GEVI for the depolarizing event but completely misses the hyperpolarizing signal [7].

The second example involves the excitation of an individual retinal ganglion cell. An ex vivo prep of mouse retinal ganglion cells expressing the GEVI, Bongwoori-R3 [9], is shown in Fig. 2a. The cell in the center is under whole current clamp. Current injection that does not illicit an action potential results in a subthreshold depolarization of the neuron that can only be detected in the soma (Fig. 2b). Stronger stimulation resulting in action potential firing yields optical signals in the soma, the axon, and neighboring cells

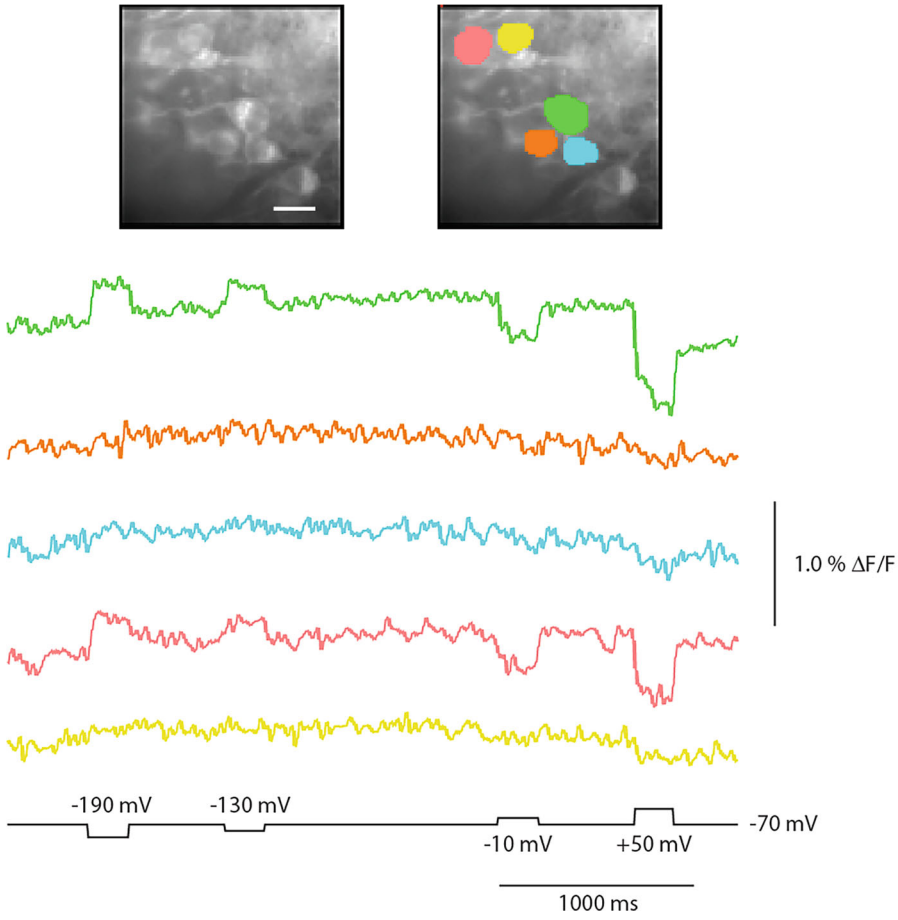

Fig. 3 Imaging an electrical synapse. Image on the left shows the resting light intensity of retinal ganglion cells expressing the GEVI, Bongwoori-R3. The image on the right shows the regions of interest corresponding to soma different retinal ganglion cells. The corresponding fluorescence traces of those cells are shown below. The cell in region one is voltage clamped (protocol at bottom in black—holding potential −70 mV). The traces are the average of 16 trials and were subjected to offline low pass Butterworth filtering of 30 Hz. (Modified from Jung et al., 2023 [10])

(Fig. 2c). Electrical synapses can also be detected using whole-cell voltage clamp (Fig. 3). Here, it is important to use hyperpolarizing pulses to confirm that the communication is via electrical synapses.

2 Materials

2.1 Animals, Reagents, and Consumables for Hippocampal Slice Voltage Imaging

1. Mice: Ca^{2+}/calmodulin-dependent protein kinase II (CaMKII) α -Cre mice (#005359; Jackson Laboratory, Bar Harbor, ME).
2. AAV1.hSyn.Flex.ArcLightDco.WPRE.SV40.
3. AAV1.Syn.Flex.GCaMP6f.WPRE.SV40.

4. Acetaminophen (Children's Tylenol, Johnson & Johnson, NJ).
5. Halothane (Sigma, St. Louis, MO).
6. Isoflurane (Sigma, St. Louis, MO).
7. 100% O_2 gas cylinder.
8. 95% O_2/5% CO_2 gas cylinder.
9. Artificial cerebrospinal fluid (ACSF; in mM; 240 Sucrose, 26 $NaHCO_3$, 2.5 KCl, 1.0 $CaCl_2$, 4 $MgCl_2$, 1.25 NaH_2PO_4, and 10 D(+)-glucose, pH 7.4, saturated with 95% O_2/5% CO_2).
10. High-sucrose artificial cerebrospinal fluid (Sucrose ACSF; in mM; 240 sucrose, 26 $NaHCO_3$, 2.5 KCl, 1.0 $CaCl_2$, 4 $MgCl_2$, 1.25 NaH_2PO_4, and 10 D(+)-glucose, pH 7.4, saturated with 95% O_2/5% CO_2).
11. D-AP5, CNQX, bicuculline, and tetrodotoxin (TTX) (all from Sigma, St. Louis, MO).

2.2 Animals, Reagents, and Consumables for Retinal Ganglion Cell Voltage Imaging

1. Retinal degenerative mice (C57BL/6J strain, or C57BL/6J-*Pde6b*$^{rd1\text{-}2J}$/J; #004766) Jackson Laboratory.
2. AAV2/2.hSyn.Bongwoori-R3 (KIST virus facility, Republic of Korea).
3. Membrane filter (Merck).
4. Ringer's solution: 124 mM NaCl, 2.5 mM KCl, 2 mM $CaCl_2$, 2 mM $MgCl_2$, 1.25 mM NaH_2PO_4, 26 mM $NaHCO_3$, 22 mM D-glucose.
5. Internal solution: 120 mM K-aspartate, 4 mM NaCl, 4 mM $MgCl_2$, 1 mM $CaCl_2$, 10 mM EGTA, 3 mM Na_2ATP, 5 mM HEPES.

2.3 Instrumentation for Both Hippocampal Slice and Retinal Ganglion Cell Voltage Imaging

1. Induction chamber (VetEquip).
2. Stereomicroscope (Nikon).
3. Digital stereotaxic instruments (Stoelting).
4. Injector and controller (World Precision Instruments).
5. Beveled needle (World Precision Instruments).
6. Stereomicroscope (Olympus).
7. Temperature controller (Warner Instruments).
8. Bath chamber (Warner instruments).
9. Slice anchor (Warner instruments).
10. Borosilicate glass capillaries (World Precision Instruments).
11. Micropipette puller (Sutter Instrument).

12. Upright fluorescence microscope system (Scientifica; equipped with both 10× and 60× water immersion objectives -Olympus, a 460 nm LED, and a GFP filter set).
13. Motorized micromanipulator (Scientifica).
14. High-speed charge-coupled-device (CCD) camera (Red Shirt Imaging).
15. Camera software (Red Shirt Imaging).
16. 10× and 60× water immersion objective lenses (Olympus; 0.30 and 1.00 NA).
17. 460 nm LED (Prizmatix; set to illuminate the specimen plane with a GFP excitation intensity of 1 mW/mm^2).
18. GFP filter (Semrock).
19. Amplifier (Molecular Devices).
20. Digitizer (Molecular Devices).
21. Patch software (Molecular Devices).

3 Methods

3.1 Population Imaging of Synaptic Connections in the Mouse Hippocampus

Optics: A high-speed CCD camera (Neuro CCD, Redshirt Imaging, Decatur, GA) was connected to the c-mount port of an upright epifluorescence microscope (Slicescope, Scientifica, East Sussex, UK), incorporating a GFP filter set (GFP-3035D-OMF, Semrock, Rochester, NY) and a 10× water immersion objective lens (UMPlanFL N; NA = 0.3, Olympus, Tokyo, Japan). 460 nm LED light (UHP-Mic-LED-460, Prizmatix, Givat-Shmuel, Israel) was connected to an EPI excitation light source port through a liquid light guide.

Electrophysiology setup: To monitor the field potential from CA1 str. pyr., an ACSF-filled glass capillary pipette (≈ 1 μm tip diameter, 5 MOhm) was connected to a patchclamp amplifier, Multiclamp 700B (Molecular Devices, San Jose, CA).

Stimulator: A bipolar tungsten electrode (30201, FHC, Bowdoin, ME) was connected to an isolator (model DS3, Digimeter Ltd., Hertfordshire, UK). The isolator can be triggered by the analog output port of the high-speed CCD camera system or the patchclamp amplifier. We prefer triggering via the camera to facilitate the coordination of the optical response and the electrical recording.

Perfusion system: To keep the brain slices functioning during the imaging, a continuous supply of oxygenated fresh ACSF to the slice is necessary. A simple conventional intravenous infusion tubing line routed through an inline temperature controller (TC-344B, Warner Instruments, CT) reaching to the

microscope slice chamber is sufficient to maintain activity at a more physiologically relevant temperature. Bath levels in the slice chamber can be maintained with a plumbing outlet connected to a vacuum pump (Linicon Vacuum Pump 6L/Min 15/14W, Nitto Kohki, Japan). Keep ACSF saturated with 95% O_2/5% CO_2 by bubbling. To prevent the dropdown of oxygen concentration in the tubing, avoid using silicon tubing. Instead, the use of oxygen impermeable tubing such as TYGON® tubes is strongly recommended.

3.1.1 AAV Injection

For an online visualized protocol of a similar AAV injection protocol, see Lowery et al. (2010) [11].

1. Adult mice older than 4 weeks were anesthetized by inhalation anesthesia using 1.5–3% isoflurane mixed with 100% Oxygen.
2. Secure the anesthetized mouse onto a stereotaxic apparatus (51730D, Stoelting, Wood Dale, IL) under a continuous administration of inhalation anesthesia.
3. Perform craniotomies (approximately 2 mm diameter) using a surgical drill (K1070; Foredom, Bethel, CT) at coordinates 1.7 mm posterior to the bregma and 1.2 mm lateral to the midline bilaterally.
4. Inject 400 nL of AAV1.hSyn.Flex.ArcLightDco.WPRE.SV40 (titer 4.83e13 GC/mL) or AAV1.Syn.Flex.GCaMP6f.WPRE.SV40 (titer, 4.38e13 GC/mL) into the dorsal hippocampus using a glass-capillary injection pipette (25 μm tip inner diameter) with 100 nL/min flow rate.
5. Suture the scalp and treat it with povidone-iodine.
6. Return the mice to their home cage, warmed by an electric blanket, and provide them with water containing 1.6 mg/mL acetaminophen (Children's Tylenol, Johnson & Johnson, NJ) until they fully recover.
7. After at least 2 weeks post-injection, mice were subjected to the following experiments.

3.1.2 Hippocampal Slice Preparation

For an online visualized protocol of a similar hippocampal slice cutting protocol, see Baccini et al. (2021) [12].

1. Anesthetize the mice deeply with halothane inhalation (Sigma).
2. After confirming the loss of reflex following the tail pinch, decapitate by sharp surgical scissors or decapitator. Immediately after the decapitation, extract the whole brain and submerge it into a chilled sucrose ACSF saturated with 95% O_2/5% CO_2 for 5 min.
3. Using a sharp razor blade, cut the whole brain coronally at the posterior end of the cerebral cortex and remove the cerebellar

cortex. Put cyanoacrilate-based instant glue (such as loctite and crazy glue) on the vibratome stage and attach the cut surface of the brain facing down on the glue. (Gluing down the agar block on the stage and support the ventral side of the brain is helpful to prevent the distortion of the brain block during the slicing.)

4. Set the vibratome stage attached with the brain prepared in the last step on the Vibratome (VT-1200, Leica, Nussloch, Germany) chamber filled with chilled sucrose ACSF, and cut acute coronal hippocampal slices (300 μm thick and approximately 1.7 mm posterior to the bregma).

Slice Preparation and Drug Application

300 μm thick acute coronal brain slices (≈1.7 mm posterior to bregma) were made after the deep anesthesia of the mice with halothane (Sigma). Isolated brain was sliced by Vibratome (VT-1200, Leica, Nussloch, Germany) in a cold, high-sucrose, artificial cerebrospinal fluid (ACSF) solution containing (in mM): 240 Sucrose, 26 $NaHCO_3$, 2.5 KCl, 1.0 $CaCl_2$, 4 $MgCl_2$, 1.25 NaH_2PO_4, and 10 D(+)-glucose, pH 7.4, by gassing with 95% O_2/5% CO_2. Slices were then placed in an interface chamber filled with ACSF oxygenated with 95% O_2/5% CO_2. Slices were incubated at 36 °C for at least 1 h. During the experiment, a slice was placed on the microscope stage chamber with continuous perfusion of ACSF at 1–2 mL/min. The temperature of ACSF on the recording chamber was adjusted to 33 ± 0.5 °C by a temperature controller (TC-344B, Warner Instruments, CT) throughout the experiment. When required, the following drugs were dissolved in perfused ACSF for perfusion: 50 μM D-AP5, 40 μM CNQX, 40 μM bicuculline and 1 μM tetrodotoxin (TTX) (all from Sigma). A minimum of 10 min of drug perfusion was done to ensure proper delivery.

Neuronal Activity Imaging

A high-speed CCD camera (Neuro CCD, Redshirt Imaging, Decatur, GA) was connected to the c-mount port of an upright epifluorescence microscope (Slicescope, Scientifica, East Sussex, UK) in combination with a GFP filter set (GFP-3035D-OMF, Semrock, Rochester, NY) and a 10× water immersion objective lens (UMPlanFL N; NA = 0.3, Olympus, Tokyo, Japan). Through the conventional EPI light source port, 8.8 mW of 460 nm LED light (UHP-Mic-LED-460, Prizmatix, Givat-Shmuel, Israel) was applied to illuminate the whole field of view (1.7 mm diameter, 3.7 mW/mm^2) (*see* **Note 1**). The fluorescent signal of ArcLight was acquired with an 80 × 80 pixel CCD camera (*see* **Note 2**). The frame rate sampling was performed at 1 kHz from the dorsal hippocampal CA1 region (500 μm × 500 μm) (*see* **Note 3**). The spatial resolution before spatial filtering was 6.25 μm/pixel. All the acquired fluorescent signals were processed as fractional

fluorescence change values [$\%\Delta F/F = ((F_x - F_0)/F_0) * 100$] with NeuroPlex (Redshirt Imaging, Decatur, GA) using an offline Butterworth low-pass filter (value 50). All the frame-subtracted ArcLight/GCaMP6f mapping images shown in this report are processed with 3 × 3 mean iteration 1 long-pass filter provided by NeuroPlex (*see* **Note 5**).

Region of Interest for Spatial Averaging of Fluorescent Signals
To obtain the fluorescence signal traces from each stratum in CA1 region, each stratum in the entire field of view was selected as a region of interest and spatially averaged. All the ANOVA analyses were performed using OriginPro (OriginLab, Northampton, MA) (*see* **Note 4**).

GEVI Imaging of Retinal Ganglion Cells
The optics and recording hardware are the same as that described for the hippocampal recordings. The lone exception being the use of a 60× water immersion objective.

1. Mice were given anesthesia using a mixture of 3–5% isoflurane in oxygen within the enclosed induction chamber. Afterward, the virus was injected into their eyes while using a stereomicroscope. To administer the injection, a beveled needle was used to make a puncture behind the outer edge of the eye. Then, 2 μL of virus solution in the administrating pipette was injected into the vitreous cavity inside the eye, with a controlled injection rate of 20 nL/s.
   (a) To perform an intravitreal injection, a glass capillary is inserted into the pars plana, which is the outer region of the front eye. The purpose of the glass capillary is to directly deliver the AAV into the vitreous humor, which fills the eye. This injection reaches a depth of approximately 1.5–1.8 mm below the surface of the eye.
   (b) It is recommended to inject AAV at high concentrations toward the retina because the intravitreal injection can potentially dilute the AAV particles before reaching the target retinal ganglion cells and the challenge of penetrating the inner limiting membrane, which hinders AAV delivery to the desired cells.
   (c) The AAV serotype 2 (AAV2) carrying Rep2 and Cap2 genes showed improved expression of Bongwoori-R3 proteins in retinal ganglion cells compared to AAV1.
2. After 2 weeks, injected mice were euthanized using cervical dislocation. Retinas were prepared in Ringer's solution allowing the retina to be separated from the eyes while using a stereomicroscope. The isolated retina was positioned with the ganglion layer facing upward on a membrane filter. To secure the retina in place, the slice anchor was used within a bath chamber beneath a one-photon fluorescent microscope.

Throughout the procedure, the solution in the chamber was constantly supplied with a mixture of 95% O_2 and 5% CO_2, with a flow rate of 1 mL/min. The temperature inside the chamber was maintained at a steady 34 °C using an automatic temperature controller.

3. An upright fluorescence microscope system was used to image fluorescence. Fluorescent images were captured by a high-speed charge-coupled-device (CCD) camera. To synchronize optical and electrical recordings, illumination, image acquisition, and electrical stimulation were all controlled by the camera software.
   (a) To allow access for electrophysiological recordings, the inner limiting membrane (ILM) was removed using a glass pipette. An exposed retinal ganglion cell expressing the GEVI was subjected to whole-cell patch clamp using micropipettes with a resistance of 5–15 MΩ.
   (b) The inner limiting membrane, consisting of astrocytes and Müller cells, acts as a protective layer situated between the retina and the gel-like vitreous humor inside the eye.
   (c) To gain direct access to the retinal ganglion cells located beneath the inner limiting membrane, a fine glass pipette is used to gently remove this membrane. This procedure allows for performing patch-clamp experiments on the RGCs, enabling the precise control of the membrane potential of a single cell.
4. The required stimulation to transition from subthreshold to suprathreshold membrane depolarizations should be determined empirically (generally 100–500 pA, 200 ms). Intercellular communication correlating only with suprathreshold (not subthreshold) stimulation of the patched cell reveals chemical synapse activity (Fig. 2).
5. Electrical synapses can also be detected by transitioning the patched cell to a whole-cell voltage clamp configuration (−120 to 120 mV, 200 ms, holding potential, −70 mV). The voltage steps applied to the plasma membrane should include hyperpolarizing steps to ensure the presence of electrical synaptic connections (Fig. 3).

4 Notes

1. GEVI use remains a difficult endeavor for several reasons [13]. Voltage transients occur at the plasma membrane. This spatial restriction limits the amount of probe, and, therefore, the total light available for reporting neuronal activity. Shot

noise due to the statistical nature of photon emission determines the accuracy of an optical recording. Measuring more photons lowers the noise relative to the mean fluorescence intensity resulting in an improved SNR. This spatial restriction also requires efficient trafficking of the probe to the plasma membrane. Internal fluorescence contributes a non-responsive background that lowers the SNR. In general, the more light the better the signal. However, strong illumination can cause bleaching as well as photo-toxicity [13, 14]. A trade-off must be considered between intensity, probe stability, and tissue health. This is usually determined empirically as variations in expression levels of the GEVI will most likely be encountered.

2. Camera considerations: Another challenge for voltage imaging is the speed of the response. While this chapter focused on synaptic activity, the experimenter will need to be able to differentiate action potentials from subthreshold activity. The time frame for an action potential is 1–2 milliseconds requiring acquisition frame rates near or above one kHz.
3. Light source intensity is critical for obtaining reliable optical signals. If the acquisition frame rate is too slow to image individual action potentials (frame rate at or in excess of 1 kHz), then the resulting temporal binning of the voltage signal will make analysis difficult. If the light level is too low for a reliable signal, multiple trials can be averaged in an attempt to improve the SNR. For more discussion of camera and light source considerations please see Braubach et al., 2015 [15].
4. Region of interest: The region of interest chosen by the experimenter can have a significant bearing on the signal seen. For example, in Fig. 2 pixels were carefully chosen to limit the contribution of non-responding fluorescence. There are multiple methods for determining a region of interest. The first is based solely on anatomy. An example of this approach is shown in Fig. 3 where the entire soma of different cells are shown. Careful analysis would reveal that the internal fluorescence yields a much smaller optical signal than the pixels correlating to the plasma membrane.

   To detect subcellular signals, algorithms can be employed to identify regions of interest. In Fig. 2 the algorithm was a simple frame subtraction replot of the optical recording. The mean fluorescence for all pixels during the stimulation (the average fluorescence of 50 msec during the stimulation for example) was subtracted from the mean fluorescence of the baseline fluorescence usually at the start of the recording. Plotting the difference can reveal which pixels experienced fluorescence change.

5. GEVI choice. There are several GEVIs available for voltage imaging [6, 9, 16–19]. Each one has strengths and weaknesses. Here we will only discuss a few important points. The first is that ΔF/F can be misleading [13]. While it is an important characteristic since it helps normalize differences in expression levels, different GEVIs have different resting intensities (F). Since ΔF/F is a function of F, a probe with a 40% ΔF/F signal may not be as good as a probe with 20% ΔF/F.

   The second misconception is that speed is the ultimate parameter. Again, speed is important, but a fast probe may not give as large as a fluorescence change as a slower probe. The on rate constant is the length of time it takes for the probe to reach 63% of its maximum fluorescence change. If a slow probe yields a much larger fluorescence change, then the number of photons detected even for fast events may be more than a faster probe that yields a smaller change in the number of photons [17]. Finally, many new GEVIs are restricted to the soma with a targeting motif [6, 16] since expression in the processes can create a large background fluorescence (Fig. 1). However, this eliminates the ability to see voltage changes in the processes which may be desirable for the question being addressed.

   We generally start with ArcLight [19] as it has one of the largest fluorescence changes of all the GEVIs published [20, 21] and is therefore a good benchmark for detecting signals. Indeed, we highly recommend new users to also try voltage dyes to ensure that a voltage-dependent optical signal can be detected by the hardware in use.

Acknowledgments

In loving memory of Dr. Lawrence B. Cohen who provided helpful comments during the writing of this submission. M.I. is funded by the National Research Foundation of Korea (NRF), grant 2022M3E5E8017395. Y.K.S. is funded by the Korea Medical Device Development Fund, project number KMDF_PR_20210527_0006. B.J.B. is funded by the Korea Institute of Science and Technology intramural funding, 2E32162.

References

1. Salzberg BM et al (1977) Optical recording of neuronal activity in an invertebrate central nervous system: simultaneous monitoring of several neurons. J Neurophysiol 40(6): 1281–1291. https://doi.org/10.1152/jn.1977.40.6.1281
2. Sepehri Rad M et al (2017) Voltage and calcium imaging of brain activity. Biophys J 113(10):2160–2167. https://doi.org/10.1016/j.bpj.2017.09.040
3. Gupta RK et al (1981) Improvements in optical methods for measuring rapid changes in membrane potential. J Membr Biol 58(2): 123–137. https://doi.org/10.1007/BF01870975

4. Loew LM (2015) Design and use of organic voltage sensitive dyes. Adv Exp Med Biol 859: 27–53. https://doi.org/10.1007/978-3-319-17641-3_2
5. Rhee JK, Iwamoto Y, Baker BJ (2021) Visualizing oscillations in brain slices with genetically encoded voltage indicators. Front Neuroanat 15:741711. https://doi.org/10.3389/fnana.2021.741711
6. Piatkevich KD et al (2019) Population imaging of neural activity in awake behaving mice. Nature 574(7778):413–417. https://doi.org/10.1038/s41586-019-1641-1
7. Nakajima R, Baker BJ (2018) Mapping of excitatory and inhibitory postsynaptic potentials of neuronal populations in hippocampal slices using the GEVI, ArcLight. J Phys D Appl Phys 51(50). https://doi.org/10.1088/1361-6463/aae2e3
8. Chen TW et al (2013) Ultrasensitive fluorescent proteins for imaging neuronal activity. Nature 499(7458):295–300. https://doi.org/10.1038/nature12354
9. Lee S et al (2017) Improving a genetically encoded voltage indicator by modifying the cytoplasmic charge composition. Sci Rep 7(1):8286. https://doi.org/10.1038/s41598-017-08731-2
10. Jung Y et al (2023) Imaging electrical activity of retinal ganglion cells with fluorescent voltage and calcium indicator proteins in retinal degenerative blind mice. bioRxiv:2023.2012.2010.571014. https://doi.org/10.1101/2023.12.10.571014
11. Lowery RL, Majewska AK (2010) Intracranial injection of adeno-associated viral vectors. J Vis Exp 45. https://doi.org/10.3791/2140
12. Baccini G, Brandt S, Wulff P (2021) Preparation of acute slices from dorsal hippocampus for whole-cell recording and neuronal reconstruction in the dentate gyrus of adult mice. J Vis Exp 170. https://doi.org/10.3791/61980
13. Rhee JK et al (2020) Biophysical parameters of GEVIs: considerations for imaging voltage. Biophys J. https://doi.org/10.1016/j.bpj.2020.05.019
14. Icha J, Weber M, Waters JC, Norden C (2017) Phototoxicity in live fluorescence microscopy, and how to avoid it. BioEssays News Rev Mol Cell Dev Biol 39(8). https://doi.org/10.1002/bies.201700003
15. Braubach O, Cohen LB, Choi Y (2015) Historical overview and general methods of membrane potential imaging. Adv Exp Med Biol 859:3–26. https://doi.org/10.1007/978-3-319-17641-3_1
16. Platisa J et al (2023) High-speed low-light in vivo two-photon voltage imaging of large neuronal populations. Nat Methods. https://doi.org/10.1038/s41592-023-01820-3
17. Yi B et al (2018) A dimeric fluorescent protein yields a bright, red-shifted GEVI capable of population signals in brain slice. Sci Rep 8(1): 15199. https://doi.org/10.1038/s41598-018-33297-y
18. Milosevic MM et al (2020) In vitro testing of voltage indicators: Archon1, ArcLightD, ASAP1, ASAP2s, ASAP3b, Bongwoori-Pos6, BeRST1, FlicR1 and Chi-VSFP-Butterfly. eNeuro. https://doi.org/10.1523/ENEURO.0060-20.2020
19. Jin L et al (2012) Single action potentials and subthreshold electrical events imaged in neurons with a fluorescent protein voltage probe. Neuron 75(5):779–785. https://doi.org/10.1016/j.neuron.2012.06.040
20. Bando Y et al (2019) Comparative evaluation of genetically encoded voltage indicators. Cell Rep 26(3):802–813 e804. https://doi.org/10.1016/j.celrep.2018.12.088
21. Armbruster M et al (2022) Neuronal activity drives pathway-specific depolarization of peripheral astrocyte processes. Nat Neurosci 25(5):607–616. https://doi.org/10.1038/s41593-022-01049-x

Chapter 15

Visualization of Synapses in Larval Stages of *Drosophila melanogaster* Using the GRASP Technique

Claudia Gualtieri and Fernando J. Vonhoff

Abstract

The flow of information within the nervous system occurs via precise connections between synaptic partners. In recent years, the development of various methods to visualize synaptic contacts has helped elucidate the connectivity within complex neuronal networks. One such method is the GRASP (GFP Reconstitution Across Synaptic Partners) technique that consists of the expression of a portion of the green fluorescent protein (GFP) at each side of the synapse, allowing the reconstitution of green fluorescence depending on the proximity of the cells expressing such tools. In *Drosophila*, various studies have shown the successful application of GRASP in adult flies to identify synaptic partners, whereas its use at earlier stages such as in first instar larval stages remains less common. Therefore, we provide here a detailed protocol for the visualization of GRASP-based neuronal contacts within previously established synaptic partners in first and third instar larvae.

Key words GRASP, Larvae, Nociceptive pathways, Confocal microscopy, Synaptic connectivity, Connectome mapping, Invertebrate

1 Introduction

Understanding how neural circuitry is formed during development often provides instructive insight into the appropriate adult connectivity within neural networks. Multiple techniques are available in *Drosophila* to analyze contacts across synaptic partners [1], which in conjunction with its tractable and stereotyped anatomy allow exquisite resolution in anatomical studies of synaptic formation and withdrawal.

Originally developed in *Caenorhabditis elegans* [2], the GRASP (GFP Reconstitution Across Synaptic Partners) technique has become one of the most widely implemented and extensively developed labeling techniques for connectome mapping in *Drosophila*

Tolga Soykan and Alexandros Poulopoulos (eds.), *Synapse Development: Methods and Protocols*, Methods in Molecular Biology, vol. 2910, https://doi.org/10.1007/978-1-0716-4446-1_15,

melanogaster. In flies, the GRASP technique can be applied using the binary expression systems, a genetic tool controlling expression via the combination of a transcriptional activator and an effector. The binary expression systems available in flies are the GAL4/UAS, the LexA/LexAop, and the Q system. With GRASP, one portion of the split GFP (split GFP tag GFP11—spGFP11) can be selectively expressed in one cell type using one binary system, while expressing the other portion of the split GFP (split GFP tag GFP1-10—spGFP1-10) in another cell type using a second binary system.

Here, we used GRASP to provide additional *in vivo* evidence regarding the connectome in the larval nociceptive sensory pathway of wildtype-like *Drosophila* and investigate the changes during development leading to proper adult synaptome morphology. The nociceptive sensory pathway is involved in the discrimination of different types of noxious stimuli such as heat, chemical, and strong mechanical stimuli via a complex neuronal network that includes a specific set of sensory neurons, the class IV sensory neurons (cIV) dendritic arborization (da) sensory neurons [3], to play a major role in nociception. The synaptic connections between the major cellular components of the nociceptive network have been characterized using electron microscopy and 3D-reconstruction approaches [4–6]. The connections between cIV nociceptive sensory neurons and their postsynaptic Basin-4 interneurons (Fig. 1) have been well-characterized at the anatomical and functional level [4] and were used in this study to visualize synaptic connectivity at early (first instar, Fig. 2a) and late (third instar, Fig. 2b) larval stages.

The fly lines used here are described in Table 1 and were received from the Bloomington Drosophila Stock Center (BDSC).

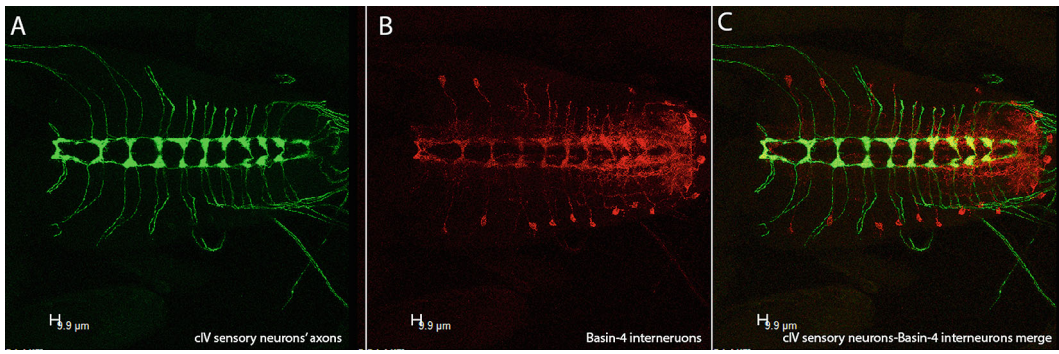

Fig. 1 Structures formed by cIV sensory neurons' axonal projections and Basin-4 interneurons in the larval ventral nerve cord (VNC). Panel **A** shows in green the axonal projections of nociceptors expressing GFP in VNC via PPK-CD4-TdGFP. Panel **B** shows in red the Basin-4 interneurons expressing TdTomato in VNC via Basin4-GAL4 > UAS-CD4-TdTomato. Panel **C** shows the concurrent pattern formed by the axonal projections of nociceptors (green) and the Basin-4 interneurons (red) location in the VNC. Images shown were collected from fixed tissue of a female third instar larva using a Leica SP5 confocal microscope

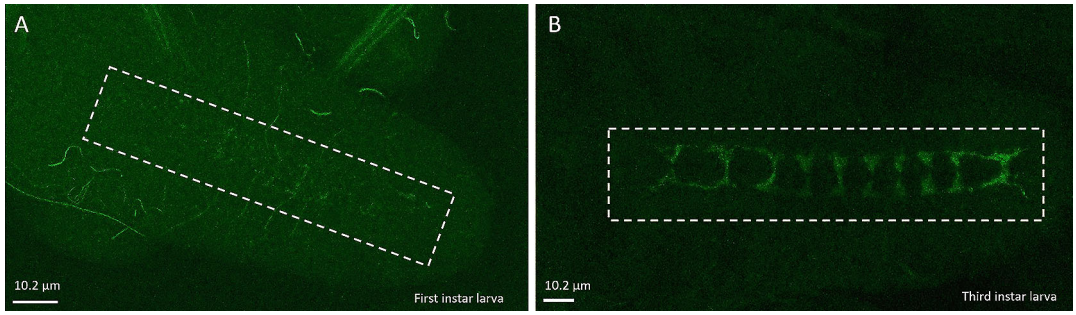

Fig. 2 GRASP signal of synapses between nociceptors and Basin-4 interneurons at different developmental stages. Panel **A** shows the GRASP signal of synapses between nociceptors and Basin-4 interneurons in a first instar larva within <6 h after embryo hatching. Panel **B** shows the GRASP signal between nociceptors and Basin-4 interneurons in a wandering third instar larva

Table 1
Fly strains

Genotype	Identification number	Source
w;UAS-CD4-TdTomato/UAS-CD4-TdTomato; Basin4-GAL4 /Basin4-GAL4	Made from RRID:BDSC 32222 and RRID:BDSC_ 46389	BDSC
w;ppk-CD4-tdGFP/UAS-CD4-TdTomato; Basin4-GAL4/Basin4-GAL4	Made using RRID:BDSC_35842	BDSC
w;UAS-nSyb-spGFP1-10,lexAop-CD4-spGFP11/ CyO	RRID:BDSC_64314	BDSC
w; Basin4 (R57F07)-LexA; ppk-GAL4	Made from (RRID:BDSC_54899 and RRID:BDSC_32079)	BDSC
y w; Sp-1/CyO; 20XUAS-post-t-GRASP, 10XQUAS-pre-t-GRASP	RRID:BDSC_79037	BDSC

2 Materials

2.1 Larvae Preparation

2.1.1 Larval Brain Dissection First Instar

1. Lid of a 35 mm × 10 mm cell culture dish.
2. Glass Pasteur Pipette.
3. P200 micropipette.
4. P100 micropipette.
5. 4% Paraformaldehyde (PFA).
6. 0.1 M Potassium phosphate buffer (PPB).
7. 0.1 M Phosphate Buffered Saline (PBS).
8. 2 Forceps (Dumont SWISSMADE—Item No. 11252-20).

2.1.2 Larval Brain Dissection Third Instar

1. Sylgard containing dissection plate.
2. Dissecting pins (Austerlitz INSECT PINS—Minutiens 0.10 mm Fine Science Tools Item No. 26002-10).
3. Forceps (Dumont SWISSMADE—Item No. 11252-20).
4. Dissecting scissors (Fine Science Tools Item No. 15000-00).
5. 0.1 M Phosphate Buffered Saline (PBS).
6. Glass Pasteur pipette.
7. Deionized (DI) Water.
8. Paint brush.
9. Three-well micro spot plate (Electron Microscopy Sciences #71561-01).
10. Dissecting microscope.

2.2 Larval Fixation

1. 0.1 M Phosphate Buffered Saline (PBS).
2. 16% PFA (Electron Microscopy Sciences #15700).
3. 0.1 M Potassium phosphate buffer (PPB).
4. Glass Pasteur pipette.
5. P1000 micropipette.

2.3 Larval Fillet/ Larval Brain Mounting

1. Microscope slide.
2. Forceps (Dumont SWISSMADE—Item No. 11252-20).
3. Glycerol.
4. Cover glass.
5. Clear nail polish.

2.4 Immunostaining

1. Microcentrifuge tube.
2. P200 micropipette.
3. Nutator.
4. 0.1 M Phosphate Buffered Saline (PBS).
5. PBS-Triton (0.1 M PBS + 0.3% TritonX100).
6. Blocking solution (PBS-Triton + BSA 10 mg/mL).
7. Anti-GFP primary antibody (rabbit anti-GFP Tag Abfinity, ThermoFisher G10362, 1:250 in PBS-Triton).
8. Secondary antibody (goat anti-rabbit Invitrogen Alexa Fluor 488, IgG A11008, 1:200 in PBS).

3 Methods

3.1 Growing Larvae

The life cycle of *Drosophila melanogaster* has four stages: embryonic, larval, pupal, and adult. The fertilized egg needs 22–24 h after egg laying at 25 °C for it to hatch into a larva. Within the larval stage, there are three substages: the first, second, and third instar. Between all three stages—the first and second lasting around 24 h each, and the third lasting 3 days—the larvae undergo molting. The third instar larva then undergoes transformation into a pupa. After about 3 days, the pupa emerges as a fully developed adult fruit fly. Our flies are reared at 25 °C in a 12/12 h light/dark incubator on standard plastic vials following a standard molasses food as described in Oyeyinka et al. 2022 [7].

3.2 Timed Egg Lays and Larval Collection

Growing first instar larvae requires setting up egg chambers where females from fly crosses can lay eggs on a (apple or grape) juice agar plate. Timed egg chambers can be set to monitor the time windows when hatching will occur. First instar larvae will appear after ~22–24 h after egg laying and the larvae can be collected directly from the juice agar plates. Depending on the experiment, young 1–8 h after larval hatching (hALH) or older 16–20 hALH larvae can be collected for dissection. Wandering third instar larvae instead can be collected from the fly vials containing food mix (yeast, molasses, cornmeal) where crosses are housed. Here, we used a commercially available grape agar mix (Flystuff 47–102 Nutri-Fly® Grape Agar Premix) and followed the vendor's instructions to make agar plates using 35 mm × 10 mm Petri dishes. Adult flies are placed in a small acrylic embryo collection cage (Flystuff #59–105) with an agar plate containing a drop of yeast paste. Cage with adult flies is placed in the 25 °C incubator and females will lay eggs on the agar surface as well as on the yeast paste. The agar plate is replaced with a fresh one every 2–4 h and the plate with eggs is kept in the 25 °C incubator to allow embryo development in a timed manner.

3.3 Larvae Preparation

3.3.1 Larval Brain Dissection and fixation - First Instar

Protocol adapted from Wu, J. S., & Luo, L., 2006 [8].

1. Pipette a few drops of 0.1 M PBS in a lid of a 10 mm cell culture dish.
2. With a paint brush collect first instar larvae from the agar plate and place them in the cell culture dish lid with 0.1 M PBS.
3. With one pair of forceps grab the larva halfway down the body while with a second pair of forceps grab the mouth hooks.
4. Gently pull the mouth hooks while holding on to the other half of the body. The brain lobes and ventral nerve cord will come out attached to the mouth hooks.

5. Place the mouth hooks/brain complex in 4% PFA. Leave to fix for ~20–25 min (*see* **Note 1**).
6. After fixation, with a pair of forceps move the mouth hooks/brain complex in PBS and leave for ~20–25 min (*see* **Note 2**).

3.3.2 Larval Brain Dissection - Third Instar

1. In a three-well micro spot plate place DI water.
2. Take a larva with a fine paint brush and gently wash it in DI water until the larva is clean of any residual food.
3. Take the larva and place it on the dissection plate.
4. Roll the larva on the dorsal side—where the two main tracheal trunks running along the longitudinal axis of the animal are visible.
5. With the forceps take a pin and pin down the larva starting at the posterior end.
6. Place another pin at the anterior end just behind the mouth hooks—make sure that both tracheal trunks are visible and lined up along the midline of the pinned larva.
7. Pipette PBS on the dissection plate so to cover the larva.
8. With scissors, make a small horizontal cut at the bottom of the pinned larva right above the bottom pin.
9. With the scissors, start cutting vertically along the dorsal midline in between the main tracheal trunks.
10. With another pin find the cuticle on the left bottom side of the pinned larva, open it, and pin it down.
11. Do the same with the top left cuticle, the bottom right and the top right cuticle as well—A total of four pins should have been used to open the larva in a fillet manner in addition to the two pins used to hold the larva from the bottom and the top.
12. Cut out and remove all fat tissue, gut, and other non-neuronal tissue (e.g., salivary glands).
13. The brain should be visible in the top middle part of the fillet, behind the mouth hooks, as a two-lobes + ventral nerve chord structure.

3.4 Larval Fixation - Third instar

1. Remove the PBS that is already present in the dissection plate where the larva is filleted.
2. Pipette 250 microliters of 16% PFA on the fillet.
3. To dilute the 16% PFA to 4%, pipette 750 microliters of PPB on the fillet.
4. Let fix for 1 h.

5. Remove the PFA solution and place it in the appropriate waste container.
6. Wash the fillet three times for 10 minutes each time with PBS.

3.5 Larval Fillet/ Larval Brain Mounting

For first instar larvae

1. Dip forceps in glycerol and place a small drop of glycerol on microscope slide (*see* **Note 3**).
2. Take the mouth hooks/brain complex from the PBS with forceps and place in the glycerol on microscope slide with brain side up.
3. Let cover glass fall on the microscope slide.
4. Seal sides of cover glass with clear nail polish.

For third instar larvae

1. Remove pins using forceps—Hold fillet down with second pair of forceps while removing the pins if needed.
2. Place a drop of glycerol on microscope slide.
3. Grab fillet at the anterior end using forceps and place it in the glycerol drop on microscope slide with brain side up. Multiple fillets can be added on the same microscope slide if needed.
4. Place a cover glass on the glycerol drop with fillet.
5. Remove glycerol excess with a kimwipe and seal sides of cover glass with clear nail polish.

3.6 Confocal Microscopy

As reported by Gordon, M. D., & Scott, K. [9], the GRASP signal can be detected without the need for immunohistochemistry. The GRASP signal can be detected with a confocal microscope and will appear as green puncta indicating the synapses between neurons. To collect these images, we used a LeicaSP5 confocal inverted microscope, objectives 40×/1.25 NA and 63×/1.4 NA, under the Argon excitation laser.

1. Place microscope slide under the confocal.
2. Locate the brain under transmitted light.
3. Scan the ventral nerve cord under laser illumination (*see* **Note 4**).
4. Identify and capture z-stack (*see* **Note 5**).

3.7 tGRASP

The GRASP technique has been further developed in *Drosophila* by Shearin H. K. et al. [10] to better target the signal to neuronal synapses. The targeted GRASP (tGRASP), indeed, targets the split-GFP portion both to the presynaptic side via a portion of the *cacophony* gene tagged with the split GFP tag GFP11 and to the postsynaptic side via a portion of the mouse Icam5 gene tagged with the split GFP tag GFP1-10. This enhances the specificity of

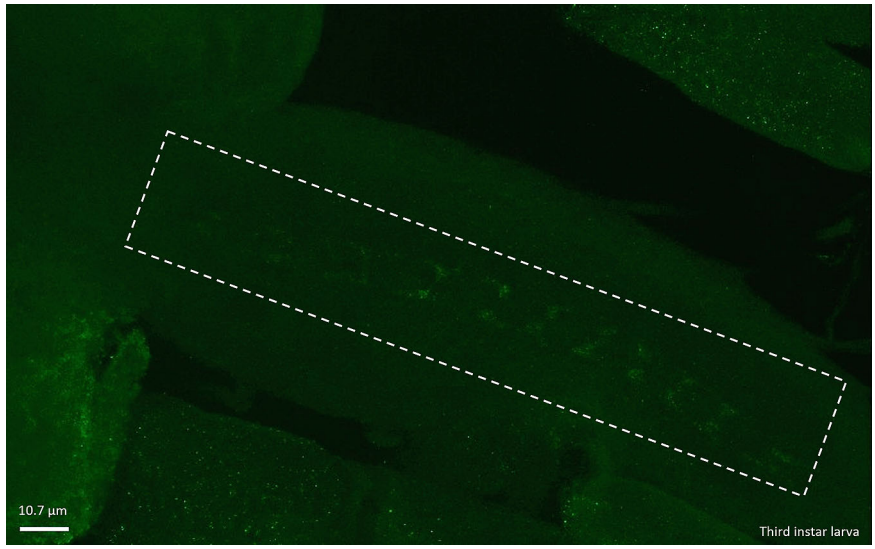

Fig. 3 tGRASP signal between cIV sensory neurons and Basin-4 interneurons in third instar larva. The synapses between nociceptors and Basin-4 interneurons are here detected via immunostaining of the signal emitted by the reconstituted GFP in a male third instar larva. In tGRASP, the split GFP portions are specifically targeted to the synapse both on the pre- and postsynaptic side

the reconstituted GFP signal, since the original GRASP only targeted the presynaptic side via the synaptic synaptobrevin protein tagged with the split GFP tag GFP1-10 in addition to the broadly membrane-localized split GFP component GFP11 via CD4. Based on our observations, tGRASP requires immunohistochemistry to detect evident GRASP signal. To confirm the GRASP signal that we detected using the classic GRASP technique, we looked at the synaptic contacts between nociceptors and Basin-4 interneurons at third instar larval stage using tGRASP (Fig. 3). The immunohistochemistry protocol followed was adapted from Wu, J. S., & Luo, L. [8] (*see* **Note 6**). For larvae preparation, fixation, and mounting (after immunostaining procedure) follow the materials and protocol as described for first instar larvae above.

3.7.1 Immunostaining

1. Add 150 uL PBS-Triton solution to a new microcentrifuge tube.
2. Place larval brains (for first instar) or fillets (for third instar) in microcentrifuge tube.
3. Close cap and turn upside down. Allow brains to set to bottom of tube.
4. Remove PBS-Triton carefully with micropipette.
5. Repeat a couple of times.
6. Add 150 uL PBS-Triton and allow brains to wash by placing tube on nutator for 20 min.

7. Repeat twice for a total of three 20 min washes.
8. Remove PBS-Triton and add 150 uL blocking solution. Allow to block on nutator for 30 min.
9. Remove blocking solution.
10. Add primary antibody (*see* **Note 7**).
11. Allow to stain on nutator at 4 °C for 2 nights.
12. Remove primary antibody (can be reused).
13. Add 150 uL PBS-Triton to the microcentrifuge tube with the brains. Close cap and turn upside down. Allow brains to set to bottom of tube.
14. Remove PBS-Triton carefully with micropipette.
15. Repeat steps #13 & #14.
16. Add 150 uL PBS-Triton and allow brains to wash by placing tube on nutator for 20 min.
17. Repeat twice for a total of three 20 min washes.
18. Remove PBS-Triton.
19. Add secondary antibody.
20. Allow to stain on nutator at 4 °C for 2 nights.
21. Remove secondary antibody.
22. Add 150 uL PBS-Triton to the microcentrifuge tube with the brains. Close cap and turn upside down. Allow brains to set to bottom of tube.
23. Remove PBS-Triton carefully with micropipette.
24. Repeat steps #22 & #23.
25. Add 150 uL PBS-Triton and allow brains to wash by placing tube on nutator for 20 min.
26. Repeat twice for a total of three 20 min washes.

4 Notes

1. Cut out the caps of microcentrifuge tubes to be used as containers where to place fixative and brains for fixation. Pipette 50 uL of 16% PFA and 150 uL of PPB (or directly ~200 uL 4% PFA) in the microcentrifuge cap. Leave the mouth hooks attached to the larval brain, this will make the brains sink better at the bottom of the microcentrifuge cap once fixed and therefore easier to grab with the forceps.
2. Cut out the caps of microcentrifuge tubes as containers where to place the PBS for washing the brains. Pipette ~200 uL of PBS in the microcentrifuge cap. For better washing, have multiple microcentrifuge caps and move the brains from cap to cap with fresh PBS every ~5 min.

3. On the microscope slide, place a circular donut sticker (or draw a circle with Vaseline) to fence a smaller area for mounting the brains. This will make it easier to find the brains under the microscope.
4. Set the laser to cover a wavelength between 496 nm and 510 nm. Also, we suggest a master gain of approximately 700, with the use of pinhole of 1 Airy Unit (AU) and bidirectional scanning.
5. Use minimal laser power (20–30%) to identify the z-stack limits first. Increase the laser power (up to 50–55%) when ready to capture the z-stack. Use approximately a 1 μm step size.
6. Carrying out immunohistochemistry on brains of first instar larvae using this protocol proved to be challenging.
7. Shearin et al. (2018) suggest the use of an antibody specifically recognizing the reconstituted GFP (rabbit anti-GFP Tag Abfinity, ThermoFisher G10362), which is the one used in this study. Additional anti-GFP antibodies could be used to detect the split-GFP portions.

References

1. Ni L (2021) Genetic transsynaptic techniques for mapping neural circuits in *Drosophila*. Front Neural Circuits *15*:749586. https://doi.org/10.3389/fncir.2021.749586
2. Feinberg EH, Vanhoven MK, Bendesky A, Wang G, Fetter RD, Shen K, Bargmann CI (2008) GFP Reconstitution Across Synaptic Partners (GRASP) defines cell contacts and synapses in living nervous systems. Neuron 57(3):353–363. https://doi.org/10.1016/j.neuron.2007.11.030
3. Grueber WB, Jan LY, Jan YN (2002) Tiling of the Drosophila epidermis by multidendritic sensory neurons. Development (Cambridge, England) 129(12):2867–2878. https://doi.org/10.1242/dev.129.12.2867
4. Ohyama T, Schneider-Mizell CM, Fetter RD, Aleman JV, Franconville R, Rivera-Alba M, Mensh BD, Branson KM, Simpson JH, Truman JW, Cardona A, Zlatic M (2015) A multilevel multimodal circuit enhances action selection in Drosophila. Nature 520(7549):633–639. https://doi.org/10.1038/nature14297
5. Hu C, Petersen M, Hoyer N, Spitzweck B, Tenedini F, Wang D, Gruschka A, Burchardt LS, Szpotowicz E, Schweizer M, Guntur AR, Yang CH, Soba P (2017) Sensory integration and neuromodulatory feedback facilitate Drosophila mechanonociceptive behavior. Nat Neurosci 20(8):1085–1095. https://doi.org/10.1038/nn.4580
6. Burgos A, Honjo K, Ohyama T, Qian CS, Shin GJ, Gohl DM, Silies M, Tracey WD, Zlatic M, Cardona A, Grueber WB (2018) Nociceptive interneurons control modular motor pathways to promote escape behavior in *Drosophila*. elife 7:e26016. https://doi.org/10.7554/eLife.26016
7. Oyeyinka A, Kansal M, O'Sullivan SM, Gualtieri C, Smith ZM, Vonhoff FJ (2022) Corazonin neurons contribute to dimorphic ethanol sedation sensitivity in Drosophila melanogaster. Front Neural Circuits 16:702901
8. Wu JS, Luo L (2006) A protocol for dissecting Drosophila melanogaster brains for live imaging or immunostaining. Nat Protoc 1(4):2110–2115. https://doi.org/10.1038/nprot.2006.336
9. Gordon MD, Scott K (2009) Motor control in a Drosophila taste circuit. Neuron 61(3):373–384. https://doi.org/10.1016/j.neuron.2008.12.033
10. Shearin HK, Quinn CD, Mackin RD, Macdonald IS, Stowers RS (2018) t-GRASP, a targeted GRASP for assessing neuronal connectivity. J Neurosci Methods 306:94–102. https://doi.org/10.1016/j.jneumeth.2018.05.014

Chapter 16

Sparse Labeling, Rapid Clearing, and Native Fluorescence Light Sheet Imaging in the Developing Rodent Cerebellum

Cheryl Brandenburg and Alexandros Poulopoulos

Abstract

This protocol outlines plasmid delivery via in utero electroporation, rapid tissue clearing using CUBIC, and light sheet microscopy with optimizations for endogenous fluorescent protein imaging to label and image neuronal cells and their projections in their native topographic context of the intact developing rodent cerebellum. This technique enables the study of neuronal migration, circuit architecture, and connectivity of cerebellar neurons, particularly focusing on Purkinje cells.

Key words CUBIC clearing, Plasmid electroporation, Purkinje cell labeling, Projection mapping, Cerebellum, Light sheet imaging

1 Introduction

Purkinje cells are organized in stereotyped microcircuitry within the cerebellar cortex, making topographic connections to output structures as well as receiving topographically organized input from other brain areas [1, 2]. However, determining the precise developmental connectivity and migration trajectories of individual Purkinje cells is difficult with currently available methods. We and others have used sparse labeling of cells via in utero electroporation for tracking of developing neurons and their projections by transfecting cells based on birthdate and anatomical location [3–5]. Here, we describe a method to label subsets of Purkinje cells with plasmids expressing fluorescent proteins and track the three-dimensional formation of the cerebellum by whole brain clearing and imaging with a light sheet microscope [6, 7].

Tolga Soykan and Alexandros Poulopoulos (eds.), *Synapse Development: Methods and Protocols*, Methods in Molecular Biology, vol. 2910, https://doi.org/10.1007/978-1-0716-4446-1_16,

2 Materials

2.1 In Utero Electroporation

1. E10.5–E12.5 Timed-pregnant mice (e.g., CD1 from Charles River Laboratories) (*see* **Note 1**).
2. Isoflurane.
3. Oxygen tank.
4. 0.1% filtered Fast green FCF in nuclease-free water.
5. Analgesic (e.g., Buprenorphine).
6. Sterile cotton tip applicators.
7. Sterile gauze or Glad Press 'n Seal.
8. Hair removal cream (e.g., Veet).
9. Sterile disposable transfer pipettes.
10. Betadine surgical scrub.
11. Sterile surgical gloves.
12. Sterile bench pads.
13. 1/2 cc syringe with 27 G needle.
14. Parafilm.
15. 50 mL conical tubes.
16. Nylon monofilament reverse cutting 3/8 c 12 mm sutures.
17. Sterile 1× Phosphate Buffered Saline (PBS).
18. Alcohol antiseptic pads.
19. Glass capillary tubes, non-heparinized, diameter 1.1–1.2 mm (e.g., Fisherbrand).
20. Eye lubricant (e.g., Puralube Vet Ointment).
21. Electroporator (e.g., Electro Square Porator ECM 830).
22. Tweezertrodes and independent electrode.
23. Light source.
24. Water heat pad set to 37 °C (e.g., HTP-1500 heat therapy pump).
25. Dry block heater with 50 mL tube block set to 40 °C (e.g., VWR mini block heater).
26. Isoflurane vaporizer.
27. Pipette puller (e.g., Narishige).
28. Pipette beveler (e.g., Narishige).
29. Dissecting microscope.
30. Sterile surgical scissors, medium and micro.
31. Sterile forceps, blunt and sharp.
32. Sterile suturing tools.

33. Aspirator tube assemblies for calibrated microcapillary (e.g., Sigma-Aldrich).
34. Red heat lamp.
35. Fluorescent stereoscope (e.g., Leica).
36. Plasmid DNA (e.g., Addgene 164469).

2.2 Perfusion

1. Surgical scissors.
2. Forceps.
3. Peristaltic pump.
4. Needles (Precision Glide 30G × 1/2″).
5. Isoflurane chamber.
6. PBS.
7. 4% PFA pH 7.0–7.4.

2.3 Tissue Clearing

1. CUBIC-L (Fisher Scientific T3741).
2. CUBIC-R+(M) (Fisher Scientific T3740).
3. Water bath set to 37 °C.
4. Glass scintillation vials (Kimble).
5. 6-well plate.

2.4 Light Sheet Imaging

1. CUBIC-R+(M) as above to fill chamber.
2. Bondic UV liquid plastic welder.
3. Zeiss Light Sheet 7.

3 Methods

3.1 In Utero Electroporation of Purkinje Cells

The Purkinje cell progenitor zone is difficult to target with bipolar electrodes; therefore, the triple electrode approach is utilized [8, 9].

3.1.1 Preparation

1. Either breed or order timed-pregnant mice to be embryonic day 10.5–12.5 on the day of surgery (*see* **Note 2**).
2. Pull glass capillary tubes with a pipette puller, then bevel with constant water flow at a 25–35° angle to create a smooth end. Ensure the appropriate pore size and check with a dissecting microscope that there are no chips in the glass that may damage the embryo. The narrow part of the tip should be at least 6 mm. Push accumulated water out of the tip and onto a Kim wipe with an aspirator.
3. Prepare plasmid DNA that expresses a fluorescent marker to track neurons that were electroporated. Combinations of DNA should stay ≤4 μg/μL total in elution buffer. For visualization

of injection into the ventricle, add fast green at a ratio of 1:10–20 DNA mix for a total volume of 20 μL.

4. Ensure heat pad and heat block come to temperature.
5. Sterile 1× PBS in 50 mL conical tubes are placed in the heat block at 40 °C.
6. The electroporator should be set with the following parameters:
   - Pulse Voltage: 25 V
   - Pulse Length: 50 ms
   - Number of Pulses: 6
   - Interpulse Interval: 1 s
7. Gather a sterile bench pad, sterile gauze, eye lubricant, sterile cotton tip applicators, alcohol antiseptic pads, iodine, parafilm, hair removal cream, sutures, beveled capillaries, aspirator, analgesic in a 1/2 cc syringe with 27 G needle, and sterilized surgical tools, then place within the surgery space.

3.1.2 In Utero Electroporation Surgery

1. Place mouse in the induction chamber with 3% isoflurane until breathing has slowed and anesthesia depth is confirmed through regular observation of respiratory rate, heart rate, and lack of response to toe pinch, or as specified by the lab's animal use protocol.
2. While the mouse is being anesthetized, cover the cap of a 50 mL conical tube with parafilm. Pipette the DNA solution on top of the parafilm, then with the aspirator, suck up the liquid with the prepared capillary needles. All 20 μL can be added to the capillary tube for repeated injections. Ensure there is no breakage of the needle end or bubbles introduced (*see* **Note 3**).
3. Place the mouse prone with its head in the nose cone and ensure deep anesthesia with a toe pinch. With a syringe, inject analgesia subcutaneously (e.g., Buprenorphine) and apply eye lubricant with a cotton tip applicator, which can be reapplied every 20 min as needed. Flip the mouse on its back with its nose to the back of the nose cone. Adjust the isoflurane level to keep breathing slow but without gasps.
4. Apply a small amount of hair removal cream (e.g., Veet) with a cotton tip applicator and spread with small circles on the center of the stomach, ensuring not to apply to the nipple area. Leave the cream on for 1–2 min, then use Kim wipes and PBS to remove all cream from the area.
5. Clean the stomach area with alcohol wipes and apply betadine to the incision area.

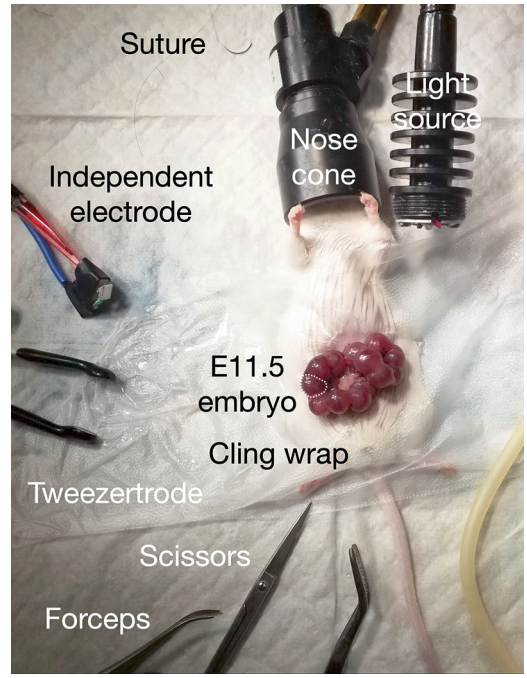

Fig. 1 Exposure of E11.5 embryos within the uterus. Embryos are pulled through the incision in the abdominal wall. Items in surgical field labeled

6. Cut a small circle in gauze or Glad press 'n seal and place the hole over the incision area so that the embryos can be placed on a sterile surface once removed.
7. If the mouse does not respond to a toe pinch, proceed with an incision along the midline of the skin of the stomach, about 3 cm in length. Create another incision along the underlying muscle layer without nicking the internal organs underneath.
8. Once the abdominal cavity is exposed, apply warm PBS with a transfer pipette to keep the embryos and organs moist.
9. Gently move the intestines and find the underlying embryos with blunt forceps. Scoop embryos out through the incision by placing forceps in the space between the embryos and pull up without pinching the forceps forcefully.
10. There will be two uterine horns with embryos. Pull each embryo out until there is slight resistance as the muscle at the end of the uterine horn is gently pulled (Fig. 1). Count the number of embryos and record.
11. Apply PBS to the embryos every few minutes as needed to keep moist and warm.
12. Avoiding the two embryos at the end of each uterine horn nearest the cervix, use gloved fingers to manipulate the embryo to become visible through the uterine wall. Look for the large

dark fourth ventricle, but do not move the embryos excessively as this can cause embryo reabsorption. If no ventricle can be found, move to the next embryo that may be in a better position. Be careful not to rupture the embryonic sac by squeezing too firmly.

3.1.3 Injection and Electroporation

1. Check that blowing through the aspirator pushes the DNA solution dropwise out of the needle. If it is blocked, choose an embryo that will not be injected and push just through the uterine wall back and forth while blowing air until liquid begins to come out.
2. Inject 4–5 μL of the plasmid solution either into the third or fourth ventricle by gently blowing into the aspirator. Injecting into the third ventricle may be less likely to result in embryo death due to the tip impaling underlying structures. Additionally, injecting into the third ventricle until the fourth ventricle is also filled allows electroporation of cells in the superior colliculus, which enables fluorescence screening after birth. Pierce the embryo with the needle just enough to reach the ventricle and not further so as not to damage brain tissue. The entire fourth ventricle should have green dye in the shape of a triangle (Fig. 2).
3. Place the tweezertrode connected to the negative lead on either side of the embryo laterally. The independent positive electrode is placed directly over the filled fourth ventricle but a bit superior so that the third ventricle is also targeted (Fig. 3). The third electrode can be manipulated a small amount left or right to target the Purkinje cell progenitor zone bilaterally or

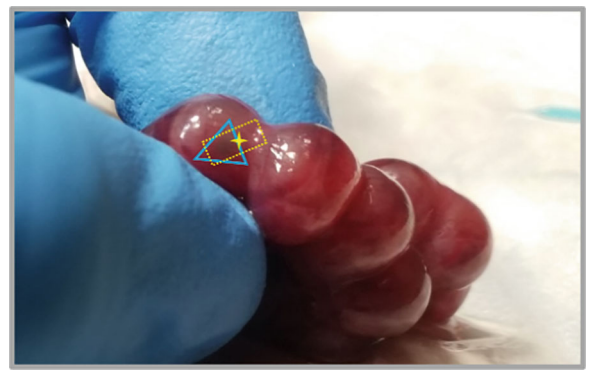

Fig. 2 Injection of DNA solution with fast green into the third/fourth ventricles. Once the entirety of the fourth ventricle is filled (blue triangle with dorsal brain toward the right), place the independent electrode over the ventricles as shown by the yellow dashed rectangle. The center of the electrode should be placed directly over the Purkinje cell progenitor zone, located on either side of the yellow star

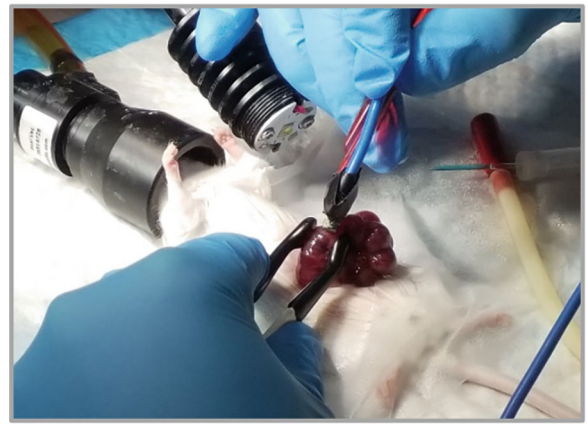

Fig. 3 Placement of triple electrode. Squeeze firmly for contact, but gently to avoid damaging the embryo and apply electrical pulses with foot pedal

both sides can be electroporated simultaneously for whole cerebellar expression.

4. With the electrodes firmly squeezing the embryo for good contact but not enough to rupture the embryonic sac, press the foot pedal to apply the series of electrical currents. To ensure an electrical field is produced at this lower voltage, put all three electrodes close together in PBS and ensure bubbles form before beginning electroporations.
5. Repeat the injection and electrical pulses on 3–6 embryos, depending on litter size.
6. Once all electroporations are complete, return the embryos to the abdominal cavity by gently pushing back through the incision with gloves or forceps and without twisting the uterus. Add a small amount of PBS into the abdominal cavity.
7. Suture the muscle layer with a continuous stitch, then suture the skin layer as well.
8. Place the mouse in its home cage on its side/back with the cage on a heat pad and a red heat lamp over the top of the cage where the mouse is underneath. Monitor to ensure the mouse wakes up and is able to flip over and walk around normally. Monitor the mouse daily for 5 days and administer buprenorphine as needed if the mouse displays signs of pain.
9. After birth, at age E18–20, screen the P0 pups for fluorescence with a dissecting microscope. The cerebellum develops postnatally and is hidden beneath other brain structures, so it is generally easier to screen the superior colliculus (*see* **Note 4**).
10. Return pups to the mother until the desired age. By P14, Purkinje cell migration is mostly complete.

3.2 Perfusion

Adapted from Hoffman and colleagues [10].

1. Prepare tools, dissecting tray, and run ice-cold PBS and 4% PFA through the tubing of the peristaltic pump (*see* **Note 5**).
2. Place the mouse in an isoflurane chamber until breathing is slowed.
3. Place the mouse on a dissecting tray with a microcentrifuge tube containing a Kim wipe and isoflurane over its nose, then if unresponsive to a toe pinch, hold down limbs with pins.
4. Make an incision along the midline of the abdominal skin, then make another incision in the muscle layer underneath without cutting the underlying organs.
5. Cut the diaphragm and sides of the rib cage, which can then be flipped and pinned back to expose the heart. Remove the tube with isoflurane from the nose.
6. Make a small cut in the right atrium to allow blood to drain.
7. Immediately run cold PBS at a speed appropriate for the mouse's age until the liver is pale and fluid leaving the right atrium is clear of blood.
8. Switch to cold 4% PFA and perfuse the mouse for 15–20 min (20–40 mL PFA) to ensure appropriate fixation that will withstand the clearing process. The PFA should cause muscle movements if the needle is placed correctly and fluid is running appropriately through the circulatory system. The animal will be very stiff at the end of 20 min.
9. Dissect the brain out of the skull. To avoid nicking the cerebellum with the scissors, cut first along one lower lateral side of the skull starting at the foramen magnum. Then cut along the midline from the olfactory bulb (place the blade between the two cortical hemispheres) until the tip of the scissors meets the midbrain. Peel one half of the skull away and then the other half, being careful not to pull off the cerebellar flocculus on either side.
10. Post-fix in 4 °C 4% PFA for 12–24 h. Wash in PBS several times, then shake in PBS overnight at 4 °C. Brains should always be kept cold to avoid loss of fluorescent signal.
11. For P0 mice, significantly decrease the perfusion to a slow drip to avoid swelling the ventricles with too much pressure.
12. If looking at embryonic developmental dates, the pregnant dam is kept under anesthesia with a nose cone, an incision is made along the midline, and the embryos are removed from the amniotic sac. The embryo is screened for fluorescence, then drop-fixed in cold 4% PFA.

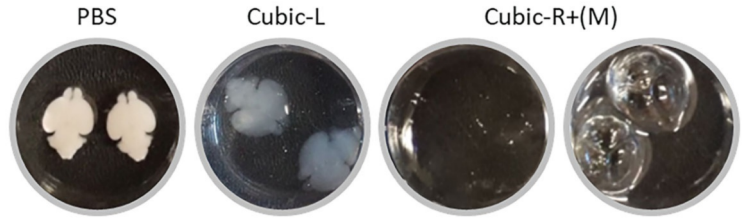

Fig. 4 P7 brains in the solution indicated within a six-well plate. After several days in Cubic-L, the brains become translucent. In Cubic-R+(M), the brains are completely transparent when covered in solution (left) but can be identified when the liquid is removed gently with a transfer pipette (right). It is normal to see some expansion of the brain. At P7, the white matter tracts are not visible, but will remain if the animals are older

3.3 Clearing with CUBIC Reagents

Modified from Matsumoto and colleagues [11].

1. With a blade, cut off the prefrontal cortex to provide a flat side for gluing to the light sheet specimen holder.
2. Place the fixed brain into fresh CUBIC-L and shake at 37 °C. Every 2 days, replace the solution with fresh CUBIC-L until the brain is uniformly opaque and white matter tracts can no longer be seen (Fig. 4). Mice under the age of P7 clear within a few days, while older mice take longer to clear. Mice several months old may not clear to the extent that younger mouse brains will, especially the white matter tracts.
3. At this stage, brains can be checked for fluorescence and imaged on a dissecting microscope if desired.
4. Remove brains from CUBIC-L with a spoon and place them in a small amount of CUBIC-R+(M). Gently shake the brains to remove the majority of CUBIC-L, then scoop brains into a new well with fresh CUBIC-R+(M).
5. Shake in CUBIC-R+(M) at room temperature for 2 days or until the brain is transparent.

3.4 Light Sheet Imaging and Analysis

1. Fill the chamber with CUBIC-R+(M).
2. Apply Bondic glue to the edges of the flat side of the cortex and use UV light to dry glue on the brain and sample holder. Apply additional glue until steadily held (Fig. 5).
3. Place the sample holder and glued brain into the chamber to equilibrate, usually a few hours, but can be left overnight. If the brains have not had enough time to equilibrate in the chamber, there may be high background and poor resolution upon imaging.
4. Click the ZEN icon to start ZEN for light sheet.

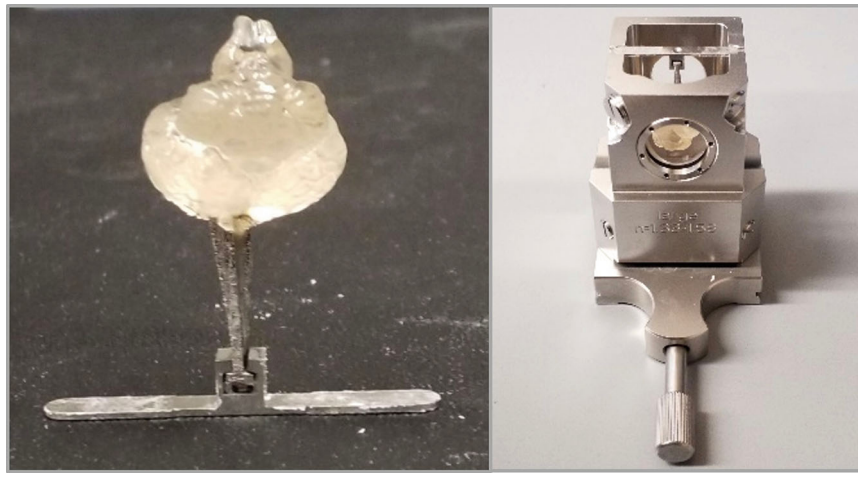

Fig. 5 P14 brains require some balancing and extra glue on the small sample holder (left). Use the cortex to glue onto the end of the metal piece. Once sturdy, can flip and place in chamber (right)

5. Click on the arrows to expand boot status and hardware configuration database and choose the clearing database under "recent." Choose "start system."
6. Once start-up is complete, ensure that the detection objective and each illumination collar is set at 1.52 to match the refractive index of the CUBIC solutions.
7. Place the chamber into the light sheet and dock the sample onto the sample holder.
8. Bring the sample above the solution so it does not interfere with alignment. Align the light sheet so that the waist is as thin and in focus as possible by turning the illumination collars.
9. Adjust the brain to be in line with the detection objective, configure the light path and laser, then press continuous to find the region of interest. It is easiest to start at a zoom of 0.4 to have a wider view and brighter fluorescence. Scroll through the z-plane to get an overview of the desired area. Decreasing the maximum range of the lookup tables so that the background is visible can help to orient within the brain when fluorescence is not visible (*see* **Note 6**).
10. While at a 0.4 zoom, set the four outer corners of the region of interest in the bounding grid tab (Fig. 6) and set the z-stack range. Setting an overlap of 15% and reducing the frame size will avoid a dark gradient at the edges of each tile. Using one side of light sheet illumination will reduce acquisition time; however, dual-side illumination can be used, if necessary, with larger brains (*see* **Note 7**).

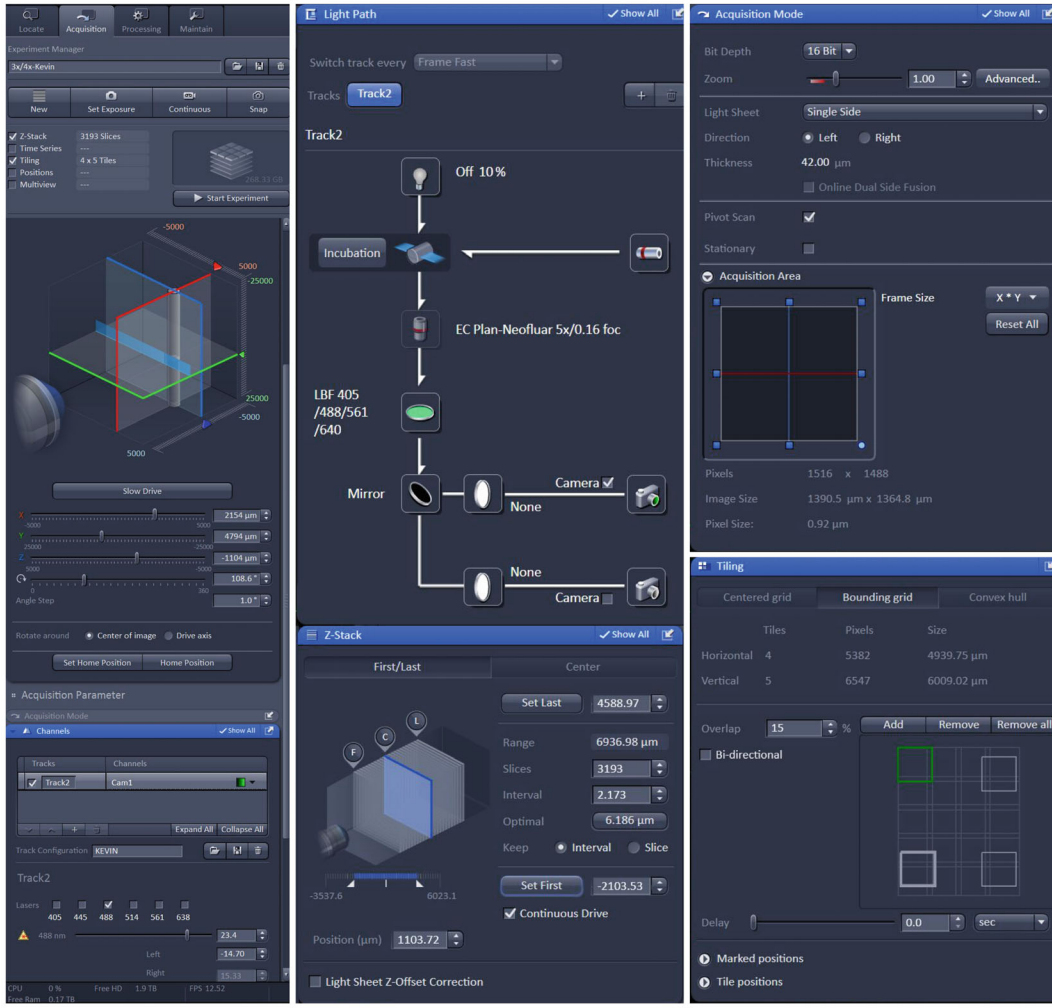

Fig. 6 Typical settings for light sheet imaging

11. Imaging will take less time if kept at a wider zoom, so can be imaged as is. Alternatively, adjust the zoom to 1, focus on a typical area, and adjust the laser power and exposure to give the desired dynamic range for imaging. Check pivot scan, then start experiment to save the file and begin imaging.
12. Once complete, the file can be opened in Zen Blue for processing or an alternative software such as Arivis. When imaging with a zoom factor, large tile artifacts are often produced so that Zen Blue does not automatically align the tiles properly. Arivis has an option to manually move tiles to a larger degree, then automatically stitch the rest together. For example, in the Tile Sorter window in the "manual" tab (Fig. 7), the left column of tiles is selected (white borders) and dragged over

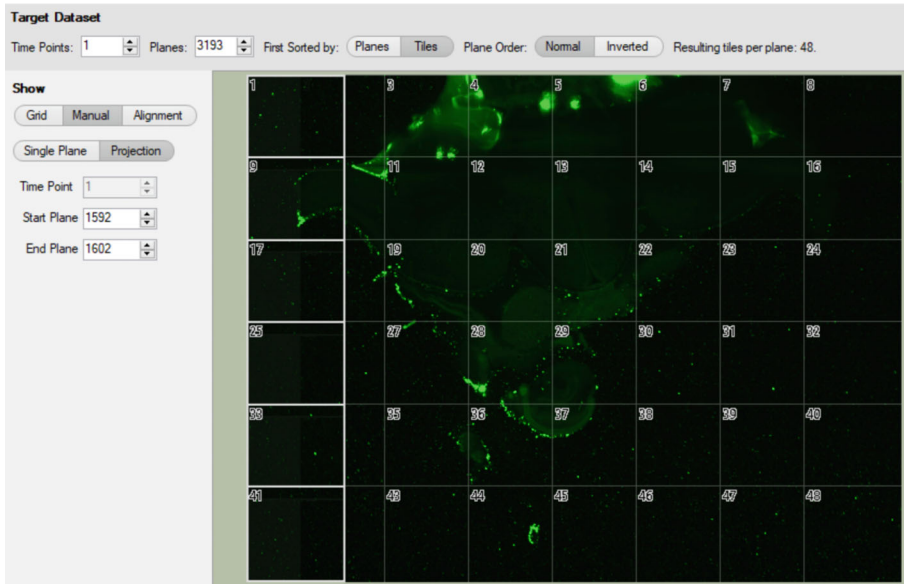

Fig. 7 Stitching tiles in Arivis

the top of the underlying tiles in which the region was imaged with a large degree of overlap (this typically occurs at each side of the image set). This manually positions the overlapping regions closer to the correct alignment so that automatic stitching can be appropriately calculated when running the "create stitched planes" operation. It is helpful to use the "projection" tab to collapse multiple z planes of each tile and use the transparency slider to correctly overlay one tile on top of another.

13. Once stitched, an Arivis pipeline can be created for standard imaging processes such as background correction and denoising as required.
14. Typically, background from brain tissue can be seen when adjusting the lookup tables. This can be helpful to orient within the brain and determine how the electroporation field is oriented in a 3D space. The 4D view control is helpful for 3D movement, and strategically placed 4D clipping planes allow movement through the image stack to visualize regions of interest more clearly (Fig. 8). Depending on the goal, downstream processes can be incorporated to quantify cell body location and map projections to output structures (*see* **Note 8**).

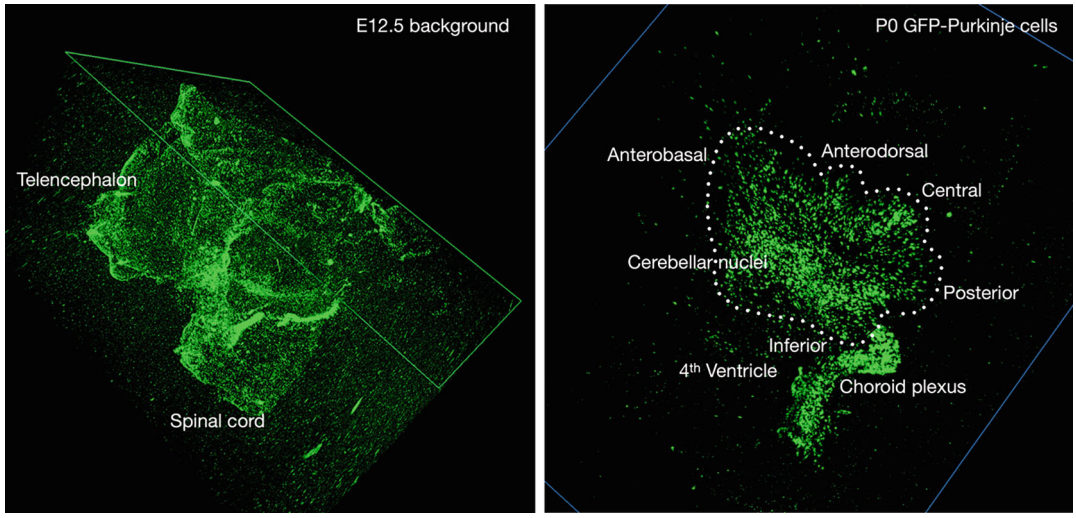

Fig. 8 Light sheet imaging examples. Left: An E12.5 brain with background fluorescence enhanced to orient the electroporation field within the whole brain. A 4D clipping plane is utilized to find the electroporation field within the stack. Right: A P0 brain Purkinje cell electroporation field with background removed, illuminating the emerging 3D structure of the cerebellum

4 Notes

1. E10.5 mice are very difficult to see through the uterine wall. Pressing LED lights directly against the back of the embryo may be required to target the ventricles. E11.5 and E12.5 are more routinely used, with 11.5 giving the largest number of electroporated cells.
2. Purkinje cells are not born outside of E10.5–E12.5.
3. After targeting a few embryos, the tip may become compromised. If there is resistance when targeting the next embryo, break the end of the tip and push out the remaining DNA solution onto the parafilm cap, then load a new needle without creating bubbles.
4. Survival rate of positive embryos is 40–50%. Important factors to increase chances of survival are using the lowest possible voltage, having a smooth end tip of small diameter and without bubbles in solution, keeping the injection depth shallow to avoid damaging underlying structures, and manipulating the embryos gently without squeezing too hard with the electrodes.
5. Keeping the brains cold at all times is important for endogenous fluorescence surviving through to the end of the clearing process.

6. The key factor in retaining enough fluorescence signal to image with light sheet is the quality of the electroporation. A strong electrical field and small plasmid sizes are needed to have a high transfection efficiency in the Purkinje cell progenitor zone. If the field is weak due to poor contact and the transfection is low, much of the endogenous fluorescence will be lost in the clearing process and will be difficult to separate from the background.
7. High laser power does not typically quench the fluorophores, so it is preferred to increase the laser power (100% is routinely used without bleaching) and decrease the exposure time for faster imaging. It is recommended to take whole brain images zoomed out since the signal is brighter for light sheet and then zoom in if specific regions are needed at higher resolution.
8. If projection mapping is required, a GPI-anchored fluorescent marker is recommended. Projections are typically brighter and better retained after clearing, although high laser power is recommended. Arivis Vision 4D accompanied with a VR headset may be useful to aid in tracing projections.

References

1. Apps R, Hawkes R, Aoki S et al (2018) Cerebellar modules and their role as operational cerebellar processing units: a consensus paper. Cerebellum 17:654–682
2. White JJ, Sillitoe RV (2013) Development of the cerebellum: from gene expression patterns to circuit maps. Wiley Interdiscip Rev Dev Biol 2:149–164
3. Poulopoulos A, Murphy AJ, Ozkan A et al (2019) Subcellular transcriptomes and proteomes of developing axon projections in the cerebral cortex. Nature 565:356–360
4. Blatt GJ, Brandenburg C, Poulopoulos A (2023) India ink to 3D imaging: the legacy of Dr. Deepak "Dee" N. Pandya and his influence on generations of neuroanatomists. J Comp Neurol 531:1875–1882
5. Poulopoulos A, Davis P, Brandenburg C et al (2024) Symmetry in levels of axon-axon homophilic adhesion establishes topography in the corpus callosum and development of connectivity between brain hemispheres. bioRxiv. https://doi.org/10.1101/2024.03.28.587108
6. Hillman EMC, Voleti V, Li W et al (2019) Light-sheet microscopy in neuroscience. Annu Rev Neurosci 42:295–313
7. Brandenburg C, Crutcher GW, Romanowski AJ et al (2024) Developmental transformations of Purkinje cells tracked by DNA electrokinetic mobility. bioRxiv. https://doi.org/10.1101/2024.08.29.610366
8. Maschio MD, Ghezzi D, Bony G et al (2012) High-performance and site-directed in utero electroporation by a triple-electrode probe. Nat Commun 3:960
9. Szczurkowska J, Cwetsch AW, Maschio MD et al (2016) Targeted in vivo genetic manipulation of the mouse or rat brain by in utero electroporation with a triple-electrode probe. Nat Protoc 11:399–412
10. Hoffman GE, Murphy KJ, Sita LV (2016) The importance of titrating antibodies for immunocytochemical methods. Curr Protoc Neurosci 76:2.12.1–2.12.37
11. Matsumoto K, Mitani TT, Horiguchi SA et al (2019) Advanced CUBIC tissue clearing for whole-organ cell profiling. Nat Protoc 14:3506–3537

INDEX

Tolga Soykan and Alexandros Poulopoulos (eds.), *Synapse Development: Methods and Protocols*, Methods in Molecular Biology, vol. 2910, https://doi.org/10.1007/978-1-0716-4446-1,

N

P

R

S

T

V